

**Neogene fluvial deposits along the south-west coast of South
Africa: understanding the palaeoclimate through proxies**

Lara Sciscio

B.Sc. (Hons.) Rhodes University

March 2011

Rhodes University

Department of Geology

Grahamstown

A dissertation submitted to the Faculty of Science, Rhodes University, Grahamstown, in
fulfilment for the Degree of Master of Science

Declaration

I, Lara Sciscio, declare that this dissertation is my own unaided work. It is being submitted for the degree Master of Science at Rhodes University, Grahamstown. It has not been submitted before for any degree or examination in any other university.

Lara Sciscio

..... Day of 20...

Abstract

Branched glycerol dialkyl glycerol tetraether (GDGTs) membrane lipids have been used as a new proxy for the reconstruction of terrestrial palaeoclimates. These biomarkers (or molecular ‘fossils’) in conjunction with palynology, have been effective in the novel analysis of Miocene organic-rich sediments from three South African west coast sites at Rondeberg, Noordhoek and Langebaanweg. Lastly, a Quaternary south coast site at Rietvlei, South Africa, was also studied to further elucidate the extent of use of this new proxy. The fluvial peat and organic-rich deposits of the Elandsfontyn Formation (Sandveld Group) were investigated at Noordhoek, Langebaanweg and Rondeberg to provide new evidence for the climate and vegetation patterns during Miocene in this region.

Drill-core and quarry samples from all four sites were freeze-dried, powdered, and prepared for biogeochemical and palynological analyses. The methylation index of branched tetraethers (MBT) and cyclisation ratio of branched tetraethers (CBT) proxies were used to calculate the mean annual air temperature (MAAT) and pH values of the organic-rich horizons at time of deposition. The Branched versus isoprenoid index of tetraethers (BIT) was used to assess the relative contributions of marine archaeal and terrestrial bacterial tetraethers, and thereby assess the validity of the MBT, CBT and calculated palaeoenvironmental factors.

The results presented in this thesis suggest that the use of the MBT/CBT proxy has significant potential in southern Africa, and may complement previously attempted palaeoclimatic and palaeoecological studies of Neogene-aged South African sediments. This type of research has the capacity to provide palaeoenvironmental information where other proxies may be absent. Results indicate that all sites yielded branched tetraether membrane lipids with the exception of Rondeberg, where GDGTs were below detection as a result of poor preservation conditions. Palynological investigation confirmed proxy derived temperatures. Furthermore palynomorph analyses supplemented earlier studies of the Noordhoek site and were piloted for the Rondeberg site, reaffirming alternating sequences of tropical and subtropical palynofloras. The MAATs, likewise, show variability and pronounced trends through time at the Langebaanweg and Noordhoek sites, generally corresponding with the variation and diversity of the pollen population. The terrestrial MAAT results appear to compliment Southern Hemisphere sea level changes associated with

Antarctic glaciations. Additionally, this data shows a pattern similar to the Southern and Northern Hemisphere marine isotope records of relative fluctuations in the global climate and sea level change from the early to middle Miocene.

The application of these past climate change indicators have been proved to be useful in the reconstruction of South Africa Miocene palaeoclimates, and may aid in understanding the consequences of climate change in the Cape region.

Keywords:

Branched glycerol dialkyl glycerol tetraether (GDGTs), biomarkers, Miocene, palaeoclimate, palynofloras, South Africa

Acknowledgements

I would like to thank my supervisor Dr. H. Tsikos as well as Dr. Y. van Breugel for their advice, contributions and encouragement in undertaking this innovative research project. I would also like to thank co-supervisor Dr. D. Roberts for his help, useful criticisms and ideas during my studies.

I am indebted to Prof. J. Sinninghe Damsté, Dr. S. Schouten and Ms. M. Baas of the Department of Marine Biogeochemistry and Toxicology, Royal Netherlands Institute for Sea Research, the Netherlands (NIOZ) for the use of the facilities, the constructive meetings and extremely valuable suggestions. I am particularly grateful to Marianne Baas for her patience, forbearance and invaluable advice during sample preparation. To Prof. Louis Scott I wish to record my sincere gratitude for his council and contributions during my brief periods in the laboratory in the Department of Plant Sciences, University of the Free State. Prof. Scott has always made me feel welcome, and through his extremely beneficial suggestions I have been able to develop a deep appreciation for palynology. I would also like to thank the Rhodes University Geology Department analytical staff (expressly Mr. J. Hepple) and Prof. Goonie Marsh for X.R.F sample analysis. I would like to acknowledge Dr. D. Gröcke for his kind stable isotopes analysis of Langebaanweg and Noordhoek samples. Finally, I wish to thank Dr. A Carr for his contribution in terms of sample material, additional bulk parameter and carbon 14 age-date data for the Rietvlei chapter.

I also acknowledge the following contributions:

- The West Coast Fossil Park and African Origins Platform,
- Mining Qualification Authority (MQA) for giving me the opportunity to lecture during my studies,
- Prof. H. Eales, Dr. E. Bordy, Dr. T. Matthews, Sean Linkermann and Kate Robey for helpful advice and encouragement whether it was dissertation-orientated or otherwise,
- Council for Geoscience for access to reports and publications,
- Staff and students of the Geology Department, Rhodes University,
- Digs-mates of 1 Bond St. (Leanne Cooper, Hailey Johnson, Matthys Kroon, Shan Ambrose, Sean Edwards and Jessie the dig's-dog) for the endless light hearted moments and general rowdy support over the years. I will sorely miss you all,

- Climbing friends: specifically Ryan Holl, Adam Ludford, Belle Johnson, Greg Carter, Nathi Nama and Gareth McAlister for the numerous bouldering and sport climbing sessions. They have taught me to have faith in my ability (as a climber), which I hope will resonate into my work.

Finally, I would like to express my deepest gratitude to my parents Mauro and Dorothy Sciscio and my sisters Romie and Gia. Their love, support and sense of humour mean more to me than words can express, and they perpetually inspire me to give of my best.

Lara Sciscio

Grahamstown, December 2010

Table of Contents

Declaration.....	i
Abstract.....	ii
Acknowledgements.....	iv
Table of Contents.....	vi
List of abbreviations	x
List of Figures.....	x
List of Tables	xiii
1 General introduction.....	1
1.1 Regional geological setting.....	5
1.1.1 Elandsfontyn Formation, Sandveld Group.....	7
1.1.2 Varswater Formation.....	7
1.2 Cenozoic climate records.....	9
1.2.1 The Climate of the Miocene Epoch.....	11
1.3 Motivation and specific objectives.....	14
2 Methodology.....	16
2.1 Part 1: Techniques in recent and current research.....	16
2.1.1 Palaeopalynology.....	16
2.1.2 Introduction to organic biogeochemical techniques.....	18
2.1.3 Organic geochemical proxies.....	23
2.2 Part 2: Methods and materials followed in current research.....	25
2.2.1 Sampling procedure.....	25
2.2.2 Palynology laboratory preparation.....	27
2.2.3 Inorganic geochemistry: Mineral petrology and bulk-rock geochemistry of the Rondeberg Clay Pit.....	29
2.2.4 Organic biogeochemistry.....	29

GDGT analysis sample preparation and analysis	30
Isotope preparation and analysis.....	30
3 Investigation of organic-rich sediments from Noordhoek, South Africa	32
3.1 Introduction	32
3.2 Regional geological setting and site description	32
3.3 Previous research in the Noordhoek area.....	34
3.3.1 Palynological studies	35
3.3.2 Pollen Zones “L and M”	37
3.4 Methodology	38
3.5 Results	40
3.5.1 Palynological results: Qualitative and quantitative analyses	40
3.5.2 Bulk organic parameters, carbon and nitrogen isotopes	49
3.5.3 The BIT Index and CBT/MBT proxy	52
3.5.4 MAAT and ‘Index/indicator’ palynomorphs	54
3.6 Discussion	55
3.6.1 Sediment description and bulk organic analyses	55
3.6.2 Palynology	56
3.6.3 Comparison to Coetzee’s (1978b) Pollen zones	60
3.6.4 Bulk organic parameters	61
3.6.5 Biogeochemical interpretation and the CBT/MBT proxy	63
3.6.6 Palaeoflora and climate.....	66
3.6.7 Stable isotope ranges.....	68
3.6.8 Southern Hemisphere comparisons and factors influencing south-west coast climate.....	70
3.6.9 Northern Hemisphere comparisons.....	73
3.7 Conclusion.....	75
3.7.1 Drawbacks and future research.....	76

4	Langebaanweg Fossil Site	77
4.1	Introduction	77
4.2	Regional geological setting and previous research	78
4.2.1	Dating of the Elandsfontyn Formation at LBW.....	79
4.2.2	LBW palaeoflora.....	80
4.3	Methodology	81
4.4	Results	81
4.4.1	Bulk geochemical parameters results.....	82
4.4.2	BIT index and CBT/MBT proxy.....	85
4.5	Discussion	88
4.5.1	Depositional setting	88
4.5.2	Regional climate and forcing mechanisms	91
4.5.3	Palynomorphs, Elandsfontyn Formation deposition and LBW climate	93
4.6	Conclusion.....	94
5	Synthesis of LBW and Noordhoek Sites	96
5.1	Introduction	96
5.2	Middle Miocene Climatic Trends	97
5.2.1	Southern African perspective of Miocene climate change	98
5.3	Results and Discussion.....	99
5.3.1	Bulk organic parameters and stable isotope record	99
5.3.2	Global and regional comparisons.....	104
5.3.3	Palynoflora.....	105
5.4	Synthesis.....	106
5.5	Future work	109
6	Case Studies from the south-west and south- east coasts, South Africa	110
6.1	Introduction	110
6.2	Case study 1: Rondeberg Clay Pit.....	110

6.2.1	Methodology	111
6.2.2	Results.....	111
6.2.3	Inorganic Geochemistry results	115
6.2.4	Discussion and conclusion.....	120
6.3	Case study 2: the Quaternary Rietvlei Site.....	122
6.3.1	Introduction.....	122
6.3.2	Methodology	125
6.3.3	Results.....	125
6.3.4	Discussion and conclusion.....	128
7	General Conclusion	131
7.1	Future research	132
8	References	134
9	Appendices	A1

List of abbreviations

BIT: Branched versus Isoprenoid tetraether Index	MMCT: Middle Miocene climatic transition (~14.5 Ma - 12.7 Ma)
CBT: Cyclisation ratio of Branched Tetraethers	OM: organic matter
EAIS: East Antarctic ice sheet	RCP: Rondeberg Clay Pit
GDGT: glycerol dialkyl glycerol tetraether	SST: sea surface temperatures
LBW: Langebaanweg	TN: total nitrogen
MAAT: Mean annual air temperature	TOC: total organic carbon (TOC) content (%)
MBT: Methylation index of Branched Tetraethers	WAIS: West Antarctic ice sheet
MMCO: Middle Miocene Climatic Optimum (~17 Ma – 14.5 Ma)	

List of Figures

Figure 1.1. The study sites at Langebaanweg, Rondeberg, Noordhoek and Stilbaai, South Africa (modified after Roberts <i>et al.</i> , 2009).....	2
Figure 1.2. Factors influencing the formation and accumulation of peat (adapted from Meadows, 1988).	3
Figure 1.3. Southern African wind patterns and ocean currents (Adapted from Chase, 2010).....	4
Figure 1.4. Geographic subsurface distribution of the Elandsfontyn and Varswater Formations of the Sandveld Group in the south-western Cape, South Africa (Adapted from Roberts, 2006b)..	6
Figure 1.5. Generalised stratigraphic log of the Elandsfontyn and Varswater Formations (Sandveld Group) at Langebaanweg indicating the presence and distribution of peat horizons (adapted from Roberts <i>et al.</i> , in review).	8
Figure 1.1 Climatic events of the Cenozoic from benthic foraminifera (adapted from Zachos <i>et al.</i> , 2001).....	13
Figure 2.1. Pollen wall terminology (adapted from Punt <i>et al.</i> , 2007).	17
Figure 2.2. Pollen and spore morphology (adapted from Traverse, 1988 and Punt <i>et al.</i> , 2007).	18
Figure 2.3. Typical bacterial core membrane lipids in comparison to the core membrane lipids recognised as archaeal (adapted from Albers <i>et al.</i> , 2000 and Weijers <i>et al.</i> , 2007c).	20
Figure 2.4. Branched GDGTs I – III and their isomers (a, b, c) (taken from Weijers <i>et al.</i> , 2007a).	22
Figure 2.5. Silicified sulphidic green nodules, Noordhoek core.	26
Figure 3.1. The borehole and locality map of the Noordhoek study site with emphasis on the subsurface extent of the Elandsfontyn Formation	33
Figure 3.2. Borehole log of the S.20 borehole previously drilled at Noordhoek and which lies approximately 3m from current Avondrustvlei core of this study (adapted from Rogers, 1982).	35
Figure 3.3. Variety of palynomorphs based on descriptive taxonomy from the Noordhoek core.	43

Figure 3.4.(A - C) Pollen diagram of the Noordhoek Avondrustvlei core.....	46
Figure 3.5. Noordhoek core bulk organic parameters.....	51
Figure 3.6. Branched vs. Isoprenoid index of Tetraethers (BIT), mean annual air temperatures (MAAT, °C), pH of soil at time of deposition, and isotope $\delta^{13}\text{C}$ values of the Noordhoek samples	53
Figure 3.7. Mean annual air temperature (MAAT), in °C, calculated from branched GDGT biomarker distribution with black dots defining samples, versus podocarp, palm and <i>Myrica/Casuarina</i> record of the Noordhoek core.....	54
Figure 3.8. Comparison between Coetzee (1978 a, b) pollen zones and parameters from the Noordhoek Avondrustvlei core of this study.	62
Figure 3.9. Carbon isotope ranges versus C/N ratio for different photosynthetic groups to aid organic matter source identification (Adapted from Shunk <i>et al.</i> , 2009).....	69
Figure 3.10. The Noordhoek core's terrestrial palaeotemperature curve in comparison to the relative sea level curve from Neogene south-west Cape coast sediments South Africa (adapted from Cole and Roberts, 1996) in comparison to global sea level (Haq <i>et al.</i> , 1987) and Southern Ocean high latitude sea surface temperatures (adapted from Clarke and Crame, 2006).	71
Figure 3.11. Continental temperature curves for Central Europe during the last 45 My (Mosbrugger <i>et al.</i> , 2005) in comparison with the global marine oxygen isotope record of Zachos <i>et al.</i> (2001), over which the Noordhoek MAAT curve has been superimposed.	73
Figure 3.12. Comparison of benthic foraminifera $\delta^{18}\text{O}$ values from the Miocene-Pleistocene (Plt) and associated recorded temperatures with that calculated from the CBT/MBT proxy for the terrestrial realm, calculating mean annual air temperatures Noordhoek.....	74
Figure 4.1. The subsurface extent of the Elandsfontyn Formation, Sandveld Group, which unconformably overlies Precambrian basement, south-western Cape, South Africa in relation to the study site at LBW and the core (S1) (adapted from Roberts, 2006a).	78
Figure 4.2. S1 borehole log (adapted from Coetzee and Rogers, 1982).	80
Figure 4.3. Log of the Elandsfontyn Formation for the Langebaanweg (LBW) core which records sediment present at borehole depths between 0 m and 35 m (Adapted from Roberts 2006b).....	82
Figure 4.4. Langebaanweg organic clay samples depths below sea level (m) and core stratigraphy with corresponding total organic carbon (TOC) content (%), total nitrogen (TN) content (%) and the TOC/TN ratio.	83
Figure 4.5. Stratigraphic down-core variability of the (A) bulk total organic carbon (TOC) contents, (B) Branched and Isoprenoid Tetraether index (BIT), (C) pH, (D) mean annual air temperature (MAAT - calculated from the CBT/MBT proxy), and (E) stable carbon and (F) nitrogen isotope values for the Langebaanweg samples. (G) and (H) are plots showing correspondence between the MAAT and pH and $\delta^{13}\text{C}$ measurements.	84
Figure 4.6. Elandsfontyn Formation log detailing samples and the corresponding mean annual air temperatures obtained from bacterial tetraether lipid composition analyses in comparison to modern MAAT	87
Figure 4.7. LBW samples $\delta^{13}\text{C}$ versus C/N data plotted onto the composite organic matter sources diagram for C_3 , C_4 vegetation and algae (Adapted from Shunk <i>et al.</i> , 2009).	88

Figure 5.1. Stratigraphic log of the Elandsfontyn Formation from the cores taken at Noordhoek and Langebaanweg, South-west Cape coast. T.....	96
Figure 5.2. Comparison of Noordhoek (blue, diamonds) and Langebaanweg (LBW: red, squares) study sites in terms of (A) Noordhoek total organic carbon (TOC) content (%), (B) Langebaanweg (LBW) TOC (%), (C) $\delta^{15}\text{N}$ record and (D) $\delta^{13}\text{C}$ record (E) C/N ratio (F) pH, (G) mean annual air temperature (MAAT), and (H) The Branched versus Isoprenoid tetraether (BIT) index	100
Figure 5.3. Noordhoek and LBW comparison of OM source.....	102
Figure 5.4. Comparison of LBW and Noordhoek MAAT with regional and global sea level and SST.....	105
Figure 5.5. Comparison between Coetzee's (1978a, b) pollen zones, Coetzee and Rogers' (1982) pollen zones and the Noordhoek pollen in addition to the Noordhoek and LBW MAAT curves	107
Figure 5.6. Palaeotemperatures and palyofloras from Noordhoek and LBW in comparison to global climatic events	108
Figure 6.1. Rondeberg Clay Pit log showing the change in lithology with stratigraphic height and the presence of wood fragments (greater than 10 cm in size) in addition to the occurrence of 'organics' – pollen and microscopic charcoal from sampled and processed material.	111
Figure 6.2. Selected photomicrographs of Rondeberg palynomorphs	112
Figure 6.3. Chart showing the percentage distribution of specific pollen types within the Rondeberg Clay Pit.	113
Figure 6.4. Pollen diagram of total counts for the most productive sample units of the Rondeberg Clay Pit, Malmesbury, South Africa.	114
Figure 6.5. Major element variation diagram with elevation above pit base at Rondeberg Clay Pit.	117
Figure 6.6. Scatter plot of SiO_2 (wt %) versus Al_2O_3 and MgO	118
Figure 6.7. Trace element data for the Rondeberg Clay pit versus lithology of the clay pit.	119
Figure 6.8. Distribution and division of modern day rainfall into three zones in relation to the study sites of Rondeberg Clay Pit (RCP) and Rietvlei wetland study area, South Africa (modified after Roberts <i>et al.</i> , 2009 and Chase and Meadows. 2007).....	123
Figure 6.9. The bulk organic parameters for the entire Rietvlei core, showing variability in TOC, $\delta^{13}\text{C}$, TN and C/N.....	125
Figure 6.10. (A) Branched vs. Isoprenoid index of Tetraethers (BIT), pH of sediment at time of deposition, mean annual air temperatures (MAAT, °C), and calibrated carbon 14 age dates for specific samples from the Rietvlei core. (B) Scatter plot of MAAT versus pH ($R^2 = 0.36$).	128

List of Tables

Table 1.1. Mio-Pliocene climate of the Southern Hemisphere in comparison to global climate change during these epochs (adapted from Clarke and Crame, 1992).....	11
Table 1.2. Comparative results for global surface temperatures and rainfall in the Middle to Late-Miocene, showing variation from modern global temperatures (adapted from Tong <i>et al.</i> , 2009).....	12
Table 2.1. Descriptive classification scheme used to classify pollen and spores.....	28
Table 3.1. Forest taxa emphasised by Coetzee (1983) as recorded during the Tertiary from the Noordhoek site, with ‘extinct’ referring to those species absent in Africa. Climatic tolerances and soil preferences (where known) have been obtained from modern species and nearest living relatives relationships	37
Table 3.2. Coetzee (1978a, b) division of south-western Cape palynomorphs into Zones M and L.	39
Table 3.3. Subzones Li to Lvii of Zone L with key indicator palynomorphs noted by Coetzee (1978a, b).	39
Table 3.4. Selected photomicrographs of palynomorphs from the Noordhoek drill core.	41
Table 3.5. Pollen, climatic tolerance and name assigned to palynomorph (template adapted and developed from that outlined by de Villiers, 1997).	42
Table 3.6. Palynomorphs abundance (%) of those pollen types (excluding the algae, incert., and unknown colpates) that exceeded 1% of the total pollen count.	44
Table 3.7. Age distribution of common elements within the Noordhoek core. Age dates obtained from de Villiers and Cadman (2001), Stevens (2001) and Raine <i>et al.</i> (2008).	50
Table 4.1. Compilation table of previous and modern nomenclature of the Varswater Formation at LBW (Adapted from Roberts, 2006d).	79
Table 4.2. Comparison between the two broad groupings of LBW samples based on measured bulk organic parameters and CBT/MBT proxy values.	86
Table 4.3. Comparison table of modern Saldanha Bay mean annual air temperatures, sea surface temperatures, carbon dioxide concentration and precipitation levels in comparison to measured and predicated Miocene values.	92
Table 4.4. Coetzee (1978b) pollen zones M and L as established from palynological studies of several west coast sites and the Langebaan site (from S1 borehole) for comparative purposes.	94
Table 5.1. Comparison of organic parameters and mean annual temperatures between groups from samples sites at Noordhoek and Langebaanweg.	103
Table 5.2. Comparison of the Noordhoek and LBW tetraethers lipid derived mean annual air temperatures (MAAT) over similar interval below sea level, and the correlation coefficient calculated for this data set (0.95).....	104
Table 5.3. Broad comparisons of organic parameters at Noordhoek and Langebaanweg (LBW) and their interpretation.	107
Table 6.1. Rietvlei organic biogeochemical parameters	127

1 General introduction

Detailed research into the sedimentary records, importantly those containing preserved organic-rich material, has become an important means to understanding palaeoclimate and palaeoecology. Palaeoclimate research serves to determine the variability of past global climate, and acts as a gauge of the effects of human industrialisation and anthropogenic forcing. This is becoming an increasingly important concept in the light of modern climate change developments (Karl and Trenberth, 2003; Bindler, 2006; Sachs *et al.*, 2007; Weijers *et al.*, 2007a, b). Grappling with more accurate palaeoclimate reconstructions requires a multistudy approach using the traditional methods of palaeopalynology, geochemistry and sedimentology. Additionally, recently developed tools, such as biomarker analysis, have become a valuable complement to palaeoclimate research. Furthermore, to have some understanding of the complexities of the forces controlling climate will significantly influence the understanding of current and past distribution, abundance and diversity of flora and fauna.

As the preservation of organic-rich deposits along the south-west Cape coast (South Africa) is rare, this dissertation sets out to examine the areas where early Neogene organic-rich deposits have been anomalously preserved (Fig. 1.1). Deposits of special interest and focus at Noordhoek and Langebaanweg (Fig. 1.1) are located stratigraphically below present day sea-level. Their preservation and position may be accounted for by deposition during times of lowered sea-level, but may also have been due to downwarping associated with flexure of the lithosphere (Du Toit, 1933; Partridge and Maud, 1987; Roberts *et al.*, 2008; Moore *et al.*, 2009). The occurrences of such deposits are of great scientific interest and value due to the palaeoenvironmental information which can be gleaned (Negri *et al.*, 2001).

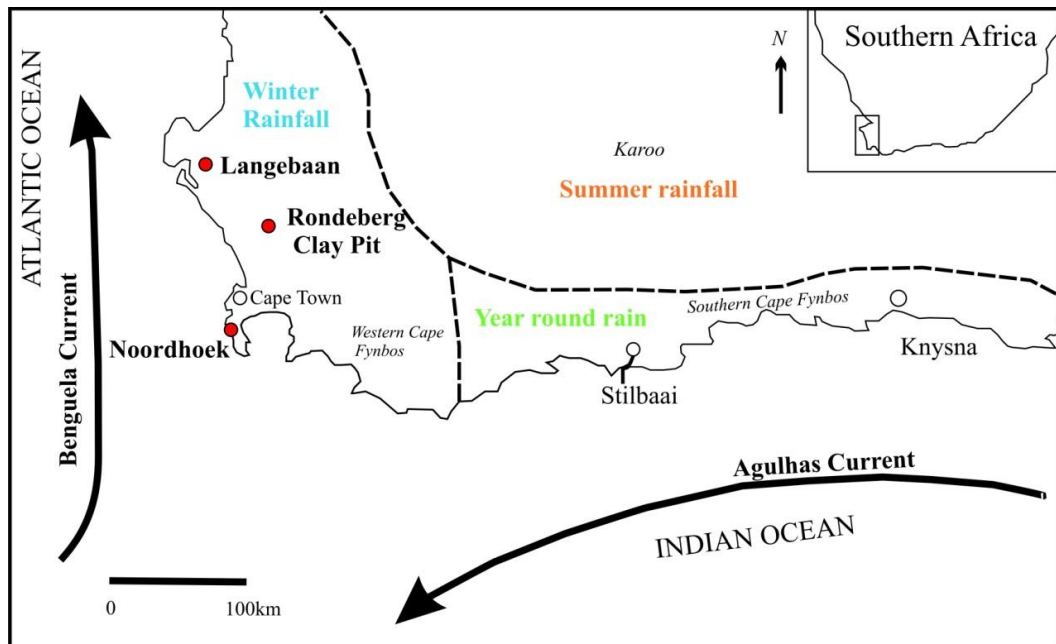


Figure 1.1. The study sites at Langebaanweg, Rondeberg, Noordhoek and Stilbaai in relation to the distribution and division of modern day rainfall along the south-west cape coast, South Africa (modified after Roberts *et al.*, 2009).

Globally, the Late Palaeogene and Neogene were periods of increased global temperatures and precipitation (Spicer, 1993; Tong *et al.*, 2009). Organic-rich sediment and peat accumulation in Southern Africa is specific to time periods of increased humidity and little seasonality (Fig. 1.2; Meadows, 1988). This is augmented by the fact that the South African coastline, on which the study sites lie, is a stable, passive intraplate margin which has not been influenced by volcanic activity nor glacio- hydro-isostatic uplift during the Cenozoic (Roberts *et al.*, 2008; Carr *et al.*, 2010d). Furthermore, low rates of denudation (estimated at less than 2 m/Ma) and uplift have also been established over this time period during which peat accumulation is likely to have been productive (Roberts, pers. comm. 2010). However, in South Africa (and indeed Southern Africa) there are a limited number of occurrences of organic material from the Palaeogene and Neogene. Organic material that may have been deposited was subsequently aerobically degraded due to the aridity of the western coast of southern Africa, created as a result of the establishment of the Benguela Current from the late Oligocene (Killips and Killips, 2005; Carr *et al.*, 2010c).

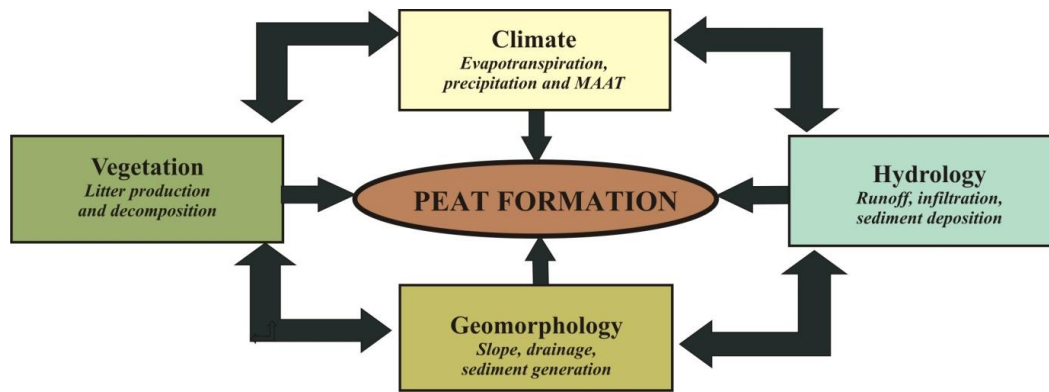


Figure 1.2. Factors influencing the formation and accumulation of peat, MAAT = mean annual air temperature (adapted from Meadows, 1988).

Molecular biomarkers have been used successfully in the interpretation of the continental mean annual temperatures and pH of Miocene sites from the Northern Hemisphere (Donders *et al.*, 2009). The novel application of these methods on organic sediments from South African sites at Langebaanweg, Noordhoek, Rondeberg and Rietvlei (Still Bay) (Fig. 1.1) has great potential to constrain local and regional evolution of palaeoclimate. The results could be compared with research from other Southern Hemisphere continents to trace Gondwanan links and to broaden and integrate palaeoclimate trends. Comparisons with the Northern Hemisphere can then be made in order to attempt to form a global-scale deduction of the dynamic nature of late Tertiary climate. Knowledge of the Southern African and Southern Hemisphere Miocene climate, in which the configuration of the continents and the flora and fauna were similar to modern times, may help in making informed opinions and models as to present climate change. This could potentially be extrapolated towards forming models to predict flora and fauna niche shifts in a changing world.

Currently, the south-western tip of South Africa is characterised by a Mediterranean climate with dry summers and wet winters which was established by the late-Miocene (Goldblatt and Manning, 2002; Cowling *et al.*, 2009). The convergence of the cold Benguela and temperate Agulhas currents, of the Atlantic and Indian Oceans respectively, near the Cape Peninsula exert a powerful influence on climate (Camberlin *et al.*, 2001; Chase and Meadows, 2007). The circumpolar westerly system (westerlies) generate cold fronts from which much of the west Coast's rainfall stems (Fig. 1.3; Carr *et al.*, 2006a; Carr *et al.*, 2006b; Cowling *et al.*, 2009). The boundaries of the regional temperate and sub-tropical atmospheric

circulation systems positions are marked by the winter rainfall zone (WRZ) of the Western Cape coast (Carr *et al.*, 2006a). These systems respond to climatic perturbations on variable timescales and are thought to be driven largely by orbital forcing (Carr *et al.*, 2006a). Annual rainfall in the Western Cape varies between 300 and 2000 mm p.a., with the waning effects of the polar frontal systems decreasing northward (Cowling *et al.*, 2009). The monthly range of temperature is 15 – 24 °C in summer, with mean annual temperatures of ~17 °C for Cape Town, and winter temperatures ranging between 9 °C and 21 °C (Adelana *et al.*, 2010; Hanekom *et al.*, 2009).

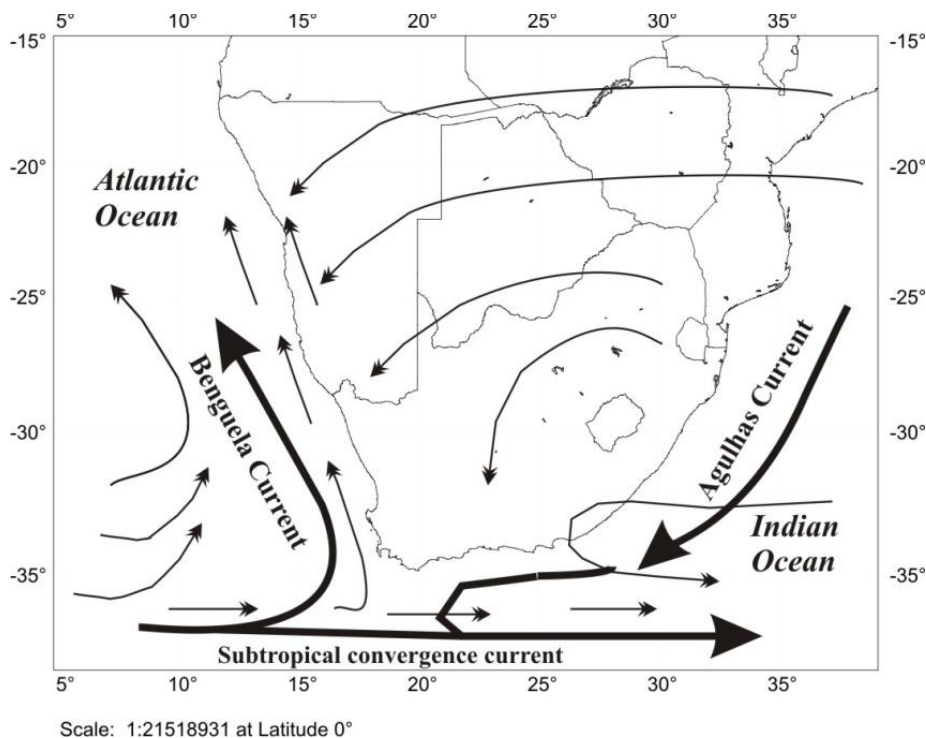


Figure 1.3. Southern African wind patterns and ocean currents. Thin double headed arrows indicate wind patterns; thick arrows indicate ocean currents (Adapted from Chase, 2010).

The south-west coast of South Africa is in the Cape Floristic Region (CFR), so called due to the extraordinarily high species diversity and richness within this 90 000 km² area (Goldblatt and Manning, 2002; Helme and Trinder-Smith, 2006; Cowling *et al.*, 2009). Families represented include Asteraceae, Ericaceae, Proteaceae, Restionaceae, Aizoaceae, Iridaceae, Rutaceae and Orchidaceae which are collectively termed ‘fynbos’ (Goldblatt and Manning, 2002; Helme and Trinder-Smith, 2006). These plants tend to be hardy and able to withstand summer drought, seasonal fires and the poor soils developed from Cape Fold Belt lithologies (Cowling *et al.*, 2009). The modern CFR is thought to have originated during the

early Pliocene through pronounced changes in climatic factors, such as increased seasonality involving a reduction of summer rainfall (Goldblatt and Manning, 2002; Cowling *et al.*, 2009). The Sandveld sub-region of the CFR predominates in the Langebaanweg, Rondeberg and Noordhoek areas and the west coast in general, and is composed predominately of restionaceous vegetation and other genera such as *Olea*, *Stoebe plumose*, *Rhus* and *Chrysanthemoides* (Goldblatt and Manning, 2002).

1.1 Regional geological setting

The study sites are along the south-western coast of South Africa (Fig. 1.4). The sites are of Neogene age, and fall within the Sandveld Group stratigraphy. The Langebaanweg and Noordhoek study sites sit on the coastal plain, with elevations of +50 m and near sea level respectively.

A diverse range of Tertiary sediments, belonging to the Sandveld Group extend from along the south-west coast of South Africa, and sporadically (unconformably) overlie the Malmesbury Group Neoproterozoic metasediments and the Neoproterozoic to Cambrian Cape Granite Suite (Pether *et al.*, 2000; Roberts, 2006a-e; Roberts *et al.*, 2006). These shallow marine, fluvial, lacustrine and aeolian sediments have been deposited during sea-level transgressions and regressions from the Miocene into the Holocene (Roberts, 2006a). The Sandveld group consists of the fluvial Elandsfontyn Formation, marine/estuarine Varswater Formation and the aeolian Prospect Hill, Langebaan, Springfontein, and Witzand Formations (Roberts, 2006c, d, and e). Focus is placed on the Elandsfontyn and Varswater Formations as they have the highest known potential for containing organic-bearing sediments of Miocene age (Fig. 1.5; Cole and Roberts, 1996).

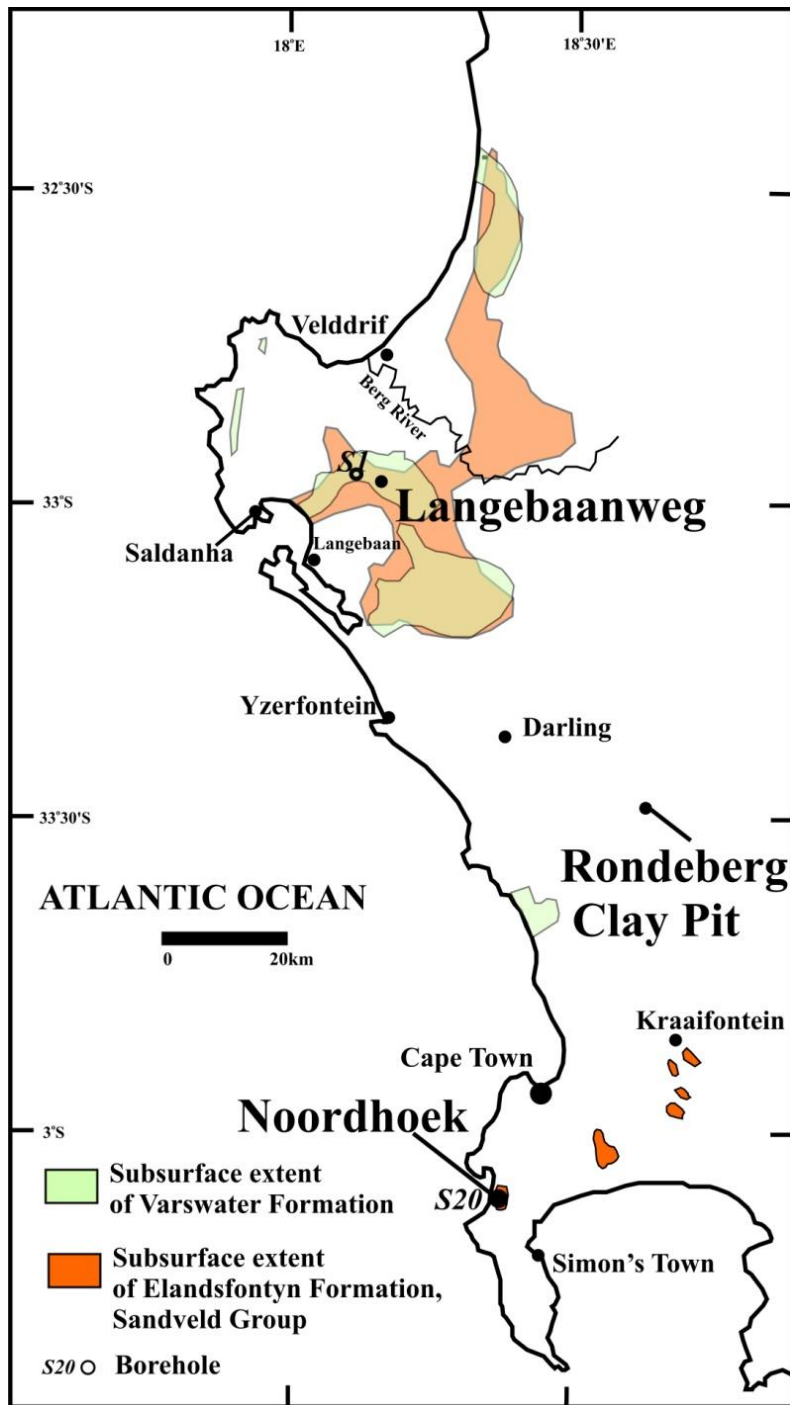


Figure 1.4. Geographic subsurface distribution of the Elandsfontyn and Varswater Formations of the Sandveld Group in the south-western Cape, South Africa (Adapted from Roberts, 2006b). The study sites at Noordhoek, Rondeberg Clay Pit and Langebaanweg are highlighted with respect to the currently known occurrence of subsurface Sandveld Group deposits.

1.1.1 Elandsfontyn Formation, Sandveld Group

Elandsfontyn Formation is the basal formation of the Sandveld Group (Fig. 1.5). Palynologically, the formation has been dated between Early to Middle Miocene on the basis of tropical and subtropical taxa (Coetzee and Rogers, 1982; Roberts, 2006a, b). It is composed of fluvial coarse-grained sands and gravels, in several fining upward sequences, deposited during periods of transgression (Cole and Roberts, 1996; Roberts, 2006b). It unconformably overlies the Cape Granite suite in some areas, and underlies the Pliocene Varswater Formation with an unconformable contact (Roberts, 2006b). It was probably deposited by the meandering palaeo-Berg River (Roberts, 2006b). The formation reaches its maximum thickness of 65 m at Elandsfontyn approximately 20km south of Langebaanweg (Roberts, 2006b).

1.1.2 Varswater Formation

Varswater Formation, named after the Varswater Quarry on Langebaan Road, is a formation of the Sandveld Group and contains four members (Fig. 1.5; Cole and Roberts, 1996; Roberts, 2006c). It conformably overlies on the Miocene Elandsfontyn Formation, and is composed of phosphorised clayey sand, fine to medium grain sand and gravel which were influenced by sea-level changes (Cole and Roberts, 1996). Additionally, lenticular lignite bodies in the Langebaanweg and Yzerfontein areas have been discovered and indicate deposition in coastal-plain peat bogs and lagoonal settings (Cole and Roberts, 1996). The biostratigraphy of this formation, on the basis of both fauna and flora, suggests an early Pliocene age (Hendey, 1981; Coetzee and Rogers, 1982; Coetzee, 1983, 1986; Cole and Roberts, 1996).

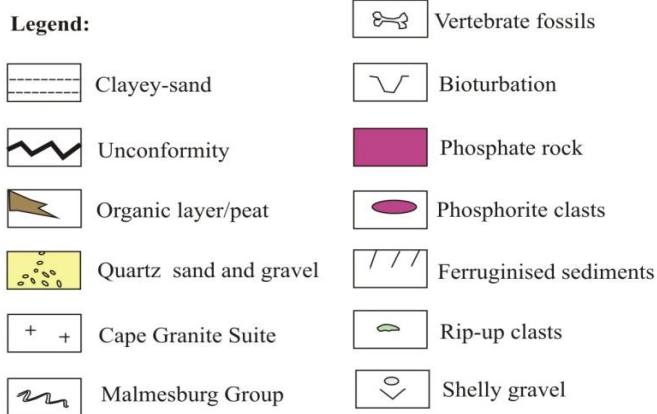
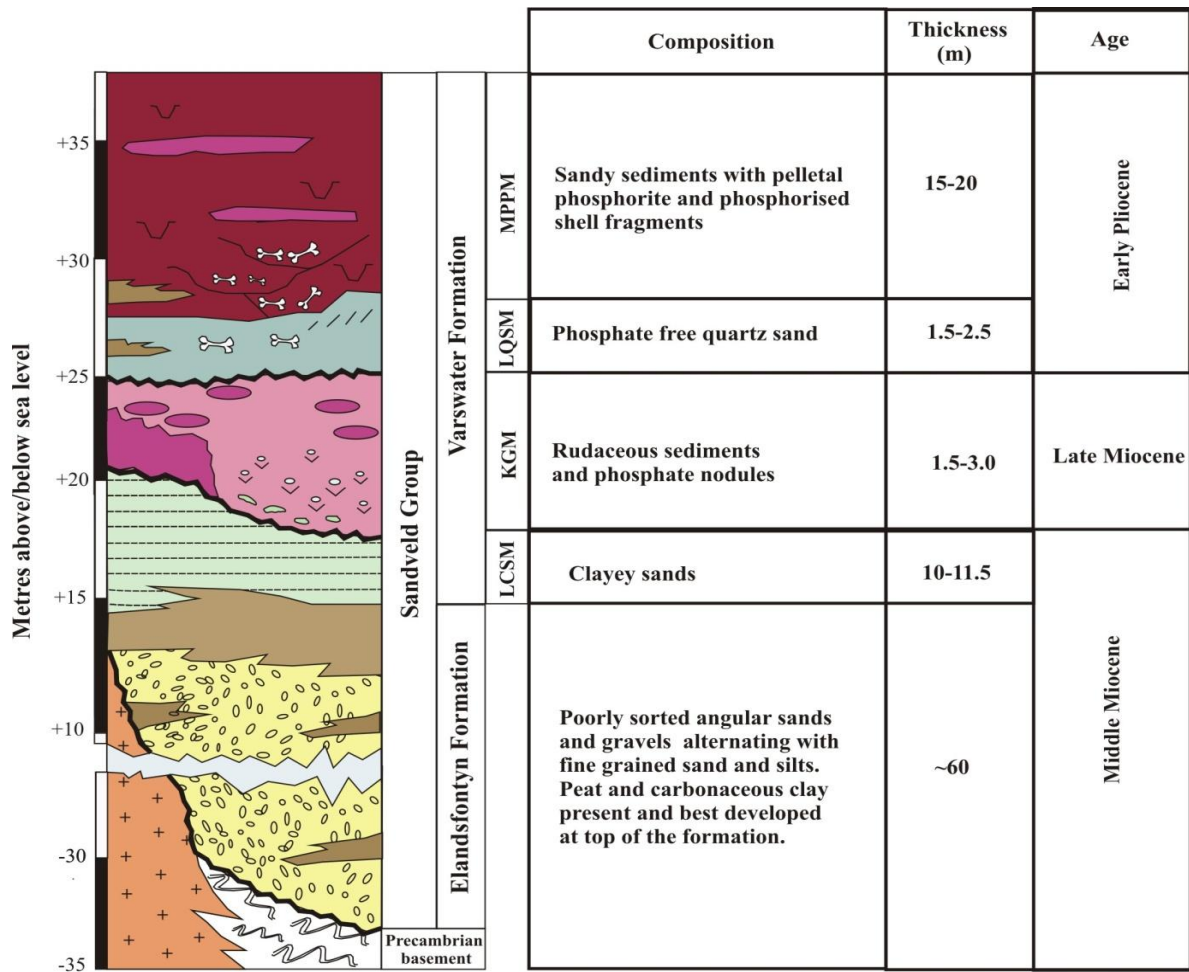


Figure 1.5. Generalised stratigraphic log of the Elandsfontyn and Varswater Formations (Sandveld Group) at Langebaanweg indicating the presence and distribution of peat horizons. Break in stratigraphy indicated by grey zig-zag. Members of the Varswater Formation are as follows: Langeenheid Clayey Sand Member (LCSM); Konings Vlei Gravel Member (KGM); Langeberg Quartz sand member (LQSM); Muishond Fontein Pelletal Phosphorite Member (MPPM) (adapted from Roberts *et al.*, in review).

1.2 Cenozoic climate records

Changes in environmental parameters influencing global and regional climate are based on external and internal forcing mechanisms (Zachos *et al.*, 2001; Maslin and Christensen, 2007). For example, global climate change, specifically its variability and frequency as recorded by geological time, is strongly controlled by Milankovitch cycles (external forcing mechanisms). These create cyclic rhythms in global mean temperatures on 10^6 - 10^7 year and shorter overlapping 10^4 - 10^5 year time periods (Clarke and Crame, 1992; Spicer, 1993; Zachos *et al.*, 2001).

Other external forcing mechanisms influential in climate change are tectonic processes. The African continent occupied a central position in Gondwana during the Jurassic, and was the first continent to break away during the Late Cretaceous (Coetzee, 1978b; Thomson, 1999; Paton, 2006; Uenzelmann-Neben *et al.*, 2007). Consequently an archaic array of flora and fauna are represented in Africa (Coetzee, 1978b; Siesser, 1978; Partridge, 1985). By the Late Oligocene- early Miocene continental positions were nearly similar to present day (Potter and Szatmari, 2009).

Miocene climate change was greatly influenced by tectonic processes which include the rejuvenation of the Alpine–Carpathian–Zagros–Himalayan Mountains and the southwestern ward opening of the East-African rift system (Potter and Szatmari, 2009). Furthermore, the opening of high latitude oceanic gateways and the closing of others at low latitudes (e.g. Tethyan Ocean closure) affected circulation and consequently a steeper meridional temperature gradient formed between the poles and equator (Potter and Szatmari, 2009). Generally, all these tectonic changes were influential in creating modern ocean-atmosphere energy transport, and contributing to the establishment of modern climatic systems (Bice *et al.*, 2000; Miller *et al.*, 2005; Potter and Szatmari, 2009; Hay, 2010).

In the Southern Hemisphere the Oligocene saw the opening of the Drake Passage and Tasmanian Gateway, which were influential in establishing the modern circulation system of the Southern Ocean through the formation of the Circumpolar Antarctic Current (Miller and Fairbanks, 1985; Potter and Szatmari, 2009). Antarctica became completely separated from South America during the Oligocene and progressively moved southwards resulting in its isolation from all other continents (Hendey, 1982; Denton, 1985; Eagles *et al.*, 2006; Gersonde and Censarek, 2006; Uenzelmann-Neben *et al.*, 2007). In so doing it initiated the

formation of the Antarctic Circum-Polar Current which began the glaciation of Antarctica, and changed the circulation of the southern wind system preventing warmer air and water masses reaching higher latitudes (Hendey, 1982; DeConto and Pollard, 2003; Holbourn *et al.*, 2005; Gersonde and Censarek, 2006; Uenzelmann-Neben *et al.*, 2007). The Benguela Upwelling System (BUS) originated through the formation of the Circum-Polar Current, and has been influential in regional and global climate, controlling heat exchange and primary productivity (Fig. 1.3; Christensen and Giraudeau, 2002; Diester-Haass *et al.*, 2001; Diester-Haass *et al.*, 2002; Wigley and Compton, 2006).

BUS flows northwards along the western margin of Southern Africa allowing exchange of heat from the south to north (Fig. 1.3; Christensen and Giraudeau, 2002; Wigley and Compton, 2006). The BUS influences the global carbon budget, and has profound implications on the diversity of vegetation along the western margin of Southern Africa and productivity of the surrounding ocean (Coetzee, 1983; Van Zinderen Bakker and Mercer, 1986; Christensen and Giraudeau, 2002; Wigley and Compton, 2006). It influenced the aridity and vegetation of the western coast and Namib through its establishment and increased upwelling by the late Miocene (Tankard and Rogers, 1978; van Zinderen Bakker and Mercer, 1986; Tyson and Preston-Whyte, 2000).

Cenozoic climate in South Africa has been inferred from previous Cretaceous-Palaeogene pollen assemblages' studies. These studies include: the Cretaceous Arnot Pipe assemblage from Banke farm (Namaqualand) (Kirchheimer, 1934; Scholtz, 1985); Thiergart *et al.*, (1963) Knysna lignites; de Villiers (1997) study of Koingnaas pollen assemblage; as well as various offshore core studies (e.g. McLachlan and Pieterse 1978; Morgan, 1978). Kemp and Harris (1975), Morgan (1978), Coetzee (1978, 1980, 1981, 1983), Coetzee and Rogers (1982), and Coetzee and Muller (1984) have studied various early-late Miocene pollen-bearing sediments from Southern Africa and the south-west coast. Coetzee (1978a, b, 1980, 1981, 1983), Coetzee and Rogers (1982), Coetzee and Muller (1984) have produced extensive works on the Neogene pollen sequences of the South-western Cape in particular. These studies indicate a warm tropical Miocene throughout southern Africa with the presence of gymnosperms and Pteridophytes such as Epheriod, Cycadophytes, Classopollis as well as angiosperms in the early Miocene. Contrastingly, a transitional stage has been recorded in the sediments of the south-west coast of South Africa between the terminal Miocene tropical/sub-tropical woodland and the typical 'modern' fynbos vegetation that has become dominant in

the Cape since the Pliocene (Coetzee, 1978a, b, 1980, 1981, 1983; Coetzee and Rogers, 1982; Coetzee and Muller, 1984; Scott *et al.*, 1997).

1.2.1 The Climate of the Miocene Epoch

The sediments studied in this thesis are largely of Miocene age, and therefore focus is placed on global and regional Miocene climate. Table 1.1 below is a summarised adaptation of Clarke and Crame's (1992) review of the Southern Hemisphere Mio-Pliocene climate. The data is mainly from oceanic research of the Southern Ocean, and little is based on the terrestrial record due to the scarcity of climatic proxies.

Table 1.1. Mio-Pliocene climate of the Southern Hemisphere in comparison to global climate change during these epochs (adapted from Clarke and Crame, 1992).

Agea	Climate	Cause	Authors
Early-early middle Miocene (23-17Ma)	Warm	Substantial increases in both surface and bottom temperatures of Sub-Antarctic waters reflects period of global warming. Neogene temperature maximum at 19.5-17Ma	Shackleton and Kennet, 1975; Kennet, 1986, Miller <i>et al.</i> , 1987
early middle Miocene -late Miocene	cool	Abrupt cooling phase from 17 to 14Ma linked to rapid expansion of East Antarctic ice-sheet (EAIS) and associated cooling of high latitude waters; marked increase in meridional temperature gradients	Shackleton and Kennet, 1975; Kennet, 1986, Miller <i>et al.</i> , 1987
Late Miocene (approx. 11-6.2Ma)	Intermittent cool-warm	General cooling trend initiated in Middle Miocene continues but is punctuated by brief episodes of climatic warming at 10.5Ma, 9-8.5Ma and 7.6-6.6Ma	Kennet, 1986; Kennet and Barker, 1990; Barron <i>et al.</i> , 1991
Lastest Miocene-earliest Pliocene transition (6.2-4.8Ma)	Cool	Moderate to severe cooling of surface waters in mid to high latitudes, development of West Antarctic ice sheet and intensification of oceanic circulation	Kennet, 1977 and 1986; Ciesieski <i>et al.</i> , 1982
Early Pliocene (4.8-3.6Ma)	warm	Another brief warm phase identified by stable isotopes and biogeographic studies, marine temperatures may have been 2-10°C warmer than today	Webb, 1990; Webb and Harwood, 1991
Middle-late plicoene (3.6-2.4Ma)	cool	A periods of sharp climatic cooling and further ice sheet development;however, mid-late Pliocene <i>Nothofagus</i> macrofossils recorded from 85°S	Kennet, 1986; Webb and Harwood, 1991
Late Pliocene – Recent (2.4-0Ma)	Cool	2.4Ma event marks onset of bipolar glaciation	Kennet and Baker (1990); Hodell and Warnke (1991)

Steppuhn *et al.* (2007) established that globally, the climate of the Miocene (23 – 5.3 Ma) was warmer, more humid and punctuated by cooling periods (Table 1.1 and 1.2). In comparison to modern standards, the poles were considerably warmer (Greenland being ice-free; Wolfe, 1985), sea-ice was non-existent and the meridional temperature gradient considerably reduced (Holbourn *et al.*, 2007; Steppuhn *et al.*, 2007; Tong *et al.*, 2009).

Carbon dioxide concentrations are said to have varied considerably between 300 and 600 ppm (Tripathi *et al.*, 2009), as shown by stomatal frequency data obtained by Kürschner *et al.* (2008) and confirmed by other author's e.g. Retallack's (2009) soil carbonate proxy. The last prolonged warming event of the Cenozoic was recorded in the Middle Miocene (Middle Miocene Climatic Optimum; MMCO) between 17 to ~14.7 Ma, with temperatures reaching up to 6 °C warmer than present (Table 1.2; Flower and Kennett, 1994; Holbourn *et al.*, 2007; Donders *et al.*, 2009; Shunk *et al.*, 2009; Tong *et al.*, 2009; Majewski and Bohaty, 2010).

Table 1.2. Comparative results for global surface temperatures and rainfall in the Middle to Late-Miocene, showing variation from modern global temperatures (adapted from Tong *et al.*, 2009).

Scenario model result	Middle Miocene	Late Miocene
Global annual mean surface temperature	+2.2 °C	+3 °C
Global annual mean total precipitation	+45 mm/a	+35 mm/a
Annual mean zonal surface temperature (tropical)	~+2 °C	~+2.5 °C
Annual mean zonal surface temperature (high latitude)	~+4 °C	~+8 °C
Annual mean surface temperature (land)	≥+5 °C	≥+8 °C
Annual mean surface temperature (ocean)	+2 °C to~+3 °C	+2 °C to~+3 °C
Annual mean total precipitation (high latitude)	+100 mm/a	+100 mm/a
Annual mean total precipitation (low latitude)	>+200 mm/a; >-200 mm/a	>200 mm/a; >-200 mm/a

The MMCO lasted for approximately 4 million years (Myr), with 100 - 400 kyr variations (long eccentricity which is regulated by obliquity) in climate parameters, and globally low ice volumes (Fig. 1.6; Holbourn *et al.*, 2007). The transition to late Miocene and early Pliocene climate can be recognised by key climatic signals based on repetitive climate and circulation patterns controlled by orbital variables (Holbourn *et al.*, 2007). These are:

1. Obliquity-influenced global cooling between 14.7 - 13.9 Ma (the Middle Miocene Climatic Transition; MMTO).
2. The present 'icehouse' conditions of 100 kyr variations (after 13.9 Ma; Flower and Kennett, 1994; Derry and France-Lanord, 1996; Holbourn *et al.*, 2007; Majewski and Bohaty, 2010)

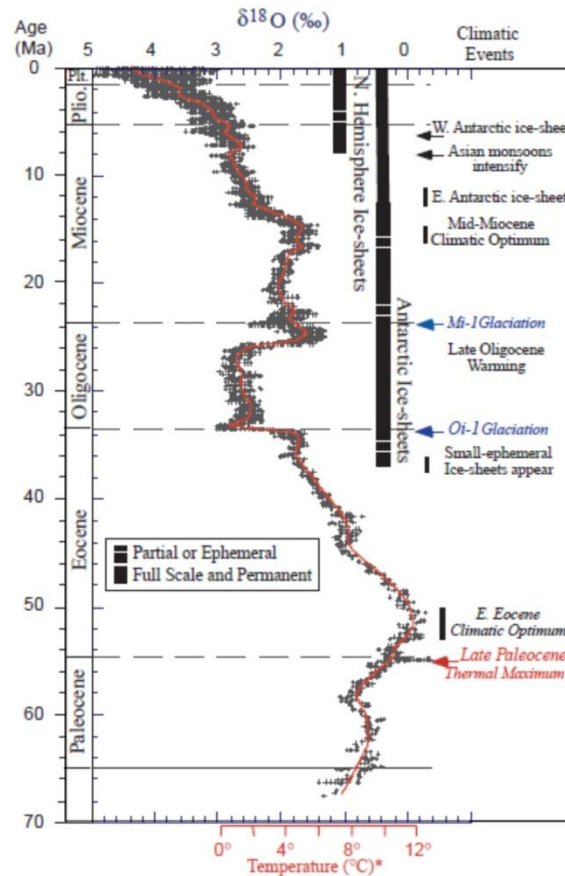


Figure 1.6 Climatic events of the Cenozoic as inferred from the global deep sea benthic foraminiferal record (adapted from Zachos *et al.*, 2001).

The period of cooling, following the MMCO, was a product of the disruption of the global carbon cycle (Flower and Kennett, 1994; Derry and France-Lanord, 1996; Majewski and Bohaty, 2010). This cooling event is highlighted by the Monterey Formation carbonaceous and siliceous marls of the middle Miocene where increased biological sequestering of carbon upset the carbon budget (Monterey hypothesis; Vincent and Berger, 1985; Flower and Kennet, 1993; Spicer, 1993; Derry and France-Lanord, 1996; Holbourn *et al.*, 2007). The Monterey Formation and the mid-Miocene Monterey excursion (17.5 – 13.9 Ma) show a pattern of benthic and planktonic foraminifera $\delta^{18}\text{O}$ and $\delta^{13}\text{C}$ records that covary, and indicate that carbon cycling, East Antarctic Ice Sheet (EAIS) growth and high-latitude deep water production are intimately associated with increased deep water cooling of 4 to 5 °C (Miller *et al.*, 1987; Flower and Kennett, 1993; Flower and Kennett, 1994; Shackleton & Kennet, 1975a, b; Zachos *et al.*, 2001; Westerhold *et al.*, 2005; Holbourn *et al.*, 2007; Majewski and Bohaty, 2010). The drawdown of atmospheric CO_2 through the deposition of these and other contemporaneous carbonaceous sediments, shown by the

positive ocean $\delta^{13}\text{C}$ ‘Monterey’ excursion, resulted in global cooling through positive feedback mechanisms that perpetuated the cycle of cooling (Vincent and Berger, 1985; Flower and Kennet, 1993; Derry and France-Lanord, 1996). Eccentricity forcing has also been described as causative in the increased carbon burial (Holbourn *et al.*, 2007). The positive increase in $\delta^{13}\text{C}$ in middle Miocene and its decline by the late Miocene, with the additional stability in benthic foraminiferal $\delta^{18}\text{O}$ values, thereafter emphasises the climatic constancy between 11 and 5 Ma (Billups *et al.*, 2008).

1.3 Motivation and specific objectives

The West Coast Fossil Park site at Langebaanweg (LBW) and a subsurface Miocene peat deposit at Noordhoek (Fig. 1.1 and 1.4) were targeted as the focus of the research. Two lesser known sites, a Quaternary Rietvlei wetland deposit and the Rondeberg Clay Pit, were also studied primarily for comparative purposes and future research potential. Palynomorphs were studied, where possible, to determine palaeovegetation and palaeoclimate using the basis of nearest living relative principles. A relatively novel organic biogeochemical technique was used to quantify the amount and composition of fossil bacterial tetraethers lipids (branched GDGTs) within the sediments. Based on a proxy developed from this analysis, the mean annual air temperatures and pH of the sediment at the time of its deposition can be calculated. Broad questions asked here are:

1. Does the MAAT-calculated data complement shifts in palaeovegetation inferred from pollen and the sedimentary setting?
2. Do changes in sedimentology have any correlation with changes in palaeovegetation and MAAT calculated?
3. How do these factors inter-relate and what are the internal and external forcing mechanisms of climate change within southern Africa? How do these mechanisms contribute to the observed changes recorded in the sediments?
4. What do the mean annual air temperatures (MAATs) and palaeovegetation tell us about the past climate and their impact on ecosystems?

The specific aim of the Noordhoek and LBW study is to determine new constraints on past climatic conditions from the terrestrial organic record in comparison to the previous studies e.g. Coetzee (1978a, 1978b). Additionally, an attempt is made to define the Coetzee

(1978a, 1978b) pollen zones in a quantitative stratigraphic sense, and relate these zones to changes in the climate as inferred from biogeochemical proxies. Lastly, the study aims to compare and contrast the modern Cape MAAT and Atlantic sea-surface temperatures (SSTs) with proxy-obtained MAAT for the terrestrial sphere and with southern ocean SSTs obtained from other studies (Dupont *et al.*, 2009). This would enable comparison with dated Neogene sites from the Northern Hemisphere. At Langebaanweg (LBW) previous studies focused on the vertebrate fossils of the Varswater Formation, but this study will investigate the older, underlying organic clays of the Elandsfontyn Formation. Thus far, no organic biogeochemical studies of the Noordhoek (Avondrustvlei Farm) and LBW peat deposits or organic-rich material from the south-western Cape has been conducted.

The studies at the Rondeberg Clay Pit (south-western Cape) and the Rietvlei study area (south Cape coast) broadly outline the use of branched tetraether membrane lipids under two different scenarios. The Rondeberg Clay Pit occurs inland and at higher elevation +90m than Noordhoek and Langebaanweg and exposures are excellent in an open pit. The study investigates the preservation of the palynomorphs and branched GDGTs at this site in comparison to relatively pristine core-derived samples. The Rietvlei study site is of Quaternary age and falls into the year-round rainfall zone, and will determine the further potential of the use of branched-GDGTs in younger age sediments. This is due to the numerous Quaternary-aged deposits in South Africa which could have significant potential for molecular biomarker research.

2 Methodology

2.1 Part 1: Techniques in recent and current research

2.1.1 Palaeopalynology

Palaeopalynology is loosely defined as the study of organic microfossils, or palynomorphs (fossil pollen), preserved in sedimentary rocks (Traverse, 1988). Extraction of palynomorphs is based on host rock composition, e.g. hydrofluoric acid treatment for silicate rocks; Faegri and Iversen, 1964; Birks and Gordon, 1985; Traverse, 1988). Identification of fossilised pollen, through the use of pollen reference collections, is often achieved by the comparison of fossil pollen and spores with modern extant specimens of known origin (Birks and Gordon, 1985). The great quantity and superior preservation capability (due to the inert chemical composition of the component sporopollenin and chitin of the exine) of palynomorphs enables them to be used widely (Faegri and Iversen, 1964; Traverse, 1988; Scott and Vogel, 2000). Palynomorphs, thus, have a range of applications in biostratigraphy, geochronology, palaeoecology and palaeoclimatology, in addition to industrial applications, notably the exploration for oil and gas-rich sedimentary units (Traverse, 1988; de Villiers, 1997; Scott and Vogel, 2000).

Palynomorphs are plant reproductive structures such as spores, produced by bryophytes and pteridophytes, and pollen, produced by gymnosperms and angiosperms, which are dislodged from their parent plant and preserved in sediment (Raven, 2001). Classification, therefore, is based on morphological description of the shape, wall sculpting and structure of the individual grains (Faegri and Iversen, 1964).

The inert outer shell of a palynomorph is composed of sporopollenin and termed the pollen wall or exine (Fig. 2.1; Traverse, 1988; Punt *et al.*, 2007). The wall is composed of several layers each of importance in providing differences in morphology between pollen types and consequently plant species (Fig. 2.1; Traverse, 1988). The thickness of the exine, and therefore quantity of sporopollenin contained within the exine, allows for preservation (Faegri and Iversen, 1964; Traverse, 1988; Scott and Vogel, 2000). Preservation is also dependent on the energy and chemistry of the depositional environment, with higher preservation rates obtained in energetically low ('quiet'), acidic, anoxic environments

(Traverse, 1988). Palynomorph preservation is chemically affected by oxidation and carbonization, which destroy the integrity of the exine (Traverse, 1988; Scott and Jones, 1994).

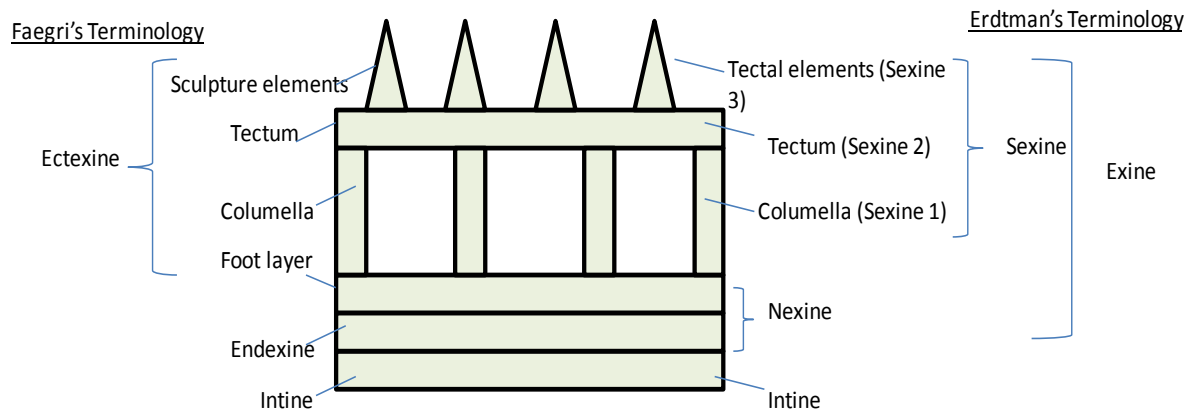
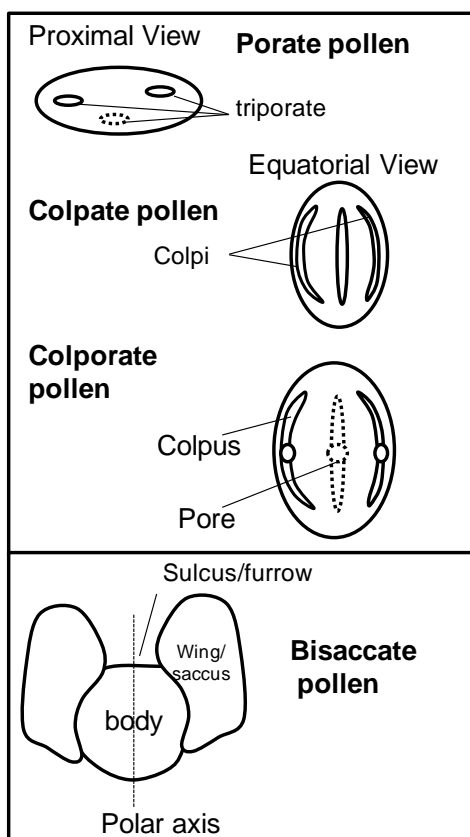


Figure 2.1. Pollen wall terminology. An adaptation of a glossary of terms used for describing structural elements of the pollen wall (adapted from Punt *et al.*, 2007).

The character of the aperture is a diagnostic feature which provides a means for the identification of spores (Fig. 2.2). Spores may also be alete (inaperturate), monolete (one laesurae) or trilete (3 laesurae; Fig. 2.2). Laesurae are the marks created on the spore surface as it developed from the spore mother cell, and are the remains of where it came into contact with the other members of the tetrad (in the case of trilete spores) (Punt *et al.*, 2007).

Pollen can be characterised by their colpi, pores and sacci as well as external sculpturing of the exine (Fig. 2.2). The nature of the sculpting of the exine, in both spores and pollen grains, albeit reticulate sinuous or branched, or echinate, provides the means by which grains can be identified to family if not genus/species level (Erdtman, 1969).

POLLEN MORPHOLOGY



SPORE MORPHOLOGY

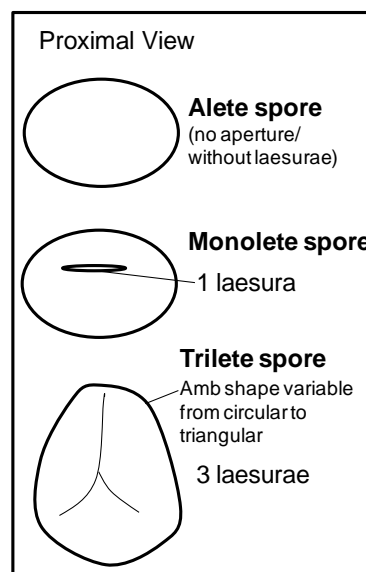


Figure 2.2. Pollen and spore morphology illustrating key terms used in the description of gross shape and features of the grains (adapted from Traverse, 1988 and Punt *et al.*, 2007).

2.1.2 Introduction to organic biogeochemical techniques

Stable isotopes – carbon and nitrogen

The atmosphere contains a ratio of 1.1:98.9 of the heavy stable isotope, ^{13}C , to the light ^{12}C in carbon dioxide (O'Leary, 1981; Schleser *et al.*, 1999; Sharp, 2007). Calculation of this ratio, expressed as $\delta^{13}\text{C}$ in parts per thousand or 'per mil' (‰), is relative to an international standard –the fossil belemnite from the Pee Dee Formation, Upper Cretaceous, U.S.A, denoted 'PDB' (Schleser *et al.*, 1999). Biological sequestering of carbon from the atmosphere slightly favours the light carbon isotope (Schidlowski, 1995; Gröcke, 2002). Plant species kinetically fractionate carbon-isotopes during photosynthesis and respiration due to the specificity of metabolic enzymes (Park and Epstein, 1960; O'Leary, 1981; Schidlowski, 1995; Schleser *et al.*, 1999). During fractionation, and depending on the type of metabolic pathway (C_3 , C_4 or crassulacean acid metabolism - CAM), plants will preferentially take up light carbon over heavy carbon (Park and Epstein, 1960; O'Leary, 1981; Cerling *et al.*, 1997; Schleser *et al.*, 1999). Additionally, with the discovery of the C_4 photosynthetic pathway, it

has been shown that different metabolic pathways sequester light and heavy isotopes in different quantities. C₄ plants have less negative $\delta^{13}\text{C}$ values in comparison to C₃ plants, and acquire a 'heavy' isotope signature (O'Leary, 1981; Sharp, 2007). The range of $\delta^{13}\text{C}$ values for C₄ plants is -10‰ to -14‰, in comparison to C₃ plants where this value is 'lighter' (more negative) with a range between of -22‰ and -30‰ (Cerling *et al.*, 1997; Sharp, 2007). These differences may either be enhanced or depressed depending on the ambient environmental conditions. For example, canopy effects on rainforest vegetation decrease ^{13}C values by as much as 5‰ to 10‰ (van der Merwe and Medina, 1989; van der Merwe and Medina, 1991; Cerling *et al.*, 1997).

Importantly for this research, it is noted that temperate terrestrial plants have an average $\delta^{13}\text{C}$ signature of -26.5‰ (Day, 1996). Furthermore, organic carbon found in sediment is preserved with little variation from the composition of the carbon source during diagenesis (Cerling *et al.*, 1997; Sharp, 2007). Lastly, carbon fractionation is enhanced (providing more negative values) by higher atmospheric concentrations of carbon dioxide (and moderately high MAAT), whereby C₃ plants will thrive over their C₄ counterparts (O'Leary, 1981; Schleser *et al.*, 1999).

Nitrogen isotopes are commonly used in palaeobiology to constrain trophic levels (Sharp, 2007). It has two stable forms, ^{15}N and ^{14}N , in a ratio of 0.37: 99.6 (Thomazo *et al.*, 2009). All N-isotopes measurements are taken against the international standard, air (Sharp, 2007; Thomazo *et al.*, 2009). Fractionation between organic nitrogen, held in nitrogen-fixing plants and soil, and nitrogen gas in the atmosphere is near zero (Meyer, 1997). Hence, soil and N-fixing plants will have $\delta^{15}\text{N}$ close to zero (Sharp, 2007). However, soil $\delta^{15}\text{N}$ -values can range between +2 to +5‰ being enriched in the heavier isotope (Sharp, 2007). There is a close link between carbon- and nitrogen-cycles in soil, with the nitrogen content of a plant (which cannot fix its own nitrogen) being close to that of the soil it grows in (Sharp, 2007). Generally, low $\delta^{15}\text{N}$ relates to soils which have profuse leaf litter (Sharp, 2007). Additionally, there is little differentiation between the $\delta^{15}\text{N}$ of plants and plant material and the $\delta^{15}\text{N}$ value of soil in nitrogen-poor soils (Sharp, 2007). Peats are reported to have a low $\delta^{15}\text{N}$ of $0.8 \pm 1.6\%$, but which can be as high as 6.8‰ (Sharp, 2007). Meyers (1997; 2003) study of nitrogen isotopes from lacustrine environments highlights a variety of methods in which this isotope in conjunction with other organic parameters (total organic carbon, $\text{C}_{\text{org}}/\text{N}_{\text{org}}$ atomic ratios etc.) can be a means to study the behaviour and determine the quality of organic compounds preserved in organic matter (OM).

Biomarkers from core membrane lipids

Biomarkers (molecular fossils) are specific biochemical compounds (i.e. lipids, lignin and pigments), often with organism specific chemical structures (Schouten *et al.*, 2000; Hopmans *et al.*, 2004; Weijers *et al.*, 2006a; Sachs *et al.*, 2007; Weijers *et al.*, 2007a, 2007b). Preservation occurs because molecular fossils are resistant biopolymers, for example plant waxes which are not easily degraded by chemical or microbial action during burial or diagenesis (Schouten *et al.*, 2000; Killops and Killops, 2005; Kim *et al.*, 2006; Weijers *et al.*, 2006a, 2007c). High preservation ability allows these molecular fossils to be used extensively for palaeoenvironmental reconstructions and proxy development (Weijers *et al.*, 2007c).

Resistant biopolymers such as membrane lipids have been recognised as biomarkers due to their ability to record palaeoenvironmental information. Typically in bacteria membrane lipids are composed of di-esters and in archaea of ether lipids; but universally they are acknowledged as molecules consisting of hydrophilic exteriors and hydrophobic interiors which maintain a barrier between an external environment and that of a cell interior (Fig. 2.3; Albers *et al.*, 2000; Schouten *et al.*, 2000; Weijers, 2007).

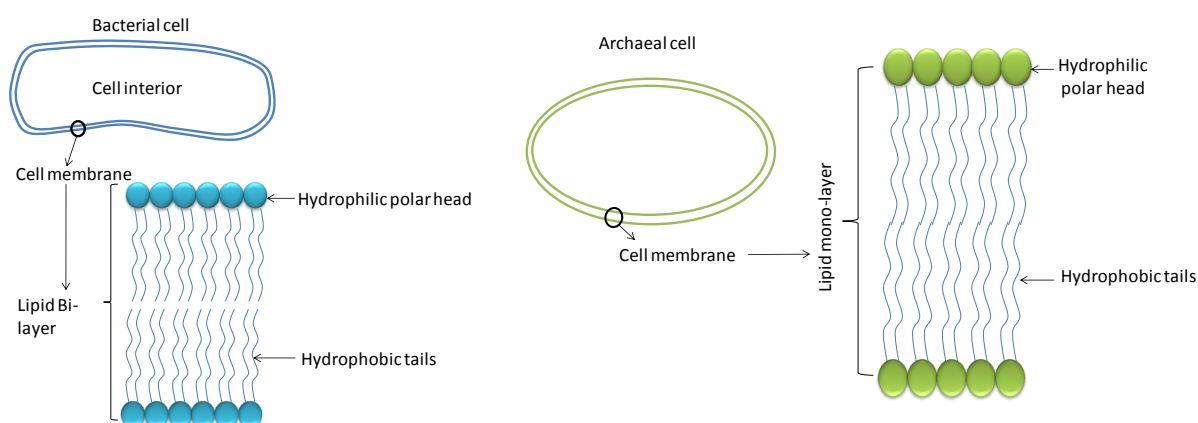


Figure 2.3. Typical bacterial core membrane lipids in comparison to the core membrane lipids recognised as archaeal (adapted from Albers *et al.*, 2000 and Weijers *et al.*, 2007c).

Archaea are typified by their ability to live under conventionally extreme environmental settings, and consequently are important in a variety of applications (Albers *et al.*, 2000; Schouten *et al.*, 2000; Weijers, 2007; Jacquemet *et al.*, 2009). Isoprenoid (straight chain) glycerol dialkyl glycerol tetraethers (GDGTs) are compounds forming archaeal membrane lipids, with the diversity of these structures reflecting different evolutionary pathways from a basal hyperthermophilic ancestor (Schouten *et al.*, 2000). Isoprenoid GDGTs are considered the conventional form of GDGTs (Schouten *et al.*, 2000; Weijers, 2007).

Analyses of isoprenoid GDGTs work on the premise that the distribution of these membrane lipids is correlated with growth temperatures of the Archaea, as these microorganisms adjust the structural and chemical composition of their cell membranes in order to maintain equilibrium with the temperature and pH of their environment (Schouten *et al.*, 2000; Schouten *et al.*, 2007; Jacquemet *et al.*, 2009). Membrane stability, under anoxia and/or a range of extreme temperatures, pressures, salinities, pHs and Ehs, is maintained through the cell membrane mono-layer formed by isoprenoid GDGTs, which is more structurally sound than the lipid bi-layer membrane of typical bacteria and eukarya (Fig. 2.3; Albers *et al.*, 2000; Schouten *et al.*, 2000; Weijers, 2006a).

Branched GDGTs

Branched GDGTs have a non-isoprenoid carbon skeleton with as many as 2 cyclopentyl moieties and 4 - 6 methyl groups (Fig. 2.4; Weijers *et al.*, 2006a; Weijers *et al.*, 2007c). Branched GDGTs are considered to be produced by bacteria (Sinninghe Damsté *et al.*, 2000). Although branched GDGTs are composed of membrane spanning tetraethers, typical of archaea, they have a branched carbon skeleton with the stereo-configuration of the glycerol moieties identical to those synthesised by bacteria and the reverse of those produced by archaea (Sinninghe Damsté *et al.*, 2000; Weijers *et al.*, 2006a; Weijers *et al.*, 2007c). Furthermore, archaea have not yet been found with branched alkyl chains, but thermophilic bacteria have been found to have branched dialkyl glycerol diethers (Sinninghe Damsté *et al.*, 2000; Weijers *et al.*, 2006a; Weijers *et al.*, 2009).

Branched GDGTs were described and identified, using nuclear magnetic resonance (NMR) spectroscopy, by Sinninghe Damsté *et al.* (2000) when studying a Northern Hemisphere Holocene peat deposit (branched GDGTs I - III; Fig. 2.4). They are typically found in lake sediments, soils and peat bogs, as well as being detected and representing the terrestrial sedimentary input in coastal sediments (Fig. 2.4; Hopmans *et al.*, 2004; Weijers *et al.*, 2006a, 2006b; Weijers *et al.*, 2007a, 2007c; Peterse *et al.*, 2009a, 2009b; Weijers *et al.*, 2009; Peterse *et al.*, 2010).

The uncertainty relating to the origin of branched GDGTs is derived from the difficulty in distinguishing with certainty between mixed bacterial and archaeal structures (Weijers, 2006a; Peterse *et al.*, 2009a, b). The branched GDGTs of these unknown bacteria, considered to be an artefact from a thermophilic ancestor, allows for stability of the cell

membrane at the conditions in which they survive (Weijers *et al.*, 2006a; Weijers *et al.*, 2007c; Sinninghe Damsté *et al.* 2008; Weijers *et al.*, 2009). In order to isolate the producer(s) of branched GDGTs, 16S rDNA analyses and membrane lipids were studied from a Swedish bog, with the result that the *Acidobacteria* phylum may contain the original micro-organisms (Weijers *et al.*, 2009).

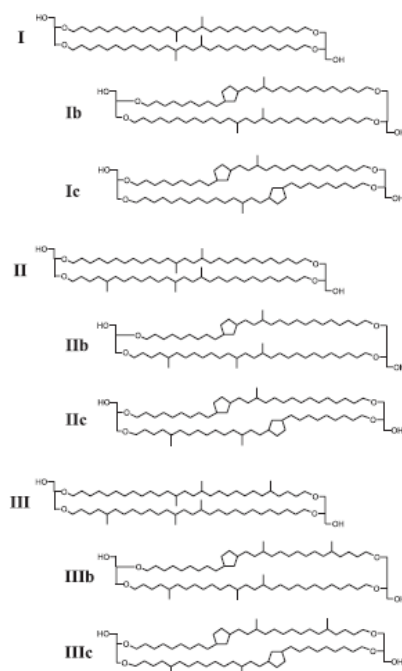


Figure 2.4. Branched GDGTs I – III and their isomers (a, b, c) used in constructing the Methylation index of Branched Tetraethers (MBT), Cyclisation ratio of Branched Tetraethers (CBT) and Branched versus Isoprenoid tetraether Index (BIT) (taken from Weijers *et al.*, 2007a).

Weijers *et al.* (2006a) established that the various branched GDGT lipids differed by two main features; i.e.

1. Number of methyl branches (attached to alkyl chains) and;
2. Number of cyclopentyl moieties.

Bacterial cell membrane composition is known to change relative to the ambient environmental conditions, and it was established that the distribution and abundance of diverse branched GDGTs was strongly controlled by the annual mean air temperature (MAAT) and soil pH (Kim *et al.*, 2006; Weijers *et al.*, 2006a; 2007a, 2007b, 2007c; Sinninghe Damsté *et al.* 2008; Peterse *et al.*, 2009b; Peterse *et al.*, 2009b). The amount of cyclopentyl moieties is related to the pH of the environment at time of deposition, and the

number of additional methyl branches may be related to both pH and temperature (Weijers *et al.*, 2006a). Using this empirical relationship, palaeoenvironmental proxies could be constructed (Weijers *et al.*, 2007a, Weijers *et al.*, 2007b).

2.1.3 Organic geochemical proxies

The MBT/CBT proxy is a molecular proxy constructed for the determination of terrestrial palaeoclimate information. This proxy uses the same principles as that of tetra-ether index (Tex₈₆) with the exception that branched and not isoprenoid GDGTs are used in a terrestrial setting. The TEX₈₆ is a recent organic proxy developed using the distribution of core membrane lipids biosynthesised by Crenarchaeota, a pico-plankton found in marine and lacustrine settings (Schouten *et al.*, 2000; 2002; 2003a; 2003b; Shah *et al.*, 2008; Kim *et al.*, 2009). The TEX₈₆ index, which refers to the 86 carbon atoms in GDGTs, allows for the determinations of sea surface temperatures (SST) from sedimentary rocks (Schouten *et al.*, 2002; 2003a; 2003b).

Hopmans *et al.* (2004) used the occurrence of branched GDGTs in marine sediment to construct the Branched and Isoprenoid Tetraether (BIT) ratio/ index (calculated using equation 1) to distinguish between the relative abundance of terrestrially produced branched GDGTs and isoprenoid marine/lacustrine GDGTs. Hopmans *et al.*, (2004) developed a protocol, using high performance liquid chromatography/ mass spectrometry (HPLC/MS) for the analysis of GDGT core membrane lipids, and allowed for the distinction between the two sources of the GDGT lipids (Hopmans *et al.*, 2004; Weijers *et al.*, 2006a; Weijers *et al.*, 2006b; Weijers *et al.*, 2006c).

As the BIT index is a measure of the amount of terrestrial tetraether lipids versus marine crenarchaeol in sediments, a low BIT index (approximately <0.77) signifies a higher crenarchaeol abundance than terrestrially-derived branched GDGTs (Hopmans *et al.*, 2004). A BIT index of 1 signifies completely terrestrially derived organic matter within a system, whereas a BIT index closer to 0 indicates only crenarchaeol GDGT IV present (Hopmans *et al.*, 2004). This index defines the depositional setting as well as providing validity to the MAAT values, with BIT indices of >0.77 indicative of reliable terrestrial values.

Weijers *et al.* (2007c) relationship between the number of cyclopentyl moieties and methyl groups of the tetraether membrane lipids is related to the soil pH and MAAT, at time of deposition, and allow for two indices to be described. These indices are: (i) Methylation index of Branched Tetraethers (MBT), and (ii) Cyclisation ratio of Branched Tetraethers (CBT) (Weijers *et al.*, 2007a; Weijers *et al.*, 2007b; Weijers *et al.*, 2007c). The CBT index allows for the calculation of soil pH and the MBT index of MAAT and soil pH, with the roman numerals in each equation (2, 3) referring to GDGT structures presented in Figure 2.4. The analytical reproducibility of these indices (0.1 units) allows for a temperature estimate reproducibility of 0.9°C (Weijers *et al.*, 2007b, c).

$$\text{BIT} = [\text{I} + \text{II} + \text{III}] / [\text{I} + \text{II} + \text{III} + \text{IV}] \quad (1)$$

$$\text{MBT} = [\text{I} + \text{Ib} + \text{Ic}] / [\text{I} + \text{Ib} + \text{Ic} + \text{II} + \text{IIb} + \text{IIc} + \text{III} + \text{IIIb} + \text{IIIc}] \quad (2)$$

$$\text{CBT} = -\text{LOG} \left[\frac{([\text{Ib}] + \text{IIb})}{([\text{I}] + [\text{II}])} \right] \quad (3)$$

MAAT is then calculated using these indices within the following calibration equation (Weijers *et al.*, 2007a):

$$\text{MBT} = 0.122 + 0.187 * \text{CBT} + 0.020 * \text{MAAT} \quad (r^2 = 0.77) \quad (4)$$

$$\text{CBT} = 3.33 - 0.38 * \text{pH} \quad (r^2 = 0.70) \quad (5)$$

The total standard error of 5.0 °C is estimated for the calculation (equation 2 and 4) of the MAATs using the transfer function, and the combined error being only 1.3 °C.

Application of the MBT/CBT proxy has been successful in numerous studies of varying geological age and location (e.g. Weijers *et al.*, 2007a; Weijers *et al.*, 2007b; Weijers *et al.*, 2007c; Schouten *et al.*, 2008; Sinninghe Damsté *et al.*, 2008; Peterse *et al.*, 2009a; 2009b). Weijers, *et al.* (2007a) was able to reconstruct the climate over the past 25 000 yrs in tropical Africa through the analysis of sediment taken from the river mouth of the Congo Basin. Additionally, Schouten *et al.* (2008) reconstructed Eocene-Oligocene mean annual temperatures, using sediments from Greenland, with these CBT/MBT MAAT proxy results complimenting the established cooling period at the Eocene-Oligocene boundary.

Sinninghe Damsté *et al.*, (2008) revealed that local soil calibrations may attain higher accuracy in the reconstruction of MAAT than solely through the use of the calibration of

Weijers' *et al.* (2007c) global soil data. Additionally, it was also noted that vegetation may have an effect on the MAAT recorded (Sinninghe Damsté *et al.*, 2008). Tierney and Russell (2009) caution the use of the MBT/CBT proxy in palaeolimnological studies because of the possible *in situ* production of branched GDGTs within lake sediments. Peterse *et al.* (2009b) highlight the importance of differentiating between GDGTs produced by living bacteria and those that are fossilised, such that the depth in the soil profile/lake sediment in which the interaction between living and fossil maybe further constrained (Powers *et al.*, 2004).

2.2 Part 2: Methods and materials followed in current research

2.2.1 Sampling procedure

All material was sub-sampled from drill-cores with one exception, the Rondeberg Clay Pit, in which outcrop was exposed and could be sampled directly. Standard techniques were used to minimise contamination of samples with modern pollen. Hence, in the case of outcrop sampling (Rondeberg) samples were not taken from the surface of each face of the quarry but excavated 5-10cm from the surface of the face. All samples were placed and sealed in aluminium foil and then into labelled plastic bags. Samples from all sites were stored in aluminium foil to minimise contamination with other organic material, such as plastics and skin fats, and then freeze-dried for best preservation of organics (bacterial tetraether membrane lipids) from contamination and deterioration. All samples were described, freeze-dried and powdered in a swing-mill in preparation for palynological, biogeochemical and inorganic geochemical analyses.

Noordhoek Drill Core (34°06'32.20''S 18°22'02.92''E)

Twenty-three samples, approximately 5cm in length, were taken at various peat-rich intervals from a 50 m drill-core. Lithological descriptions of the samples were made (Appendix Table A.1). The uppermost 2.5 m of core (being Quaternary in age) was studied due to the presence of dark colouration and fibrous plant material and for comparison with lowermost peaty units.

A pure-quartz sand unit, which does not contain organic-material, occurs between 2.5 m and 18 m depth below surface. Additionally, many sand 'pockets' are interbedded with the peat and clay-peat units which meant sampling of the organic material was not continuous. Sample intervals varied with the presence or absence of these sandy units, with sample intervals being greater or smaller depending on distance between organic horizons. Two

‘unconformities’ were encountered at 26.5 m and 32.50 m depth below surface which affected the distance at which samples were taken (Fig. 2.5). At these depths there is a locally developed (over intervals of 5 - 10 cm) fine-grained, green coloured, sulphide-rich sandstone (?).

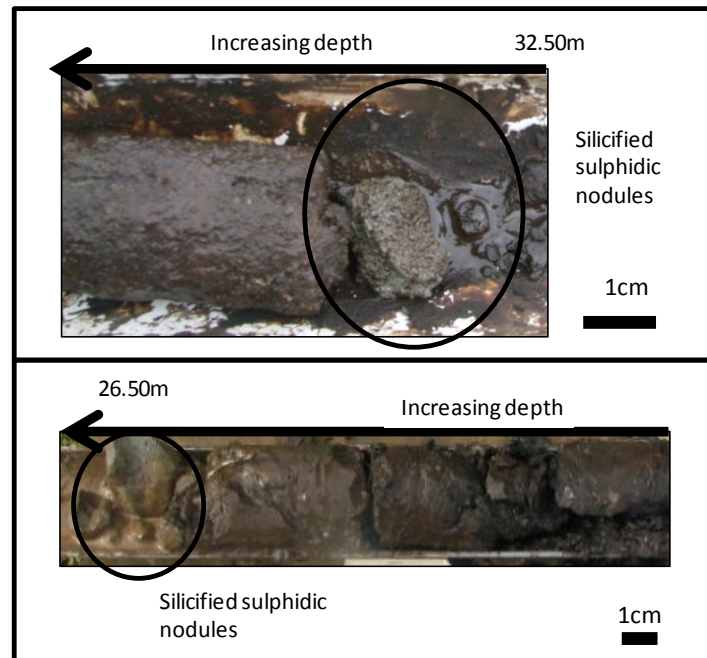


Figure 2.5. Silicified sulphidic green nodules found at 26.50 m and 32.50 m below surface interbedded with dark brown peaty-clay, Noordhoek core.

Langebaanweg drill core (33°10'32.01''S 18°09'59.74''E)

Seven samples were provided for this study from the Bernard Price Institute (B.P.I of the University of the Witwatersrand), where the LBW subsamples from a Council of Geoscience core is kept. Approximately 5 g of sample was taken from a previously sub-sampled core between 17 m and 33 m depth below sea level where organic horizons were prevalent. Lithological descriptions of the samples were made prior to sub-sampling (Table A. 6).

Rondeberg Clay Pit (33°27'04.71''S 18°43'19.03''E)

A total of 26 samples were collected from the Rondeberg clay pit (RCP) (Table A. 8). The outcrop contained 2 thin organic-rich horizons and samples were collected at regular intervals of 20 cm until sample ‘RCP19’ at 6.32 m above sea level, where the sample interval increased to 50 cm. Vertical sampling at 20 cm intervals allowed for the best representation of vertical variation of lithological differences. At 6.32 m a 50 cm sample interval was used

for coarser sand-rich upper portion of section, in light of the nature of the sediment being less likely to contain organic material (pure fine grained sand).

Rietvlei samples (-34.335381 S; 21.461968 E)

Sub-samples (of 5 – 10 g) were obtained solely for the purpose of organic biogeochemical analysis. Sub-samples were obtained by Lynn Quick at the University of Cape Town from the core RVSB-2 taken at Still Bay. This forms part of a larger study of Dr. A. Carr of the University of Leicester, United Kingdom.

2.2.2 Palynology laboratory preparation

Standard palynological extraction techniques were used as outlined by Gray (1965), Traverse (1988) and Erdtman (1969). Material from Noordhoek and Rondeberg Clay Pit were processed for palynomorphs.

Disaggregation and chemical extraction

Noordhoek and RCP samples were washed with distilled water and/or the outer layer is shaved off with a clean sterile knife to remove any contamination. Samples were then crushed into small chips (disaggregation) using a pestle and mortar, and not ground into a fine-powder which can damage palynomorphs and sporomorphs. Powdered weights were recorded, and samples were placed into labelled plastic beakers or test tubes.

As the RCP samples appeared to be more quartz- and clay-rich than the Noordhoek samples a different initial chemical extraction was used. To remove carbonate and silicates the samples were treated with HCl (10%) and HF (48%). Sample treatment with HF varied in time from 1 – 3 hours to 48 hours, and extraction was only considered successful when stirring a sample mixture one could not see any large undigested solids. Samples are then washed with 15 ml 10% hydrochloric acid to precipitate calcium fluoride and this is followed by washing and centrifuging several times with distilled water.

Noordhoek samples were treated with KOH (10%) which was used instead of HF because of the low quartz and clay content of the samples (peat rich). Sample powder and 20 ml KOH (10%) were placed in a glass beaker over a low-temperature hot plate and stirred continuously. Once sample was dissolved it was washed and centrifuged several times with distilled water.

Density Separation

Density separation, due to the disparate specific gravities of the organic material and minerals, was utilised to remove any heavy minerals present. A zinc chloride ($ZnCl_2$) solution with specific gravity of 2 g/cm^3 was used. Palynomorph-containing organic residue collected from density separation process was flushed with distilled water, to remove the zinc chloride prior to mounting.

Slide Mounting

Slide mounting, in glycerol jelly, uses roughly 1 cm^3 of the organic residue collected. All sample preparation was carried out in the Dept. of Plant Sciences, University of the Free State, and slides were labelled and stored in the Geology Department, Rhodes University. Transmitted light microscopy was carried out with a Zeiss light microscope using X250 and X1000 (oil immersion) magnifications for palynomorphs identifications and counts.

Classification and Taxonomy

Palynomorphs were classified as either spores or pollen based on key morphological features. Table 2.1 illustrates the manner in which palynomorphs were described using a modified scheme outlined by de Villiers and Cadman (2001).

Table 2.1. Descriptive classification scheme used to classify pollen and spores

Description	
Spores:	Pollen:
Shape of the amb	Shape of the amb
Number of laesurae	Number of colpi and or pores
Description of Cingulum	Number of pores
Exospore	Exine
Ornamentation	Sculpturing
Dimensions	Dimensions (Diameter/length)

Data was collected by describing and point-counting the different palynomorphs per slide. The quantitative and qualitative descriptions of pollen dimensions (amb shape, height diameter at equator and exine thickness) being of special importance when grains were not able to be identified or were poorly preserved/damaged. Representative specimens were photographed (See Noordhoek pollen catalogue in appendix pages A16 - A33; Table 3.4; Fig.

6.2). The palynomorphs identified were described using the taxonomic classification system erected by de Villiers and Cadman (1997) and using the reference collection of published photos and slides of Tertiary and modern pollen, respectively.

2.2.3 Inorganic geochemistry: Mineral petrology and bulk-rock geochemistry of the Rondeberg Clay Pit

The Rondeberg Clay Pit samples were washed thoroughly and air-dried, contaminated parts of the samples (weathering) were removed and the remnants were milled. The powder obtained was collected, catalogued and placed in glass vials. The fine powder was used for press pellet and fusion disc preparation for X-ray fluorescence (XRF).

Press powder pellets were made through the use of 5 grams of powder from each sample. This was mixed, in a mortar and pestle, with a binding agent (Mowial) until the mowial was even distributed throughout the sample. The mixture was then placed within a cylindrical tube and pressed by hand until compact and forming a circular briquette. Boric acid was then placed into the cylinder over the pressed briquette and this was then compressed at 10 kPa for 1 minute.

Fusion Disc preparation

The procedure followed and techniques used are outlined in Norrish and Hutton (1969).

X-Ray Fluorescence analyses were conducted in the Department of Geology, Rhodes University using a Philips PW 1480 X-ray spectrometer. The XRF technique obtained whole rock chemical composition. The analytical runs were calibrated through the use of in-house standards.

2.2.4 Organic biogeochemistry

Bulk organic carbon and nitrogen isotope analyses of Noordhoek and LBW peats were carried out by Dr. D. Gröcke of the Department of Earth Sciences, Durham University. GDGT-analyses were carried out at the Netherlands Institute for Sea Research (NIOZ), Texel.

GDGT analysis sample preparation and analysis

Freeze-dried and powdered samples (approximately 1 - 2 g of all 23 samples) were extracted with an accelerated solvent extractor (ASE Dionex 2000) using a dichloromethane (DCM):MeOH 9:1 (v/v) solvent mixture in three cycles under conditions of 100°C and 1000 Psi (5 min static, 100% flush, 90 s purge). The extracted solution, after rotary evaporation, was then separated over an activated Al₂O₃ column into an apolar fraction (eluent hexane/DCM, 9:1, v/v), a pure DCM-fraction, a tetraether fraction (eluent DCM/MeOH, 95:5, v/v) and a polar fraction (eluent MeOH/DCM, 1:1, v/v). The apolar and polar fractions of each sample was dried under N₂-gas. The polar fraction, which contained the branched GDGTs, was dissolved in hexane:propanol 99:1 (v/v) mixture to produce a 2 mg ml⁻¹ solution, and placed in an ultrasonic bath. The mixture was then filtered through a 0.45 µm PTFE filter (Alltech) in preparation for High performance liquid chromatography- mass spectrometry (HPLC/MS) analysis. For separation, an Alltech Prevail Cyano column (150 mm × 2.1 mm; 3 µm) was used. Samples were run with a hexane:propanol (99:1, v/v) eluent. An Agilent 1100 series/1100MSD series instrument, equipped with auto-injector and HP Chemstation software was used. A pure crenarchaeol standard was used to prepare a typical standard curve for quantification of the GDGT. Using Hopmans *et al.* (2000) methodology, after samples were run through HPLC/MS, quantification of branched GDGTs was achieved through the comparison and integration of the area of the protonated molecular ion [M+H]⁺ peaks with an isoprenoid GDGT crenarchaeol external standard of known quantity (Huguet *et al.*, 2006).

Isotope preparation and analysis

Sample preparation required all samples to be placed in 10% HCl for 2 hours, with intermittent stirring to ensure all carbonate materials were removed. The samples were then freeze-dried and 5 to 10 mg of sample was used for isotopic analyses.

A Costech Elemental Analyser (ECS 4010) coupled to ThermoFinnigan Delta V Advantage was used for all stable-isotope measurements. The contribution of ¹⁷O in carbon-isotope ratios was corrected (Craig, 1957). The accuracy of data was monitored through analyses of in-house standards which are calibrated against international standards (e.g., USGS 40, USGS 24, IAEA 600, IAEA N1, IAEA N2). Analytical uncertainty for δ¹³C_{org} and δ¹⁵N_{tot} measurements is typically <0.2‰ on replicate sample analysis, and ±0.1‰ for replicate analyses of the international standards. Total organic carbon (TOC) and total

nitrogen (TN) data was obtained as part of the isotopic analysis using an internal standard (i.e., Glutamic Acid, 40.82% C and 9.52% N).

Calculation of carbon and nitrogen isotopes, expressed as $\delta^{13}\text{C}$ and as $\delta^{15}\text{N}$ respectively in parts per thousand or 'per mil' (‰), is relative to an international standard (Sharp, 2007). Organic matter carbon and nitrogen isotope values are reported as a ratio of the samples relative to the standard, thus:

$$\delta = [(R_{\text{samples}} - R_{\text{standard}}) / R_{\text{standard}}] * 1000$$

Where:

R_{samples} = ration of heavy to light isotope (e.g. $^{13}\text{C}/^{12}\text{C}$) of the organic matter

R_{standard} = ratio of heavy to light isotope in the standard (e.g. for carbon the PDB standard).

3 Investigation of organic-rich sediments from Noordhoek, South Africa

3.1 Introduction

Studies and reconstructions of the terrestrial Miocene palaeoenvironment in South Africa are infrequent and unrefined (Coetzee, 1983). The majority of the biogeochemical and palynological research focuses on Upper Pliocene and Quaternary-aged sites (Scott *et al.*, 1997). Palaeogene and Neogene palynological reference materials with reliable age-constraints are scarce. Many of the palynomorphs studied are of uncertain affinity as parent taxa are unknown and are most likely extinct, making it difficult to assign these palynomorphs to family or genus-level (Scott, pers. comm.). This reduces the degree of understanding as to their ecological and environmental significance (Scott, pers. comm.).

This chapter investigates samples taken from the Noordhoek area on the Farm Avondrustvlei (Fig. 3.1) on the western margin of the Cape peninsula. The significance of the new Noordhoek ‘Avondrustvlei’ core is twofold. Firstly palynomorphs obtained can be used for comparison purposes with previous palynological work accomplished by J.A. Coetzee (1978a, b). Secondly, it provides a relatively complete record of changes in the regional terrestrial climate over a large time range from the Miocene. Samples are organic-rich with abundant cellulose fibers and were immediately processed from the fresh drill core. This meant that the material had not been significantly degraded by any processes during storage making it extremely valuable for biogeochemical studies, and preparation for use in the terrestrial palaeotemperature proxy of Weijers *et al.* (2007c).

3.2 Regional geological setting and site description

The Noordhoek site lies in a fault-controlled low altitude area (<10 m above mean sea level) parallel to and roughly 2 km inland from the coast (Fig. 3.1; Roberts and Brink, 2002). The regional geology of this area and data from a previous borehole (S20) study suggest that this deposit is Neogene (~Miocene) in age (Coetzee, 1978a, b).

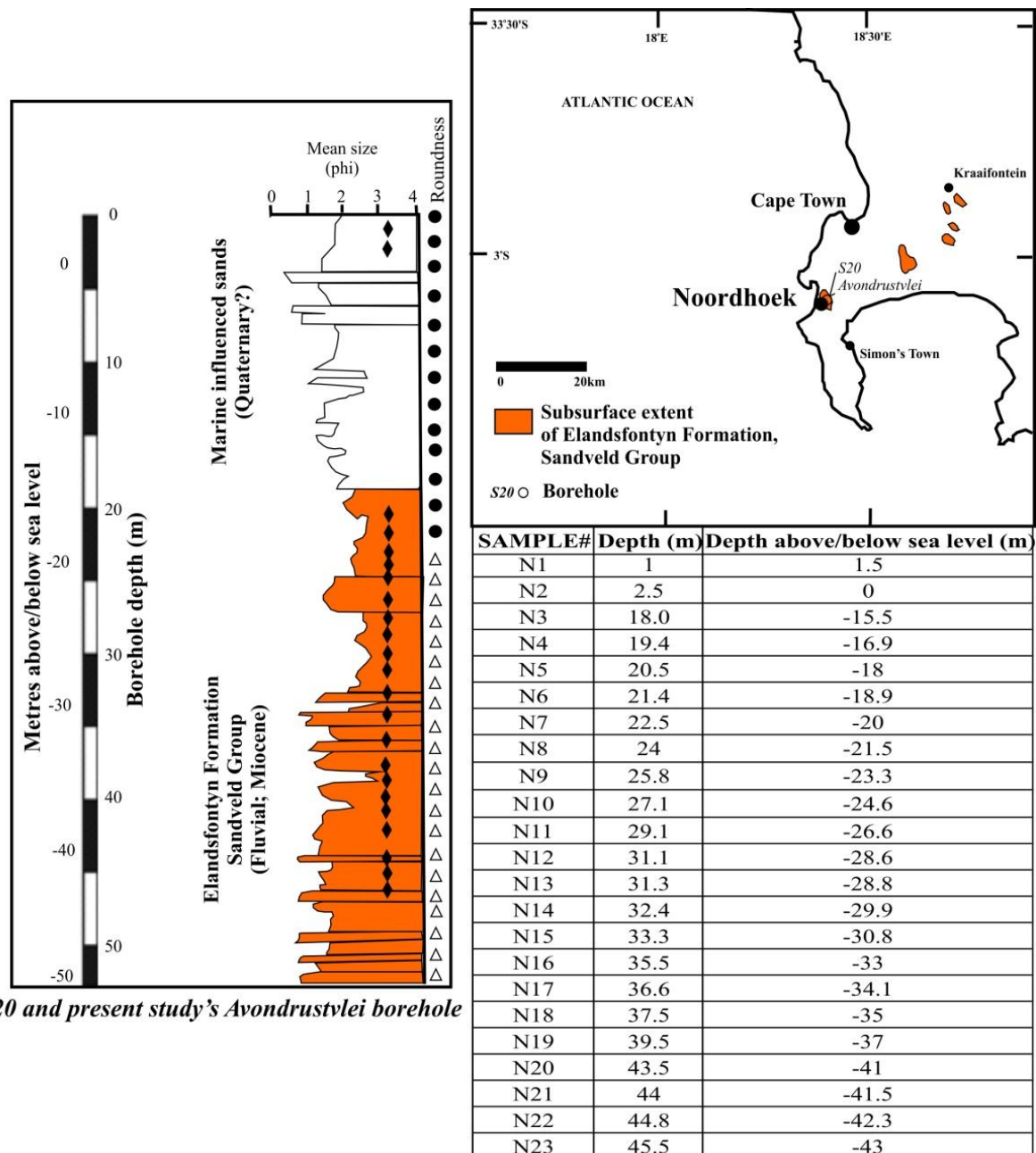


Figure 3.1. The borehole and locality map of the Noordhoek study site with emphasis on the subsurface extent of the Elandsfontyn Formation (indicated in orange). The locality map showing the Cape Peninsula indicates the sites of the 2 Noordhoek boreholes (S20 and the present study's Avondrustvlei borehole). The log shows the lithology present subsurface (orange indicating Elandsfontyn Formation) as logged from the S20 core (Rogers, 1982) and the currently studied Avondrustvlei core. The table provides sample numbers and sample depths for the current study. Samples are denoted on the log by a black diamond symbol. Rounding of grains is denoted by triangles (poorly) and circles (well-rounded) on right-hand side of the log.

Generally, the Elandsfontyn Formation comprises several upward-fining fluvial sequences each having been deposited during transgressive events when sea-level rose above present levels (Siesser and Dingle, 1981; Cole and Roberts, 1996; Roberts, 2006b). During

these periods rivers would aggrade, dumping coarse bedload and immature channel-fill clastics in fining upward sequences. The uppermost of these fining upward cycles consists of mud, clay and organic-rich overbank swamp deposits which are of interest for palaeoclimatic studies (Roberts, 2006b). There were three main transgressive events during the Late Miocene interrupting the overall global cooling trend of the Cenozoic, where sea levels dropped as global cooling brought about several pulses of Antarctic glaciation (Roberts *et al.*, 2006). Evidence of these time periods may likely be captured in the Elandsfontyn Formation's overbank fines deposits. Partridge and Maud's (1987) Post African erosion cycles I and II, in the early and late Miocene respectively, associated with the uplift events cause by plume activity would have led to the rejuvenation of many river systems. However, as there is not significant quantitative information to validate these events sea level has been considered the main driving force of Elandsfontyn Formation deposition.

3.3 Previous research in the Noordhoek area

Preceding studies of the Elandsfontyn Formation at Noordhoek have focused on sedimentological and palynological descriptions of an earlier core (assigned 'S20'; Fig.3.2; Coetzee, 1978a, b; Rogers, 1982). This core, drilled approximately 3m away from the new core obtained for this study, provided initial insight into the vegetation and climatic conditions of the south-west coast during the Neogene. The age formerly suggested for the sediments of the S20 core according to Coetzee's (1978a, b; 1983) palynological work is Early/Middle Miocene to Pliocene (Coetzee and Rogers, 1982; Roberts, 2006a, b, c).

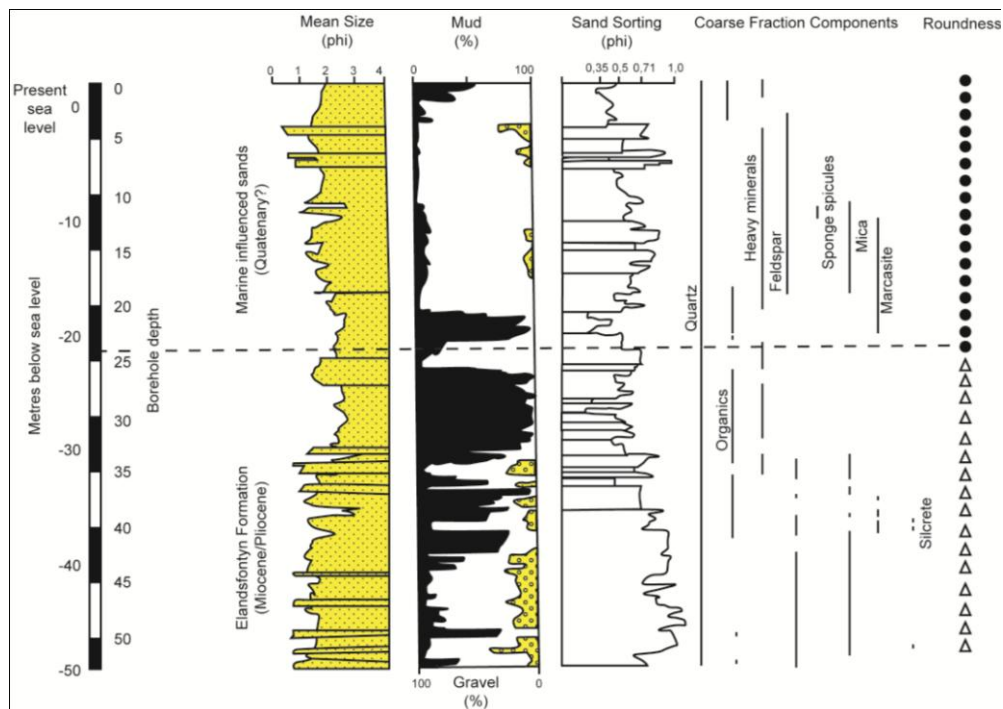


Figure 3.2. Borehole log of the S.20 borehole previously drilled at Noordhoek and which lies approximately 3m from current Avondrustvlei core of this study (adapted from Rogers, 1982).

3.3.1 Palynological studies

Prior to the drilling of the S20 core, Coetzee (1978a) conducted a pilot study of the ‘O’-borehole at Noordhoek, from which 14 samples were taken between the depths of 0.76 m and 33.4 m (Coetzee, 1978a, 1978b). Later the 50m S20 drill core (Rogers, 1982) was studied to supplement the original work (Coetzee, 1978a, 1978b; Coetzee, 1983; Coetzee *et al.*, 1983; Coetzee and Muller, 1984; Coetzee and Praglowski, 1984). Pollen identifications were done via morphological features (Coetzee, 1978a) with comparisons to other literature from Tertiary sites in Australia, New Zealand and Europe (Coetzee, 1978a). The study of several Cenozoic (Mio-Pliocene) ages sites (e.g. Noordhoek, Cape Flats, Mamre, Saldanha; Coetzee, 1978a) around the south-west Cape, intended for stratigraphic correlation, led to the establishment of pollen zones.

Comparisons of Coetzee’s S20 and S1 boreholes at Noordhoek and Langebaanweg, in terms of sedimentology and pollen, allowed for a more specific age-constraint (of early – to late Miocene) of the Noordhoek peat between 21 m and 50 m depth to be assigned (Coetzee and Rogers, 1982; Coetzee and Praglowski, 1984). The age-date of late Miocene was ascribed to palynomorphs from the Elandsfontyn Formation in the S1 borehole, as

constrained by their association with the overlying intensely studied early-Pliocene (~5 Ma) fauna of the Varswater Formation (Coetzee and Muller, 1984; Coetzee and Praglowski, 1984). Reaffirmation of these Langebaanweg Varswater Formation faunal dates was based on comparative analysis of local W. Cape sea-level fluctuations (from coastal and continental shelf deposits) with global Tertiary sea-level (Franz-Odendaal *et al.*, 2002). The comparison of the Elandsfontyn Formation pollen in the S1 and S20 boreholes established an earlier middle Miocene age for the latter (Coetzee and Praglowski, 1984).

Tropical vegetation, coniferous forest and swamp elements were evident in the original S20 core from Noordhoek (Coetzee, 1978a). The distinct alternating successions of these vegetation types, i.e. between the dominance of palm species, indicating a decidedly tropical climate, and coniferous forest and swamp elements with the abundance of temperate Restionaceae and the now extinct *Algaoreidia qualumis* Partridge (resembling that from Australia; Coetzee, 1978a, b), allowed for patterns and zones to be established; with biological tolerances of each taxa playing a vital role in their distribution (Table 3.1).

Noordhoek pollen records indicated that the now common Asteraceae pollen is sparse in the upper parts of the core, and completely absent in the lower part (Coetzee, 1983). The *Clavatipollenites/Ascarina* complex, ancient angiosperm, is well represented from 32.4m to 45 m in depth, and rarely present above this depth in the S20 core (Coetzee, 1983). The 'older' parts of the core, below 21 m depth, show distinct assemblages of pollen types, typically with the presence of *Ascarina*, Winteraceae, Podocarpaceae, *Microcachrys*, Sarcolaenaceae, *Sparganiaceapollenites*, *Cupaniopsis*, *Casuarina/Myrica* and Palmae (Table 3.1) (Coetzee, 1978a, b, 1983).

The extinction of certain subtropical elements by the early Pliocene and the appearance of plant pollen taxa typifying this epoch (such as fynbos floras) is established from the younger Saldanha assemblages, and other Southern hemisphere sites (Lakhanpal, 1970; Schalke, 1973; Kemp and Harris, 1975; Markgraf *et al.*, 1995). Fynbos elements (e.g. Proteaceae), however, were present throughout the Tertiary period in the Noordhoek and Saldanha regions with fluctuating abundance (Coetzee, 1983).

Table 3.1. Forest taxa emphasised by Coetzee (1983) as recorded during the Tertiary from the Noordhoek site, with ‘extinct’ referring to those species absent in Africa. Climatic tolerances and soil preferences (where known) have been obtained from modern species and nearest living relatives relationships. Soil preferences and climatic tolerances taken from Coetzee (1983), Coetzee and Muller (1984), Jiménez-Moreno *et al.*, (2005), Jiménez-Moreno and Suc, (2007); Lovett *et al.*, (2007), Orwa *et al.*, (2009), Jiménez-Moreno *et al.*, (2010).

<i>Plant Family/genus (if known from nearest living relatives)</i>	<i>Climatic tolerances</i>	<i>Soil preferences</i>
• <i>Podocarpus</i> spp (Podocarpaceae)	Temperate	Acidic soils
• <i>Microcachryidites</i> sp. Cf. <i>M. antarcticus</i> (Podocarpaceae, extinct)	Temperate	Acidic soils
• <i>Widdringtonia</i> (Cupressaceae)	Temperate	Acidic soils
• <i>Cupanieidites</i> sp. Cf. <i>C. Orththeichus</i> (Sapidaceae, Cupanieae, tropical to subtropical)	Subtropical	Acidic soils
• <i>Haloragacidites</i> sp. Cf. <i>H. Harrisii</i> (Casuarinaceae, extinct)	Temperate Drought intolerant	
• Myricaceae	Temperate Drought intolerant	
• <i>Echiperiporites</i>	Tropical (?)	
• <i>Croton</i> sp. (Euphorbiaceae, tropical)	Tropical	
• Palmae (locally extinct)	Tropical	Cannot tolerate water logging
• Myrtaceae	Tropical Some may be drought tolerant	
• <i>Alchornea</i> sp. (<i>Psilatricolporites operculatus</i> , Euphorbiaceae)	Tropical	
• <i>Rauvolfia</i> sp. (<i>Margocolporites rauvolfii</i> , Apocynaceae, tropical)	Tropical	
• <i>Cunonia</i> sp. (Cunoniaceae)	Tropical	
• Sapotaceae	Tropical Drought intolerant	
• Combretaceae/Melastomataceae-type	Tropical	

3.3.2 Pollen Zones “L and M”

Palynologically, the Noordhoek sequence shows some strong similarities with New Zealand Neogene floras (Coetzee, 1978b; Markgraf *et al.*, 1995). However, in comparison to palaeoflora patterns described by Germeraad *et al.* (1968), Coetzee’s (1978a) palynological

investigations erected new Southern Africa zonations (Zones M and L; Fig. 3.2) based on several south-west Cape Mio-Pliocene deposits (Saldanha, Noordhoek, Cape Flats, Mamre). Although assigning pollen zones to south-west coast Mio-Pliocene sediments Coetzee (1978a, b) does not provide averaged depth measurements for the position of these zones within the Sandveld stratigraphy. There is no report on whether there were any distinctions between lithologies of these zones, or any key geological features (Coetzee, 1978 a, b). Zone L refers to samples at deeper stratigraphic levels, and therefore of greater age, while Zone M refers to stratigraphically higher, younger samples (likely of Quaternary age; Coetzee, 1978a, b).

A characteristic of the uppermost pollen zone (Pollen Zone M; Table 3.2) is the dominance of fynbos elements which presently occur in the region of this study. Pollen types typifying this zone are Proteaceae, Restionaceae, Rutaceae, Ericaceae, Cyperaceae, various Compositae, *Cliffortia* and *Passerina* (Coetzee, 1978b).

Conversely, Pollen Zone L is defined by an increase in the abundance of sporomorphs which are now extinct in the Cape. The type locality for Pollen Zone L is the Noordhoek O-borehole as there are noticeable differences in specific pollen abundances which can be used for stratigraphic and palaeoecological purposes (Coetzee, 1978a, b). These samples capture a depth between 0.76 m and 33 m. The precise presence/absence of many palynomorph families allowed for the subdivision of Zone L into 7 subzones (Table 3.3). There are no photomicrographs or morphological descriptions of K36-monosulate or any of the other morphotypes mentioned by Coetzee's work for comparison purposes.

3.4 Methodology

Methods used are outlined in Sections 2.2.1, 2.2.2 and 2.2.4.

Table 3.2. Coetzee (1978a, b) division of south-western Cape palynomorphs into Zones M and L, with further subdivision of Zone L into 7 subzones based on the appearance of key indicator palynomorphs. This table was based on Coetzee's work conducted at Noordhoek as well as several south-western Cape sites (Langebaan, False Bay, Cape Flats, Mamre, and Saldanha).

Pollen zone	Vegetation	Abundance of pollen (%)	Climate	Suggested stratigraphy	
M	Present macchia	Ericaceae: 30-37%	Present	Quaternary	
Lvii	First strong development of macchia	Last appearance of palm pollen	Colder drier	C E N O Z O I C	Pliocene
Lvi	Forest: Coniferae Casuarinaceae Cupaniidites	Podocarp (1-9%) Casuarineaceae (40%)	Cool wet		Late Miocene
Lv	Palmae	Palms: 34%	Subtropical, tropical		Middle Miocene
Liv	Restionaceae swamp	Podocarp: \pm 20%	?temperate, locally wet		Early Miocene
Liii	Forest: Coniferae, first Compositae		Cool wet		
Lii	Palmae	Palms (32%) (Podocaps: 1-9%)	Subtropical, tropical		
Li	Forest coniferae	Podocarp \pm 20%	Cool wet		Late Oligocene

Table 3.3. Subzones Li to Lvii of Zone L with key indicator palynomorphs noted by Coetzee (1978a, b). K36monosulcate, K35-colpate, K53-3 refer to unidentified palynomorphs for which there are no literature, descriptions or photographs.

Pollen subzone	Dominant Palynomorphs and sporomorphs
Lvii	macchia pollen types with the presence of K36-monosulcate and <i>Triorites</i> pollen
Lvi	<i>Triorites</i> , <i>Aglaoreidia</i> and <i>Microcachrydites</i>
Lv	K36-monosulcate, <i>Tricolpites pilatus</i> , K35-colpate echinate with the presence of <i>Clavatipollenites</i> .
Liv	<i>Tricolpites pilatus</i> , K53-3-colpate echinate with the presence of <i>Clavatipollenites</i> .
Liii	<i>Aglaoreidia</i> and <i>Podocarpus</i> .
Lii	K36-monosulcate
Li	<i>Tricolpites Pilatus</i> and <i>Podocarpus</i> .

3.5 Results

The Noordhoek Avondrustvlei samples of this study are fine grained, clay-rich (80%), homogeneous and contain dark brown fibrous material. Sections of the core below 20.5 m held macroscopic woody-fibrous material ranging in size from <1 cm to 3 cm in length. The uppermost samples at 1 m and 2.5 m depth below surface were composed of fine grained sand and organic matter in form of fibrous material. The sand unit between 2.5 m depth and 17 m depth below surface was not studied as it was liable not to contain organic material.

The core intersects at approximately ~18 m to 50 m below the surface the Miocene Elandsfontyn Formation, Sandveld Group (Fig. 3.1, 3.2). The core contains massive peat layers, interbedded with fine- to medium-grained, subrounded pure quartz sands which became progressively more poorly-sorted and angular with depth (>~21 m). The peat horizons extend over an interval roughly 30 metres in depth.

3.5.1 Palynological results: Qualitative and quantitative analyses

Pollen counts were made of up to ~300 pollen grains per slide, for the most part, with some samples yielding better (>300) and poorer (<200) results. All percentages are expressed as total numbers of pollen grains and spores with stratigraphic depth.

All palynomorphs were described based on distinct morphological features (shape, size, exine thickness, texture etc.; Table 2.1) and each spore/pollen type was related to modern taxonomic assemblages where possible and its environmental tolerances (Tables 3.4 and 3.5). Commonly occurring taxa (>1%) are presented in Table 3.6. Age-diagnostic taxa and all morphotypes are presented in the Noordhoek pollen catalogue (Appendix pages A17-A34).

Figure 3.3 indicates the variety of pollen morphological types that are represented in the entire core. The relative abundances of morphological pollen types which exceed 1% of the total pollen count (which excludes unknown colpates, algae and *incertae sedis*) are presented in Table 3.6. The variation of palynomorphs with stratigraphic depth and mean annual air temperature (MAAT), calculated using the MBT/CBT proxy, are indicated in the pollen diagrams (Fig. 3.4 A-C).

Table 3.4. Selected photomicrographs of palynomorphs which represent tropical (1, 2, 3, 7, 9, 10) temperate (4, 5, 6, 8) and wet (9, 10) environments from the Noordhoek Avondrustvlei drill core. All specimens were photographed under a transmitted light microscope. Each specimen is represented by a sample number (1-15), name, ecological tolerances and depth of occurrence. Scale bar = 10µm.

Name assigned	Habitat	Depth of occurrence
(1) Pteridaceae, <i>Pellaea</i> -type	moist and rocky habitat	18 m – 40 m.
(2) Polypodiaceae, <i>Polypodiisporites</i> sp. A	moist habitat	18 m – 40 m.
(3) Arecaceae/Palmae ‘Large palm’	tropical to subtropical	18 m – 40 m
(4) <i>Podocarpidites</i> sp.	subtropical to temperate	18 m – 40 m
(5) Myrtaceae, <i>Myrtaceidites parvus</i> Cookson and Pike 1954	subtropical subcanopy vegetation	18 m – 40 m
(6) Restionaceae	temperate	1-2.5 m and 18 m – 40 m
(7) Oleaceae, <i>Olea</i> -type	Warm temperate to tropical but requires being near water (riparian flora), predominating flora in montane forests in Africa	18 m – 40 m
(8) Rosaceae, <i>Cliffortia</i> spp.		
(9) <i>Myrica/Casuarina</i>	tropical, can grow in acidic peat bogs, drought intolerant, symbiosis with N-fixing bacteria in roots	1 - 2.5m (<i>Myrica</i> only); 18 m – 40 m (<i>Casuarina</i> and/or <i>Myrica</i>)
(10) Sapotaceae	Riverine forest; drought intolerant	29 m
(11) Compositae, Tubuliflorae group.		18 m – 40 m
(12) Chloranthaceae, <i>Clavatipollenites-Ascarina</i> complex		18 m – 40 m
(13) Sarcolaenaceae, <i>Xyloolaena</i> -type (Coetzee and Muller, 1984)	Endemic to Madagascar; subtropical	18 m – 40 m
(14) <i>Striatricolpites</i> spp. (15) <i>Tricolporites reticulate</i> sp. C		18 m – 40 m

Table 3.5. Pollen, climatic tolerance and name assigned to palynomorph (template adapted and developed from that outlined by de Villiers, 1997).

Division	Order	Family	Genus	Morphology	Climatic Tolerance	Palynomorph
Pteridospermophyta						
	Filicales	Polypodiaceae	Microsorium	Terrestrial, epiphytic	Tropical/temperate	<i>Polypodiidites, Polypodiisporites polypodiidies</i>
			Pellaea-type			
Coniferophyta		Podocarpaceae		Forest tree	Tropical and temperate	<i>Podocarpidites</i>
Angiospermophyta						
Class Liliopsida (monocotyledonous)						
Subclass	Order	Family	Genus	Morphology	Climatic Tolerance	Palynomorph
Liliidae	Liliales	Liliaceae		Geophytic herbs	Temperature to subtropical	<i>Liliacidites</i>
Class Magnoliopsida (Dicotyledonous)						
Subclass	Order	Family	Genus	Morphology	Climatic Tolerance	Palynomorph
Hamamelidae	Casuarinales	Casuarinaceae		Evergreen trees and shrubs	Tropical and subtropical	<i>Casuarina</i>
Magnoliidae	Piperales	Chloranthaceae		Herbaceous	Tropical and subtropical	<i>Clavatipollenites</i>
Dilleniidae	Ebenales	Sapotaceae		trees and shrubs	Tropical and subtropical	<i>Sapotaceoidaepollenites</i>
	Ericales	Epacridaceae		Evergreen trees and shrubs	Subtropical and temperate	
Rosidae	Proteales	Proteaceae		Evergreen trees and shrubs	Tropical and subtropical	<i>Proteacidites</i>
	Myrtales	Thymelaceae		trees and shrubs	Cosmopolitan	
	Celastrales	Aquifoliaceae	<i>Ilex</i>	Small trees and shrubs	Cosmopolitan	<i>Ilex-type</i>
			<i>Olea</i>			<i>Olea</i>
	Sapindales	Rutaceae		trees and shrubs	Tropical and subtropical	
Polygalales	Polygalaceae		trees, shrubs and woody	Cosmopolitan		
Asteridae	Asterales	Asteraceae		Herbs	Cosmopolitan	
	Rubiales	Rubiaceae		trees, shrubs and woody	Tropical and subtropical	<i>Stephanocolpate grains</i>

Palynomorphs showed decreasing degrees of preservation with depth, with many forms being unidentifiable due to damage (Table A.3). Low palynomorph abundances were generally coeval with high charcoal counts and fragmentary organic matter (Table A.3). Palynodebris and charcoal fragments were present in high proportions between the depths 24 - 25.8 m, 31.3 - 33.3 m and 43.5 - 45.5 m (Table A.3). The highest charcoal estimates were obtained from samples at depths between 32.4 m and 33.3 m, where charcoal constituted 80% of the material, were relatively well rounded with a size range distribution of $1.3 \pm 0.23 \mu\text{m}$.

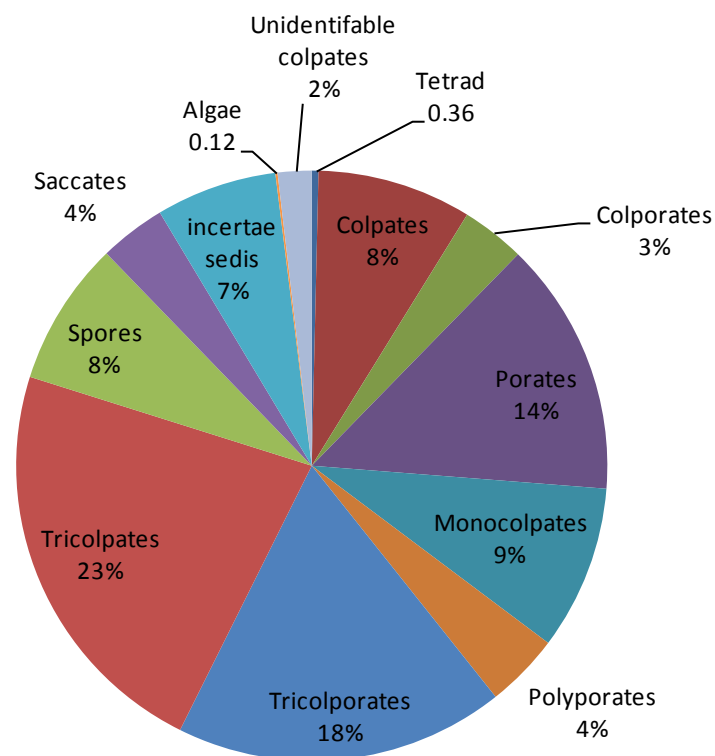


Figure 3.3. Variety of palynomorphs based on descriptive taxonomy from the Noordhoek Avondrustvlei core, and indicating the dominance of tricolpates (23%).

The variety of pollen found within the Noordhoek core, when based on descriptive taxonomy, highlights the predominance of tricolpates (23%), tricolporates (18%) and porates (14%). Saccate (4%), such as *Podocarpus*-type pollen, colpates (8%) and monocolpates (9% - i.e. palms) pollen were under-represented within the core, in comparison to the previously mentioned pollen forms (Fig.3.3). Eight percent of the population was composed of spores.

Table 3.6 illustrates dominate palynoflora within the total pollen count with morphotypes *Tricolpites reticulata* A (4.9%), *Tricolpites psilate* B (4.7%). *Tricolporites reticulata* D (4.6%) and *Tricolporites reticulata* C (3.6%) featuring heavily.

Table 3.6. Palynomorphs abundance (%) of those pollen types (excluding the algae, incert., and unknown colpates) that exceeded 1% of the total pollen count.

Palynomorph	Percentage (%)
Carpacoce	1.11
Celastraceae	3.19
Crassulaceae	2.23
Large Palmae	3.89
Liliaceae	2.41
Myrica/ Casuarina	6.01
Myrtaceidites parvus	0.96
Olea	2.75
Pellaea-type	3.39
Periporate reticulate (4 pores)	1.27
Poaceae	1.27
Podocarpus	3.86
Polypodiaceae	1.79
Proteaceae	5.00
Restionaceae	2.56
Sapotaceae	1.84
Small Palmae	2.80
Stephanoporate A	1.09
Tricolpites psilate A (round)	1.35
Tricolpites psilate A (small)	1.66
Tricolpites psilate B (trilobate)	4.69
Tricolpites reticulate large B	2.54
Tricolpites reticulate E (long baculae)	2.38
Tricolpites reticulate F (round large)	2.18
Tricolpites reticulate small A	4.92
Tricolporites psilate A	2.20
Tricolporites psilate C (Small round triloba	2.28
tricolporites psilate D (large, elongate)	2.72
Tricolporites psilate E (small)	1.24
Tricolporites reticulate C (large elong)	3.60
Tricolporites reticulate D (small, elong)	4.64
Trilete triangular cingulate spore	1.06

Small and Large Palmae (6.7%), Proteaceae (5%), Podocarps (3.9%), *Myrica/Casuarina* (6%) and Celastraceae (3.2%) were also important contributors to the overall palynoflora assemblage. Dominant spores were Polypodiaceae (1.8%) and *Pellaea*-type (3.4%). Less prominent pollen types were the Crassulaceae (2.2%), Liliaceae (2.4%), *Olea*-type (2.8%), Restionaceae (2.7%), Poaceae (1.3%) and Sapotaceae tetracolporate palynomorphs (1.7%).

Pollen distribution with stratigraphic depth and calculated MAATs

When comparing the MAATs and pollen abundance for the entire core, the greatest abundance of pollen types can be seen with the higher MAATs (Fig. 3.4A-C). This is especially true for the high MAAT interval between 18 m and 31.3 m depth. The abundance and diversity of plant species lessens lower in the stratigraphy (between 32.4 m and 45.5 m depth below surface) with cooler MAATs recorded. In this 'cool' MAAT interval a predominance of temperate flora is noted (Fig. 3.4, 3.7; Table A.4). The period of coldest MAATs, of 11 °C and 13 °C between 43.5 m and 44.8 m depth, did not contain any pollen but merely fragmentary organic material and charcoal fragments (~40%) (Table A.3, Table A.4). Low abundance and absence of pollen is also seen between 32.4 m and 33.3 m depth with corresponding MAATs of 20 °C and 18 °C respectively. These samples are also characterised by fragmentary organic material and the presence of charcoal (~60 - 80%).

The number and abundance of colpate, tricolporate and tricolpate pollen is increased below 20 m depth below surface (Fig. 3.4B-C). Tricolporate psilate grains occur in the upper 18 - 30 m depth below surface. Tricolpate psilate grains had a wide distribution, occurring between 20 m and 38 m depth below surface, but at low abundance. Tricolporate reticulate grains were dominant below 25 m - 40 m depth below surface (Fig. 3.4 B). Tricolpate reticulate grains had a narrow distribution, in comparison to tricolpate psilate grains, and only occurred between 23 and 35 m depth below surface. The polyporate pollen grains only occurred below 35 m depth below surface (Fig. 3.4 C). Colpates have a wide distribution, mainly occurring below 20 m to 40 m depth below surface. Crassulaceae and Poaceae pollen are seen to principally occur in the upper portion of the core at 19.4 m to 31.1 m and 18 m to 22.5 m depth below surface, respectively. All spores were low in relative abundance throughout the core (exceptions being the *Pellaea*-type and Polypodiaceae), and were predominately present below 18 m depth below surface, with the exception of Verrucate spore 'A'. There were microscopic charcoal (fusain) fragments in stratigraphically lower samples (24 - 25.8 m, 31.3 m - 33.3 m and 43.5 - 45.5 m) (Table A.3).

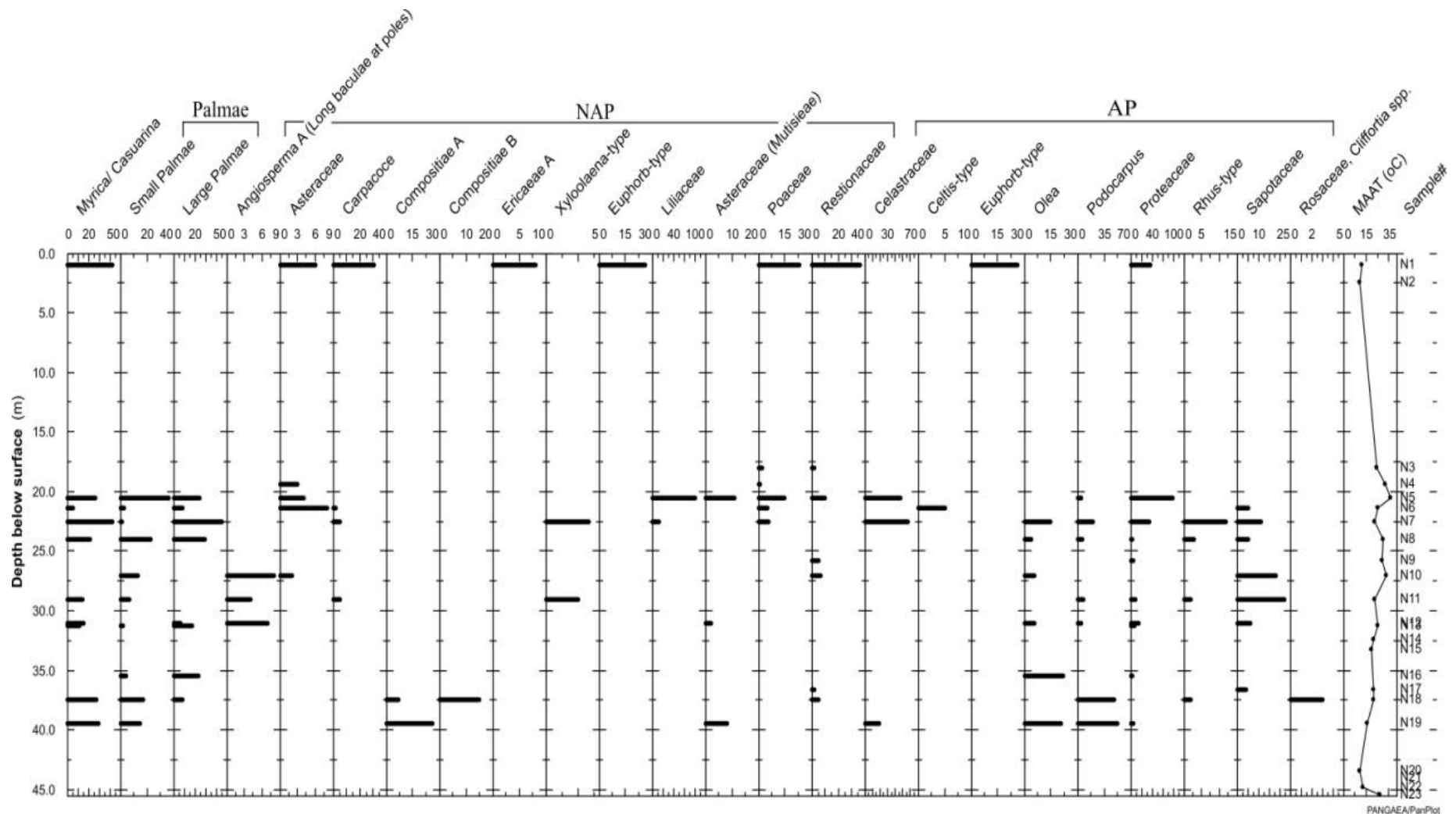


Figure 3.4.(A) Pollen diagram of the Noordhoek Avondrustvlei core used as the basis for palaeoenvironmental reconstructions, NAP- non-arboreal pollen, AP – arboreal pollen. The mean annual air temperature (MAAT) calculated using the CBT/MBT proxy is shown on the far right hand-side of the diagram with samples numbers (N1-N23). The gap in data between 2.5 m and 17 m is due to palynological and biogeochemical sterile quartz sands.

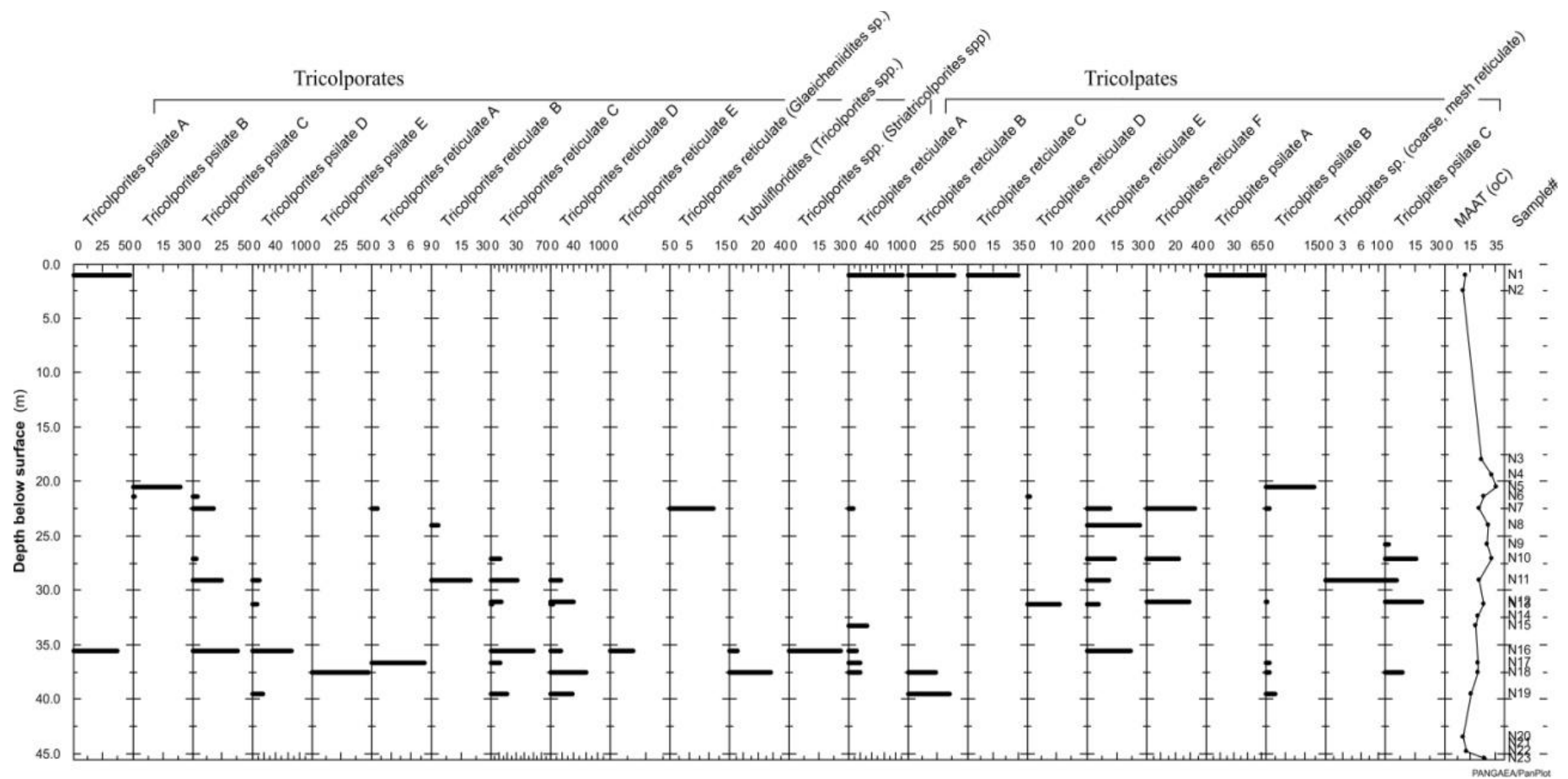


Figure 3.4 (B) Pollen diagram of the Noordhoek Avondrustvlei core used as the basis for palaeoenvironmental reconstructions. The mean annual air temperature (MAAT) calculated using the CBT/MBT proxy is shown on the far right hand-side of the diagram with samples numbers (N1-N23). The gap in data between 2.5 m and 17 m is due to palynological and biogeochemical sterile quartz sands.

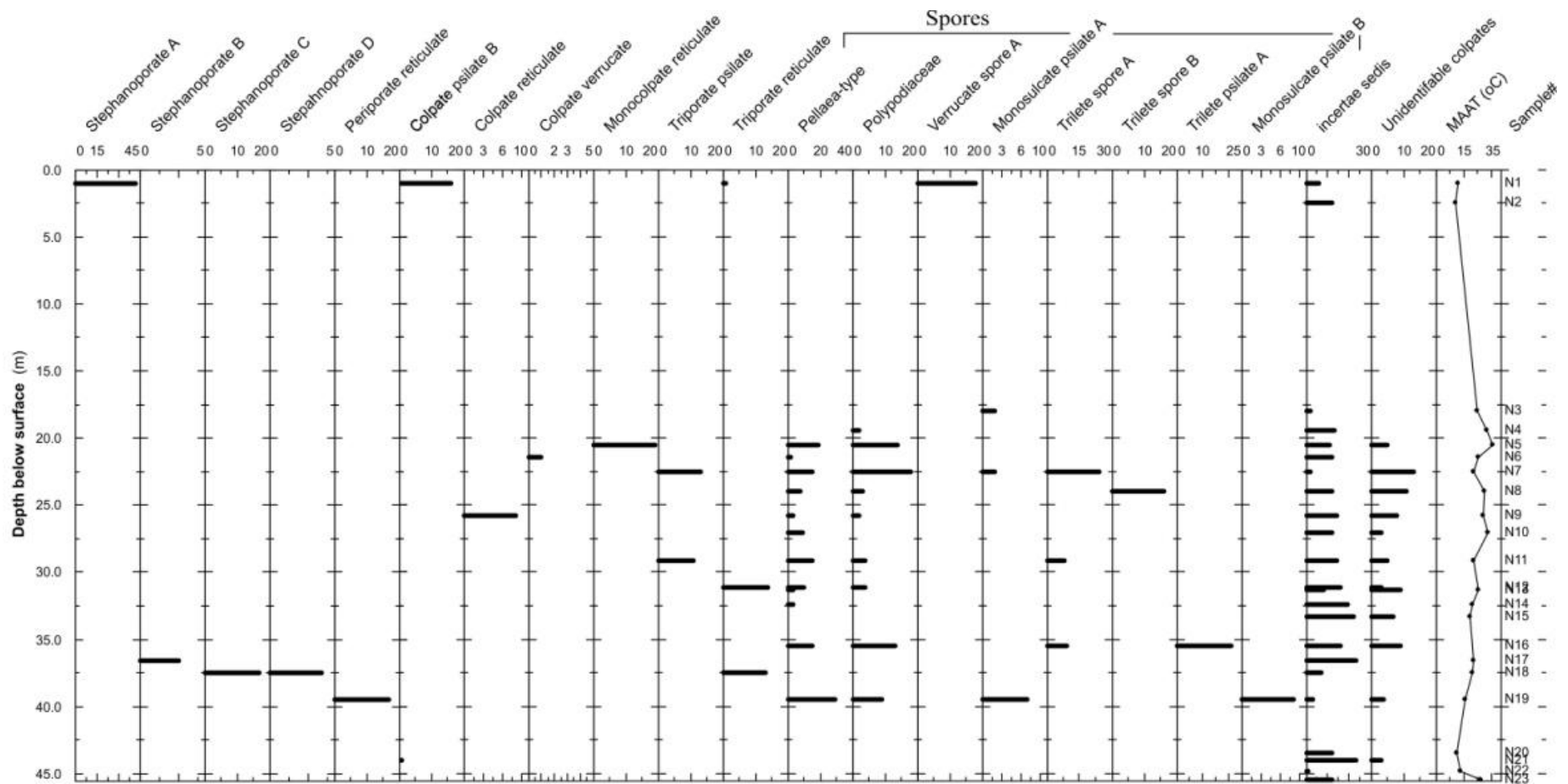


Figure 3.4 (C) Pollen diagram of the Noordhoek Avondrustvlei core used as the basis for palaeoenvironmental reconstructions. The mean annual air temperature (MAAT) calculated using the CBT/MBT proxy is shown on the far right hand-side of the diagram with samples numbers (N1-N23). The gap in data between 2.5 m and 17 m is due to palynological and biogeochemical sterile quartz sands.

The distribution and abundance of palms (indicative of tropical climates), *Myrica/Casuarina* (subtropical water-dependent species) and podocarps (temperate climates) indicate an alternating pattern (Fig. 3.4 A). Palms decrease in abundance with depth, first appearing at 20.5 m and disappearing by ~38 m depth below surface. The largest numbers of palms (large and small morphotypes) is between 20.5 m and 24 m depth below surface, with some localised occurrences lower in the core (e.g. increased abundance at 31.3 m and 35.5 m for ‘large palm’) (Fig. 3.4 A). Podocarps are spread throughout the core but dominate lower in the stratigraphy with peak abundances at 37.5 m and 39.5 m depth below surface.

Age-limits

The oldest possible age for the Noordhoek core based on the presence of Asteraceae (*Tubulifloridites* sp.) is Upper Palaeocene – Eocene, as the work of Zavada and de Villiers (2000) on South African onshore and offshore material report this as the earliest occurrence of Asteraceae in the fossil record (Table 3.7). The youngest possible age of Quaternary, for the uppermost 1 m - 2.5 m of the core, is based on the high abundance of fynbos elements (e.g. *Myrica*, *Carpacoe*) still present today, and the lack of locally extinct flora such as Areaceae. The youngest maximum age for the peat horizons, starting at 18 m depth below surface, is late Miocene –early Pliocene based on the presence of *Croton*-type pollen (Table 3.7) (Macphail and Cantrill, 2006).

3.5.2 Bulk organic parameters, carbon and nitrogen isotopes

The total organic carbon (TOC) content of the Noordhoek samples is highly variable with a range between 0.1% and 63.4% (Fig. 3.5, Table A.2). The highest values are recorded between 20.5 m and 31.3 m below surface, with an average TOC value of 52.7%, and these decrease towards 44 m where there is a second peak in TOC in excess of 48% between 44 m and 44.8 m below surface (Fig. 3.5). The total nitrogen (TN) content ranges between 0.03 and 0.77 with values less than 0.03 being analytically irreproducible and not used in this study (Table A.2; Fig. 3.5). The TOC/TN ratio is highly variable with a range between 24 and 286 (Table A.2).

Table 3.7. Age distribution of common elements within the Noordhoek core. Age dates obtained from de Villiers and Cadman (2001), Stevens (2001) and Raine *et al.* (2008).

Boundary ages (Ma)	Age	Pteridospermophyta		Angiospermophyta																					
		Pellaea-type	Polypodiaceoispontes	Asteraceae	Palmae	Capraceae	Celastraceae	Celast-type	Chloranthaceae	Clavipollenite s-Acuarina complex	Casuarinaceae (Casuarina)	Ericaceae	Liliacitides	Low spine Asteraceae (Mutisieae)	Myricaceae (Myrica)	Myrtaceitides parvus	Oleaceae (Olea)	Proteaceae (Proteacidites)	Restoniaceae (Restia)	Rutaceae	Rosaceae	Sapotaceae (Genus:Sapotaceoidites)	Sarcocaulaceae (Xylocaula-type)	Tubifloridae group	
1.81	Pliocene	late																							
5.332	Miocene	late																							
23.03		middle																							
33.9	Oligocene	early																							

The $\delta^{13}\text{C}$ values ranges from -27.1‰ to -24.3‰ with an average $\delta^{13}\text{C}$ value of -25.9‰, and the $\delta^{15}\text{N}$ record ranges from 0.03‰ to 4.76‰ (Table A.2; Fig. 3.5, 3.6). The highest $\delta^{15}\text{N}$ values (4.76‰ and 4.16‰) are recorded at 19.4 m and 32.4 m, respectively. The $\delta^{13}\text{C}$ and $\delta^{15}\text{N}$ values do not co-vary ($R^2 = 9\text{E-}05$; Fig. 3.5G). The $\text{C}_{\text{org}}/\text{N}_{\text{org}}$ ratio of the OM is highly variable and ranged between 43.8 and 333.9 when all values are considered (Table A.2). The highest $\text{C}_{\text{org}}/\text{N}_{\text{org}}$ ratio corresponds with higher TOC versus TN values as would be expected (Fig. 3.5). Generally, the samples between 18m and 31.3m below surface show the highest TOC and largely the highest $\delta^{15}\text{N}$ values (Fig. 3.5).

The data set shows an increase in $\delta^{13}\text{C}$ from more negative to less negative values with stratigraphic depth (Fig. 3.5). Samples at 1.0m and 2.5m depth below surface (N1 and N2, respectively) have strongly negative $\delta^{13}\text{C}$ values of -26.5‰ and -26.1‰ (Fig. 3.5). Figure 3.6 shows a general trend of increasingly more negative $\delta^{13}\text{C}$ values from 18 m to 31.1 m with 3 spikes, to less negative values, at 21.4 m (-25.4‰), 25.8 m (-25.6‰) and 31.3 m (-26.0‰). At 32.4 m depth below surface, the trend is reversed whereby $\delta^{13}\text{C}$ values become less negative until 45.5 m. The trend of increasingly heavier values is disrupted by 2 spikes to more negative values at 32.4 m and 37.5 m (Fig. 3.6).

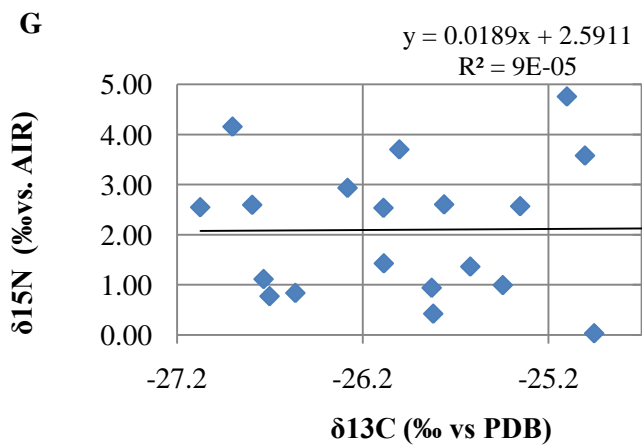
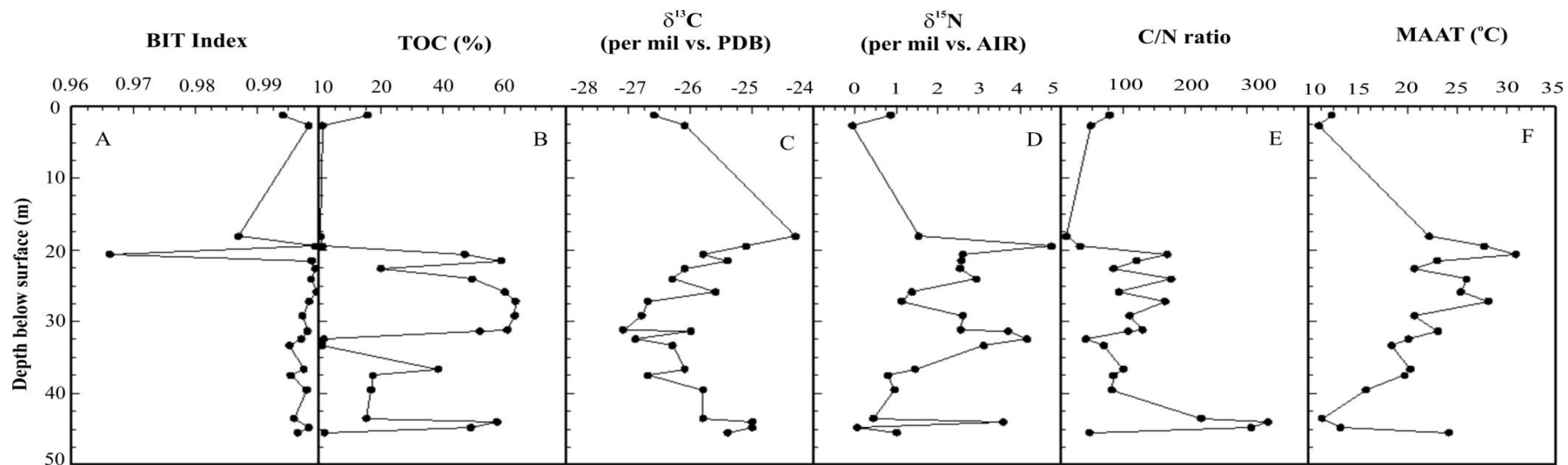


Figure 3.5. Noordhoek Avondrustvlei core bulk organic parameters and branched versus isoprenoid (BIT) index data for the entire 45m of core. (A) Branched versus Isoprenoid tetraether (BIT) Index-black dots defining samples, (B) Total organic carbon (TOC) content of samples, (C) $\delta^{13}\text{C}$ -isotope plot, (D) $\delta^{15}\text{N}$ -isotope plot, (E) the total organic carbon to nitrogen ratio ($C_{\text{org}}/N_{\text{org}}$ ratio) curve, (F) Mean annual temperature (MAAT) plot obtained from the CBT/MBT proxy recording the MAAT over entire borehole (G) R^2 value for carbon and nitrogen isotope comparison.

3.5.3 The BIT Index and CBT/MBT proxy

Branched GDGTs in samples at 31.1 m, 35.5 m and 44.7 m respectively, were below the detection limit (Table A.4). The BIT indices for samples yielding GDGTs were all ≥ 0.99 (Table A.4; Fig. 3.5; 3.6). The MBT index varied between 0.63 – 0.89, and the CBT index varied between 0.74 -1.92 (Table A.4).

Samples at 1.0 m and 2.5 m record MAATs of 12 °C and 11 °C, respectively. Samples between 18 m to 45.5 m depth below surface have a temperature range from 11 °C to 31 °C with an average temperature of 20.62 ± 5.8 °C. Samples at 19.4 m, 20.5 m, 27.1 m and 29.1 m record the highest MAAT's of 28 °C, 31 °C, 28 °C and 28 °C, respectively. There is a positive correlation between the MAAT and the pH with an R^2 value of the distribution is 0.7 (Fig. 3.6). A higher MAAT corresponds with the less acidic, more neutral pH values (Fig. 3.6).

Samples spanning a depth of 13.3 m, between 18 m and 31.3 m depth below surface, record relatively constant high temperatures of ≥ 21 °C, and an averaged MAAT of 25 °C over this interval (Fig. 3.6). A gradual decline in MAAT is recorded from the samples commencing at 32.4 m to 44.8 m depth below surface with the lowest MAAT (11 °C) recorded at 43.5m. The sample at 45.5 m records an increase of 11 °C from 13 °C, at 44.80 m, to 24 °C (Fig. 3.6).

Generally, the MAAT and $\delta^{13}\text{C}$ values show no significant co-variation with an R^2 value of 0.01, although a lower MAAT corresponds with an increase in higher, less negative, δ values (Fig. 3.6).

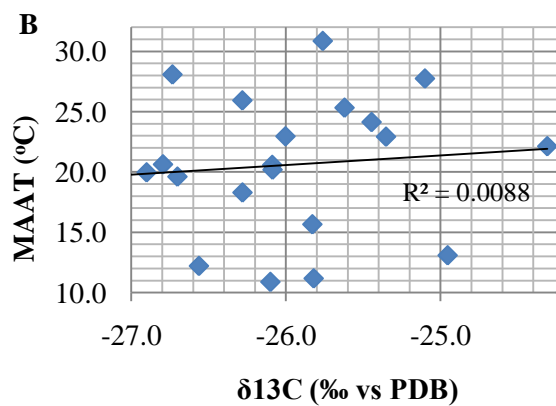
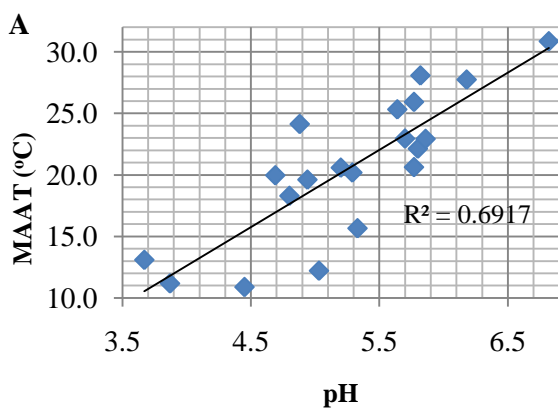
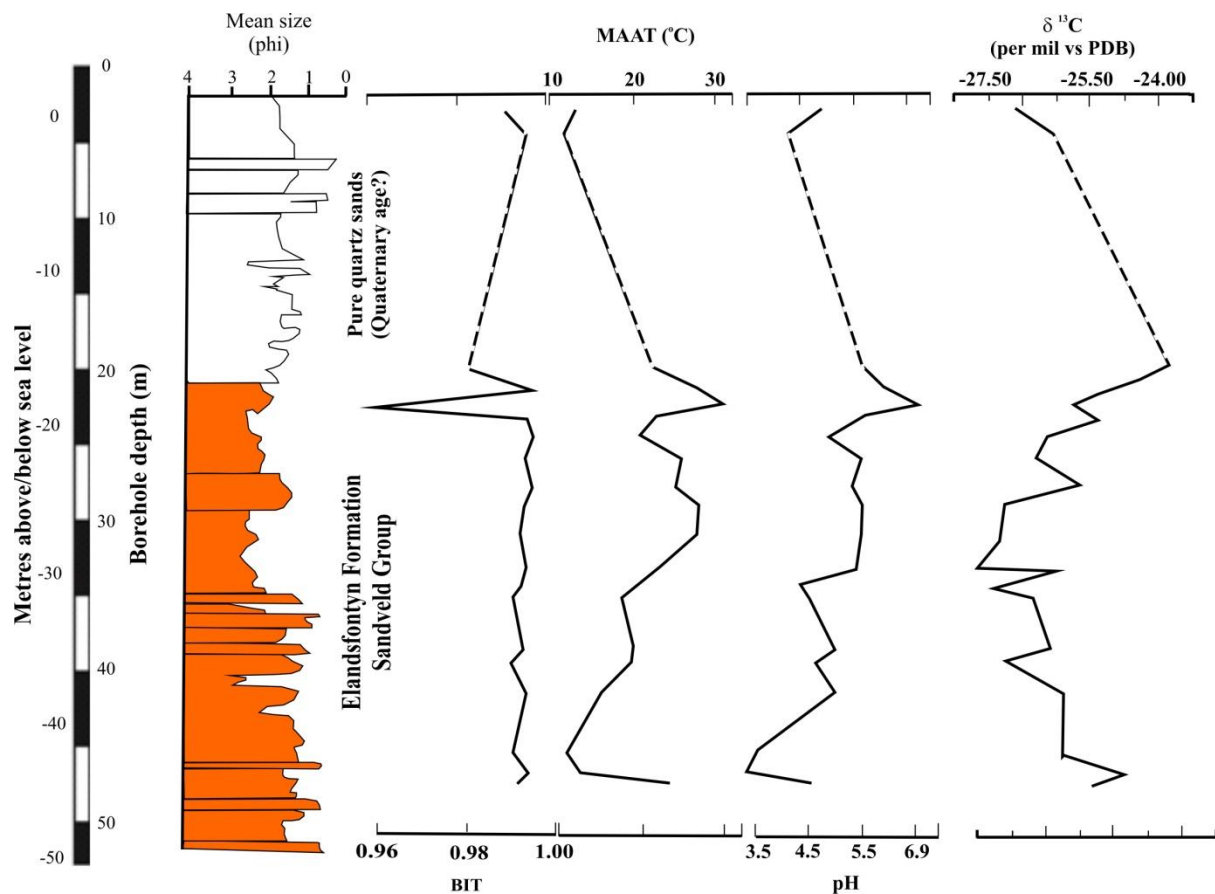


Figure 3.6. Branched vs. Isoprenoid index of Tetraethers (BIT), mean annual air temperatures (MAAT, °C), pH of soil at time of deposition, and isotope $\delta^{13}\text{C}$ values of the Noordhoek samples from entire 45.5m of core. Simplified log on left-hand side shows peat distribution (orange); no data was taken from pure quartz sand interval in the core profile between 2.5 m-18 m (log adapted from Rogers, 1982). (A) Scatter plot of MAAT versus pH ($R^2 = 0.7$), and (B) $\delta^{13}\text{C}$ ($R^2 = 0.008$).

3.5.4 MAAT and 'Index/indicator' palynomorphs

Figure 3.7 targets the variation of three 'index' palynomorphs with stratigraphic depth, and versus the calculated mean annual temperature. *Myrica* (*Myrica* /*Casuarina*) and podocarps appear at 20.5 m (with the exception of the uppermost sample at 1 m for *Myrica* pollen), with low abundances, and increase in number with the depth and age of the core (Fig. 3.7).

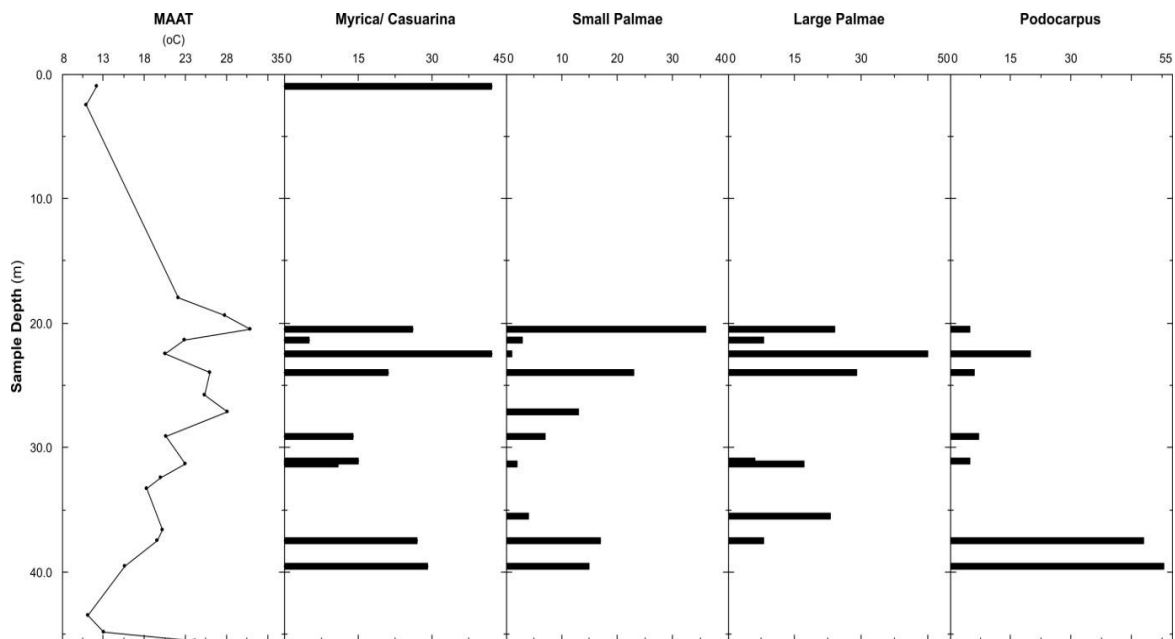


Figure 3.7. Mean annual air temperature (MAAT), in °C, calculated from branched GDGT biomarker distribution with black dots defining samples, versus podocarp, palm and *Myrica/Casuarina* record of the Noordhoek core. Note that the first appearance of the podocarp and palm pollen is below 20 m depth. *Myrica* pollen shows a similar trend (occurring first below 20.5 m) but there is a deviation due to its occurrence in the upper 1.0m.

The trend of increasing abundance (especially with regards to podocarps) with increasing depth follows closely the decreasing MAAT with depth (Fig. 3.7), obtained from the CBT/MBT proxy. The greatest abundance of *Podocarpus* pollen was found at 37.5 and 38.5 m depth. *Myrica* pollen shows a degree of variation to this trend; *Myrica* abundances peak when the MAATs are lowered, and decrease in abundance as temperatures increase. The greatest abundance of podocarps is found at 39.5 m, which coincides with a period of lowered MAAT between 36.6 m and 44.8 m depth (Fig. 3.7). Neither small palms nor podocarps occurred between 31.1 and 33.3 m depth, when MAAT's were moderate between 18 °C and 22 °C. *Myrica* pollen was found at depths of 31.1 m and 33.3 m but in low

abundance. One sample at 31.3 m yielded more abundant large palm pollen in comparison to the other pollen types.

3.6 Discussion

3.6.1 Sediment description and bulk organic analyses

The Elandsfontyn Formation peats (and interbedded sandy units) have been interpreted as having been deposited in a lagoonal and back-barrier environment (Rogers, 1982). Relatively continuous peat deposits of this age are of particular interest because of their scarcity in southern Africa, and allow for reconstruction of Miocene climate in this region. The extensive thickness of the peat units (almost 30 m) implies a long period of deposition on a stable plain with little clastic input, as would be expected from a stable margin (Killops and Killops, 2005). With this in mind, and the fact that the Noordhoek peat deposit formed in such close proximity to the ocean, it seems that it must have been protected from marine incursions through a barrier complex of bars or spits (?). Rogers (1982) reports a marine incursion at 11 m to 13 m depth below the surface evident due to the presence of sponge spicules. This occurrence is in the back barrier beach deposits above 18m depth below surface which were not studied here. All material analysed reflects a pristine terrestrial organic source (Table A. 4).

Sedimentologically, the Noordhoek core can be divided into two sections: a fine grained peat-rich lowermost unit and an overlying medium-grained quartz sand unit. The division of these two units occurs at approximately 17.5 m below surface, suggesting a coarsening-upward sequence, with stratigraphically lower massive clayey- and silty-peat abruptly transitioning into overlying fine to medium-grained, well-sorted and rounded quartz sands (Fig. 3.1, 3.2).

The organic sediments (between 18 m and 45 m below sea level) are likely to represent the overbank fines of a distributary system (Miall, 1985). The fine-grained interval consisted mostly of silty- and clay-rich peats, generally massive but with stratigraphically lower intervals showing lamination, with two probable unconformity or palaeosol horizons characterised by sulphidic sandstone layers of 2 - 4 cm thickness (Fig. 2.5). It was initially suspected that these silicified sulphidic green nodules, found interbedded with dark brown peat at 26.50 m and 32.50 m below surface, might indicate transgressive events which

increase the sulphur content of the sediment (Fig. 2.5; Killops and Killops, 2005). However, given the high BIT-indices of the neighbouring samples (Table A.1 and A.4), a marine influence is not apparent, and these nodules may therefore represent an anoxic period of non-deposition or erosion following regression (and lowering of base line). In general, excessive flooding of the floodplain interrupts the deposition and formation of peat, and deposits significant clastic material which is not apparent at these intervals (Killops and Killops, 2005).

The massive peats are interbedded with fine-grained, angular and poorly-sorted sand units probably representing crevasse splay deposits (Miall, 1985). Due to the nature of the core, however, the lateral continuation of these deposits cannot be established. The fine-grained peaty-overbank fines unit is overlain by massive medium-grained, rounded and well-sorted quartz sand (back-barrier beach deposit?). This sand unit has a thickness of 15 m. Lastly, the uppermost 2.5 m of the core is likely Quaternary (Holocene?) in age, but radiocarbon dating is necessary to establish this age.

3.6.2 Palynology

Assigning ‘form-genera’ (or form-taxa) is an artificial means of classifying fossil pollen and spores which are deficient of morphological characteristics that would place them easily within natural botanical affinities (Traverse, 1957). It is, however, also considered improper to use extant families and generic names for the naming of fossil pollen – even where there is direct evidence for this assignment (Traverse, 1957). Generally, artificial taxa are assigned when palynomorphs are of unknown botanical affinity.

There are several reasons why form genera are maintained and palynomorphs are not referenced to extant genera. One of the most important reasons being that it is not possible to be convinced that fossil form taxa are one species or several of the known natural genera, or does not belong to either (Traverse, 1957). However, the expression “-type” and the assignment of form-taxa has been used when referring to fossil palynomorphs in this core bearing morphological characteristics similar to that of a modern genera; thus indirectly relating the pollen to a modern genus/ family for the purpose of reconstructing palaeoenvironment. Similarly for fossil forms for which there were no clear form-taxa association morphotypes were assigned.

There was some confusion with naming the pollen which closely resembled *Myrica* (modern and extinct) but which also shows strong similarities (morphologically) with *Casuarina* (now extinct in the Cape). In this thesis I have broadly considered these pollen types to be the form genera *Myrica* in terms of palaeoenvironmental tolerances. Although Coetzee and Pragłowski (1984) establish on the basis of LM, SEM and TEM studies that both *Myrica* and *Casuarina* (now not indigenous to South Africa) occurred within the southwestern coast sediments, it is difficult to distinguish between the two without SEM work.

Many of the morphotypes (e.g. *Tricolpites* spp.) described from the core may be representing now extinct genera when considering the age of the material (early to middle Miocene) (Scott, pers. comm.). Unknown pollen types with similar morphological features, e.g. tricolporate and reticulate, were grouped together and assigned names based on these features (Fig. 3.4; Table A.3 and Noordhoek pollen catalogue). This meant that in some cases the approach used led to quite broad classification of palynomorphs. The tricolporate and tricolporate pollen grains could not be identified to family level given the variety of parent families which these relatively common pollen grains could belong (Scott, pers. comm.). What can be inferred from these grains is that their sheer number does represent heightened biological diversity at the time of their deposition.

In other cases, where pollen was similar to that of other fossil taxa from other continents, it allowed for form-genera to be assigned to some palynomorphs (e.g. *Pellaea*-type and *Podocarpidites* spp. with botanical affinities to Podocarpaceae). This again led to a broad classification, for instance, the palms were of two broad morphotypes which could only be distinguished based on their size ranges, i.e. “small” (anything less than 15 μm) and “large” (greater than 20 - 25 μm). These taxa may have different ecological tolerances and may represent different species especially when considering they seem to be somewhat separated in occurrence in the core.

Although numerous palynomorphs were not identified to Family or Genus level, and were classified through descriptive taxonomy, botanical affinities were inferred from literature where feasible (Table 3.4, 3.5).

‘Marker’/‘Index’ taxa, (palms, podocarps, *Myrica*) were specifically employed because of their significant abundance, high preservation within most slides and their presence/absence which may largely be controlled by environmental factors/niche tolerance, (Fig. 3.7; see appendix for Noordhoek pollen catalogue, page A16). Other palynofloras could

indicate contradictory climatic information. The few marker palynomorphs were used on the basis of their abundance throughout the core, and the assumption that these ‘index’-palynofloras would highlight main trends in the palaeoclimate.

To constrain a relative age-date more objectively for the material, since chronometric dating was not feasible, Noordhoek pollen suites were correlated with other similar southern African (and Southern Hemispheric) pollen between sequences and sites (e.g. comparisons to work by Germeraad *et al.*, 1968; Coetzee, 1978a, b; Coetzee and Muller, 1984; de Villiers, 1997; de Villiers and Cadman, 2001; Shaw *et al.*, 2008; Raine *et al.*, 2008; Logan *et al.*, 2009; Holdgate *et al.*, 2009). Literature from South Africa is heavily focused on the Quaternary Period (e.g. Scott, 1982, 1993, 1994, 1996; Scott and Vogel, 2000; Scott and Woodborne, 2007), or falls more largely into the upper Mesozoic or Palaeogene era (Zavada and de Villiers; 2000; de Villiers and Cadman, 2001; Zamalola, 2004), and meant that age-comparable sequences in South Africa were difficult to obtain. Poor chronostratigraphic constraints have hindered this research, and independent dating means would significantly add to this work.

Much of the relevant research on Cenozoic southern African floras used Southern Hemisphere descriptions to classify and name African floras, because of both the greater extent of well-preserved and dated Neogene pollen records, and the Gondwana connection. The duration of southern Africa’s split from other Gondwana provinces (~130 Myr; mid-Cretaceous; Gheerbrant and Rage, 2006), even when considering Gondwanic inheritance, is great enough to instil a sense of risk when comparing, naming and dating pollen using this method (Linder 1987; Gheerbrant and Rage, 2006). This is emphasised by the fact that Africa, surprisingly, lacks several taxa (flora and fauna) which are present, extinct (fossilised) or extant, on other Gondwana provinces (e.g. *Nothofagus*; Gheerbrant and Rage, 2006; Macphail and Cantrill, 2006). This means that African floras of this and other cores could be markedly different from other Gondwana provinces. However, at this time it remains the most valuable way of achieving a coherent record of South Africa’s palaeofloras. Furthermore, it is strange that there is not more interest and research placed on the Mio-Pliocene floras of the south-western Cape, given that it is today a biodiversity hotspot (Cowling *et al.*, 2009). Tracing the evolution of this important floristic region would have significant effects on the understanding of the origin of many endemic genera (Cowling *et al.*, 2009).

That being said, the Noordhoek palynomorphs, below 18 m depth below surface, based on this study and the original study by Coetzee (1978a, b), and in comparison to other Southern African (e.g. Schalke, 1973; Morgan, 1978; Coetzee and Rogers, 1982; Coetzee *et al.*, 1983; de Villiers and Cadman, 1997) and Southern Hemisphere sites (e.g. Kemp and Harris, 1975; Markgraf *et al.*, 1995; MacPhail and Cantrill, 2006), for the middle Miocene age, held comparable:

- *Clavatipollenites-Ascarina* complex,
- *Liliacidites*,
- Sarcolaenaceae: *Xyloolaena*-type
- *Palmae*,
- *Podocarpus* -types,
- *Euphorbia*-type,
- Myraceae: *Myrtacidites parvus* Cookson and Pike 1954
- *Myrica/Casuarina* -type

The Noordhoek pollen assemblage of this study does show similarities with the older Scholtz (1985) Arnot Pipe assemblage but more so with that of de Villiers and Cadman's (1997) Koingnaas Paleogene pollen assemblage, with the presence of fern spores, Myraceae, *Myrica*, *Podocarpidites*, *Liliacidites* etc. This implies a lowermost age of upper Cretaceous-Paleogene (Table 3.7). However, the presence of Mutisieae, an accepted stratigraphic marker, at 39.5m depth in the Noordhoek assemblage, places a maximum Oligocene-Early Miocene age for these lowermost sediments (Fig. 3.4, Table 3.7; Zavada and DeVilliers, 2000). This would complement the age of Coetzee's (1978a) S20 core where the first occurrence of Compositae pollen delineated a late Oligocene-early Miocene age.

The sparse abundance of Poaceae at a depth greater than 22.5 m below surface within the Noordhoek core is significant in defining the age of the deposit in the knowledge that grasses have been around since the Cretaceous (Germeraad *et al.*, 1968; Muller, 1981). This could point to an older (Cretaceous) age for these deposits. The numerous Angiosperm and Asteraceae pollen (indicating winter rainfall and therefore emplacing an upper age limit of ~10 Ma; Cowling *et al.*, 2009) at Noordhoek however again points to a younger age. Although having many commonalities with Koingnaas as there is no independent dating of this or the Koingnaas assemblage it would be difficult to further specify an age.

Therefore, the preferred age for the peat unit of the Noordhoek core, based on this study and in comparison to the previously drilled S20 core of Coetzee (1978a, b; 1983) is early to middle Miocene. This applies specifically to the Noordhoek material occurring below 18m depth below surface. Although the oldest possible age, based on the Asteraceae (Mutisieae) pollen, is roughly Eocene (Zavada and de Villiers, 2000; Scott *et al.*, 2006), the occurrence of other flora and stratigraphic relationships to other laterally coeval Mio-Pliocene sites (e.g. at Langebaanweg; Coetzee and Rogers, 1982, Coetzee and Muller, 1984) gives validity to the Miocene hypothesis. Notably, the common occurrence of subtropical and temperate vegetation (Palmae, Sapotaceae, *Olea*, Restionaceae, Celastraceae, *Euphorbia*-type), and their occurrence at other Neogene locations in the Southern Hemisphere reaffirms a Miocene age for the material (Martin and McMinn, 1993; Macphail and Cantrill, 2006; Coetzee, 1978a, b; Coetzee and Rogers, 1982; Coetzee and Muller, 1984; de Villiers and Cadman, 1997, 2001).

The upper 2.5 m of core has been considered separately from the remaining core because of the disparity in the ages of the two separated units of sediment. The age-range for the uppermost samples, 1 m and 2.5 m in depth, is Quaternary, based on the modern pollen found in sample N1 (e.g. *Carpacoce*, Proteaceae), and the lowermost ‘youngest’ age range is Pliocene (based on the presence of one fern spore, absence of palms, etc.; Coetzee, 1983).

3.6.3 Comparison to Coetzee’s (1978b) Pollen zones

Figure 3.8 highlights similarities and differences between the Noordhoek core and Coetzee (1978b) pollen zones, as well as comparing the palynological results from both studies to the bacterial tetraether lipid derived MAATs from the current study’s samples. Coetzee’s (1978b) zones, although highlighting certain repetitive elements which make palaeoenvironmental reconstruction more probable, do not account for the depths of pollen occurrences or geological associations (Fig. 3.8). Thus, the zones describe key taxa at undefined intervals and do not report their occurrence in a more quantitative manner; both in terms of average depths of each zone and average taxa abundance characterising the zone. The Noordhoek pollen suite presented here did not fit the erected zones absolutely, as would be expected due to key influencing factors such as provincialism, as well as undefined zone depths (Fig. 3.8). The pollen zones and known climatic tolerances of taxa support (and to an extent validate)

the calculated MAATs. Pollen assemblage variation between mesothermic and megathermic elements does show an agreement with variability in MAATs, with temperate floras abundance being greatest when calculated MAATs are low (e.g. podocarps and *Olea*; Fig. 3.7, 3.8).

3.6.4 Bulk organic parameters

The high TOC, $\delta^{13}\text{C}$ and $\text{C}_{\text{org}}/\text{N}_{\text{org}}$ ratio indicate that the organic matter of the peat was derived from higher plants without a lacustrine (algal) influence (Meyers and Lallier-Vergès, 1999). The TOC values of the samples vary with stratigraphic depth (0.1% to 63.4%) but seemed to do so with no clear pattern. The generally high TOC values, which act as indices for quantity of OM preserved in the sediment, indicate high abundance and preservation of OM during and subsequent to deposition (Meyers, 2003). The degradation of animal and plant OM and the quality of the OM can be deduced through the measured total nitrogen (TN) content of the samples (Meyers, 2003; Mielnik *et al.*, 2009). The Noordhoek samples range from reliably low values of 0.19% to 0.77%, reflecting low protein content (absence of abundant algae), and therefore the likelihood that much of the OM present was derived from cellulose and lignin-rich plant materials (Meyers, 2003; Table A.2). This is further affirmed by the high $\text{C}_{\text{org}}/\text{N}_{\text{org}}$ ratios with most $\text{C}_{\text{org}}/\text{N}_{\text{org}}$ ratios being variable and in some cases extremely high. For example, at 43.5 m below sea level (44 m depth below surface) a value of 334 was obtained. Meyers and Lallier-Vergès (1999) show that $\text{C}_{\text{org}}/\text{N}_{\text{org}}$ ratios greater than 20 are due to OM which is derived purely from higher plants, with lower $\text{C}_{\text{org}}/\text{N}_{\text{org}}$ ratios being indicative of OM rich in protein (such as that derived from algae) and poor in cellulose and lignin.

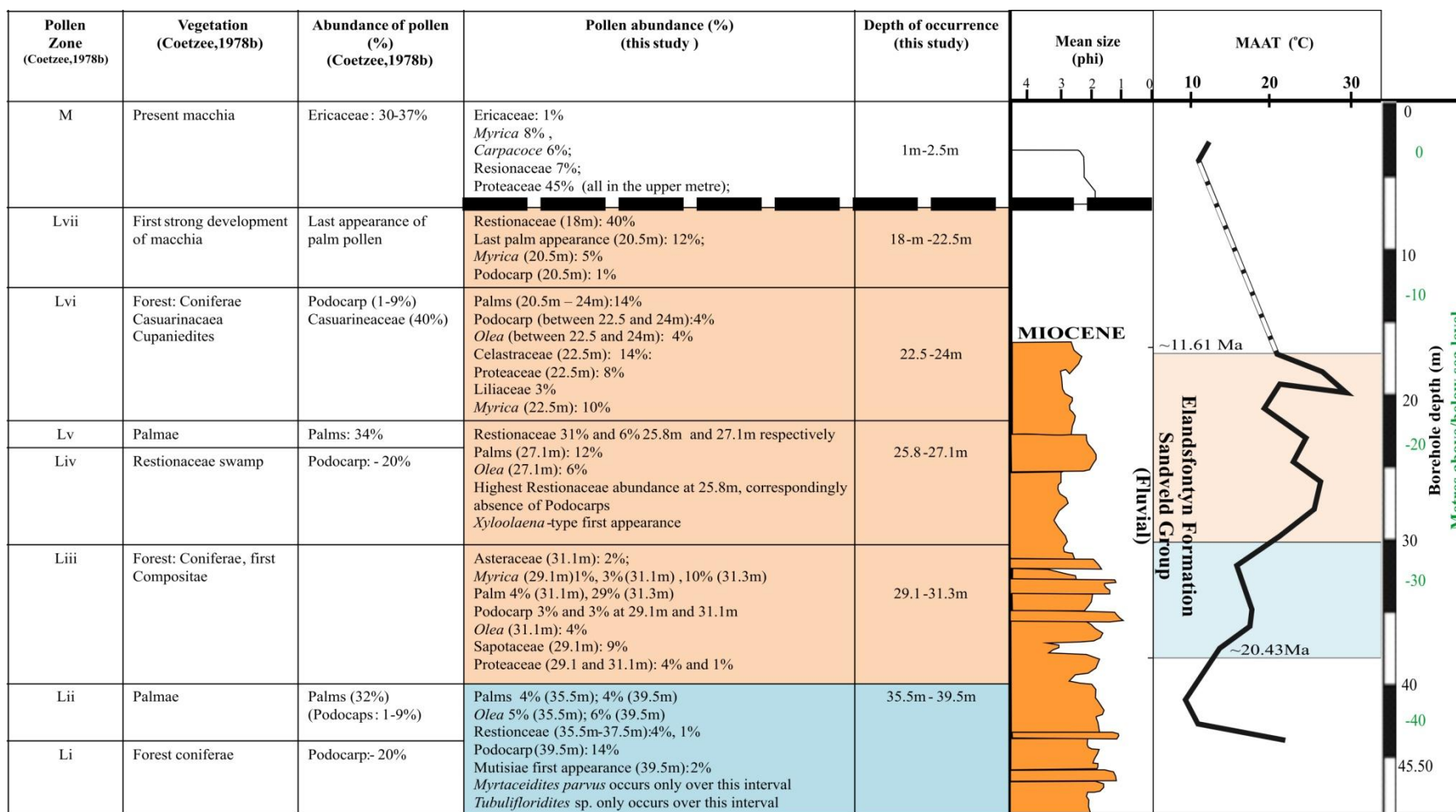


Figure 3.8. Comparison between Coetzee (1978 a, b) pollen zones and the Noordhoek core of this study (sample between 1 - 2.5 m and 18 - 39.5 m depth below surface). Pollen of this study showed a degree of congruency with Coetzee's (1978b) pollen zones (M-Li). The calculated mean annual temperature (MAAT) curve, from the MBT/CBT proxy, of this study is given, as well as the stratigraphic log for the Noordhoek core (adapted from Rogers, 1982). Broken lines indicate a stratigraphic break over which no samples were analysed because the interval constituted well-sorted quartz sands. Temperatures higher (orange) and lower (blue) than present day Cape MAAT (17 °C) are indicated.

Samples, which were exceptions to the general pattern, occurred at 1 m and 2.5 m below surface, 18 m - 19.4 m depth below surface and 33.3 m depth below surface. These show low TOC values of less than 0.7% and correspondingly low TN values. The C_{org}/N_{org} ratios obtained from these samples were treated with caution due to the concentrations of these elements being very low. The low TOC and TN values may be indicative of increased inorganic input through increased sedimentation rates. It could also be indicative of high levels of degradation of the OM (Meyers, 2003; Mielnik *et al.*, 2009). Pollen counts from these specific intervals were low, and in all cases the presence of charcoal fragments was noted (Table A.3). The low TOC, palynomorphs and charcoal point to poor preservation as a result of seasonal fires with drying of the overbank fines/wetland area (Fig. 3.5, Table A.2). The presence of fire means that much of the OM present would have been combusted. As temperature is a key factor in the nature of fires in an ecosystem it would be expected that the MAATs calculated from these samples would be high. This was indeed the case for the samples at 18 m (22 °C), 19.4 m (27 °C) and 33.3 m (18 °C). Samples at 18 m and 19.4 m depth below surface were preceded by samples showing significantly elevated MAATs, e.g. sample interval at 20.5 m (stratigraphically below sample at 19.4 m) having a MAAT of 31 °C.

Conversely, the interval between 20.5 m depth and 31.3 m had the highest TOC values with an average value of 52.7% (Fig. 3.5). This interval coincides with high pollen counts, the highest MAATs, and indicates a time of elevated primary productivity with favourable preservation conditions (Fig. 3.4, 3.5; Table A.3). However, a second peak lower down in the stratigraphy, between 44 m and 44.8 m, has elevated TOC values (57.4% and 48.9%, respectively) corresponding to lowered MAATs and no pollen preserved, but only broken organic material (Fig. 3.5; Tables A.2 and A.3).

3.6.5 Biogeochemical interpretation and the CBT/MBT proxy

Analyses of the bacterial tetraether lipid composition of the Noordhoek material established a purely terrestrial origin of the sediments. They contained little crenarchaeol and no marine signature as illustrated by BIT indices > 0.99 (Weijers *et al.*, 2006b). This is despite the site's relative proximity to the coast and the likelihood of influence of marine or estuarine elements even if sea levels are likely to have been periodically low.

The MAATs reported suggest a temperate/subtropical to tropical climate which is supported by the palaeoflora represented in the core (Fig. 3.8). In focusing on Miocene MAATs calculated between 18 m and 45.5 m below the surface in more detail, there is a general pattern of increasingly cooler conditions with stratigraphic depth (Fig. 3.6, 3.8). The warmer temperatures cover the sample interval 18 m – 31.3 m in depth, with climax temperatures recorded as 20.5 m (31°C) and 27.1 m (28°C). The averaged MAAT over this period is 24.2 ± 6.4 °C. Warmer mean annual temperatures are correlated with less acidic sediments (averaged pH 5.9 ± 0.6) (Fig. 3.6).

In contrast, the stratigraphically lower samples between 32.4 m and 45.5 m depth showed cooler temperatures, where the averaged MAAT over the interval corresponded to 18.3 ± 4.3 °C (Fig. 3.6). The lowest MAAT over this interval was 11 °C at 43.5 m depth below surface. This suggests cool and wet conditions, which are reinforced by the palynofloras, and ideal for peat formation (Fig. 3.8; Meadows, 1988; Killips and Killips, 2005). The lower MAATs corresponded with more acidic sediment pH values averaging 4.7 ± 0.6 . The relatively low pH values obtained are typical of humid soils supporting forest floras such as the podocarps and *Olea* reported (Fig. 3.6, 3.8; Schalke, 1973; Chesworth *et al.*, 2008). The trees *Podocarpus* and *Olea* are sensitive to soil moisture and thrive in soils of pH between 4.8 and 5.5 (Schalke, 1973), a range into which the average pH of 5.3 fits.

Soil pH and precipitation are linked with an increase in rainfall corresponding to the production of more acidic soil profiles (Weijers *et al.*, 2007a). When temperatures are high, generally accounting for increased precipitation (through increased evapotranspiration), the pH of the soil will become increasingly more acidic (Weijers *et al.*, 2007a). The converse is seen in the Noordhoek core with near-neutral conditions complementing high MAAT. By this account the low MAAT group of samples, lower in the stratigraphy, with acidic sediment profiles would have likely experienced higher rates of rainfall, low decomposition, and thereby, increased rates of peat accumulation.

Importantly, under elevated carbon dioxide (as modelled for the Miocene; 300 ppm-600 ppm; Kürschner *et al.*, 2008) and water availability, plants sequester and discern a greater amount of carbon dioxide, providing a lighter $\delta^{13}\text{C}$ signature. It has also been shown that lower $\delta^{13}\text{C}$ values are recorded when precipitation is high, as a result of increased stomatal conductance (Farquhar *et al.*, 1982; Liu *et al.*, 2004). In light of the present data from Noordhoek, the light $\delta^{13}\text{C}$ values would imply that the carbon dioxide concentration and

water availability were not limiting factors. However, the latter contradicts the presence of charcoal and lowered pollen counts at various intervals, which suggest seasonality or periodic drought. Inferring rainfall from sediment pH and MAAT is not absolute by any means, as many other edaphic factors are influential in determining the sediment pH.

The Quaternary Noordhoek samples at 1.0 m and 2.5 m depth below surface, likely to be the best analogue for modern climate, gave MAATs of 12 °C and 11 °C, respectively. This correlates with the mean annual winter temperature (12.5 °C) of the Cape Town area and falls below the modern MAAT of 17 °C (Fig. 3.8). Microbial productivity in the Cape, where plant productivity is intimately related to winter rainfall (since roughly 10 Myr ago; Cowling *et al.*, 2009), is likely to be highest in the winter. This could be a potential reason that the MBT ratio does not reflect a mean annual temperature but one biased towards winter temperatures.

Could this imply that the anaerobic bacteria producing the branched GDGTs are influenced by increased bio-productivity associated with winter months (with higher rainfall)? If this is based on the assumption that winter productivity would be higher and decomposition rates lower because of the ambient conditions in the Cape? Additionally, as a Mediterranean climate was only established at approximately 10 Ma, the results from 'older', stratigraphically lower samples should show a shift in this bias (if indeed there is a bias) from a summer rainfall dominated climate. Peterse *et al.*, (2009b), however, affirmed that tetraether-derived temperatures are comparable to instrumental temperature measurements in a study of modern high latitude soils from Svalbard, Norway. Interestingly, nevertheless, Zink *et al.* (2010) have also questioned whether MAATs derived from the MBT/CBT proxy may be skewed towards months of higher productivity, where bio-production is enhanced due to favourable environmental variables. Ultimately, Zink *et al.* (2010) have proved that the MAATs are representative of the averaged annual signal. Furthermore, a report of palaeotemperatures from three different proxies obtained from an Arctic Pliocene peat by Ballantyne *et al.* (2010) incurred the same annual temperature signal with very little variation. This further verifies the assumption that the palaeotemperatures derived from the proxy are records of mean annual temperatures. The recorded MAAT for the Noordhoek samples (1.0 m and 2.5 m) may represent a period where the MAAT was cooler than present, perhaps indicative of a transition in environmental conditions linked to a Quaternary glacial (?).

3.6.6 Palaeoflora and climate

The pollen evidence suggests the palaeoflora varied, from ferns, herbaceous plants and shrubs (e.g. *Myrica/Casuarina*, Liliaceae) to trees (e.g. Sapotaceae, palms, Podocarps) constituting woodland and open forested areas (Fig. 3.4; Table 3.4). These are predominately subtropical/tropical and temperate floras which would have occupied the coastal plain wetlands of a Neogene Noordhoek. Saccate pollen, belonging to podocarps, suggest forested areas are likely to have existed throughout the Cape Peninsula extending northwards as far as Saldanha Bay and south-eastwards towards Knysna (Coetzee and Rogers, 1982; Carr *et al.*, 2010a). In South Africa, the closed Knysna Forest is a remnant of this once large expanse of temperate forests, and today contains a few extant podocarps (e.g. *Podocarpus falcatus*, *P. Elongates*; Schalke, 1973).

The palynomorph assemblages and stable carbon isotopes indicate an open riparian forest due to the abundance of arboreal pollen (e.g. palms, *Olea*, podocarps, Sapotaceae) and groundcover (e.g. Celastraceae pollen – which may be vines or small trees; *Pellaea*-type spores and other trilete fern spores). These taxa are influenced by the availability of water (specifically *Myrica* and Sapotaceae; Jiménez-Moreno *et al.*, 2010), and generally indicate a warmer (more subtropical) climate with reduced seasonality. A lack of seasonality could be due to the raised global temperatures (associated with MMCO) and the lack of a steep pole-to-equator temperature gradient (Potter and Szatmari, 2009). It would be interesting to relate these vegetation shifts to increased upwelling of the BUS and the increasing aridity it brought about along the west coast.

The greatest abundance of palynomorph types broadly coincides with elevated MAATs (Fig. 3.4). This pattern is especially pronounced for the high MAAT interval between 18 m and 31.3 m depth below surface. Peaks in palm abundance indicating humid and tropical temperatures and well-drained soils show correspondence with elevated MAATs, e.g. at 20.5 m depth below surface the highest palm abundance is recorded as well as MAATs measured (31 °C) (Fig. 3.4).

The abundance and diversity of plant species lessens with stratigraphic depth, and with increasingly cooler MAATs recorded between 32.4 m and 45.5 m depth below surface. The predominance of temperate, mesothermic flora (e.g. podocarps) within the core, indicating lower mean annual temperatures, was observed to coincide with the cooler MAAT

interval (Fig. 3.4). The occurrence of these temperate taxa with the lowered MAAT may reaffirm the use of the CBT/MBT proxy for palaeoenvironmental reconstruction in the south-west Cape. The period of coldest MAATs, 11 °C and 13 °C between 43.5 m and 44.8 m depth, did not have any pollen but merely fragmentary organic material and charcoal fragments (~40%). Fragmentary organic material, the presence of charcoal (~50-60%) and very low abundances of pollen are also recorded between 32.4 m and 33.3 m depth with corresponding MAATs of 20 °C and 18 °C respectively; pointing to periods of increased seasonality.

There are a number of extinct tropical and subtropical pollen found in the core, (e.g. palms and cf. *Casuarina*) which have been considered extinct since late Miocene in the south-west Cape; Coetzee, 1978a, b), but still extant in other tropical areas in the southern hemisphere (e.g. *Xyloolena*-type, which is present in the Noordhoek Avondrustvlei core and now endemic to Madagascar). A subtropical/ tropical climate supporting tropical and temperate vegetation (i.e. palms), is completely different to the xerophytic fynbos dominant in the Cape today (Fig. 3.4).

Restionaceae which are present in the Noordhoek core are limited in present distribution to cool and moist climatic conditions (Cowling *et al.*, 2009). Restionaceae therefore act as a good 'indicator' family for increased aridification along the south-western coastline, and their abundance decreases with depth in the core (Chase and Meadows, 2007; Coetzee *et al.*, 1983). However, the climatic tolerance of modern *Restios* to cool, moist conditions and nutrient poor soils contrasts their highest abundance being recorded at 20.5 m and 27.1 m depth during periods of highest recorded MAATs (31 °C and 28 °C, respectively). This might be due to the fact that Restionaceae are also indicative of winter rainfall, and their variable stratigraphic abundance may be linked to periods when rainfall seasonality was varied, with their presence and greatest abundance falling predominately in a winter rainfall regime (Shi *et al.*, 2000). The upper metre of Quaternary sediments contained the greatest overall abundance of Restionaceae representing the modern state.

Myrica was used as 'indicator' pollen (Fig. 3.7) as it needs sustained high water resources for abundance, and therefore grows proximal to water ways (Jiménez-Moreno *et al.*, 2010). It shows three peak periods, firstly between 40 m and ~37.5 m depth corresponding with colder conditions and high podocarps abundance; secondly, between ~20 and 24 m with correspondingly warmer temperatures and increased palm abundance, and

lastly within the uppermost 2.5 m of the core (Fig. 3.7). The appearance in the uppermost 2.5 m can be confirmed as *Myrica* pollen and not *Casuarina* due to latter's extinction in the Cape by Pliocene (Coetzee, 1986).

The distribution and abundance of *Myrica/Casuarina* (Fig. 3.7) which is a subtropical, water-dependent species shows a clear pattern, with its absence over 32.4 m - 33.3 m depth (charcoal present – likely drought-prone), and reoccurrence with increasing abundance immediately following (with increasing stratigraphic height above 31.3 m) likely to indicate periods of wet and dry. Additionally, its presence and abundance over extremely warm periods (e.g. at 20.5 m and 22.5 m) indicates that these are time frames which despite high MAATs are not arid (Fig. 3.7, 3.8).

The alternating abundance and presence/absence of taxa representing mesothermic conditions (i.e. more temperate plants such as the Podocarps and *Restios*) with megathermic ones (e.g. tropical/subtropical elements such as Sapotaceae, *Myrica*, Palms, Euphorbia) show general patterns which complement cooling MAATs with depth and age. These repetitive transitional shifts in vegetation on the south-west coast could imply tropical periods being characterised by flora adapted to summer rainfall (Fig. 3.7, 3.8). Asteraceae (in particular Mutisiaea) pollen, first appear at a borehole depth of 39.5 m, and these ancient angiosperms are known to prevail even under summer rainfall (Doyle, 1998).

3.6.7 Stable isotope ranges

The $\delta^{13}\text{C}$ range of values (-27.1‰ and -24.3‰) corresponds to vegetation dominant in C_3 plants ($\sim -28.1\text{‰} \pm 2.5\text{‰}$; Day, 1996). Temperate plants have a carbon isotope signature (-26.5‰; Day, 1996) closer to that of the averaged signal (-25.9‰) obtained from the peats (Fig. 3.6, 3.9). As the palaeoflora reported here suggest the presence of arboreal plants, the $\delta^{13}\text{C}$ values reported in forested areas was considered for comparison purposes. The $\delta^{13}\text{C}$ values may be affected by position of plant species in the biome, as gradients of increasingly negative $\delta^{13}\text{C}$ with depth from canopy top have been reported (van der Merwe and Medina, 1989). Palynological data from this study suggests a predominance of trees and ferns (forested landscape), but the carbon signal implies an open riparian forest not prone to the fractionation measured in modern dense forests. Other intrinsic and extrinsic factors affect the $\delta^{13}\text{C}$ value, such as specific environmental parameters (humidity, temperature) and the plant's physiological tolerances (e.g. podocarps which assimilate carbon less efficiently even

under elevated CO₂ levels) which ultimately affects the degree of carbon isotope fractionation (Schleser *et al.*, 1999; Bechtel *et al.*, 2008; Royer, 2006; Tong *et al.*, 2009). These perturbations (in ambient light, carbon dioxide, rainfall) reflect restrictions to the plants productivity under given environmental factors. Under ideal conditions of optimal light, carbon dioxide concentrations and water availability the δ¹³C values of plant OM would be light, which is what is noted in the Noordhoek data (Day, 1996).

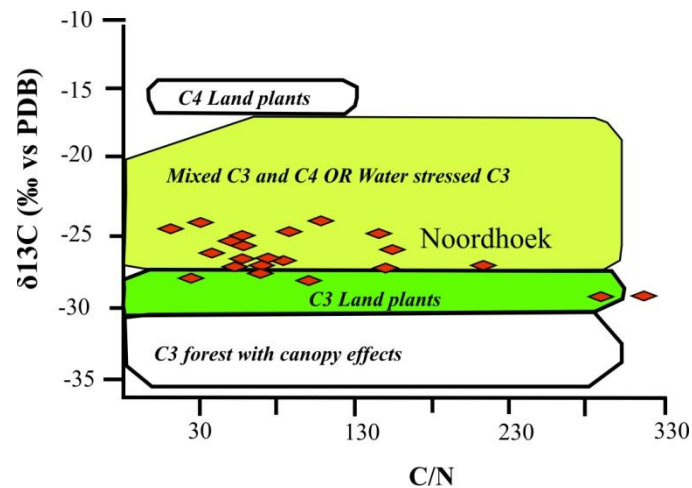


Figure 3.9. Carbon isotope ranges versus C/N ratio for different photosynthetic groups to aid organic matter source identification. Noordhoek Avondrustvlei core material overlaps the C₃ land plant zone and a mixed C₃/C₄ or water stressed C₃ zone (Adapted from Shunk *et al.*, 2009).

The averaged δ¹³C value of -25.9±0.8‰ for the high MAAT unit over the depth interval 18 m to 31.3 m is comparable with that of the low MAAT group's of (-25.9±0.7‰), even given the significant differences in vegetation type and abundance (Fig. 3.6, 3.9). It can be assumed that the conditions during plant growth were not limited by temperature, as both high and low MAATs recorded isotopically light signatures. The abundance of podocarps lower in the stratigraphy and their inability to assimilate carbon dioxide efficiently under high carbon dioxide concentrations, however, could imply that carbon dioxide concentrations were not elevated during this period; therefore this greenhouse gas would not have been a factor in moderating climate over this period. This is further reinforced by the lower MAATs. The Noordhoek δ¹⁵N values average 2.1 ±1.4‰, which falls into the range of most soils (+2 to +5‰), but implies high leaf litter content (Sharp, 2007). This would fit the environment of deposition and a forested scenario. This low δ¹⁵N value further complements the idea of a neutral to acidic pH wetland environment at the time of deposition (Fig. 3.5). Higher δ¹⁵N values do not necessarily correlate with higher TN or TOC values (Fig. 3.5). However, there is

a general positive linear correlation (correlation coefficient of 0.54) with raised MAATs and increased $\delta^{15}\text{N}$ values (Fig. 3.5).

3.6.8 Southern Hemisphere comparisons and factors influencing south-west coast climate

Study of Pliocene sediments from the Cape Basin ODP site 1085 has allowed for rainfall to be indirectly inferred by Sancetta *et al.* (1992). This demonstrated that Pliocene interglacial periods, between Antarctic glaciations, are characterised by high marine primary productivity and increased terrigenous input related to summer rainfall (Sancetta *et al.*, 1992). Dowsett and Willard's (1996) study confirmed that both terrestrial and marine changes along the south-west coast were linked to sea surface temperatures changes; ultimately controlled by the southward movement of subtropical high pressure cells during warmer interglacial intervals. Diester-Haas *et al.* (2002) application of these results to the late Miocene core, taken from ODP Site 1085, allowed for the inference that during cool periods (e.g. between 6.7 and 6.5 Ma) winter rainfall predominated with summer precipitation falling during interglacials.

The Noordhoek area currently has a winter rainfall climate related to the complete glaciation of Antarctica and the related changes in atmospheric and oceanic circulation starting at ~14 Ma (Zachos *et al.*, 2001; Cowling *et al.*, 2009). Noordhoek samples (between 18 m and 31.1 m depth below surface) appear coincidental with the middle Miocene climatic optimum (MMCO), due to elevated MAATs and correspondence with the regional sea level curve for the south-west Cape of Cole and Roberts (1996). This would place them with into a Miocene interglacial meaning rainfall may have been likely in summer months (Fig. 3.10). The Noordhoek core could provide a unique insight into the transition from summer- to winter- rainfall dominated climate and the resulting floristic changes. These samples are also broadly correlated with elevated temperatures of the Southern Ocean and with an early-Middle Miocene transgression (Fig. 3.10; Cole and Roberts, 1996). The pollen of this sample interval is characterised by the presence of palms (cold intolerant) which are a good index species for global warming (Fig. 3.7; Walther *et al.*, 2007). As palms cannot endure freezing and frost damage typically associated with winter rainfall this could further imply summer rainfall regime (Walther *et al.*, 2007). Importantly, Coetzee (1978a) bases the extinction of *Palmae* from the Noordhoek site as a result of increased Antarctic re-glaciation at around 14 Ma. This is likely on the basis that the ecological tolerance of palms is narrow when

considering decreasing temperatures, increased seasonality and decreasing rainfall limited to winter months. This has been noted before as the palm record from Northern Hemisphere sites show extinction related to Northern Hemisphere early-late Pliocene glaciations (Coetzee, 1978a).

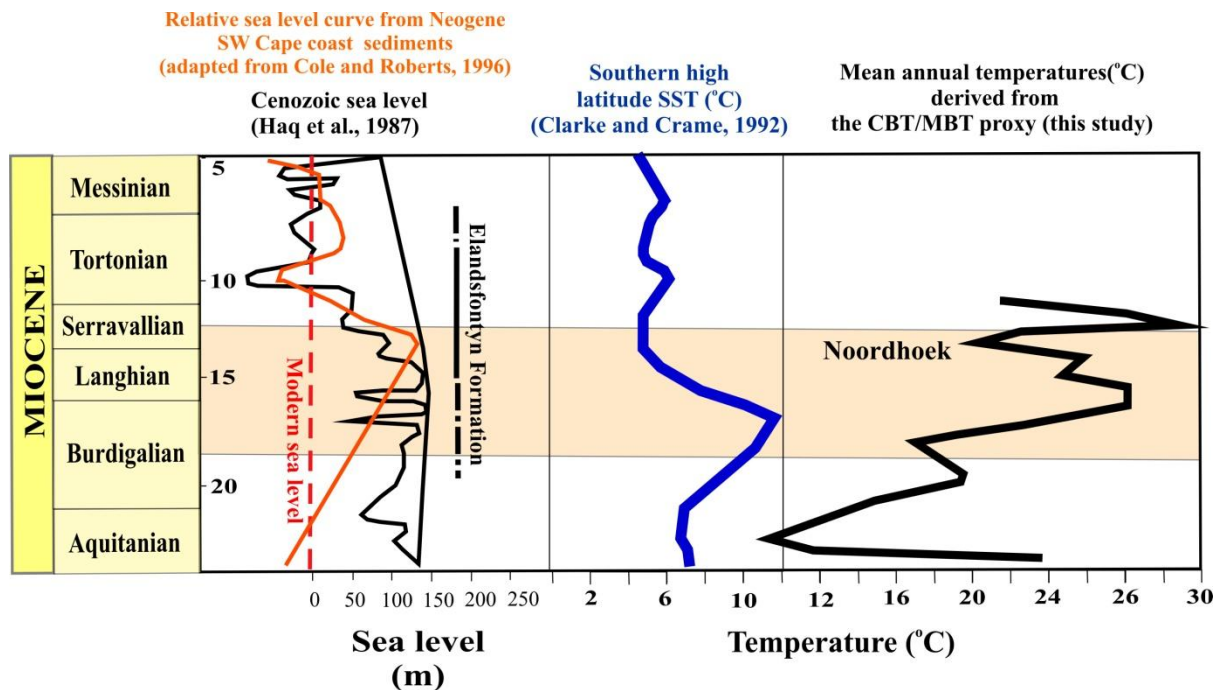


Figure 3.10. Relative sea level curve (orange) from Neogene south-west Cape coast sediments South Africa (adapted from Cole and Roberts, 1996) in comparison to global sea level (thin black line; Haq *et al.*, 1987) and Southern Ocean high latitude sea surface temperatures (blue curve; adapted from Clarke and Crame, 2006). The Noordhoek Avondrustvlei core sediment’s bacterial tetraether lipid derived terrestrial palaeotemperature curve (mean annual air temperatures; thick black line). Pale orange block denotes time interval over which the Middle Miocene Climatic Optimum (MMCO) occurred.

Figure 3.10 captures the variability of the Noordhoek tetraether membrane lipid derived MAATs against the south-western Cape’s Miocene relative sea level, global sea level and Southern Ocean SSTs. Encouragingly, the tetraether derived MAATs in association with the pollen results present a good fit with the middle Miocene transgression recorded from south-west coast sedimentary archive (Cole and Roberts, 1996). Given the broad age range (from pollen data) and the elevated period of MAATs a best fit of this data was attempted onto the regional and global sea level curves with respectable results (Fig. 3.10).

Open ocean oxygen isotopes and SST, calculated using the TEX_{86} and UK'_{37} proxies from Cape Basin sediments at ODP Site 1085, show a gradual decline in Miocene sea temperatures from extremely high (~27 °C) values at roughly 14 Ma (and prior) to 18 °C by

the late Miocene (~5 Ma) (Dupont *et al.*, 2009). These high SSTs are related to global ocean warming of the MMCO, with the lowered temperatures a result of the glacioeustatic sea-level fall (due to West Antarctic ice sheet growth at 8.5 Ma; Gersonde and Censarek, 2006), and bottom water cooling (associated with increased upwelling; Westerhold *et al.*, 2005; Dupont *et al.*, 2009). Modern SSTs in this region (at ~16°S) are much lower on average (20.6 °C; Ansorge and Lutjeharms, 2007). Elevated Miocene SST would allow for maintained high terrestrial temperatures and humidity, which gives credential to the elevated terrestrial MAATs at Noordhoek between 18 m and 32.4 m below surface (Fig. 3.10).

This clear-cut scenario may be more complicated when considering that re-glaciation periods in the evolution of Antarctica affect climate; with ‘interglacial’ periods, related to transgression along the south-west coast (Fig. 3.10), influencing rainfall in summer (Diester-Haas *et al.*, 2002). The stimulation of changes in the atmospheric circulation over Southern Africa which would lead to these changes is largely dependent on the Southern Oscillation, Walker circulation and other forcing mechanisms ultimately affecting the moderation of extreme climatic events (Camberlin *et al.*, 2001; Vogel, 2003).

The reported Southern high latitude SSTs (Clarke and Cramer, 1992; Zachos *et al.*, 2001) do not appear markedly elevated for MMCO conditions and the SSTs data reported by Dupont *et al.* (2009). The low SSTs from high latitude sites near Antarctica may report noticeably lowered temperatures due to the establishment of the Circumpolar Current and its prevention of warmer tropical waters flowing further south (Bice *et al.*, 2000; Potter and Szatmari, 2009). Modelling of Southern Ocean palaeo-heat transport illustrates that there is a general decrease in heat transport to the pole during the Miocene, which could contribute to a higher gradient between the pole and 33°S (Bice *et al.*, 2000). Furthermore, elevated SSTs alter the low- and high-phase Southern Oscillation and therefore are integral to this southern Africa climate forcing mechanism (Vogel, 2003). Sporadic upwelling of the cold (modern – 12 °C ±2 °C) westerly running BUS in the early to middle Miocene meant that the offshore west coast waters were still warmer than present (Schalke, 1973; Tankard and Rogers, 1978; Cowling *et al.*, 2009). Presently, continuously high SSTs are associated with increases in rainfall (Camberlin *et al.*, 2001; Vogel, 2003). Higher SSTs (in the region of 28 °C) and lower terrestrial MAATs, as for the samples between 18 m and 31.3 m depth, are likely to have resulted in a steeper ocean-atmosphere-land gradient. The supplementary influence of the BUS as it became a dominant influence on terrestrial climate in the middle Miocene

would mean a significant variation in the amount of rainfall received onshore (Marlow *et al.*, 2000; Pegion and Kumar, 2010).

3.6.9 Northern Hemisphere comparisons

As the MMCO was a global phenomenon it was likely that data from both hemispheres would be comparable. The coupling of terrestrial and marine climate records taken in the Northern Hemisphere, thus, acted as a basis and a correlative for the Southern Hemisphere comparisons (Fig. 3.11 and 3.12; Zachos *et al.*, 2001; Mosbrugger *et al.*, 2005; Kürschner *et al.*, 2008; Donders *et al.*, 2009). Figures 3.11 and 3.12 deal with the comparison of the Noordhoek MBT/CBT proxy derived MAATs with European terrestrial and marine palaeotemperature records. It is acknowledged that there are poor chronostratigraphic constraints of the Noordhoek sediments and that the uppermost samples, between 1 m - 2.5 m, are Quaternary, have been removed for the purpose of comparison (Zachos *et al.*, 2001; Mosbrugger *et al.*, 2005; Donders *et al.*, 2009; Jiménez-Moreno *et al.*, 2010).

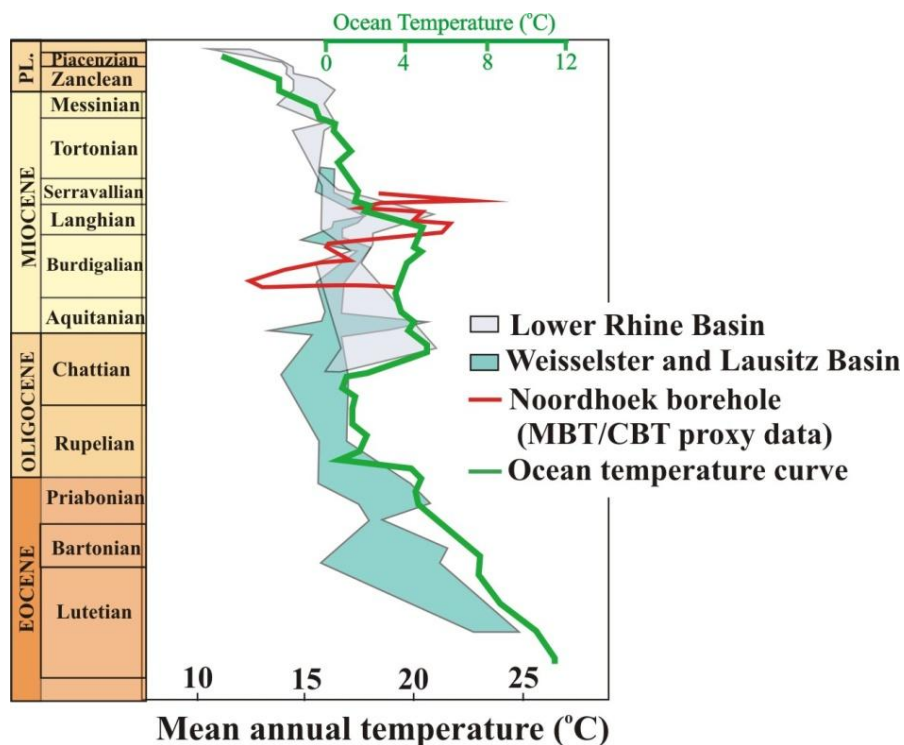


Figure 3.11. Continental temperature curves (Blue coloured blocks) for Central Europe during the last 45 My (Mosbrugger *et al.*, 2005) in comparison with the global marine oxygen isotope record (green curve) of Zachos *et al.* (2001), adapted to the International Commission on Stratigraphy 2004 time scale. Superimposed over these temperature curves is the MAAT record (thick red curve) from the Noordhoek borehole, representing the terrestrial record of climate for the Miocene period in south-western Cape, South Africa.

During the MMCO (~Burdigalian - middle Serravallian) Europe experienced elevated MAATs, ranging between 21 °C and 28 °C, and global SSTs (Fig. 3.11, 3.12; Zachos *et al.*, 2001; Kürschner *et al.*, 2008; Jiménez-Moreno *et al.*, 2005; Jiménez-Moreno *et al.*, 2010). Mega-mesothermic to mesothermic flora transitions in Europe (specifically Spain, Southern France, Austria and Hungary) establish that there was a decrease in MAAT from the middle Miocene (temperatures averaging ~23 °C), to ~14 °C by the early Pliocene (Fig. 3.8, 3.11; Mosbrugger *et al.*, 2005; Kürschner *et al.*, 2008; Jiménez-Moreno *et al.*, 2005; Jiménez-Moreno and Suc, 2007; Jiménez-Moreno *et al.*, 2010; Ivanov *et al.*, 2010).

A relationship was noted when comparing the global middle Miocene temperature peak of the Mosbrugger *et al.* (2005) study with the MAATs derived from the Noordhoek core, based on the palynomorph-derived age range and sea-level history (Fig. 3.11). It appears that European MMCO terrestrial temperature records are similar to the ‘high’ temperatures measured between 18 m and 31.3 m depth below surface at Noordhoek (Fig. 3.11; Kürschner *et al.*, 2008; Jiménez-Moreno and Suc, 2007; Jiménez-Moreno *et al.*, 2010). This indicates that palaeoflora tolerances recorded from Northern and Southern Hemispheric sites indicate similar climatic regimes during this period (Fig. 3.11).

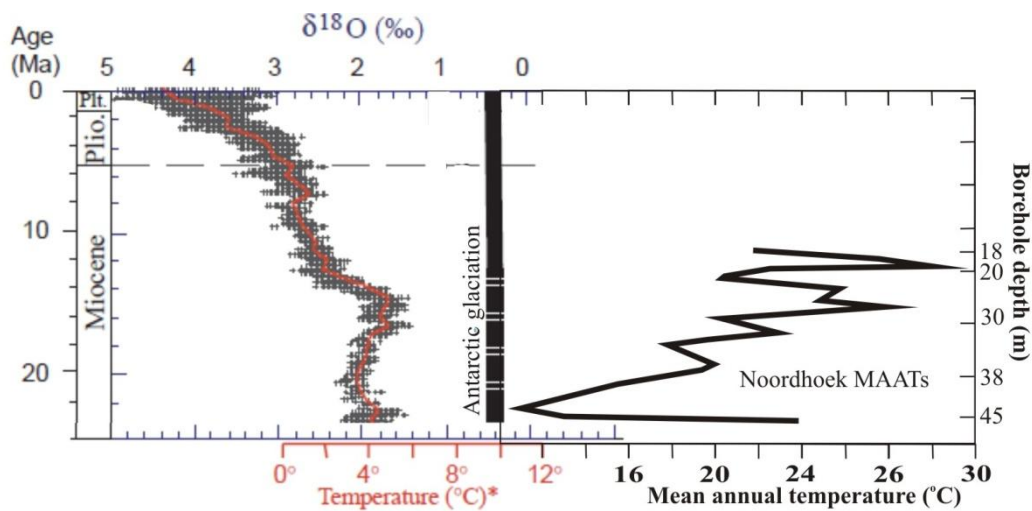


Figure 3.12. Comparison of benthic foraminifera $\delta^{18}\text{O}$ values from the Miocene-Pleistocene (Plt) and associated recorded temperatures (red curve) with that calculated from the CBT/MBT proxy for the terrestrial realm, calculating mean annual air temperatures (MAAT °C – black curve) for Noordhoek on the south-western Cape coast, South Africa (Adapted from Zachos *et al.*, 2001). Sample interval shown is between 18 m and 45.5 m depth below surface and has excluded uppermost Quaternary samples at 1 m and 2.5 m depth.

Mosbrugger's *et al.* (2005) megaflora study has demonstrated that both long term variations and short term oscillations in European Mio-Pliocene continental climate co-vary with the marine isotope studies. This account from the Northern Hemisphere appears to be comparable with that of the Noordhoek samples which show a similar temperature pattern with the offshore data (including global sea level data), and interestingly the Northern Hemisphere (Fig. 3.11, Zachos *et al.*, 2001). The rate of cooling on continental and oceanic scales after the MMCO are staggered (Mosbrugger *et al.*, 2005; Donders *et al.*, 2009). Continental cooling is much slower than that documented by in the marine record, and this seems to hold true for the Noordhoek data (Fig. 3.10, 3.12; Zachos *et al.*, 2001; Mosbrugger *et al.*, 2005; Donders *et al.*, 2009).

These associations have been cautiously attempted because of the difficulty in linking data with other Northern Hemisphere (or even southern African) sites, especially in light of the lack of a comprehensive chronology for the Noordhoek sediments. Moreover, if these sediments cannot be placed in more precise geological time frame, then estimating influencing factors of environmental change from other global sites is more complicated and more intensely subjective. Departure from Northern Hemispheric trends, after the MMCO, is likely because of hemispheric discontinuity associated with changes in atmospheric and oceanic circulation.

3.7 Conclusion

Although sparsely sampled, the Noordhoek core shows interesting palaeoclimatic results and the potential for further more detailed study. The palynological study of the Noordhoek 'Avondrustvlei' core in comparison to Coetzee's (1978a, b) work and that of other authors from southern Africa and the Southern Hemisphere provide a Miocene age for the peat unit below 18 m depth below surface. Furthermore, this work has provided idealised depth constraints for the pollen subzones of Coetzee's (1978a) pollen zone L (Fig. 3.8). It has also been used to infer palaeoenvironmental change of the south-west coast. Cool and temperate climate palynoflora of the stratigraphically lower samples (below 32.4 m depth below surface) give way to mega-mesothermic taxa and increasingly tropical climatic conditions with stratigraphic height to 18 m depth surface (Fig. 3.8). The presence of charcoal and lowered palynomorph counts at specific stratigraphic intervals indicate times of climatic stress linked to drought and fire. The upper 2.5 m have not been included in this analysis as

these samples represent Quaternary climate change. The MBT/CBT proxy results indicate increasing temperatures with increasing stratigraphic height, with a clear division between temperate and tropical climatic conditions (Fig. 3.8). The palynoflora confirmed the bacterial membrane lipid derived temperatures, and affirm their use in South Africa (Fig. 3.7, 3.8). The comparison of the Miocene south-west coast's regional climate with those reported from Southern and Northern Hemispheres show similar patterns (Fig. 3.10, 3.11 and 3.12).

Importantly, for Quaternary-aged climate studies it has been noted that the global pattern of climate change, gathered from marine isotopes, does not seem to reflect the regional conditions within Southern Africa (Chase, 2010). If this is the case for the relatively well-studied past 2 million years then, potentially, there is greater room for error when considering the past 20 million years in South Africa. Caution must be taken in viewing and interpreting these results.

3.7.1 Drawbacks and future research

A drawback encountered both from a palynological and biogeochemical perspective was that the organic sediment was not continuous. Light coloured, pure quartz sands occur continuously through a large portion of the core (~15 m) and sandier horizons were interbedded in the peat succession below 18 m depth below surface. These units do not contain any/enough pollen or organic material for analyses. Consequently large intervals between certain samples (e.g. 2.5 m and 18 m depth below surface) cannot be avoided. Importantly, finer resolution sampling would provide a more detailed study of the terrestrial Miocene palaeoenvironment in Southern Africa. This could only improve the understanding of Miocene climate regionally and in the Southern Hemisphere. Moreover, this would compliment Northern Hemisphere research for a more encompassing perspective of global climate, especially in light of climate change. With this in mind, it would be useful to calibrate the CBT/MBT proxy for use in Southern Africa. Lastly, to firmly and independently date the Noordhoek core would greatly add to the significance of this palaeoenvironmental data, as well as that of future studies.

4 Langebaanweg Fossil Site

4.1 Introduction

The largest lagerstätte of excellently preserved Mio-Pliocene terrestrial fauna in South Africa is located at Langebaanweg (Saldanha region; Fig. 4.1). The Langebaanweg (LBW) research area, a National Heritage Site, is an internationally known deposit which was originally a large scale phosphate mine and now forms the West Coast Fossil Park (Hendey, 1982; Roberts *et al.*, in review). The West Coast Fossil Park is located between Hopefield and Vredenburg, 120km north of Cape Town along the south-west coast (Fig. 4.1). It lies on an established coastal platform with the Great Escarpment to its landward site (Roberts *et al.*, in review).

The core drilled at the West Coast Fossil Park at Langebaanweg ‘E’ Quarry captures the Elandsfontyn and Varswater Formations of the Sandveld Group. Previous palynological studies and reviews of the Elandsfontyn and Varswater Formations by Coetzee and Rogers (1982), van Zinderen Bakker and Mercer (1986) and Scott *et al.* (1997) illustrate a change in palaeovegetation, from riparian tropical and temperate forest to the expanding Pliocene grasslands, and winter rainfall fynbos biomes.

Grasslands are thought to have broadened globally during the late Miocene-early Pliocene, and gave rise to summer-rainfall dominated savanna biomes now firmly established in southern and east Africa (Cerling *et al.*, 1997; Franz-Odenaal *et al.*, 2002). Coetzee and Rogers (1982) state that the Western Cape fynbos taxa today are likely to carry the remnant signature of this summer-rainfall dominated climate due to their rapid vegetative growth spurts at the end of summer, when rainfall is the lowest in the south-western Cape.

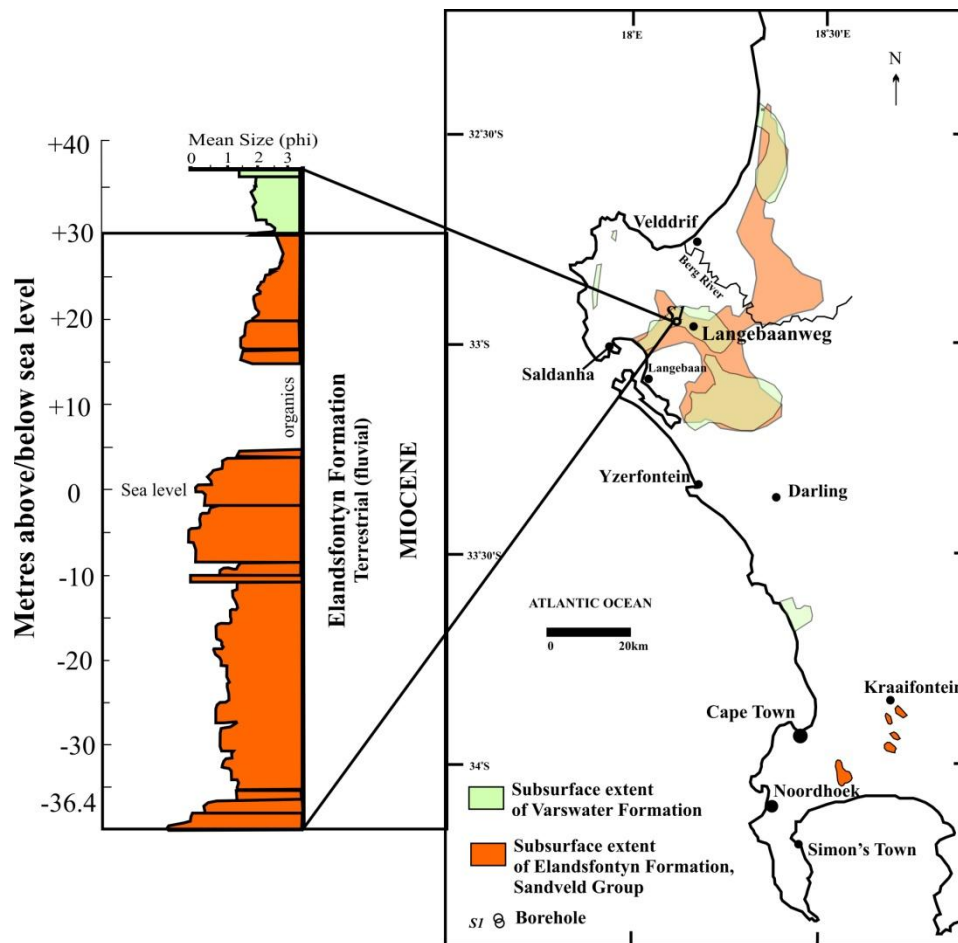


Figure 4.1. The subsurface extent of the Elandsfontyn Formation, Sandveld Group, which unconformably overlies Precambrian basement, south-western Cape, South Africa in relation to the study site at LBW and the core (S1) (adapted from Roberts, 2006a).

4.2 Regional geological setting and previous research

The sediments at LBW have undergone various nomenclature changes since their first informal names were assigned (Table 4.1). Roberts (2006a, b, c and d) revised the coastal Cenozoic lithostratigraphy of the south-western Cape and established the Sandveld Group, comprising the Elandsfontyn, Varswater, Langebaan and Springfontyn Formations (Fig. 4.1).

Table 4.1. Compilation table of previous and modern nomenclature of the Varswater Formation at LBW (Adapted from Roberts, 2006d).

Hendey (1970)	Tankard and Rogers (1978)	Rogers (1982)	Roberts (2006)
Bed 3	Pelletal Phosphorite member	Pelletal Phosphorite member	Muishond Fontein Peletal Phosphorite Member (MPPM)
Bed 2	Quartzose sand member	Quartzose sand member	Langeberg Quartz sand member (LQSM)
	Gravel member		Konings Vlei Gravel Member (KGM)
Bed 1	Kaolinitic clay and fine quartzose member	Saldanha Formation	Langeenheid Clayey Sand Member (LCSM)
	Saldanha formation (mottled silty clay)	Elandsfontyn Formation	

4.2.1 Dating of the Elandsfontyn Formation at LBW

Biostratigraphic dating has been conducted on the Mammalians of LBW, especially of the upper Varswater Formation, because of their large numbers and variety; very little focus has been placed on the flora of the underlying Elandsfontyn Formation (Coetzee, 1978b; Tankard and Rogers, 1978; Hendey, 1974, 1981, 1982, 1983; Coetzee and Rogers, 1982; Franz-Odendaal *et al.*, 2002; Matthews *et al.*, 2006; Matthews *et al.*, 2007).

A biostratigraphic age of middle Miocene has been assigned to the Elandsfontyn Formation and Mio-Pliocene to the Varswater Formation (Dingle *et al.*, 1979; Hendey, 1974, 1981, 1982, 1983; Coetzee and Rogers, 1982). These ages are reaffirmed by correspondence of the Cenozoic Western Cape sea-level fluctuations to global Cenozoic sea-level trends (Tankard, 1976; Haq *et al.*, 1987; Shackleton, 1995; Franz-Odendaal *et al.*, 2002).

To place an independent uppermost age-constraint on the Elandsfontyn Formation the conformably overlying unfossiliferous Langeenheid Clayey Sand Member (LCSM), the lowermost member of the Varswater Formation, was analysed using palaeomagnetic dating. This was not, however, absolutely successful for the analyses only yielded one sample of Normal polarity (Roberts *et al.*, in review).

4.2.2 LBW palaeoflora

Coetzee's (1978a) pilot study of the organic-rich unit (uppermost Elandsfontyn Formation), below the main fossil bed at LBW, first gave clues as to the tropical floral assemblages present. This was later supplemented by a more detailed study of the peaty-clay and organic silty-clay horizons from the S1 borehole (33°58.20'S and 18°6.97'E; Fig. 4.1, 4.2) on Langeberg 188 Farm by Coetzee and Rogers (1982).

In comparison to the work of Tankard and Rogers (1978) of the Varswater Formation floras, Coetzee and Rogers (1982) study is comprehensive of the underlying LBW floras of the Elandsfontyn Formation. It establishes two pollen zones within the uppermost Elandsfontyn Formation of the S1 borehole (Fig. 4.2).

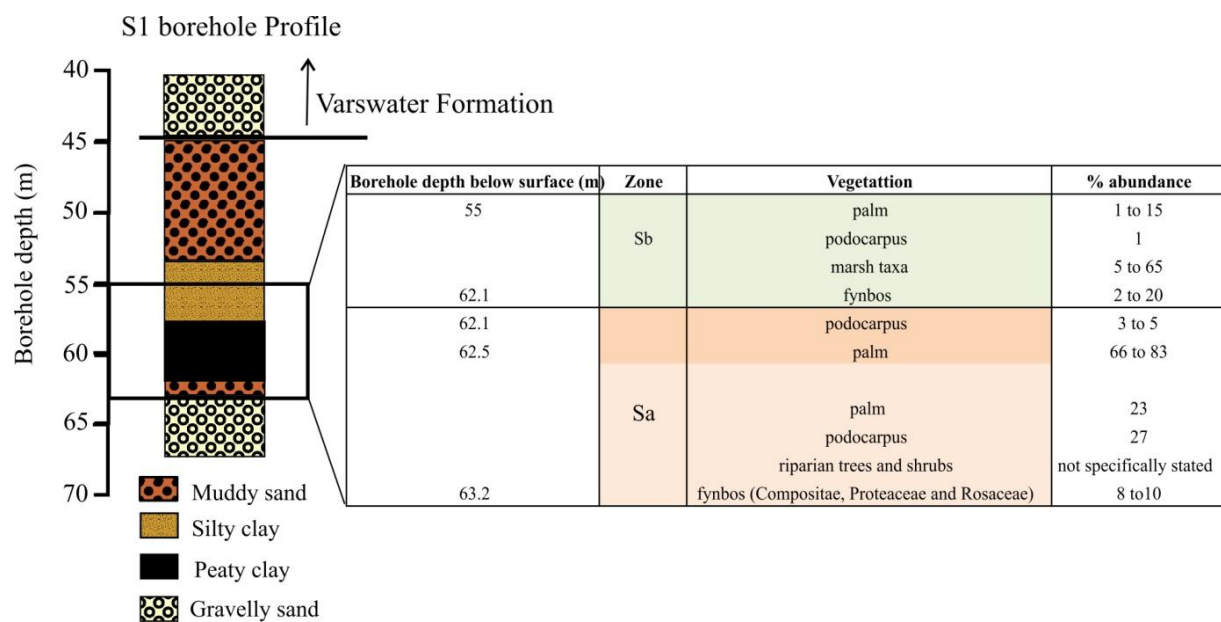


Figure 4.2. S1 borehole log (adapted from Coetzee and Rogers, 1982) highlighting the peaty- and silty-clay units of the study. Black box indicates depth over which samples were taken from the Elandsfontyn Formation. Inserted table provides percent abundances for the zones Sb (green) and Sa (orange) described by Coetzee and Rogers (1982). The Sb zone (orange) is characterised by an uppermost sample unit with high abundances of palm pollen (66-83%) and dramatic reduction of *Podocarpus* pollen (3-5%).

The lowermost pollen zone (Sa) between 62.1 m and 63.2 m borehole depth (2.95 m to 4.0 m above sea level) is dominated by palms (21-23%), *Podocarpus* (26-27%) as well as tropical forest and riparian plants such as Oleaceae, Celastraceae, *Celtis*, Casuarinaceae and others no longer occurring in the south-western Cape (Coetzee and Rogers, 1982). Fynbos

floras are present throughout the zone, e.g. Compositae (1-2%), Proteaceae (1-4%), and Rosaceae (1-9%). In the upper part of the Sa-zone, between 62.1 - 62.5 m depth below surface, there is a reduction of forest taxa with dominance in palms (66-87%) and lesser amounts of *Podocarpus* (3-5%; Coetzee and Rogers, 1982). Generally, this zone shows a decrease in 'wetness' of the environment over time.

The upper zone (Sb) is between 55.0 m and 61.2 m depth below surface, and shows a dramatic reduction in palm abundance (1-15%; Coetzee and Rogers, 1982). Forest elements are still present, but only as a result of their long-distance dispersal capability, as is the case with *Podocarpus* pollen ($\pm 1\%$; Coetzee and Rogers, 1982). This zone is considered to be deposited in a freshwater environment, and contains high proportions of marsh taxa (Coetzee and Rogers, 1982).

These studies exhibit the interplay of alternating wet and dry period floras (Coetzee and Rogers, 1982). However, Coetzee and Rogers (1982) largely account for the change in vegetation due to the meander and lateral migration of the river channel over time with the influence of sea-level variation. Thus, a change from river channel with significant representation of riparian forest (*Podocarpus* and other arboreal taxa) being developed proximal to it and earlier in succession, to later developed proximal and distal floodplains, where palm and swamp vegetation dominate on poorly drained soils (Coetzee and Rogers, 1982).

4.3 Methodology

Methods used are outlined in Sections 2.2.1 and 2.2.4.

4.4 Results

The seven LBW samples provided for analysis are homogeneous argillaceous (~80% clay) sediments, with the presence of organic matter noted by the dark colouration (brown to black; Fig. 4.3; Table A.5). Samples are siltier with stratigraphic depth (Fig. 4.3; Table A.5). The samples of this study form part of a fine-grained assemblage which caps an upward fining sequence of the fluvial Elandsfontyn Formation (Fig. 4.3).

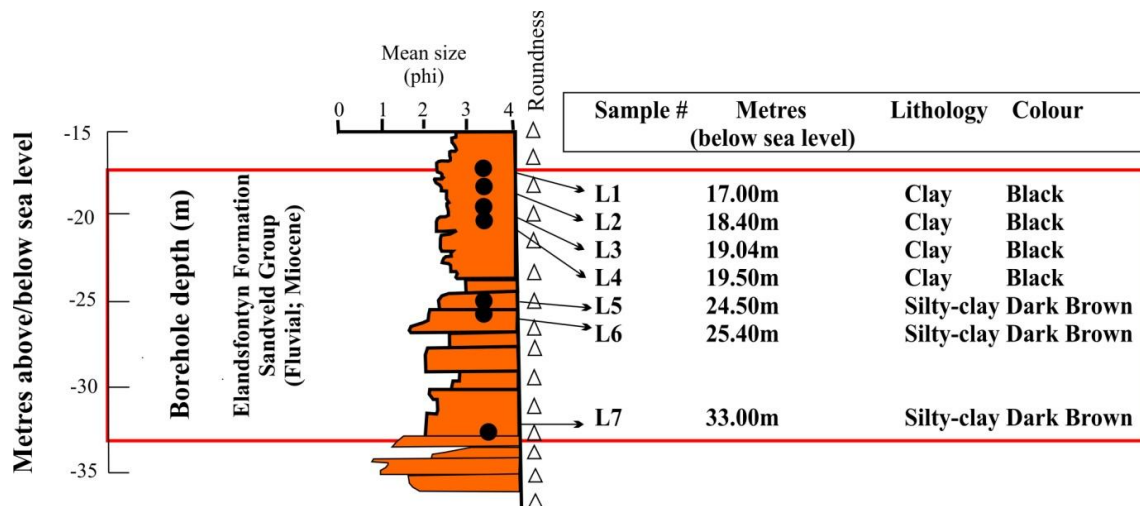


Figure 4.3. Log of the Elandsfontyn Formation for the Langebaanweg (LBW) core which records sediment present at borehole depths between 0 m and 35 m (Adapted from Roberts 2006b). Roundness refers to the degree of rounding of grains from which transport distances and depositional energy can be inferred. Red square denotes interval over which LBW samples were taken and table states sample numbers, depths, lithologies and their colouration.

4.4.1 Bulk geochemical parameters results

The total organic carbon (TOC) content of the samples ranges between 2.3% to 10.7% (Fig. 4.4; Table A.6). The highest TOC values (5.1 and 10.7) are recorded between 19.14 m and 19.50 m. The TOC values decrease, below 19.50 m, with stratigraphic depth and age (Fig. 4.4). Total nitrogen (TN) values are low, and range from 0.09% to 0.22% with an average of 0.14%. The TN values follow the same trend as the TOC values of decreasing percentages with depth (Fig. 4.4).

The TOC/TN ratios vary from 23 to 48.6% rising steadily from 18.40 m to 19.50 m before decreasing to the lowest ratio at 33 m depth below sea level (Fig. 4.4). The core samples are characterised by a negative spike at 18.40 m to low TOC, TN and TOC/TN ratio, followed by an increase to high TOC, TN and TOC/TN ratio at 19.50 m (Fig. 4.4).

The $\delta^{13}\text{C}$ record ranges from -25.5‰ to -24.3‰, with the averaged $\delta^{13}\text{C}$ values being -24.8‰ with the lightest value (-25.5‰) obtained at 19.50 m depth below sea level (Fig. 4.5E). The heaviest $\delta^{13}\text{C}$ values are recorded at 18.40 m and 19.14 m depth below surface.

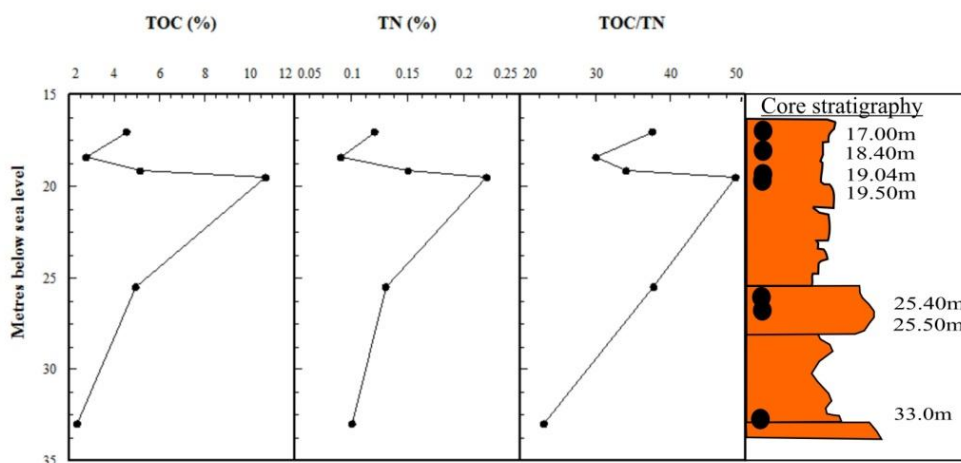


Figure 4.4. Langebaanweg organic clay sample depths below sea level (m) and core stratigraphy with corresponding total organic carbon (TOC) content (%), total nitrogen (TN) content (%) and the TOC/TN ratio.

The $\delta^{15}\text{N}$ values also show a narrow range of values between 2.4‰ (19.14 m) and 3.7‰ (17 m). The uppermost samples, between 17 m and 18.4 m depth, show low TOC values, moderately light $\delta^{13}\text{C}$ values and largely the most enriched $\delta^{15}\text{N}$ values in comparison to other samples within the study (Fig. 4.5A, E and F). Generally, the relationship between the $\delta^{13}\text{C}$ and $\delta^{15}\text{N}$ is antithetic with stratigraphic with a low R^2 value of 0.1 (Fig. 4.5E, F). The $C_{\text{org}}/N_{\text{org}}$ ratio had an average value of 40.9 and ranged between 27 (at 33 m depth below sea level) to 57.4 (at 19.5 m below sea level) (Table A.6).

The TOC values increase and then decrease with depth, whereas the $\delta^{13}\text{C}$ measurements show increasing values with stratigraphic depth (Fig. 4.5A). A peak in both TOC and $\delta^{13}\text{C}$ values is reached at 19.50 m depth below sea level with values of 49% and -25.5‰, respectively (Fig. 4.5A, E). These elevated values at 19.50 m then steadily decline to 33 m with a TOC and $\delta^{13}\text{C}$ values of 23% and -25.5‰, respectively (Fig. 4.5A, E). The uppermost samples taken at 17.0 m and 18.40 m depth below sea level have low TOC and $\delta^{13}\text{C}$ values, but elevated $\delta^{15}\text{N}$ values. In contrast, all other samples (between 19.14 m – 33 m depth below sea level) show elevated and steadily declining TOC and $\delta^{13}\text{C}$ values, with low $\delta^{15}\text{N}$ (Fig. 4.5).

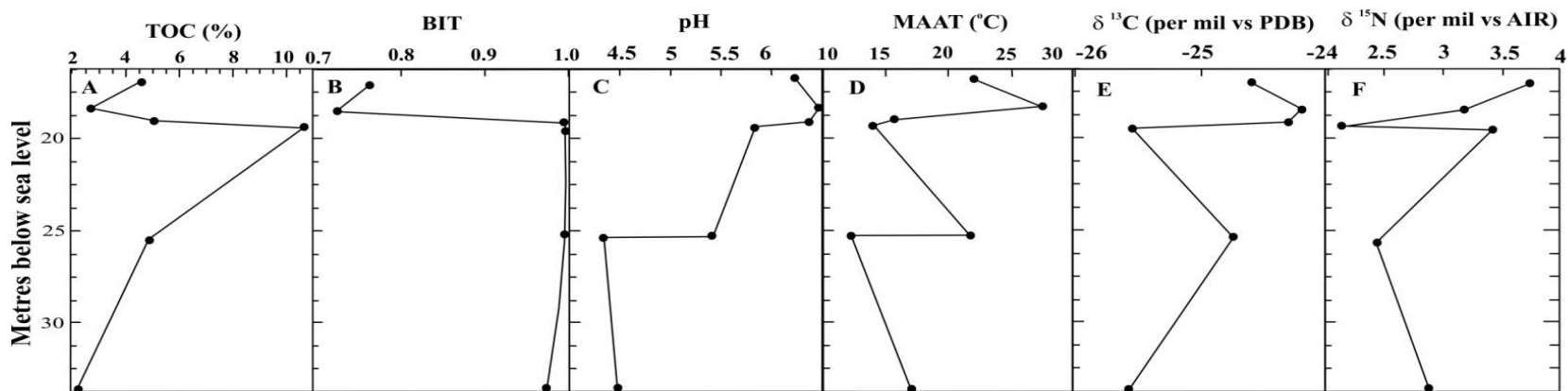
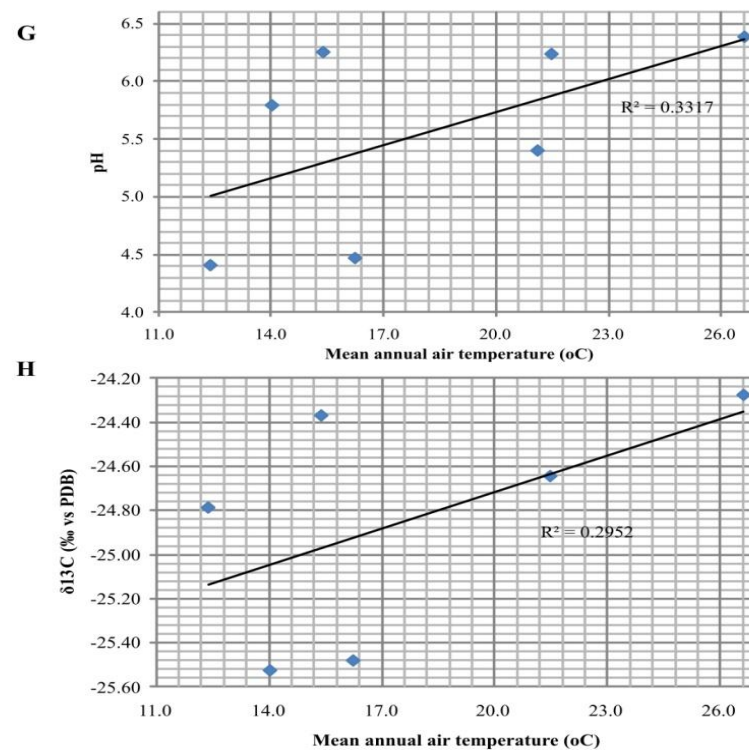


Figure 4.5. Stratigraphic down-core variability of the (A) bulk total organic carbon (TOC) contents, (B) Branched and Isoprenoid Tetraether index (BIT), (C) pH, (D) mean annual air temperature (MAAT - calculated from the CBT/MBT proxy), and (E) stable carbon and (F) nitrogen isotope values for the Langebaanweg samples. (G) and (H) are plots showing correspondence between the MAAT and pH and $\delta^{13}\text{C}$ measurements. Samples were obtained from a fluviolacustrine sequence, Elandsfontyn Formation, Sandveld Group, between 17 and 33 m depth below sea level. Sample at 25.40 m has no $\delta^{13}\text{C}$ and $\delta^{15}\text{N}$ reading.



4.4.2 BIT index and CBT/MBT proxy

The LBW core yielded seven samples for bacterial tetraether lipid analyses, and all samples showed a positive result (Fig. 4.5; Table A.7). The BIT indices for samples ranged from 0.78 to 1.0 (Fig. 4.5). The lowest BIT indices were recorded from samples at 17 m and 18.4 m of 0.78 and 0.74, respectively. All other samples showed high BIT indices above 0.98 (Fig. 4.5).

The MBT/CBT proxy was used to calculate mean annual temperatures (MAAT) and pH of the soil at time of deposition. The LBW samples have MAATs which range from 12.4 °C to 26.6 °C with a pH range from 4.4 to 6.4 over the 16 m's studied (Fig. 4.5, 4.6). There is a positive linear correlation, with low R^2 values, between MAAT, pH and stable carbon isotope values of samples (Fig. 4.5 G, H). Interestingly the MAATs, relative to the present day MAAT, show two distinct groupings:

1. 'Low' (<16°C) temperatures (samples between 19.14 – 33 m depth; with one high temperature anomaly at 25.40 m of 21.1 °C; Fig. 4.5, 4.6; Table 4.2)
2. 'High' (>21.5°C) temperatures (samples between 17 – 18.40 m depth)(Fig. 4.5, 4.6; Table 4.2)

Furthermore, a distinction can be seen in the BIT derived from bacterial tetraether composition of the samples. The samples falling into the 'high' temperature group have low BIT values, whereas the 'low' temperature group of samples have BIT indices of >0.98 (Fig. 4.5). In comparison to the other samples, the 'high' temperature group have several other distinguishing characteristics. They exhibit high $\delta^{15}\text{N}$ values with correspondingly higher $\delta^{13}\text{C}$, low TOC and near neutral pH of the sediment at time of deposition (Table 4.2). The predominately 'low' temperature group shows contrasting values to the uppermost samples, at 17 m and 18.4 m, with high BIT index, low $\delta^{13}\text{C}$ and variable and high TOC values, but lower MAATs and pH values (Fig. 4.5; Table 4.2).

Interestingly, the sample at 19.04 m depth below sea level showed very low $\delta^{15}\text{N}$ values with heavy $\delta^{13}\text{C}$ values and a correspondingly moderate to low TOC content which correspond to a low MAAT. The sample stratigraphically below it at 19.50 m shows the opposite trend, with high $\delta^{15}\text{N}$ values, enriched $\delta^{13}\text{C}$ values and extremely high TOC content corresponding to a low MAAT value (Fig. 4.6). These samples both record very low MAATs but show different and opposite trends regarding their bulk organic parameters. Similarly,

there is a pattern of high MAATs corresponding with heavy $\delta^{13}\text{C}$ values and lowered $\delta^{15}\text{N}$ values (e.g. sample at 25.40 m depth below sea level).

Table 4.2. Comparison between the two broad groupings of LBW samples based on measured bulk organic parameters and CBT/MBT proxy values. MAAT – mean annual air temperature.

	<i>'Low' MAAT group</i> <i>19.04– 33 m</i>	<i>'High' MAAT group</i> <i>17 – 18.40 m</i>
MAAT	Moderate to low (12.4 °C -21 °C; av. 16±3 °C):	High 21.5 °C -26.6 °C; av. 24±4 °C
pH	Neutral to acidic (4.4-6.3; av. 5.0± 0.8	Near neutral (6.2-6.4; av.6.0±0.11)
BIT	0.98-1.0	0.74-0.78
$\delta^{13}\text{C}$ (‰ vs. PDB)	Av.-25.1±0.6 ‰	Av. -24.5±0.3 ‰
$\delta^{15}\text{N}$ (‰ vs. AIR)	2.8±0.5‰	3.5±0.3‰
TOC	Av. 5.75±3.5	Av. 3.6±1.3
C_{org}/N_{org}	37.6±6.4	42.5±12.7

Additionally, when comparing the stable isotope values of the uppermost 'high' temperature group with that of the lower samples there is a trend of increasingly lower $\delta^{13}\text{C}$ values with depth (Fig. 4.6); with the highest $\delta^{13}\text{C}$ values recorded between 17 m and 19.14 m (Fig. 4.6). Broadly, there is a positive correlation (low R^2 value of 0.3) between the carbon isotope values and MAAT obtained, with samples of more negative $\delta^{13}\text{C}$ value correlated to lower MAATs (Fig. 4.5 G).

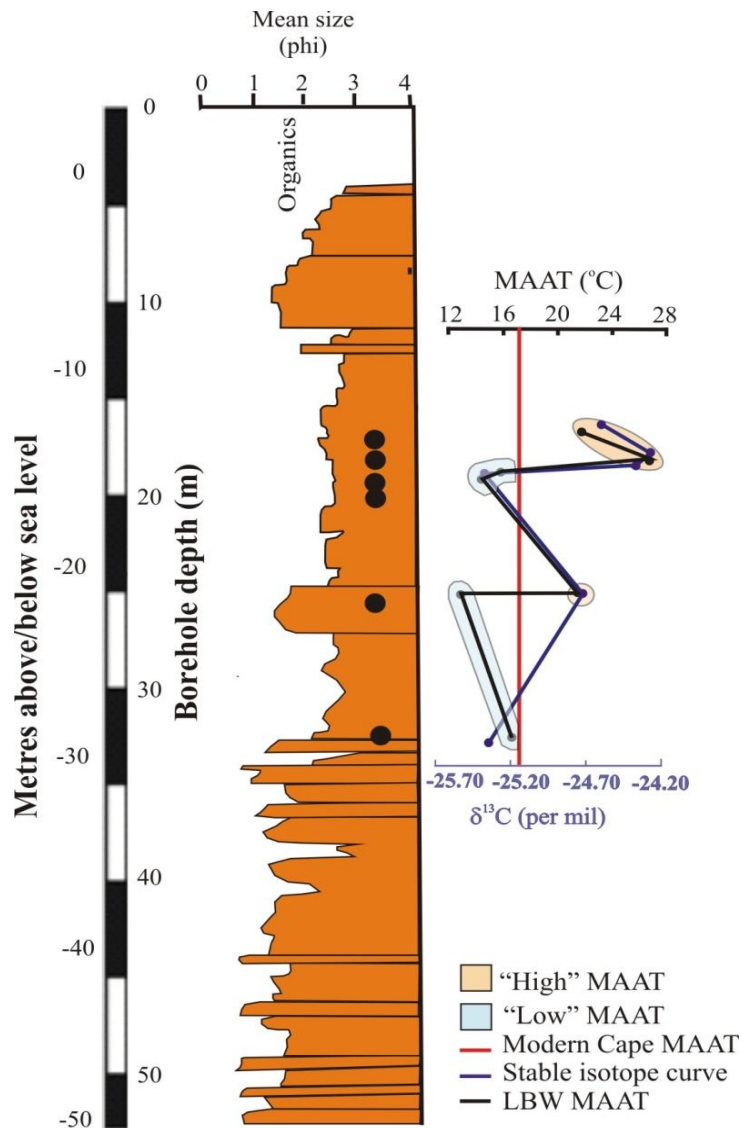


Figure 4.6. Elandsfontyn Formation log detailing where samples were obtained (below sea level; black filled circles) and the corresponding mean annual air temperatures (MAAT; black line) obtained from bacterial tetraether lipid composition analyses. The coloured areas indicate MAAT which were high (orange) and lower (blue) than the modern MAAT recorded for the Western Cape, presently (17°C). Stable carbon isotope curve (purple line) is shown in comparison to the MAAT.

Figure 4.7 is a comparison of this study's $\delta^{13}\text{C}$ and $\text{C}_{\text{org}}/\text{N}_{\text{org}}$ data with a composite organic matter source diagram adapted from Shunk *et al.* (2009). LBW samples have a narrow, light (more negative) $\delta^{13}\text{C}$ value distribution and low $\text{C}_{\text{org}}/\text{N}_{\text{org}}$ ratios. The $\delta^{13}\text{C}$ value range versus $\text{C}_{\text{org}}/\text{N}_{\text{org}}$ ratio illustrated that LBW samples fell into the category of 'mixed C_3 and C_4 vegetation OR water stressed C_3 ' (Fig. 4.7).

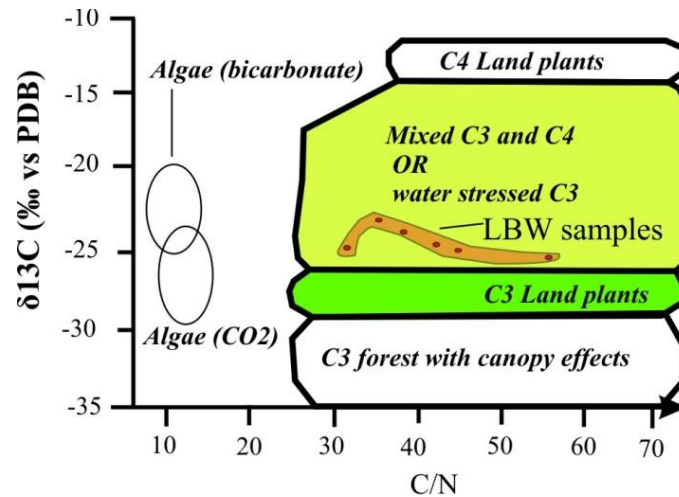


Figure 4.7. LBW samples $\delta^{13}\text{C}$ versus $\text{C}_{\text{org}}/\text{N}_{\text{org}}$ data (red dots circled by orange shape) plotted onto the composite organic matter sources diagram for C_3 , C_4 vegetation and algae (Adapted from Shunk *et al.*, 2009).

4.5 Discussion

4.5.1 Depositional setting

The sample sediments have been ascribed to deposits of the palaeo-Berg River (Roberts, 2006b). The size, uniformity and homogeneity of grains (from hand specimen and Council for Geoscience log) of all samples indicate deposition from suspension. Descriptive sedimentology of the samples showed no significant changes in colour, grain size or sorting between samples (Fig. 4.3). They are likely to represent the overbank fines, formed in the low lying alluvial plain of the coastal platform, owing to their clay-rich nature and the presence of organic material (pollen, charcoal) which is terrestrially derived (Fig.4.1, 4.3; Miall, 1985). Palynomorph studies currently being undertaken (by Dr. F Newmann of the B.P.I., University of Witwatersrand) show that the samples of this study contain pollen and charcoal.

The TOC index, a proxy for the measurement of the amount of OM in a system, was low (between 2.7% and 10.7%) and indicated that the OM source was diluted with significant inorganic clastic input during deposition, or OM was degraded after deposition (Meyers, 2003; Mielnik *et al.*, 2009). The high TOC/TN (averaged 35; standard deviation 3.01) and $\text{C}_{\text{org}}/\text{N}_{\text{org}}$ (averaged 41; standard deviation 10.52) ratios imply that the bulk organic matter contained cellulose and lignin and was not derived from algae in a lacustrine setting which exhibit low TOC/TN ratios (with a typical $\text{C}_{\text{org}}/\text{N}_{\text{org}}$ ratio of 13-14; Table A.6), but solely from terrestrial, higher-plant material (Fig. 4.4; Meyers and Lallier-Vergés, 1999; Meyers,

2003). The increased TOC and $\delta^{13}\text{C}$ values are likely indicative of increased productivity to 19.50 m depth, which is followed by a period of decreasing productivity to 33 m depth (Fig. 4.5). The spike in productivity at 19.50 m corresponds to an increase in the BIT index (to 1.0) which signifies a purely terrestrial source of the OM during sediment deposition (Fig. 4.5). The uppermost samples (17.0 m -18.40 m) show low BIT, TOC, elevated, less negative $\delta^{13}\text{C}$ values and elevated $\delta^{15}\text{N}$ values and MAATs which suggests that these samples are likely lacustrinal in origin.

The LBW samples showed two distinct groups of MAATs, and the BIT index reflected two different depositional environments for the sources of the organic matter (OM) within these groups. The 'low temperature' samples with BIT indices of >0.98 indicate all OM is terrestrial (Hopmans *et al.*, 2004). This confirms the overbank fines deposition of these sediments by the palaeo-Berg River, and suggests no influence by marine/lacustrinal OM. In contrast, samples at 17 m and 18.4 m record low BIT indices (<0.78) representing an increasing lacustrinal and/or coastal marine OM contribution (Fig. 4.5; Hopmans *et al.*, 2004; Weijers *et al.*, 2006b).

The meandering nature of the palaeo-Berg River means that channels may be periodically abandoned forming ephemeral (ox-bow) lakes (Miall, 1985; Nichols and Fisher, 2007). Furthermore, transitional lakes may form in the distal regions of a distributary system, on the alluvial plain, during periods of increased water supply (Nichols and Fisher, 2007). The changes in the proxy signal may also be related to the lateral migration of the river system and the concurrent changes in facies. The overbank fine deposits are likely to contain branched GDGTs within a developed soil profile which are unlikely to be affected by riverine branched GDGT production. Whereas, the MBT-CBT index of channel fills are likely to be influenced by the *in situ* production of branched GDGTs within the river system. It is important to note facies change as they are most likely to have bearing on the production and preservation of branched GDGTs, and therefore the interpretation of the proxy signal.

On the basis of basement configuration studies of the LBW area by Roberts *et al.* (in review), the Langebaan embayment, at the mouth of Saldanha Bay, is likely to have periodically held an expanse of water into which palaeo-Berg River sediments (Elandsfontyn Formation) were deposited. The location of the core in this study is within the Langebaan embayment making this assumption valid (Fig. 4.1). Ultimately, with lateral migration of the river system, the inter-fingering of channel, overbank fines and lacustrinal facies will develop as seen in the LBW core stratigraphically and geochemically (Fig. 4.1, 4.3).

Given the altitude of the site above modern sea level (~50 m), and taking into consideration a Miocene sea level high stand (Haq *et al.*, 1987; Kominz *et al.*, 1998) potentially of 150m, it is possible that the LBW coastal platform would have been periodically inundated. This is even if a pulse of uplift in the early-middle Miocene of 150 m is considered (Partridge and Maud, 1987). Ultimately, this would also allow for the higher crenarchaeol abundance within the BIT indices noted for samples at 17m and 18.40 m depth. It would also account for the lowered TOC and $\delta^{13}\text{C}$ values which would have meant that productivity would have declined with estuarine development/salt water intrusion, or lead to conditions of poorer preservation, into the wetland of the overbank fines (Meyers, 2003). The high $\text{C}_{\text{org}}/\text{N}_{\text{org}}$ ratio of these uppermost 'high' MAAT samples, a good indicator of the presence of lignin and cellulose of higher (non-aquatic) plants, points to a higher plant derived depositional setting (Sharp, 2007). The contribution of higher plant material therefore greatly outweighs that which may have been supplied by aquatic plants and/or lacustrine algal organic matter contribution (Meyers, 2003; Sharp, 2007).

There is little differentiation between the $\delta^{15}\text{N}$ of plants/plant material and the $\delta^{15}\text{N}$ value of soil in nitrogen-poor soils (Meyers, 2003; Sharp, 2007). Given the bedrock geology this is presently and most probably a past characteristic of the LBW area. The $\delta^{15}\text{N}$ values for the LBW samples fall within the accepted norm of soils of between +2‰ to +5‰ (Sharp, 2007).

The pH of the LBW samples all fell within near-neutral to slightly acidic values (Fig 4.5). The samples with low MAATs corresponded with more acidic sediment pH values (Fig. 4.5). Modern soil acidity is related to rainfall, with acidic soil profiles linked to increases in precipitation (Weijers *et al.*, 2007a). It can be inferred that sediments deposited below 19.50 m depth, experienced consistently high rainfall, and that plant matter deposition and decomposition facilitated the maintenance of low pH sediments (Killops and Killops, 2005). It is generally known, however, that lowered MAAT (as shown by the samples between 19.50 and 33 m) are likely to decrease the rate of organic matter degradation, and raise the sediment pH, as lesser amounts of humic substances are produced (Coûteaux *et al.*, 1995; Killops and Killops, 2005). The uppermost samples at 17 m and 18.40 m depth below sea level have high MAAT and near neutral pH. These samples are associated with warm temperatures and are likely to also represent a period of high rainfall and a sea level high stand during the late middle Miocene (Roberts, 2006d). This leads to a contradiction, as increased rainfall should lower the acidity of the sediment, however, if these uppermost samples are lacustrine in origin it is likely that they were buffered by the water column.

4.5.2 Regional climate and forcing mechanisms

On a regional scale pollen evidence, from sediments of uppermost Elandsfontyn Formation, indicates periodic flooding and drought within the Saldanha environs during the late middle Miocene (Fig. 4.7; Hendey, 1981; Franz-Odenaal, 2001; Franz-Odenaal *et al.*, 2003). Globally, the middle Miocene is considered a time of reduced seasonality and relatively stable climate with elevated temperatures, high humidity and rainfall. At LBW rainfall variability, with strongly developed wet (i.e. implied from palynomorph taxa) and dry (charcoal) year distinctions, are likely the result of changes in the strength and position of the westerlies, cloud bands and SSTs (Table 4.2; Coetzee and Rogers, 1982; Scott, 1994; Vogel, 2003). These forcing parameters of continental climate are strongly linked to Southern Ocean conditions (Gallagher *et al.*, 2001; Romero *et al.*, 2005), and ultimately coupled with Milankovitch cycles.

The ‘low’ mean annual temperatures (15.8 ± 3.3 °C) from stratigraphically lower (older) samples are comparable with modern winter mean annual temperatures for the Cape region today (average ± 12.5 °C; Table 4.2 and 4.3; Cowling *et al.*, 2009), but are more closely associated with the modern MAATs (17°C). These low MAATs, for the locality of the sample site and in the knowledge that the Miocene Epoch is generally typified by raised global temperatures, is unusual.

The samples with recorded ‘high’ MAATs (24 ± 3.6 °C) were deposited most probably during the late middle Miocene marine transgression due to the low BIT indices, high MAATs and sedimentology (Table 4.3). Study of the palaeo-Atlantic through the offshore Cape Basin sediments from ODP Site 1085 indicate declining Miocene SSTs during this time from (Table 4.3; Westerhold *et al.*, 2005; Dupont *et al.*, 2009). These high SSTs at the end of the MMCO would complement the high MAATs obtained for samples at 17 m (22 °C) and 18.40 m (27 °C) depth when it is considered that the ocean is a strong forcing mechanism of continental air temperatures (Dommenget, 2009).

Furthermore, during the deposition of these samples it is likely that rainfall was elevated. In southern Africa higher rainfall would be expected with elevated SSTs due to fluctuations in parameters of the Southern Oscillation such as evaporation and wind (Table

4.3; Lutjeharms *et al.*, 2001). Elevated SSTs give rise to the thermal expansion of ocean water and a concurrent rise in sea level; supporting the late Miocene transgression reported on the west coast (Kennett, 1977). Additionally, warm oceans have a lowered capacity for the storage of CO₂, further increasing the amount of this greenhouse gas in the atmosphere and the raising of global temperatures (Kürschner *et al.*, 2008).

The middle to late Miocene global cooling trend, as known from co-varying planktonic and benthic foraminifers stable oxygen isotope studies, is punctuated by several glaciation events (Mi-events) (Westerhold *et al.*, 2005). The cooling of SSTs (Table 4.3) has been related to glacio-eustatic sea-level fall (due to the WAIS growth), and bottom water cooling associated with increased upwelling (Westerhold *et al.*, 2005; Dupont *et al.*, 2009).

Table 4.3. Comparison table of modern Saldanha Bay mean annual air temperatures, sea surface temperatures, carbon dioxide concentration and precipitation levels in comparison to measured and predicated Miocene values.

Simulation	Mean annual temperature (°C)	Southern Ocean Mean annual sea surface temperatures (°C)	Atmospheric carbon dioxide (ppmv)	Average annual rainfall (mm)
Saldanha Bay (Present day)	17 °C (Adelana <i>et al.</i> , 2010). Mean annual summer air temperature range: 18.4 – 27.5 °C; Mean annual winter temperature range: 7.1 °C – 14.9 °C (Hanekom <i>et al.</i> , 2009)	16.3 °C (http://www.surf-forecast.com). Ranges from 10 °C - 16 °C within the Bay	387 ppmv (Tripathi <i>et al.</i> , 2009)	256 mm
Middle Miocene	3-6 °C higher globally 21.1 – 26.6 °C (this study); But also MAATs lower by 1 - 5 °C than modern Cape MAAT.	~ 27 °C at 14 Ma, decreasing to 18 °C at 5 Ma (Dupont <i>et al.</i> , 2009)	Globally 300 – 600 ppmv (Kürschner <i>et al.</i> , 2008)	Globally higher than present by at least 200 mm (Tong <i>et al.</i> , 2009))

There is an intimate connection between marine carbon drawn-down and SST cooling and continental climate, with short- and long-term oscillations of Mio-Pliocene terrestrial climate (of the Northern Hemisphere) seen in the marine isotope record (Mosbrugger *et al.*, 2005). This may also be the case with the western coast LBW site; however, more detailed

sampling would be required stratigraphically higher in the section following the high MAATs of the uppermost samples at 17 m and 18.40 m depth below sea level.

4.5.3 Palynomorphs, Elandsfontyn Formation deposition and LBW climate

Palynology of the S1 constrains palaeovegetation during the middle to late Miocene in the LBW area. Palynologically, the LBW core is periodically dominated by subtropical elements (palms) and temperate forested ones (Podocarps), as well as marsh elements with increasing stratigraphic height (Fig. 4.2; Coetzee and Rogers, 1982), which indicates a wetter less seasonal climate. This is especially true when compared to the present succulent shrubland and fynbos flora which thrive on winter rainfall and hot, dry summer months (Coetzee & Rogers, 1982; Hendey, 1982; Goldblatt and Manning, 2002; Cowling *et al.*, 2009).

Based on data of the Pollen Zones Sa and Sb from S1 borehole and that of the west coast Mio-Pliocene Zone L, I have attempted to consolidate these two schemes given estimated ages and taxa occurrence (Table 4.3). This proves difficult as Zone L is not furnished with borehole depths for zone occurrence but merely presence/absence data. Additionally, the palynological study presented by Coetzee and Rogers (1982) does not present a large enough database of palynomorphs for a detailed comparison of pollen types between Zones. Zone comparison was undertaken because the initial zones (M and L) erected by Coetzee (1978a) were a corollary of a compilation of all west coast Mio-Pliocene pollen, and therefore should act as a basis for future comparative work.

Palaeovegetation evolution, as stated by Coetzee (1978a) and Coetzee and Rogers (1982), suggest a gradual decrease in continental temperatures and rainfall with stratigraphic height, which is illustrated by a transition from subtropical and tropical vegetation (palms, riparian floras such as *Olea*) over time. Nonetheless, the limited portion of the S1 core studied may simply reflect a transition in the depositional environment with lateral migration of facies, and hence plant types associated with and distinctive of, the particular facies rather than significant regional climatic effects (Coetzee and Rogers, 1982). However, the rather significant decrease in the abundance of certain flora with stratigraphic height suggests that potentially climate may also have played a role in determining the presence and maintenance of certain taxa. Coetzee and Rogers (1982) only briefly considered the ecological tolerances of certain taxa (e.g. palms) in coping with extended water logging that characterises the Sb

zone of the core. Palm abundance decreases and abundance of swamp taxa increases with stratigraphic height, and this may be a factor of the lack of tolerance of palms to prolonged flooding which has been noted by Coetzee and Rogers (1982) (Fig. 4.2; Table 4.4). The presence of swamp elements indicates the inundation of the coastal plain, which may be a result of a rise in sea level, and could account for the wetland expansion landwards.

Table 4.4. Coetzee (1978b) pollen zones M and L as established from palynological studies of several west coast sites and the Langebaan site (from S1 borehole) for comparative purposes. Blue colouration highlights potential overlap between the Sa and Sb zones and that of Zone L.

Pollen zone (Coetzee, 1978b)	Vegetation (Coetzee, 1978b)	Abundance of pollen (%) (Coetzee, 1978b)	Pollen zones as established in Coetzee and Rogers (1982)	Suggested stratigraphy	
M	Present macchia	Ericaceae: 30-37%		Quaternary	
Lvii	First strong development of macchia	Last appearance of palm pollen	~Sb/Sa	TERTIARY	Pliocene
Lvi	Forest: Coniferae Casuarinaceae Cupanioidites	Podocarp (1-9%) Casuarineaceae (40%)	~Sb/Sa		Late Miocene
Lv	Palmae	Palms: 34%	~Sa		Middle Miocene
Liv	Restionaceae swamp	Podocarp: ±20%			Early Miocene
Liii	Forest: Coniferae, first Compositae				
Lii	Palmae	Palms (32%) (Podocaps: 1-9%)			
Li	Forest coniferae	Podocarp: ±20%			Late Oligocene

4.6 Conclusion

The south-western coastal plain's regional climate is a complex interaction of multiple factors. The depositional setting, riparian terrestrial floras and bulk organic parameters suggest a subtropical wetland environment which likely experienced the effects a sea level high stand during the middle Miocene (Table 4.3). Sedimentology and BIT indices of samples at 17 m and 18.40 m indicate elevated MAATs, and deposition of sediments within a lacustrine setting which may have been influenced by a marine incursion (likely linked to the eustatic sea level rise in the early-middle Miocene; Haq *et al.*, 1987) that ultimately disrupts productivity (lower TOC and $\delta^{13}\text{C}$ values). This disruption may be a factor of prolonged water logging through raised water table levels or as a factor of salt water intrusion

to which many plants are intolerant. Absolute age dating would be required to guarantee whether this assumption is valid. Sediments falling below these elevated samples record MAATs similar to present day conditions within Saldanha Bay (Fig. 4.5). Ultimately, perturbations in the SSTs during the middle Miocene caused changes in the Southern Oscillation which ultimately affected forcing mechanisms controlling continental climate change (Preston-Whyte and Tyson, 1988; Vogel, 2003; Dommenges, 2009).

5 Synthesis of LBW and Noordhoek Sites

5.1 Introduction

Although geographically separated the Noordhoek and Langebaanweg sites are considered lithostratigraphic and possibly temporal correlatives based on geology (both attributed to the Elandsfontyn Formation of Miocene age) and palynological associations (Fig. 5.1; Coetzee and Rogers, 1982).

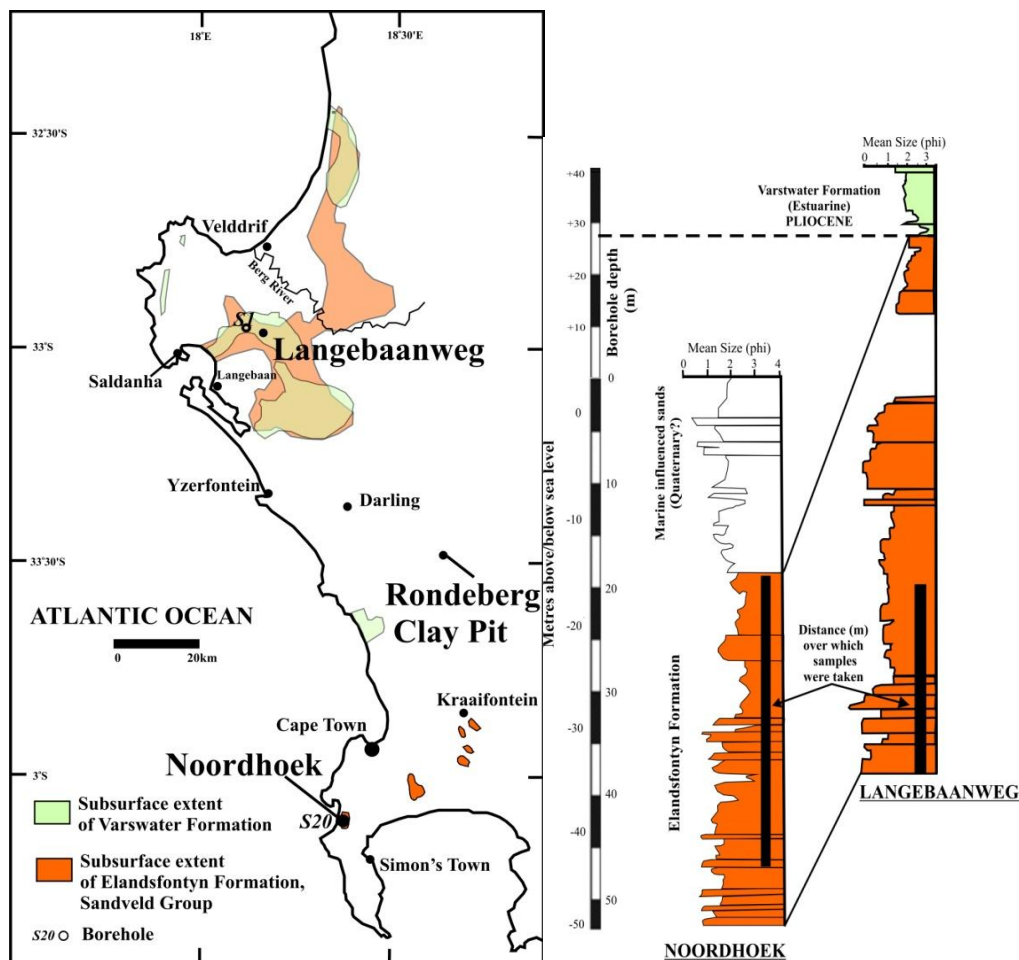


Figure 5.1. Stratigraphic log of the Elandsfontyn Formation from the cores taken at Noordhoek and Langebaanweg, South-west Cape coast. The thick black line indicates the distance over which samples were taken for the comparative studies. Sample intervals overlap between 17 m and 33 m depth.

This chapter focuses on comparing and contrasting these sites in terms of their biogeochemistry and palynology, with the assumption that the climate at two sites share

similar trends in mean annual air temperature (MAAT) variation. The organic parameters of the Miocene LBW and Noordhoek cores are discussed in the light that regional palaeoenvironmental and palaeoecological parameters may further enhance knowledge of the southern African climate in the early Neogene. A comparison between the two sites highlights the potential use of the mean annual air temperature record, in close conjunction with sedimentology and palynology, as a potential stratigraphic tool for geographically and geological coeval sites. Currently the two sites are situated in different climatic zones, with rainfall at LBW (~300 mm) being only ~one third of that at Noordhoek (~900 mm) due to northward attenuation of the polar frontal systems (Kruger, 2004). The question arises therefore-did this humidity gradient exist in Miocene times?

5.2 Middle Miocene Climatic Trends

The Middle Miocene Climatic Optimum (MMCO) and the Middle Miocene Climatic Transition (MMTO) appear to be appropriate analogues for modelling future climate change (Kutzbach and Behling, 2004). This is because the MMCO, ~17.9 to 13.9 Ma, represents the last period of augmented global warmth, and the MMCT best describes the period after episodic warming (Ennyu and Arthur, 2004; Kutzbach and Behling, 2004). A better understanding of the Miocene can, therefore, contribute to better understanding of present global climate change and aid in prediction and modelling of the impact of future climate change (Schindler, 1999; Royer, 2006; Steppuhn *et al.*, 2007; Schmittner *et al.*, 2008; Hay, 2010).

Global Miocene climate studies have demonstrated elevated sea (~ 6 °C at mid-latitudes relative to the present; Flower and Kennett, 1994) and continental temperatures (MAATs 3 - 6 °C higher than present; Zachos *et al.*, 2001; Royer, 2006; Holbourn *et al.*, 2007; Donders *et al.*, 2009; Dupont *et al.*, 2009).

To understand global warming during the Miocene some of its probable causes need to be highlighted. There has been much speculation and debate concerning the role of carbon dioxide in the middle Miocene warming event (Adams *et al.*, 1990; You *et al.*, 2009). Numerous studies suggest atmospheric CO₂ ranged from pre-industrial and modern levels (Pearson and Palmer, 2000), to levels ranging between 300 ppm – 700 ppm (Cerling, 1991; Kürschner *et al.*, 2008) and finally to seeming extremes of over a 1000ppmv (Retallack, 2001). A decoupling of carbon dioxide and temperature has been suggested as a factor

leading to the disparity and contradiction of models and proxies of Miocene carbon dioxide levels (Adams *et al.*, 1990). Most estimates have been above present day concentrations of 387 ppmv (Tripathi *et al.*, 2009) with You's *et al.*, (2009) model constraining it down to between 460 – 580 ppmv. Models doubling the levels of atmospheric carbon dioxide have shown to create a disparity of 1 – 3 °C between land and sea temperatures, with an increase in continental temperature of 2 - 5 °C only being met by a sea surface temperature (SST) increase of 2 - 3 °C (Tong *et al.*, 2009). Additionally, models predicted enhanced continental and oceanic precipitation (Tong *et al.*, 2009). The Miocene is also known as a period of high global humidity due to records of increased kaolinite concentrations in marine sediments (Robert and Chamley, 1987); with additional data from foraminiferal $\delta^{11}\text{B}$ values which indicate that sea surface waters were strongly alkaline (at ~ 20Ma) (Zachos *et al.*, 2001; Pagani *et al.*, 2005).

These extreme conditions subside after ~14 Ma, during a transitional period (the MMCT), whereby atmospheric carbon dioxide levels drop by 200 ppmv, sea levels are lowered by west Antarctic ice sheet (WAIS) growth, surface waters become more neutral and general atmospheric temperatures are reduced (Flower and Kennett, 1994; Zachos *et al.*, 2001; Pagani *et al.*, 2005; Miller *et al.*, 2005; Holbourn *et al.*, 2007; Donders *et al.*, 2009; Shunk *et al.*, 2009; Tong *et al.*, 2009; Tripathi *et al.*, 2009; Majewski and Bohaty, 2010). Shevenell *et al.* (2004) and Verducci *et al.* (2007) indicate a dramatic drop in SSTs in the Southern Ocean by approximately 6 – 7 °C with associated deep water cooling during the MMCT; and these concomitantly give rise to increased seasonality.

5.2.1 Southern African perspective of Miocene climate change

The opening of oceanic gateways in the Southern Hemisphere in the Late Oligocene- early Miocene resulted in the thermal isolation of Antarctica by the middle Miocene, and established new atmospheric and oceanic circulation systems (Miller and Fairbanks, 1985; Miller *et al.*, 1987; Holbourn *et al.*, 2005; Miller *et al.*, 2005; Potter and Szatmari, 2009). These were influential in establishing the reduction in MMCO temperatures in the Southern Hemisphere.

On the south-west coast, increased global temperatures and subsequent sea-level changes are recorded by a series of sea level high stands (Hendey, 1982; Clarke and Crame, 1992; Wigley and Compton, 2006). Miocene terrestrial palynological studies by Coetzee (1978a) places the MMCO between 19 Ma – 14 Ma in South Africa. This age range is

relative, and largely based on the presence of palm-dominated subtropical-tropical vegetation (Coetzee, 1978a) indicating increased regional temperatures and reduced seasonality.

5.3 Results and Discussion

The organic rich sediments at LBW and Noordhoek have comparable palynofloras. Both are intimately associated with fluvial environments and are overlain by marine-influenced strata. This forms the basis for a hypothesis that they may be direct temporal correlatives, which can be tested by comparing their biogeochemical signatures with sample depth (Fig. 5.1). Whereas all the Noordhoek organic horizons are well below sea level, their counterparts at LBW are situated above this datum. Given the fact that LBW is located some 20 km inland and Noordhoek only ~3 km inland and taking account of seaward palaeoslope, this situation is supportive of the proposed correlation i.e. this suggests a similar sea level regime at both sites during OM accumulation.

5.3.1 Bulk organic parameters and stable isotope record

The total organic carbon (TOC) content is an important means to assess the contribution and preservation of organic matter (OM) within sediment, and can reflect changes in OM source during deposition (Meyers, 1997). TOC content is highly variable (range between 0.1% and 63.4%) in samples from the Noordhoek core in comparison to the narrow range of the LBW samples (averaged $5.0 \pm 3.01\%$) (Fig. 5.2A, B). This discrepancy is likely to be a reflection of the higher ratio of clay particles diluting the total organics present, and the degree of sorting of the sediment which excludes larger fragmentary organic matter in comparison to the Noordhoek peat. The LBW TOC values decreased with stratigraphic height and increased sorting of the sediment, with the highest values of 5.1% and 10.7% recorded between 19.14 m and 19.50 m depth, respectively (Fig. 5.2B).

The TOC values for the Noordhoek and LBW core are intimately linked to the original input and preservation of OM during deposition and burial. The Noordhoek samples in particular showed a trend of lowered TOC values corresponding with poor preservation of pollen, lower pollen counts and increased abundances of charcoal and degraded organic fragments (Table A.3).

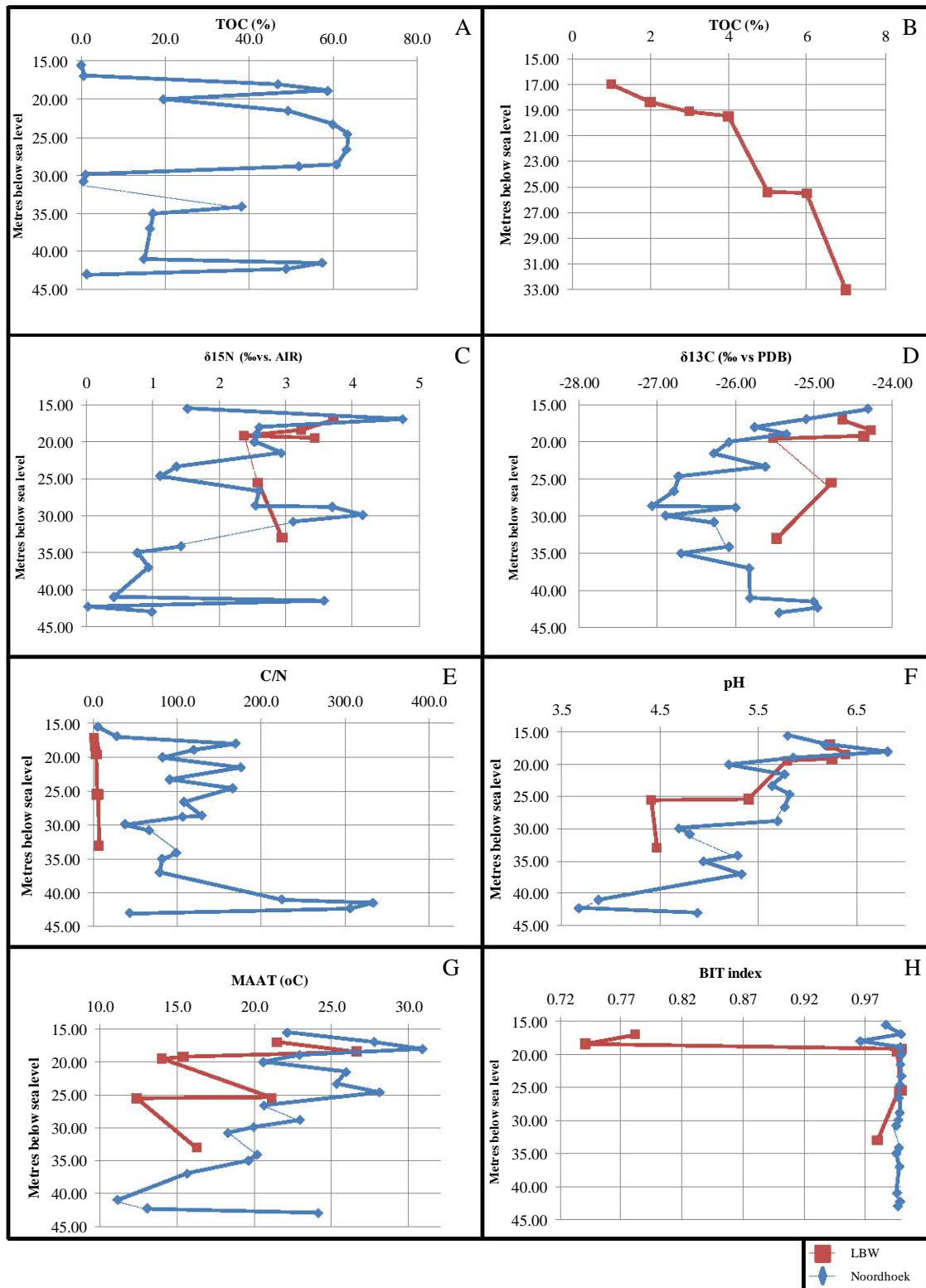


Figure 5.2. Comparison of Noordhoek (blue, diamonds) and Langebaanweg (LBW: red, squares) study sites in terms of (A) Noordhoek total organic carbon (TOC) content (%), (B) Langebaanweg (LBW) TOC (%), (C) $\delta^{15}\text{N}$ record and (D) $\delta^{13}\text{C}$ record (E) $C_{\text{org}}/N_{\text{org}}$ ratio (F) pH, (G) mean annual air temperature (MAAT), and (H) The Branched versus Isoprenoid tetraether (BIT) index. Dashed lines link samples between which data is missing because samples gave no result.

The considerably lower TOC values and range for LBW samples, when compared to those of Noordhoek may reflect a greater degree of subsequent oxidation or lower initial OM input, with non-organic detritus playing a larger (diluting) role. (Meyers and Lallier-Vergès, 1999; Killops and Killops, 2005).

The $\delta^{15}\text{N}$ values are a means to measure the amount, quality and change in OM and organic compounds with stratigraphic depth and changing lithology (Jenkyns *et al.*, 2001; Meyers, 2003). Noordhoek $\delta^{15}\text{N}$ values range from 0.03‰ to 4.8‰ with LBW showing a narrow range between 2.4‰ and 3.7‰ with enriched values being obtained from stratigraphically higher samples (Fig. 5.2C). The contribution of inorganic nitrogen from clastic input potentially enriches the $\delta^{15}\text{N}$ signal at LBW with stratigraphic height.

Noordhoek and LBW samples show no strong relationship between TOC, TN and $\delta^{15}\text{N}$ values (correlation coefficients of 0.09, 0.22 and 0.09, respectively). This is most likely a factor of the source material being nitrogen-poor, as would be expected from OM derived from lignin and celluloses (which compliment the TOC, $C_{\text{org}}/N_{\text{org}}$ and $\delta^{13}\text{C}$ records) (Jenkyns *et al.*, 2001).

Noordhoek core's $\delta^{13}\text{C}$ record range (-27.1‰ to -24.3‰) in comparison to LBW's range (-25.5‰ to -24.3‰) is much larger, and lighter by 0.4 - 1.6‰ (Fig. 5.2D). Noordhoek and LBW sites, however, both reflect C_3 -dominated palynofloras that may have periodically undergone water stress (Fig. 5.3; Shunk *et al.*, 2009). This is clearly seen at the Noordhoek site, where periodically lowered TOC values, increased charcoal (linked to seasonal fire?) and fluctuations in pollen abundance most likely linked to seasonality (and drought) (Fig. 5.3). These may be linked to orbitally-driven climate fluctuations. The increasing abundance of charcoal with increasing stratigraphic height within the Noordhoek core is most likely linked with increased abundance of more 'modern' fynbos flora. These are stimulated to reproduce after fire which is a fundamental dynamic in the ecosystem (Scott and Jones, 1994).

The elevated $C_{\text{org}}/N_{\text{org}}$ ratios of Noordhoek and LBW (Fig. 5.2E, Table 5.1) characterising Om derived from higher plant material (a $C_{\text{org}}/N_{\text{org}}$ range of ≥ 20 ; Meyers, 1997). The larger range of $C_{\text{org}}/N_{\text{org}}$ values in the Noordhoek samples (Fig.5.2E) may be accounted for by low sedimentation rates and no significant inorganic nitrogen source which could potentially decrease $C_{\text{org}}/N_{\text{org}}$ values (Meyers, 2003; Mielnik *et al.*, 2009). The relatively high $C_{\text{org}}/N_{\text{org}}$ ratio of the LBW samples (Fig.5.2E) does not show a significant

algal contribution even though the BIT indices imply a lacustrine depositional setting for the uppermost samples (Fig.5.2E, H; Table 5.1). Moreover, the greater the degree of sorting with stratigraphic height for the LBW samples will induce a lower contribution of larger intact plant material and a lower C_{org}/N_{org} value (Meyers, 1997). Importantly, inorganic nitrogen may be absorbed onto clays during burial which may further depress the C_{org}/N_{org} signal (Meyers, 1997), but because the LBW and Noordhoek samples show consecutively low TN values this is unlikely to be the case.

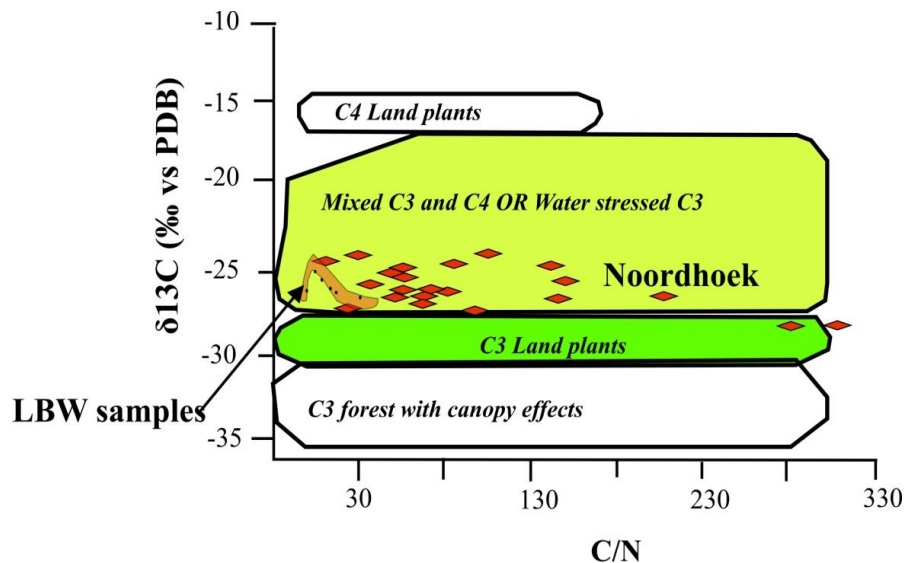


Figure 5.3. The composite organic matter source diagram, adapted from Shunk *et al.*, (2009), comparing the organic matter sources of the Langebaanweg (LBW – orange array) and Noordhoek (Avondrustvlei core - red diamonds) samples.

Lowered BIT indices were recorded for LBW uppermost samples at 17 m and 18.4 m. These contain crenarchaeol which implies deposition within a lacustrine and/or marine environment (Fig. 5.2H). A purely terrestrial signal is, however, seen in the remaining LBW samples and all of the Noordhoek samples, with BIT ranges between 0.96 and 1.0 (Fig. 5.2H; Hopmans *et al.*, 2004; Weijers *et al.*, 2006b).

The LBW and Noordhoek samples could be grouped into two classes of ‘low’ and ‘high’ MAATs with samples lower in the stratigraphy at both sites recording cooler temperatures (below modern MAAT of 17 °C; Table 5.1; Adelana *et al.*, 2010).

Table 5.1. Comparison of organic parameters and mean annual temperatures between groups from samples sites at Noordhoek and Langebaanweg.

	LANGEBAANWEG (LBW)		NOORDHOEK	
	<i>'Low' MAAT group</i> 19.14– 33 m <i>below sea level</i>	<i>'High' MAAT group</i> 17 – 18.40 m <i>below sea level</i>	<i>'Low' MAAT group</i> 29. -43 m <i>below sea level</i>	<i>'High' MAAT group</i> 15.5 – 28.8 m <i>below sea level</i>
MAAT	Moderate to low (12.4 °C -21 °C; av. 16±3 °C):	High 21.5 °C -26.6 °C; av. 24±4 °C	Moderate to low (11 °C -24 °C; av. 18±4 °C):	High 21 °C -31 °C; av. 25±3 °C
pH	Neutral to acidic (4.4-6.3; av. 5.0±0.8)	Near neutral (6.2-6.4; av.6.0±0.11)	Acidic- near neutral (3.7-5.3; av.5.0±0.6)	Near neutral (5.2-6.8; av.6.0±0.4)
BIT	1.0	0.74-0.78	1.0	1.0
δ¹³C (‰ vs. PDB)	Av. -25.1±0.6 ‰	Av. -24.5±0.3 ‰	Av. -25.9±0.7 ‰	Av. -25.9±0.8 ‰
δ¹⁵N (‰ vs. AIR)	2.8±0.5‰	3.5±0.3‰	1.2±1.2‰	2.7±1.3‰
TOC (%)	Av. 5.8±3.5%	Av. 3.6±1.3%	Av. 21.8±21.4%	Av. 43.2±24.5%
C_{org}/N_{org}	37.6±6.4	42.5±12.7	167±119	110±48

The high MAATs groups of both Noordhoek and LBW show a MAAT averaging between 24 - 25 °C with small annual ranges (Table 5.1). This is higher than present day MAATs by 7 - 8 °C, and higher than the average temperatures from the “low MAATs” groups by 8 - 9°C (Table 5.1). The pH of the sediment at LBW and Noordhoek during ‘high MAATs’ periods is near neutral with acidic profiles reported for the ‘low MAAT’ groups (Table 5.1). The pH of the ‘low MAATs’ groups are similar to the acidic soil profiles of a modern day fynbos setting indicating well drained, nutrient poor conditions (Fig. 5.2F; Cowling *et al.*, 2009).

As the MAAT data between these geographically separated sites showed a matching pattern of increasing values relative to the top of the organic succession in each core (Fig. 5.2G), a correlation co-efficient was calculated using data at points similar within the organic horizons (Table 5.2). The correlation coefficient of 0.95 implied a near perfect positive linear relationship between the variables at the two sites (Table 5.2). This correlation is based purely on sample depth below the top of the organic beds, a logical chosen datum given the poor chronostratigraphic correlation between the sites, and does not take into consideration the likely disparities in depositional, burial and compaction histories. Compensating for these

variables could further increase the resolution of the correlation, and further improve understanding and interpretation of the palaeoenvironmental data. Fundamentally the data reflect similar climate fluctuations at spatially disparate locations, which impinged on the environment and therefore the flora and organic preservation in analogous ways. The biogeochemical correlation between LBW and Noordhoek illustrates the power of biogeochemistry to resolve and correlate climate fluctuation over space and time.

Table 5.2. Comparison of the Noordhoek and LBW tetraethers lipid derived mean annual air temperatures (MAAT, °C) over similar interval below sea level, and the correlation coefficient calculated for this data set (0.95).

Noordhoek		Langebaanweg	
Depth above/below sea level (m)	MAAT (°C)	Depth above/below sea level (m)	MAAT (°C)
16.9	27.75	17	21.5
18	30.86	18.4	26.6
18.9	22.92	19.14	15.4
20	20.59	19.50	14.0
24.6	28.08	25.40	21.1
26.6	20.63	25.50	12.4
34.1	20.19	33.00	16.2

CORREL:	0.95
---------	------

5.3.2 Global and regional comparisons

Figure 5.4 is a comparison between the regional and global sea level, high latitude Southern Ocean sea surface temperatures and the proxy data obtained from LBW and Noordhoek for Miocene continental temperatures. The correlation between increasing LBW and Noordhoek terrestrial MAATs shows a relationship with an increase in SSTs near Antarctica (Clarke and Crame, 1992).

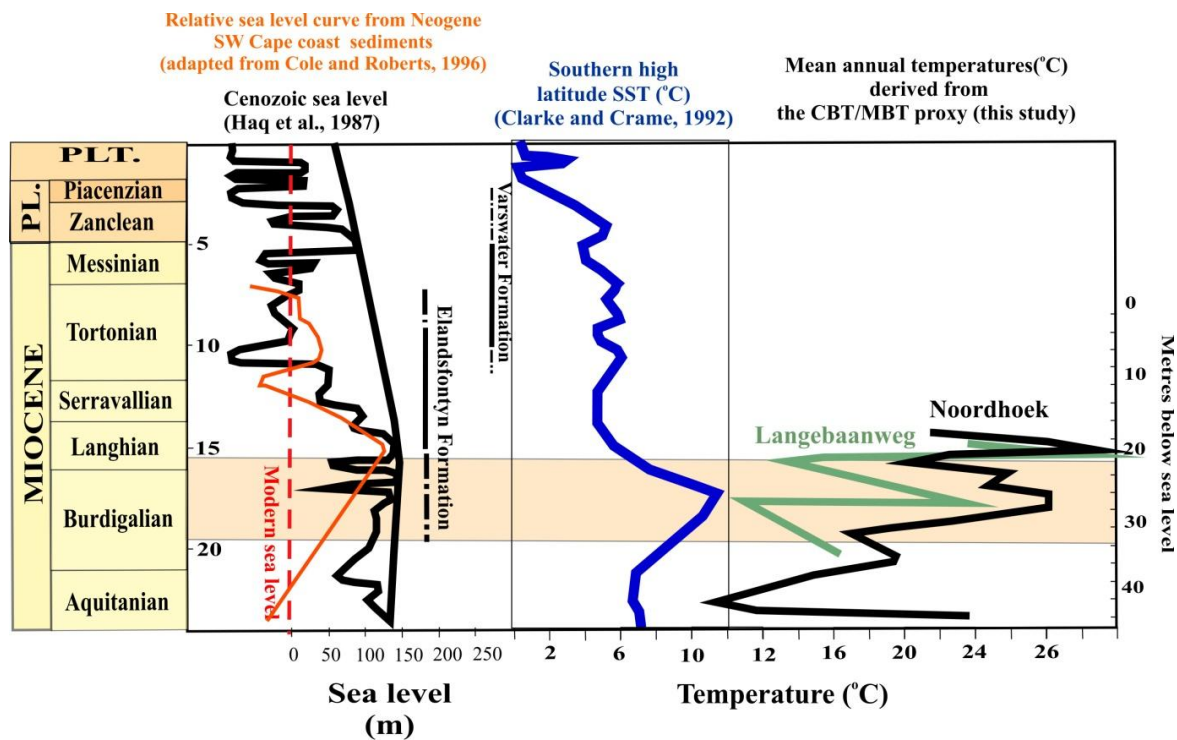


Figure 5.4. Comparison of the Langebaanweg (green) and Noordhoek (black) mean annual air temperature curves derived from the MBT/CBT proxy, in relation to the Cenozoic sea level.

Closer to the south-west coastline elevated SSTs ($\sim 28^{\circ}\text{C}$ at 14 Myrs ago; Dupont *et al.*, 2009) have been recorded from sediments at ODP Site 1085, and these are likely to be influential in contributing to elevated continental temperatures (Fig. 5.4). The largest oceanic warming event, therefore, has been broadly correlated with the significantly increased continental temperatures at both sites, given the probable delayed response of the continental signal to the oceanic stimulus (Fig. 5.4). The correspondence to elevated global and regional sea levels would be expected if both oceanic temperatures and continental temperatures were elevated during this period, which appears to be the case. This may further confirm an early to middle Miocene age for the sediments at Noordhoek and LBW. However, the low MAATs of the lowermost samples, at least from the Noordhoek site, could point to an older age – perhaps pertaining to the cold Oligocene.

5.3.3 Palynoflora

The Noordhoek palynofloras identified in this study, and those by Coetzee (1978a, b) and Coetzee and Rogers (1982) broadly supported the MBT/CBT proxy MAATs from both

Noordhoek and Langebaanweg (Fig. 5.5). When the ecological tolerances of some of the flora are considered it becomes apparent that environmental factors such as MAATs and pH are intrinsically linked, and that other environmental parameters which cannot directly be studied (such as humidity and drought) can also be inferred (Fig. 3.7, 3.8). The low to near-neutral pH values of the Noordhoek and LBW sediments at time of deposition is consistent with the presence of arboreal taxa which flourish in soils of pH between 4.8 and 5.5 such as podocarps and *Olea* (reference to Fig. 3.4, 3.8; Schalke, 1973; Chesworth *et al.*, 2008).

Furthermore drought-intolerant flora (palms, *Casuarina*, *Myrica* and the family Sapotaceae; Jiménez-Moreno and Suc, 2007) are prolific during elevated MAATs in the Noordhoek core, and are present in LBW core (Newmann, pers. comm.). This suggests high humidity and/or precipitation. Their absence within the Noordhoek core at specific intervals is significant and points towards drought or flooding (Jiménez-Moreno and Suc, 2007; Jiménez-Moreno *et al.*, 2010); with other taxa thriving at these intervals, such as *Olea* which is known to be drought-tolerant (Scott *et al.*, 2006; Jiménez-Moreno and Suc, 2007; Jiménez-Moreno *et al.*, 2010; Orwa *et al.*, 2009).

5.4 Synthesis

The terrestrial organic proxies for the Elandsfontyn Formation at LBW and Noordhoek show similar fluctuations in time and space, and provide an interesting insight into studies of regional climate during the Miocene (Fig. 5.5).

OM contribution and the BIT index of the uppermost LBW samples indicate deposition influenced by a lacustrine or marginal marine setting; likewise the Noordhoek core grades upwards into marine-influenced beds. This suggests that both sites developed under conditions of rising sea level which is consistent with the higher MAATs in the upper part of both organic-rich successions. Furthermore, this sea level rise may be glacio-eustatic in origin. The dominant OM contributions during deposition based on TOC, TN, C_{org}/N_{org} and carbon isotopes appears to represent a dominantly terrestrial higher plant source (Table 5.3).

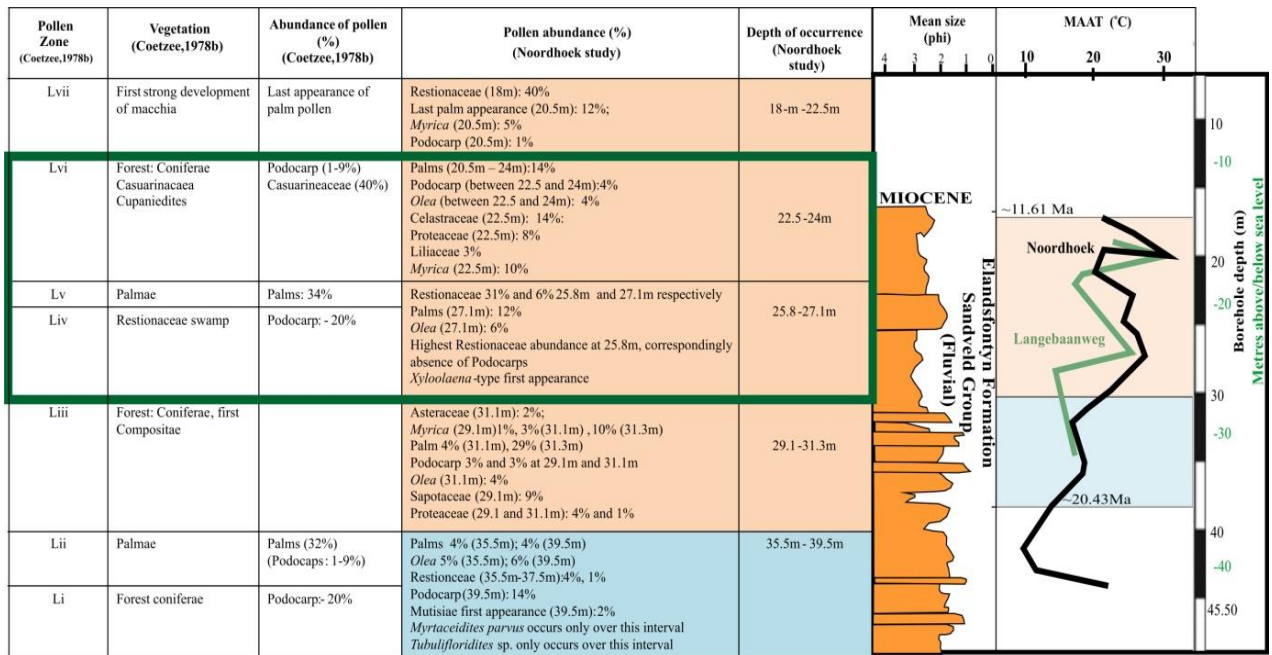


Figure 5.5. Comparison between Coetzee (1978 a, b) pollen zones, Coetzee and Rogers (1982) Sb and Sa zones occurrence determined by pollen comparisons to Pollen zone L (indicated by green box) and the Noordhoek core of this study (sample between 18 m- 39.5 m depth). The Noordhoek (black) and Langebaanweg (green) calculated mean annual temperature (MAAT) curves, from the MBT/CBT proxy, of this study for the samples between the depths 17 m and 43 m depth against stratigraphic log (adapted from Rogers, 1982). Palaeoflora and CBT/MBT proxy temperatures higher (orange) and lower (blue) than present day MAAT (17°C) are indicated.

Table 5.3. Broad comparisons of organic parameters at Noordhoek and Langebaanweg (LBW) and their interpretation.

	LBW	Noordhoek
MAAT	Uppermost samples are above modern MAAT by 1 - 10 °C	Uppermost samples are above modern MAAT by 1 – 13 °C
Charcoal	Known that overlying samples (Varswater Formation) experienced seasonality linked to drought and fire	Presence is correlated with high MAAT, low TOC, TN and lowered pollen counts/poorly preserved palynomorphs
BIT	Uppermost samples show BIT indices indicating lacustrine OM deposition	All terrestrially deposited OM
$\delta^{13}\text{C}$ (‰ vs. PDB)	Heavier	Light
$\delta^{15}\text{N}$ (‰ vs. AIR)	low	low
TOC (%)	Low	High
$\text{C}_{\text{org}}/\text{N}_{\text{org}}$	Above 20; OM is derived from high plants' lignin and cellulose	Variable and above 20; OM is derived from high plants' lignin and cellulose

Figure 5.6 is a summary of the global and regional climate events and palynofloras present in South Africa during the Miocene. Mercer (1978) had suggested a two part increase in warming in the Miocene at 19 Ma and 14 Ma which was recorded in the south-west coast by Coetzee (1978a). This increase can be generally seen in the CBT/MBT proxy data from the Noordhoek and LBW site, where there are 2 peaks in elevated MAATs which could correspond approximately to these time periods (Fig. 5.6). These peaks show a general pattern with elevated SSTs during the time periods mentioned, but show a time-lag in response to globally increased sea temperatures and levels.

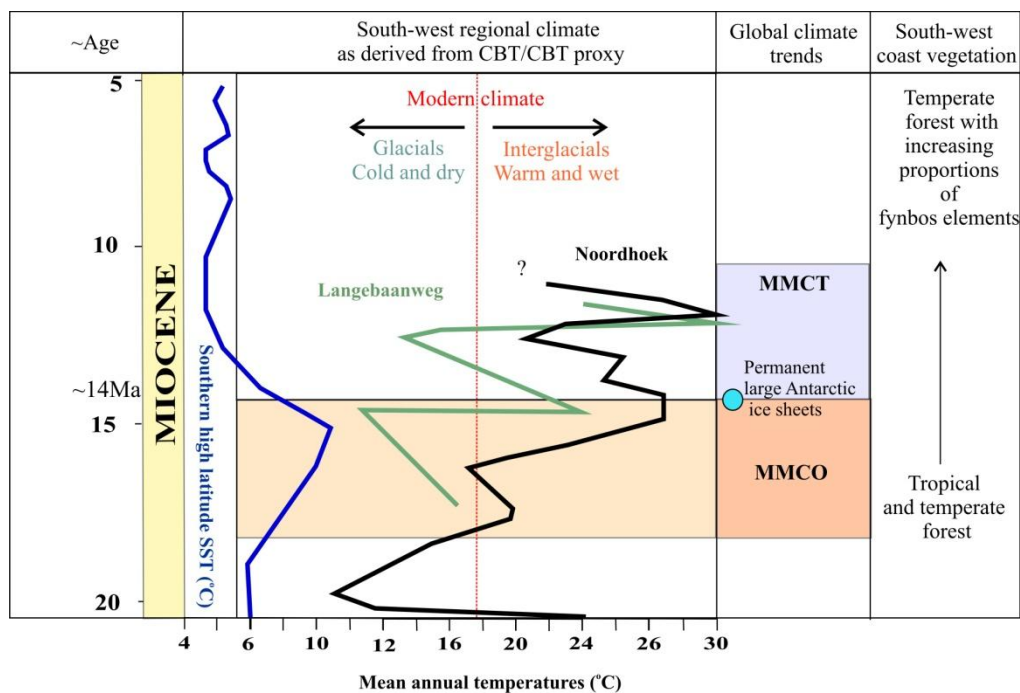


Figure 5.6. Palaeotemperatures and palynoflora from Langebaanweg and Noordhoek (MAATs) plotted against approximate age of the sediments, based on biostratigraphic correlations of the Noordhoek core, in comparison to global climate trends (e.g. Southern high latitude sea surface temperature, SST, of Clarke and Crame, 1992) and in response to regional climate trends.

Given the connection between sea and continental temperatures, terrestrial proxy data shows a delayed response to sudden increases/ decreases in global sea surface temperatures (Mosbrugger *et al.*, 2005). The second period of elevated temperature discussed by Mercer (1978) is prior to the glaciation of the West Antarctic ice sheet (WAIS) at 14Ma, and is followed by a substantial drop in Southern Ocean temperatures (Clarke and Crame. 1992; Billups *et al.*, 2008). There is a significant drop in MAATs from the Noorhdoek and LBW sites but no further resolution of the data could be obtained for time periods after this interval

as this was the uppermost limit of the peat deposits at Noordhoek. The Elandsfontyn Formation in the south (at Noordhoek) in comparison to that in the north at LBW has a more continuous extent of relatively continuous massive peat layers, but neither site seems to (organically) capture (at this rough level of sampling) the time period following WAIS growth.

5.5 Future work

The terrestrial record of MAAT derived from branched GDGTs was a novel approach aimed at illuminating the palaeoclimate of the Southwestern Cape during the Miocene. The Noordhoek and Langebaanweg branched GDGT, palynomorph and stable isotope studies are in substantial agreement with the marine records for the Southern Ocean during this period (Haq *et al.*, 1987; Clarke and Crame, 1996, Cole and Roberts, 1996). Future studies should focus on consistency in MAAT and palynomorphs data obtained through more rigorous sampling and more extensive work. This will still further greatly impinge on constraining the age of these deposits, and will be hindered in the fact that, as many of the fossil taxon represented works on nearest living relative (NLR) assumptions, estimations will never be accurate. Other cores through the Elandsfontyn Formation in more distal settings are available in the LBW environs and may show substantially different palaeofloras because of a higher water table and therefore greater affinity with Noordhoek.

6 Case Studies from the south-west and south- east coasts, South Africa

6.1 Introduction

This chapter examines two case studies involving sites of different ages to one another and in comparison to the Noordhoek and Langebaanweg sites. These additional sites have been used to assess the application of the new biogeochemical proxy in different depositional settings of variable age within South Africa. The first site discussed is the Rondeberg Clay Pit on the south-west coast. The second site (Rietvlei) lies on the south coast and experiences a different climatic regime in addition to being significantly younger than the preceding sites.

6.2 Case study 1: Rondeberg Clay Pit

The Rondeberg Clay Pit (RCP) is situated approximately 60km north of Cape Town near the town of Malmesbury, Western Cape Province. Mining activity has exposed extensive fluviolacustrine clay deposits (informally named the Rondeberg clays). The Rondeberg clay sequence lies at an altitude of ~100m above modern sea level, and is included in the Elandsfontyn Formation (Roberts, pers. comm.) since it has a fluviolacustrine origin and is possibly a palaeo-Diep River deposit. The modern Diep River is situated only a few kilometers from the site. From its geomorphic setting and compacted sediments, it was assumed to be of considerable age. However, prior to this study its true age was highly uncertain and palynology was the only means to resolve the chronology.

The RCP allows for a three-dimensional study of exposed Elandsfontyn Formation which can be compared in regards to relative age and stratigraphic relationship with borehole samples of the Elandsfontyn Formation at other sites (i.e. Noordhoek and Langebaanweg).

RCP is composed of green-ish-grey coloured clay, silts and very fine-grained sands. Borehole data shows that it unconformably overlies the Malmesbury Group (Neoproterozoic metasediments). The exposure is approximately 12 m thick, stratified and coarsens-upward, with channels filled with silty sediment at the top. It contains 2 thin black organic-rich

horizons with conspicuous charcoal, woody fragments and *in situ* tree stumps. The general appearance of the clays (greenish-grey colour) suggested little organic material was present.

6.2.1 Methodology

Methods used are outlined in Sections 2.2.1, 2.2.2, 2.2.3 and 2.2.4.

6.2.2 Results

The clay pit consisted of a coarsening upward sequence with clay grading into silts and very fine sands (Fig. 6.1; Table A. 8). Clays appeared homogeneous and were laterally continuous over the area of the pit (approximately 25 m²). Small strike slip faults were noted in the south-western part of the pit but not within the section of the pit where samples were taken. Fine-grained sand channels transect the pit margin obliquely in the north-west of the pit.

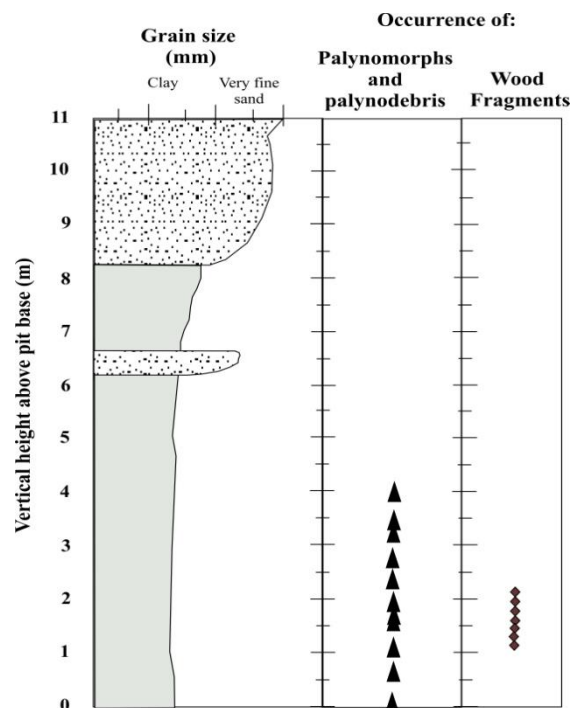


Figure 6.1. Rondeberg Clay Pit log showing the change in lithology with stratigraphic height and the presence of wood fragments (greater than 10 cm in size) in addition to the occurrence of ‘organics’ – pollen and microscopic charcoal from sampled and processed material.

Branched tetraether membrane lipid extraction was attempted on the most organic-rich (black coloured horizons) at 1.62 m and 3.18 m above the base of the succession, but their tetraether yield was below detection levels.

Palynomorphs varied from spores (Pteridophytes) to pollen (gymnosperms and angiosperms) (Fig. 6.2). Palynomorphs were generally poorly preserved and low in abundance (Table A.9 and A.10). Palynomorphs were identified to family level through the use of literature and the pollen reference collection held at the Department of Plant Sciences at the University of the Free State or described and named according to morphological features where identification was uncertain.

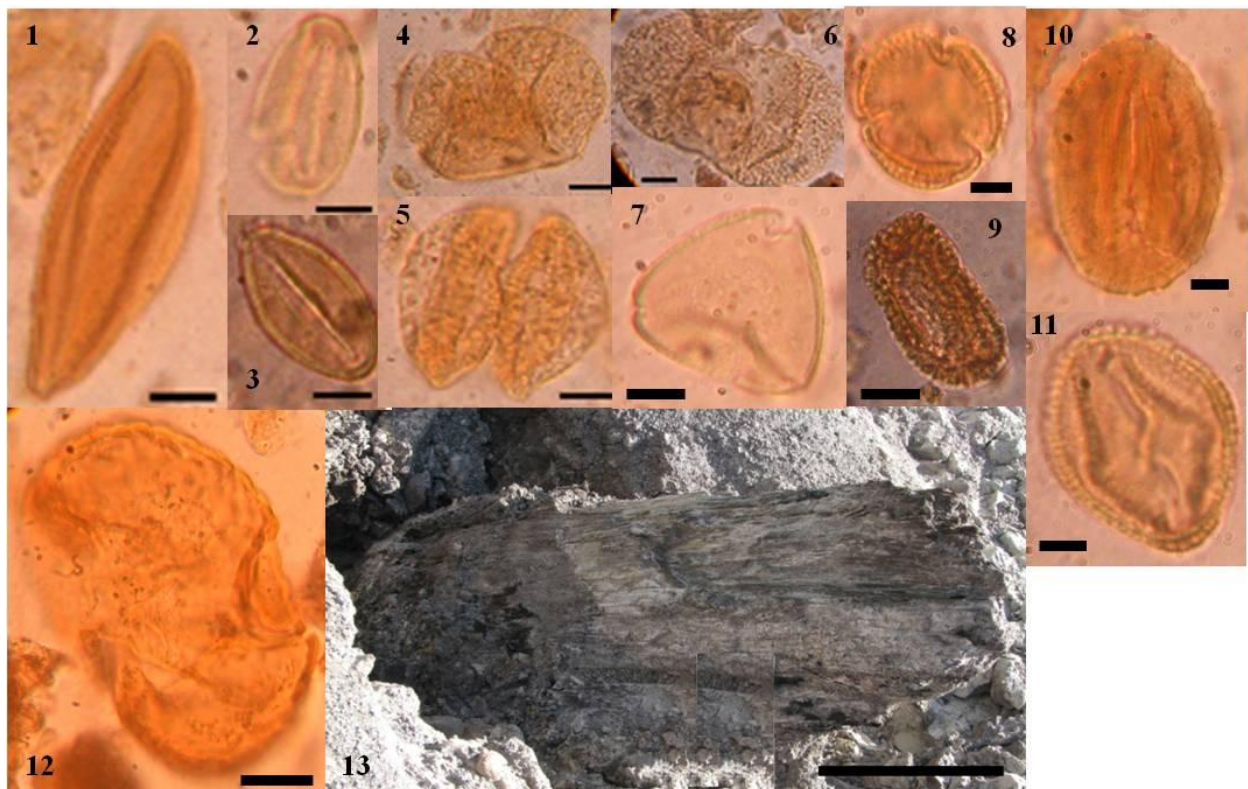


Figure 6.2. Selected photomicrographs of Rondeberg palynomorphs which represent tropical (1, 2, 3, 7, 8, 9, 10) temperate (4, 5, 6, 8, 11, 12) environments. 1: Angiospermae: Arecaceae/Palmae, ‘Large Palm’, 2, 3: Arecaceae/Palmae, ‘Small Palm’, 4, 5, 6: Gymnospermopsida: Coniferophyta, Podocarpidites sp. A, 7: Rhamnaceae, 8: Angiospermae: Oleaceae, *Olea*-type, 9: Rutaceae, 10: Tubuliflorae group, *Mutisia*, 11: Aizoaceae, 12: Spore: Polypodiaceae, *Polypodiisporites* sp. Scale bar = 10µm. 13: Charred log (Podocarp?), scale bar = 15cm.

Palynomorphs (Fig.6.3 and 6.4; Table A.10) are present in reasonable abundance at specific intervals (1.1 m, 1.76 m, 1.96 m), but most samples yielded sparse material of poor

quality (poor preservation). The ‘unknown’ category accounted for 19% of total counts. The overall assemblage is dominated by palms (31%), *Podocarpus*-type (11%), Asteraceae (8%) and Rhamnaceae (7%). Modern fynbos elements, such as Restionaceae (2%), Proteaceae (triporate, triangular amb; 5%) and Ericaceae (3%) are present but with lowered abundances (Fig. 6.3).

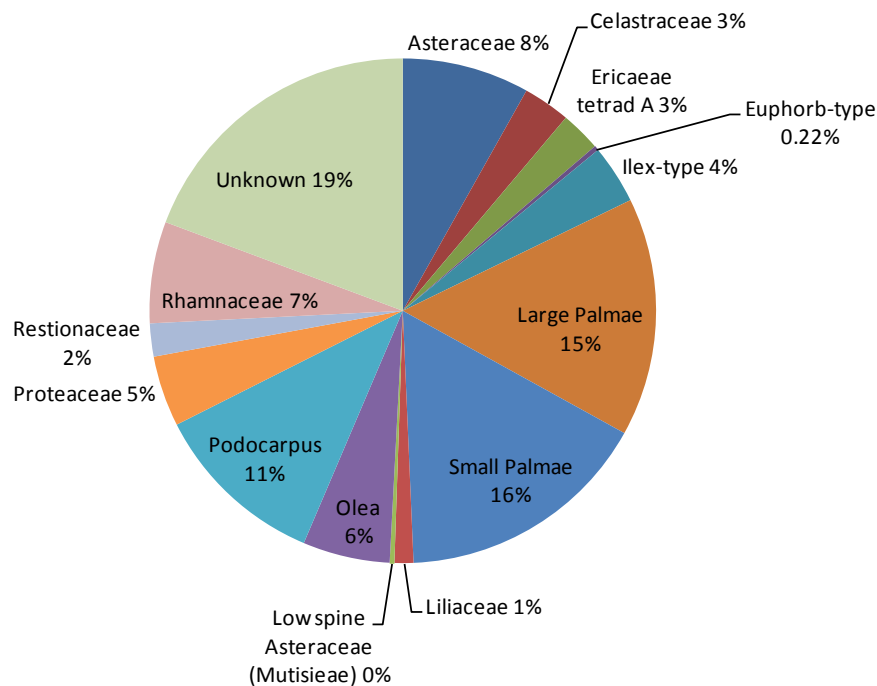


Figure 6.3. Chart showing the percentage distribution of specific pollen types within the Rondeberg Clay Pit. All percentages are given against total pollen counts for entire section.

The lowermost productive sample unit (1.1 m above pit base) contained abundant *Pellaea*-type and Polypodiaceae fern spores (Fig. 6.4). Asteraceae, Ericaceae, Mutisieae and abundant Rhamnaceae were present at this level (Fig.6.4). *Ilex*-type grains were also present and relatively abundant in comparison to other grains. Palms (both large and small morphotypes) were low in abundance and there were no recorded *Podocarpus*-type pollen present.

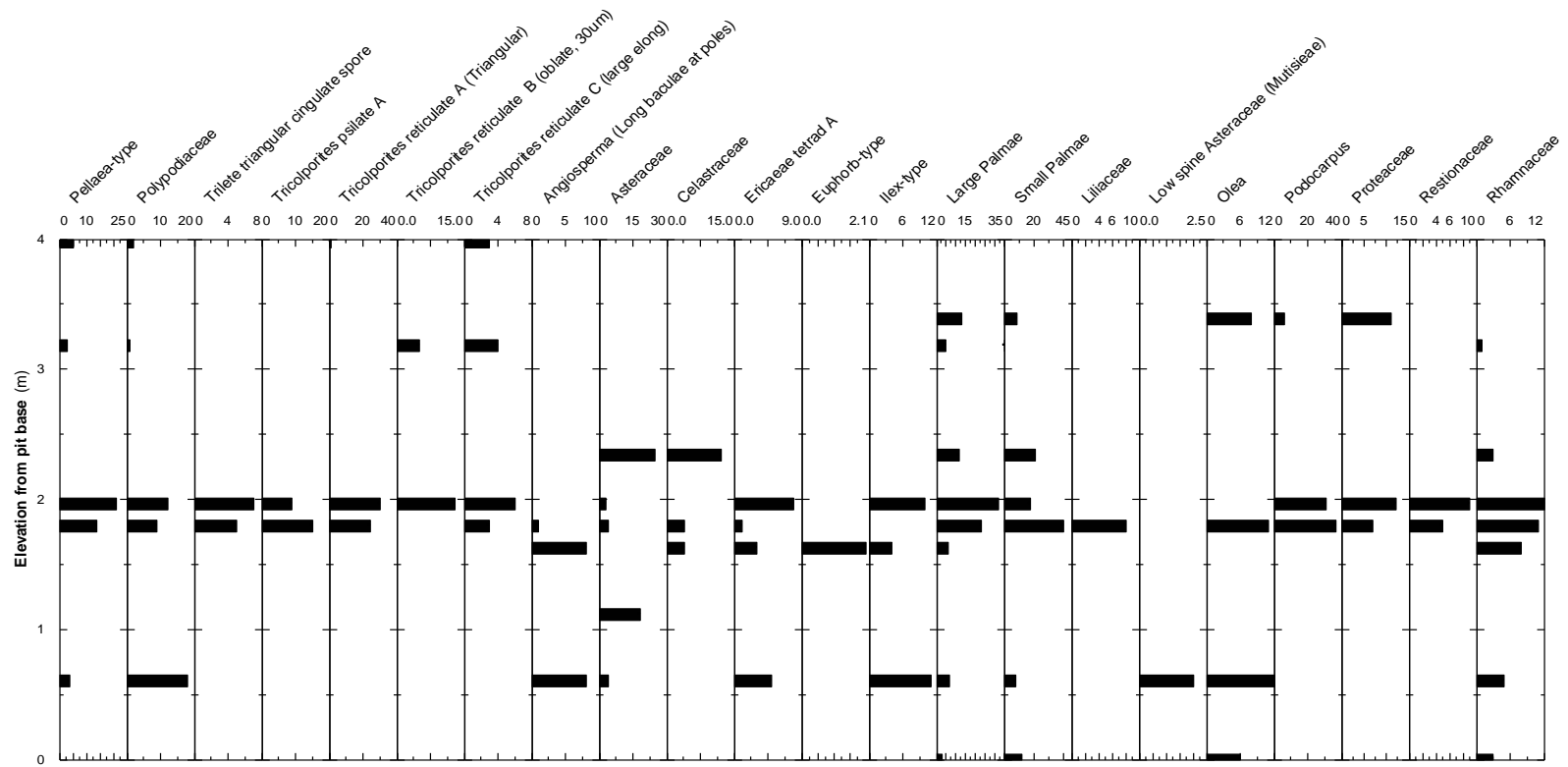


Figure 6.4 Pollen diagram of total counts for the most productive sample units of the Rondeberg Clay Pit, Malmesbury, South Africa.

The critical interval of highest abundance and preservation of palynomorphs was between 1.79 m and 1.96 m above the pit base. There is a general increase in the abundance of palms, Rhamnaceae, Asteraceae and the first appearance of Podocarpaceae at 1.79 m. At this level the first appearance of various, tricolporate psilate and reticulate species as well as Celastraceae, *Euphorb*-type, Liliaceae and an unidentified trilete triangular amb spore were recorded. A decrease in pollen abundance and preservation is noted with an increase in charcoal appearance and concentration (Table A. 9).

The pollen diagram illustrates a generally lower abundance of pollen above 2.5 m above the pit base (Fig. 6.4). Tricolporate reticulate grains 'A', 'B' and 'C' were present at 1.79 m and 1.96 m below 2.5 m – 4.0 m elevation. There were microscopic charcoal (fusain) fragments in all samples (Table A.9).

6.2.3 Inorganic Geochemistry results

Thin sections were made of all samples taken, and analysed to identify any detrital grains which may indicate source rock(s).

The modal distribution of major elements was correlated to the stratigraphic profile description and attempts were made to relate this to thin sections of representative samples, but without success due to the small and fractured nature of many mineral grains. Thin sections all showed very fine-grain size with all particles being of clay or silt size. The upper 2.08 m proved the exception and was composed of very fine-grained quartz sand. The major element data records a transition from clay-rich unit (0 m - 8.27 m elevation above pit base) to a sandy unit between 8.92 m and 11.04 m (Table A. 12). The sandier unit (8.92 m to 11.04 m) is characterised by a distinct increase in SiO₂ content from 43 wt % at 8.92 m to 83 wt % at 11.04 m (Fig. 6.5). There is a SiO₂-rich very fine sand interval within the predominately silty-clay horizon below 8.92 m which starts at 6.32 m and ends at 7.72 m with SiO₂ varying between 72.0 wt % and 92.4 wt % (Fig. 6.5).

SiO₂, MgO and Al₂O₃ concentration show a negative linear relationship ($r^2 = 0.54$) with high SiO₂ corresponding to lowered MgO concentrations and this pattern is predominant in the sandier units (Fig. 6.6). High MgO concentrations are recorded in the clay-rich units below 6.3m elevation (Fig. 6.5). Mobile elements, specifically K₂O and Na₂O show increased

concentration in sandy units versus clay-rich units. K_2O shows high variability with stratigraphic depth, and is significantly depleted directly below the sandy unit between 7.5 m and 6.5 m (Fig. 6.5).

Figure 6.7 deals with trace elements that are largely controlled by lithological changes and barriers. Strontium (Sr) and neodymium (Nd) peak at 8.92 m below the uppermost sand unit (Fig. 6.7). The base of the silty-clay unit between the uppermost sand unit (8.92 m to 11.04 m) and the second sand unit (6.32 m - 7.72 m) is characterised by increases in Nd, Sr, Y and Pb which decrease with height towards the top of the uppermost sand unit (Fig. 6.7). Zr shows an opposing pattern to that demonstrated by Nd, Sr, Y and Pb. Figure 6.6 shows a peak in Ce, Nd, La, Cr, V, Cu, Y, U and Th at 3.18m which coincides with the black organic horizon. Zn and Co are the only trace elements which show considerable depletion over this interval (Fig. 6.7).

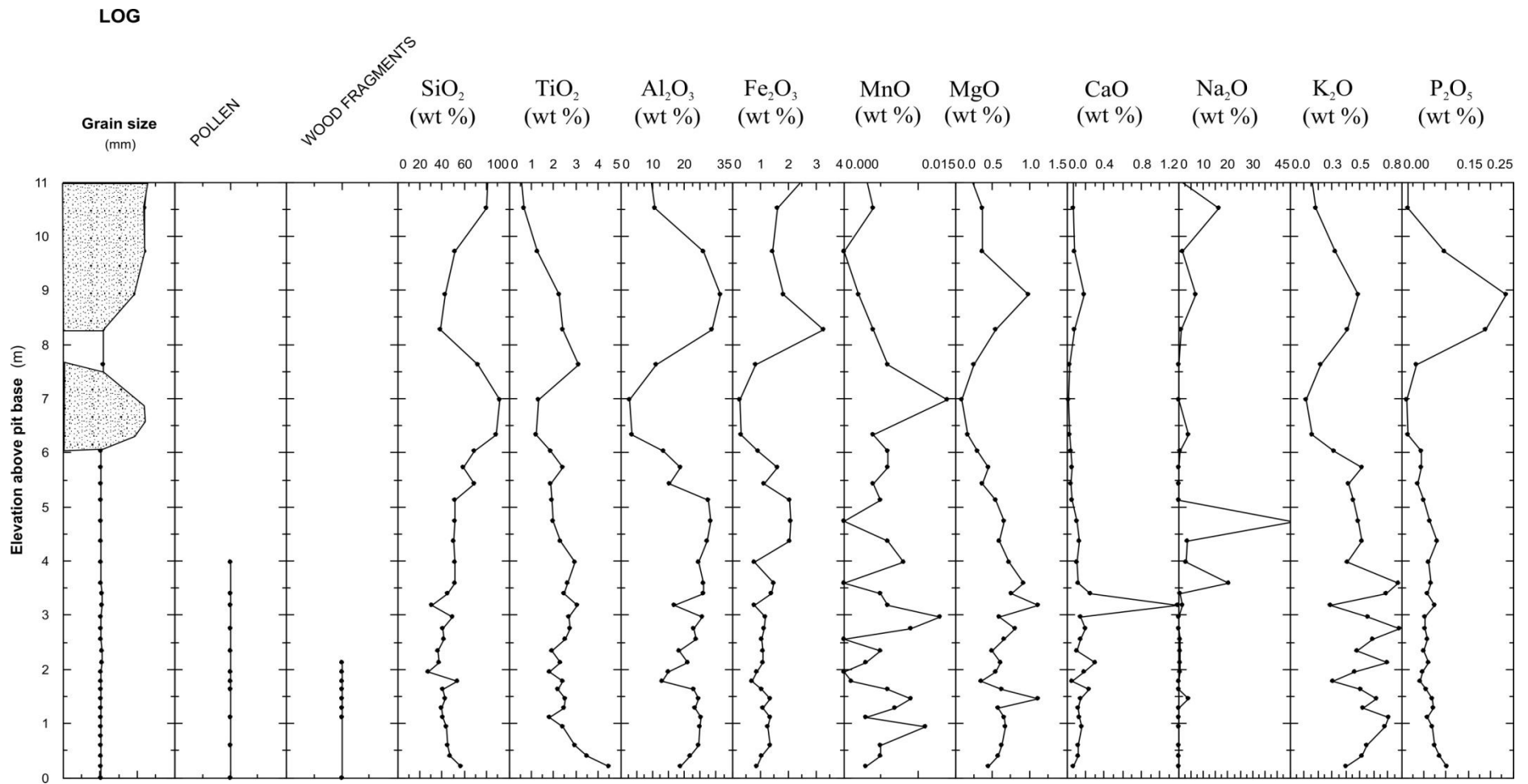


Figure 6.5. Major element variation diagram with elevation above pit base at Rondeberg Clay Pit.

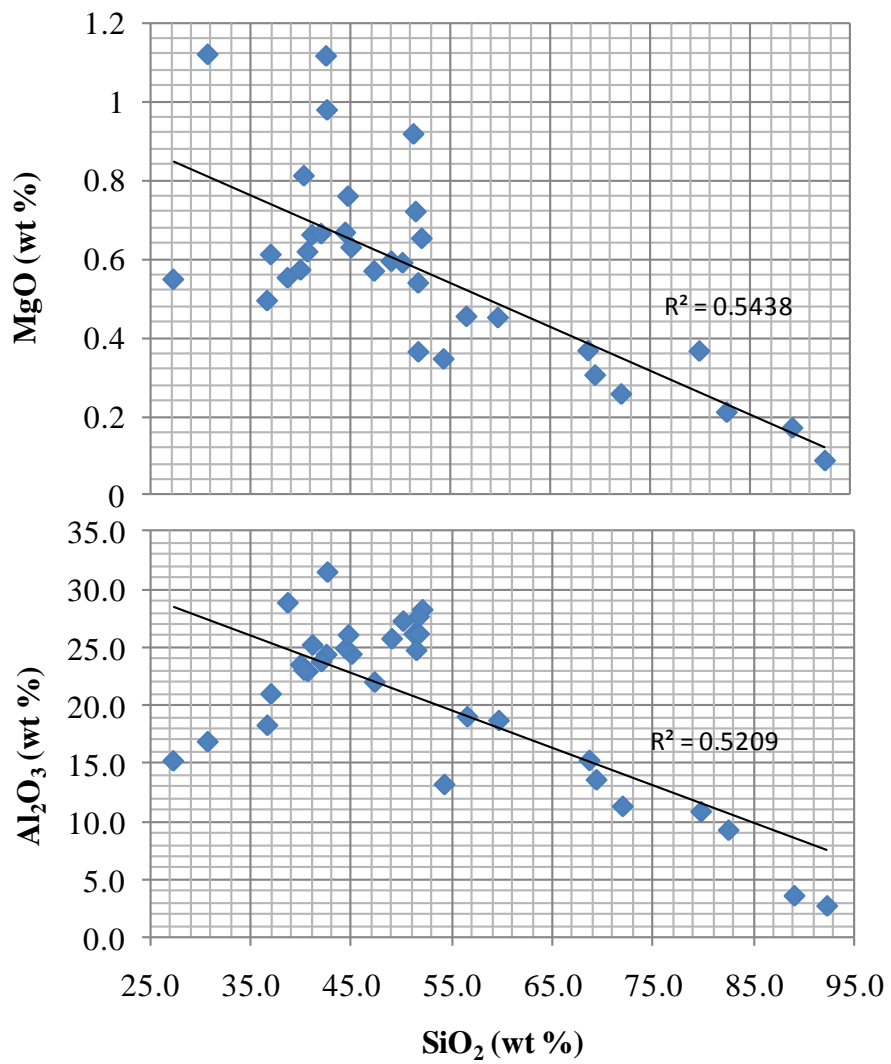


Figure 6.6. Scatter plot of SiO₂ (wt %) versus Al₂O₃ and MgO showing a negative linear relationship.

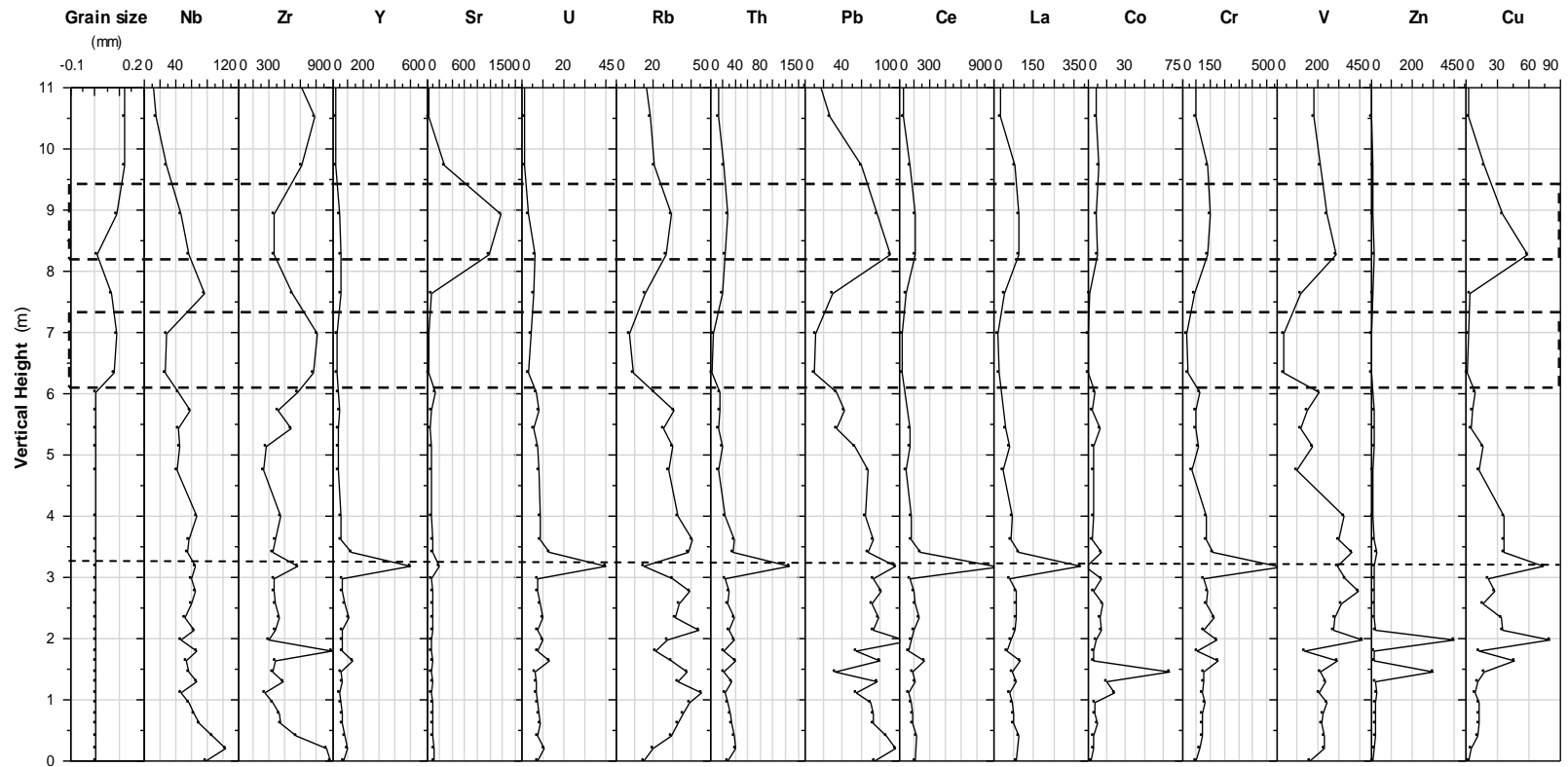


Figure 6.7. Trace element data for the Rondeberg Clay pit versus lithology of the clay pit. Dashed boxes and line indicate where lithological changes show groupings in trends in trace element data.

6.2.4 Discussion and conclusion

The variation and concentration of major element data was strongly controlled by the lithology and therefore mineralogy. However, comparisons between thin section petrography and major element data proved unsuccessful due to the very fine-grained, sparse and fractured nature of the mineral grains. Changes in lithology from clay-rich to sandier (quartz sand) units lead to changes in the percentages of major element components. Increases in SiO_2 were associated with decreases in Al_2O_3 , MgO , and Fe_2O_3 , but elements such as NaO and K_2O showed no significant variation with SiO_2 . This is likely to be a factor of their mobile nature as the percolation of fluids can significantly affect their distribution with depth. This is clearly illustrated by peaks in concentrations of mobile elements at lithological boundaries between permeable (silt and sandier units) and impermeable clay units. The soluble nature of trace elements and CaO , NaO and K_2O would allow for their movement with the percolation of fluids.

The concentration of trace elements was largely controlled by lithological changes with elements such as Y, Pb and Nd becoming concentrated at the contact between permeable sandier units and impermeable clay-rich units. This is likely a factor of fluid flow which would, if predominately originating from rainwater, percolate downwards through porous and permeable layers (sand-rich horizons at 6.32 m - 7.72 m and 8.92 m-11.04 m) and concentrate elements at the boundary to impermeable clay layers where fluid flow becomes restricted. The contact between sandier horizons and the clay horizons thereby being marked by a distinct peak in abundance of many trace elements.

The black organic horizon at 3.18 m showed peak abundances in many trace elements. The thin section, biogeochemical and palynological studies of this sample interval confirmed the presence and abundance of charcoal. It is likely that the peak in abundance in trace elements in this sample is a factor of the charcoal forming process, as well as the porous and therefore absorptive nature of the charcoal fragments during deposition, burial and diagenesis (Jenkins, 1989). Furthermore, the charcoal remains themselves may contribute marginally to the trace elements detected some of these elements may be utilised during plant growth and will be variable depending on taxa and environmental conditions (Jenkins, 1989). The depletion of Zn and Co may be a factor of loss during carbonisation of wood and the elements low concentration within source rock (Jenkins, 1989).

The preservation organic matter, whether palynomorphs or tetraether membrane lipids, is generally poor. The high fraction of charcoal (microscopic and macroscopic) and charred *in situ* stumps of (likely) *Podocarpus* (30 – 50 cm in length), indicate frequent fires that are likely to have caused membrane lipid and pollen degradation. The poor preservation and low abundance of pollen may additionally affected by the well-sorted nature of the sediments (Traverse, 1988), environmental factors during and following immediate deposition (drought) and diagenetic factors.

Fire is controlled by climate (such as seasonality and rainfall variability in general) and availability of fuel. Periods of drought/seasonality are further indicated by relatively pronounced growth rings of the charred tree stumps, and sequences of upward decreasing organic content grading into pedogenically influenced (ferruginised) horizons in the Rondeberg area (Fig. 6.2, 6.4). This tentatively suggests a wetland prone to seasonality and fire regimes ultimately controlled climate change associated with orbitally forced glacial/interglacial periods.

The fossil pollen evidence suggests that the Rondeberg deposits are of Neogene age and experienced a subtropical/ tropical climate dominated by meso-megathermic (*Palms*, *Ilex*-type) and mesothermic (*Podocarpus*-type) palynofloras. This is a completely different association compared with the fynbos-type dominant in the Cape today. The Rondeberg palynofloras include large forest trees (*Podocarpidites* spp. bisaccate pollen) and shrubs (Rutaceae), to primitive Asteraceae (Mutisieae) and ferns (*Pelleae*-type). These floras suggest the landscape was at least partially forested. Palmae, typical of humid subtropical to tropical climates, were observed in high abundances (up to 31%) over specific intervals at the pit (Fig. 6.4), and are also found at other sites in the region as studied by Coetzee (1978a, b), Coetzee and Rogers (1982) and Carr *et al.*, (2010b). The palm pollen and those palynomorphs such as the Rhamnaceae, *Euphorb*-type, and *Ilex*-type complement the high abundance of spores indicative of wetter, warmer weather (Fig. 6.4).

Modern fynbos elements also make up the pollen assemblage at RCP (e.g. Ericaceae, Restionaceae) but are significantly depleted in comparison to other floras (such as Asteraceae) and in comparison to present day scenario. The ‘unknown’ category placed palynomorphs of uncertain affinity due to fragmentary nature into one group comprising a significant proportion (19%) of the total pollen counted. These can be classed with the tricolporate psilate and reticulate species representing high diversity of palynofloras.

The findings confirm the regional trend of temperate and tropical forest vegetation in the south-west Cape during the Palaeogene and into the Neogene (Axelrod and Raven, 1978). The age of the deposit which was initially based on impressions from geomorphological criteria as late Miocene-early Pliocene is likely to be older. The presence of the ancient angiosperm, Mutisieae, places a lowermost age of late Oligocene-early Miocene age for the deposit (Scott *et al.*, 2006).

6.3 Case study 2: the Quaternary Rietvlei Site

6.3.1 Introduction

The Rietvlei site comprises an extant, localised coastal inter-dune wetland about 50 m from the present beach, which is washed by the warm Agulhas Current (Fig. 6.8). The site therefore holds significant potential for comparing ecological processes of the past with the present (Carr *et al.*, 2010c). The Rietvlei site is located near the town of Still Bay in a year-round rainfall zone affected by the cyclonic and anticyclonic weather systems (Fig. 6.8; Roberts *et al.*, 2008; Carr *et al.*, 2010c). This study focuses on sub-samples from a core (RVSB 2) taken from the Rietvlei wetland by Dr. A Carr of the University of Leicester. The chronology of the Rietvlei core is constrained by radiocarbon dating, and spans the period from ~27.5 ka to 1 260 yrs , which includes the Last Glacial Maximum (LGM). This study was undertaken in order to determine the efficacy of applying the branched GDGTs method in younger organic-rich sediments in southern Africa. Furthermore, there is also potential for comparison with south-west coast sites which have winter rainfall environments in comparison to Rietvlei's year round rainfall, as well as oceanographic contrasts. Branched GDGTs may also, however, potentially reflect the differences in age, preservation and organic productivity.

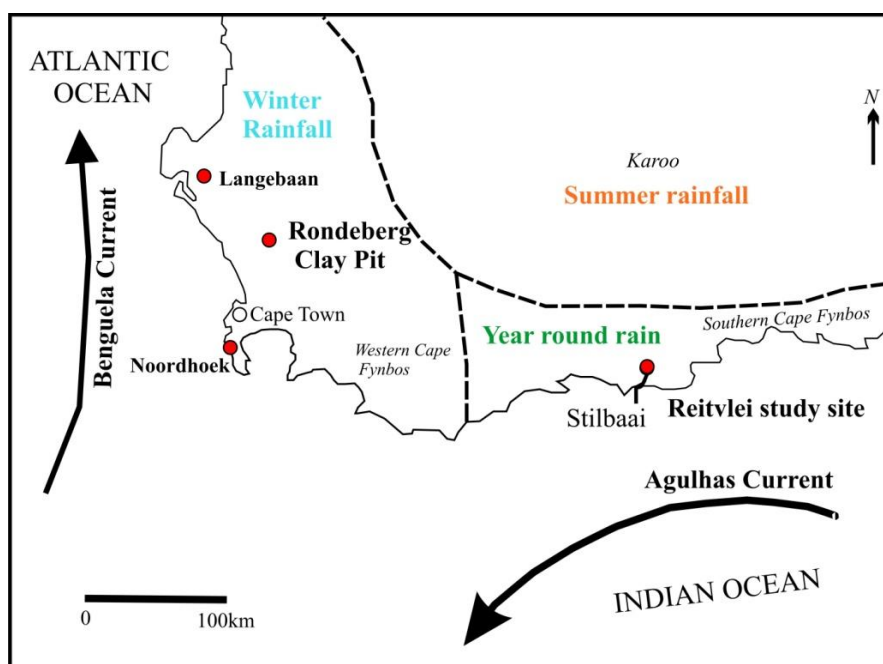


Figure 6.8. Distribution and division of modern day rainfall into three zones in relation to the study sites of Rondeberg Clay Pit (RCP) and Rietvlei wetland study area, South Africa (modified after Roberts *et al.*, 2009 and Chase and Meadows. 2007).

Regional geological setting

The basement rocks underlying the wetland consist of the Devonian Bokkeveld Group shales of the Cape Supergroup that are in places overlain by marine Late Tertiary gravels, deposited during marine transgressions (De Hoop Formation), and contemporary aeolinite of the Wankoe Formation (Roberts *et al.*, 2008). The dune cordons decrease in age (from Tertiary to Holocene) towards the sea (Roberts *et al.*, 2008). The sub-samples obtained comprised silt and fine-grained calcareous sand with a large organic component.

Previous research

The Rietvlei samples presented here form part of a larger study by Carr *et al.* (2010c), in which they report the type, extent of preservation and degradation of Rietvlei's molecular compounds using pyrolysis-gas chromatography mass spectrometry (py-GC/MS). The Carr *et al.* (2010c) study illustrates periods of increased organic matter production in the surrounding terrestrial and aquatic realm of the Rietvlei wetland, over time, as well as variability in the preservation of organic matter (Carr *et al.*, 2010c). Carr *et al.* (2010c) found that there was generally a low concentration and diversity of pyrolysis products, even resistant primary polysaccharides of fresh cellulose, throughout the core. Instead the microbial degradation

products, such as secondary polysaccharides, were present in abundance, with low total organic carbon (TOC) values of most samples reflecting a high degree of degradation (Carr *et al.*, 2010c). Furthermore, they also found a close correlation between the diversity of pyrolysates and TOC value. In contrast, lignin (a resistant polymer) was present in abundance in the uppermost samples, indicating a modern source, as well as an environment which may not be conducive to rapid lignin degradation (Carr *et al.*, 2010c). The abundance of lignin decreased appreciably with depth indicating warmer and more humid climatic conditions in the past, favouring lignin degradation. This is controlled by the pH of the environment which itself is controlled largely by the (alkaline) geology of the area, which has remained relatively constant at ~7.5 (Roberts *et al.*, 2008; Carr *et al.*, 2010c).

Algal and terrestrial OM variability and degree of preservation were found to contribute to an understanding of the Rietvlei wetland environment as well as the terrestrial setting in the immediate vicinity. Aquatic algal organic matter contribution becomes significant within the core between 0.9 m and 2.04 m depth, but terrestrial input and preservation is still considerable during this period (Carr *et al.*, 2010c). It was found that all Rietvlei samples above 2 m depth within the core have a low abundance of aromatic compounds versus a higher contribution of aliphatic and lignin-derived signal, which suggests that terrestrial OM preservation and input, in alliance with algal contribution, increased. Samples lower in the stratigraphy, between 2.3 m and 3.3 m, had lowered TOC with an absence of aliphatic components indicating changes in the preservation of the terrestrial OM signal. Moreover, it was noted that the fatty acid methyl esters and their pyrolysates contribute to the aliphatic signal which would imply an algal lipid source for the OM (Carr *et al.*, 2010c).

The core showed variable trends which repeated themselves down-core with respect to the preservation and variation in OM sources. The samples taken between 1.3 m and 0.9 m depth showed a decrease in the amount of aquatic OM, a general decrease in TOC and increased degradation of the organics present (Carr *et al.*, 2010c). Furthermore, a decrease in the degree of degradation and increases in preservation and productivity of the lake's organics was seen between 0.9 m and 0.7 m depth. Carr *et al.* (2010c) noted that the reverse trend is seen between 0.7 m and 0.3 m depth where preservation and lake productivity decrease once more. The top of the core to 0.3 m depth records both a decrease in degradation and the amount of organic matter input from aquatic sources.

6.3.2 Methodology

Methods used are outlined in Sections 2.2.1 and 2.2.4.

6.3.3 Results

The following bulk organic parameters and radiocarbon ages were obtained from Dr. A Carr of the University of Leicester. Four radiocarbon ages were obtained from 0.9 m, 1.7 m, 2.5 m and 2.89 m. The ages range from 1 260 yrs to 27 630 yrs straddling the transition from the Pleistocene into the Holocene.

The total organic carbon (TOC) content was variable, ranged from 0.96% to 16.3%, and showed a slight increase with stratigraphic height (Fig. 6.9). The total nitrogen (TN) value varied between 0.04% and 0.86%, and showed a similar trend to that of the TOC values with increasing stratigraphic height (Fig.6.9). The $\delta^{13}\text{C}$ values are highly variable and range between -19.8‰ to -25.1‰ (Fig. 6.9). The $\text{C}_{\text{org}}/\text{N}_{\text{org}}$ ratio ranged from 6.67 to 30.52 and showed an increase in value with stratigraphic depth.

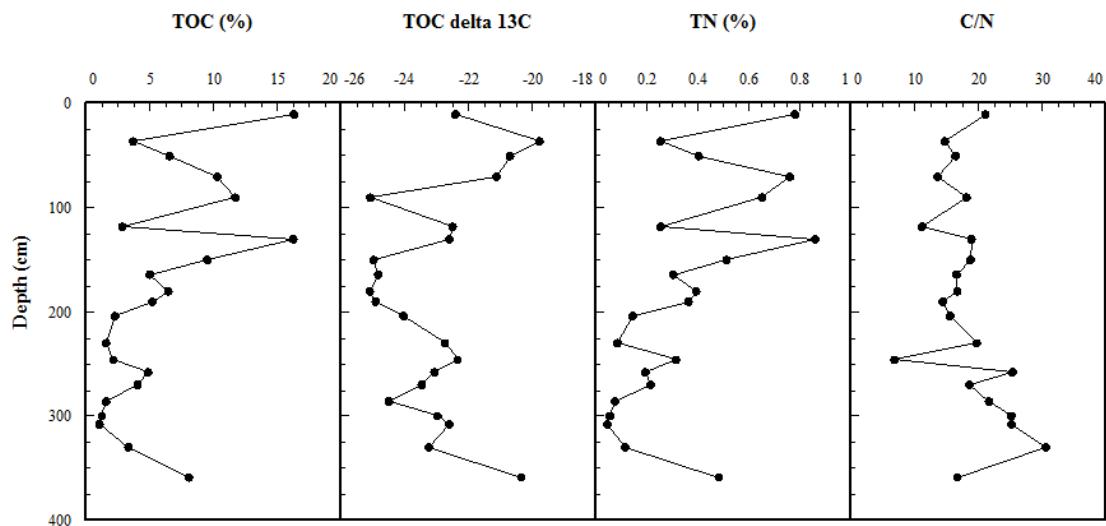


Figure 6.9. The bulk organic parameters for the entire Rietvlei core, showing variability in TOC, $\delta^{13}\text{C}$, TN and C/N ($\text{C}_{\text{org}}/\text{N}_{\text{org}}$).

Table 6.1 provides the range of values obtained from bacterial tetraether membrane lipid extraction from the Rietvlei samples. All samples yielded branched tetraether membrane lipids with BIT indices ≤ 0.90 , and a range between 0.74 and 0.90 (Table 6.1). The lowest BIT values were recorded between 0.9 m (1 260 cal. yrs BP), 2.30 m and 2.51 m depth, and all fell below 0.78. The highest BIT index (0.9) was obtained from the penultimate sample at 2.55 m depth which has an age of 10 250 cal. yrs BP. The Pleistocene sample at 2.89 m (27 630 cal. yrs BP) has a BIT index of 0.84. The higher BIT indices decrease with stratigraphic depth.

The MBT index was low and varied between 0.29 – 0.63, and the CBT index between 0.11 and 0.29 (Table 6.1). The mean annual air temperatures (MAATs) ranged from 9.85 °C at 0.085m depth to 22.74 °C at 2.89 m depth below surface. The lowest MAAT was recorded from the uppermost sample, samples between 0.9 and 2.5 m depth recorded intermediate MAATs (av. 16.9 °C), and the samples between 2.55 and 2.89 m recorded the highest MAATs (Fig. 6.10). The pH of the sediment at time of deposition from all samples was alkaline and ranged from 8.0 to 8.96 (Fig. 6.10, Table 6.1). The highest pH was recorded at 0.085 m depth.

Figure 6.10A illustrates the variation of BIT, pH and MAAT with increasing stratigraphic depth and age. There is a negative relationship between the MAAT and the pH of the samples with a low R^2 value of the distribution of 0.36 (Fig. 6.10A, B). Broadly, higher MAATs correspond with neutral to slightly alkaline pH values (Fig. 6.10A), and lower MAATs correspond to more strongly alkaline pH of the sediment. There is a general trend of increasing temperature with increasing stratigraphic depth and age (Fig. 6.10). The highest MAATs of 20.3 °C and 22.7 °C are recorded at 255 cm and 289 cm depth below surface. The lowest temperatures are found higher in the stratigraphy at 8.5 cm (9.9 °C) and 230 cm (15.7 °C) depth below surface.

Table 6.1. Rietvlei organic biogeochemical parameters, Branched vs. Isoprenoid index of Tetraethers (BIT), Methylation index of branched tetraethers (MBT), cyclisation ratio of branched tetraethers (CBT). The CBT and MBT indices are used to calculate the pH of sediment at time of deposition and mean annual air temperatures (MAAT, °C).

SAMPLE NAME	Depth (m)	BIT	MBT	CBT	pH	MAAT (°C)	AGE median probability (cal yr BP)
Rietvlei 1 (RVSB - 2 - A)	0.085- 0.0105	0.88	0.30	0.11	8.96	9.85	
Rietvlei 2 (RVSB - 2 - B)	0.90 -0.91	0.78	0.50	0.17	8.33	17.50	1130
Rietvlei 3 (RVSB - 2 - C)	1.70-1.71	0.80	0.53	0.24	8.12	18.04	6092
Rietvlei 4 (RVSB - 2 - D)	2.30-2.31	0.74	0.49	0.29	8.03	15.72	
Rietvlei 5 (RVSB - 2 - E)	2.50-2.51	0.78	0.49	0.24	8.13	16.23	
Rietvlei 6 (RVSB - 2 - G)	2.55-2.56	0.90	0.63	0.29	8.00	20.34	11 870
Rietvlei 7 (RVSB - 2 - F)	2.89-2.99	0.84	0.62	0.14	8.40	22.74	

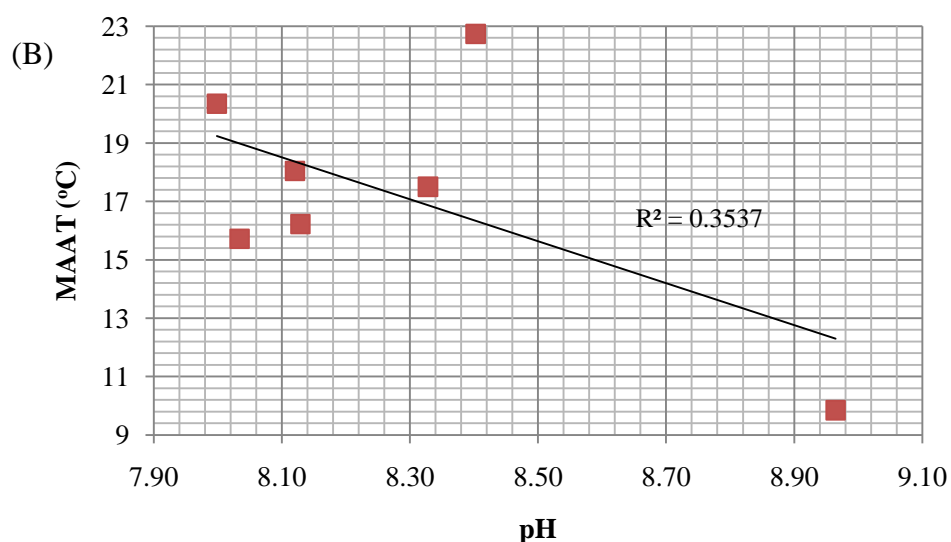
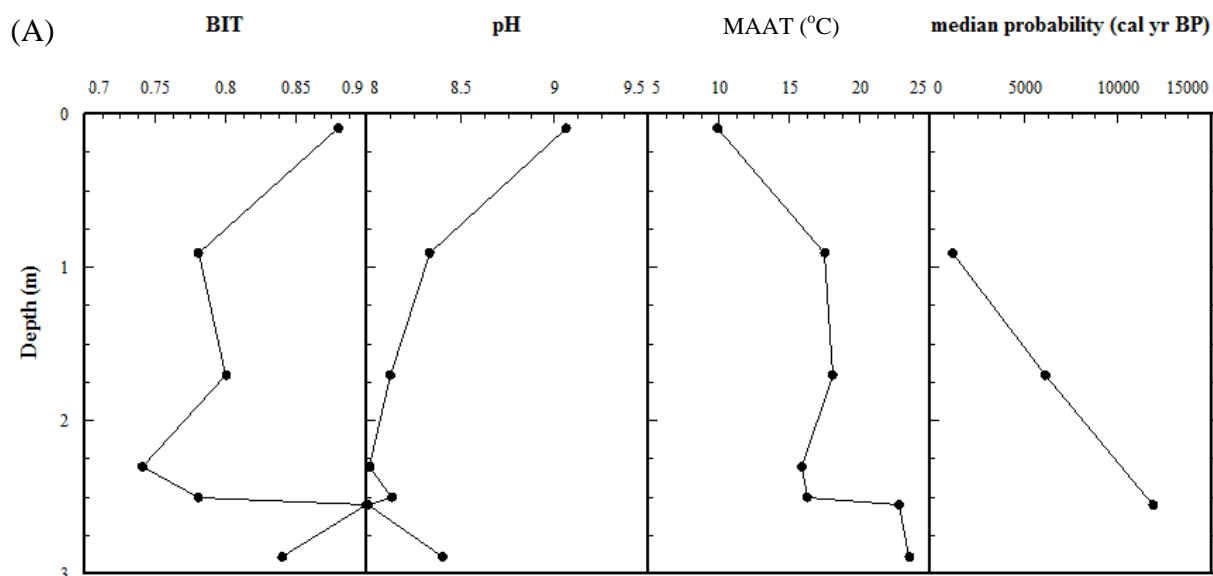


Figure 6.10. (A) Branched vs. Isoprenoid index of Tetraethers (BIT), pH of sediment at time of deposition, mean annual air temperatures (MAAT, °C), and calibrated carbon 14 age dates for specific samples from the Rietvlei core. (B) Scatter plot of MAAT versus pH ($R^2 = 0.36$).

6.3.4 Discussion and conclusion

The samples span the Holocene with an age range from 11 870 cal yr BP at 2.55 m depth to present day. The lowermost samples, at 2.55 m and 2.89 m depth, poor preservation of OM is likely to be a result of the aridity associated with the last glacial maximum and lowered SSTs (Stokes *et al.*, 1997; Carr *et al.*, 2010c). The MAATs recorded from the branched GDGTs show increasing temperatures with increasing sample depth and age (Fig. 6.10A).

The Holocene samples lying above 2.55 m depth show lowered degradation of organic constituents with contributions from both the aquatic and terrestrial realm (Carr *et al.*, 2010c). The low C_{org}/N_{org} ratio indicates an algal influence for the source of much of the organic matter within the samples. The concurrently high TN values are likely a result of nitrogen derived from the proteinaceous algae. The $\delta^{13}C$ values range between -19.8‰ to -25.1‰, with an average value of -23.0‰ (Fig. 6.9). These values indicate C_3 vegetation contaminated by aquatic material.

The Rietvlei samples yielded a range of MAATs from 9.9 °C to 23 °C, and alkaline pH values. There is a negative relationship between the pH of the sediment at time of deposition and the MAAT, which showed a moderately low R^2 value (this correlation, however, is dependent on a single point) (Fig. 6.10B). The alkaline nature of the sediment is to be expected given the alkaline geology and marine-influenced wetland-marsh environment (Roberts *et al.*, 2008; Carr *et al.*, 2010c).

The Rietvlei MAATs can be subdivided into three trends with the lowermost samples (2.55 m – 2.89 m) recording the highest temperatures. These samples are older than 11 870 cal yr BP and may relate to the late glacial maximum and early Holocene, and possibly correlate with increased aridity along the south-eastern Cape coast (Carr *et al.*, 2010c). The elevated temperatures of this interval (greater than 20 °C) complement Carr's *et al.* (2010c) data; as increased degradation of OM would be higher under elevated temperatures. However, considering these are reported during the late glacial maximum it is the reverse of what would be expected for this colder period. The intermediate MAATs, averaging at 17 °C for samples between 2.5 m and 0.9 m depth, are of Holocene age and correspond with the MAAT (20.1 °C) of the Knysna area today (Koen and Crowe, 1987). Deacon *et al.*, (1984) and Carr *et al.*, (2010c) affirm that the Holocene period of the southern Cape was humid contrasting with the present low rainfall state (400 mm pa). This is likely to have increased production and preservation of algal and terrestrial OM within the system, as well as the surrounding environs which would agree with the MAATs derived in this study (Fig. 6.10A; Carr *et al.*, 2010c).

The very low MAAT recorded for the uppermost sample of the Rietvlei core is more difficult to explain in relation to the semi-arid conditions and MAAT of the region today. Instead this low MAAT shows a relationship with the minimum mean annual temperature recorded for the Knysna region (11 °C; Koen and Crowe, 1987). This could be a reflection of

times of higher productivity where the production of branched GDGTs may be biased towards colder, winter months of higher rainfall. However, as this site receives year-round rainfall it still presents an ambiguity and may represent a significantly cold period over the past ~ 1 000 years. Carr *et al.* (2010c) study shows that samples taken above 0.9m depth had highly variable TOC contents with phases of enhanced preservation/degradation of OM during the late Holocene. This would complement cycles of increasing and decreasing aridity of the area. The samples over this period also saw a decrease in degradation and the amount of aquatic organic matter input. This could mean a more terrestrially derived signal, but the BIT index of the uppermost sample is 0.88 indicating a mixture of terrestrial and aquatic sources.

Importantly, the low MBT values of all samples question the reliability of the branched GDGT derived palaeotemperatures and pH of these lake derived sediments; as sediments that are stratigraphically close to the surface may be influenced by modern day bioturbation. These sediments experience periodic and more often perennial water-logging, and are likely to have inconsistent MBT and CBT results as a likely result of modern day bacterial lipid contribution (Table 6.1). This, therefore, suggests that the branched GDGT palaeoenvironmental data is questionable in this shallow setting. The sample depth (less than 3 m depth below surface), the nature of a wetland ecosystem and the function modern bacteria producing tetraether membrane lipids are all factors which need consideration.

There is a significant change in MAAT at 11 870 yrs BP with high temperatures of 20 - 22.7 °C recorded for samples between 2.55 m and 2.89 m depth. Above 2.55 m the MAATs of samples between 1 130 yrs BP and 6 092 yrs BP record temperatures which are similar to that of the modern day setting (averaging 17 °C) (Fig. 6.10). The uppermost sample from 0.085 m depth recorded a significantly low MAAT of 9.9 °C which is comparable to modern day Cape winter temperatures. The presence of modern lignin (Carr *et al.*, 2010c), within the near surface samples, further indicates the likelihood that there may be contamination of modern branched-GDGTs with those produced in the past. The presence of the vegetation mat (*Phragmites australis*; Carr *et al.*, 2010c) is also another concern and can affect the microclimate, thereby affecting the composition of the tetraether membrane lipids.

7 General Conclusion

Palaeoenvironmental factors were deduced from two proxies: firstly, the traditional use of palynology to give a broad understanding of palaeoenvironmental and palaeoecological factors; and secondly, the employment of a novel proxy using bacterial branched tetraether lipids (GDGTs), preserved in peat and organic-rich sediments, to calculate precise mean annual air temperatures and sediment pH.

These proxies were applied to each study site, where feasible, and complimented other techniques (e.g. stable isotopes). Results indicate that the sediments from Langebaanweg, Noordhoek and Rondeberg are early to late Miocene in age. They experienced seasonality and periods of significantly elevated mean annual air temperatures (MAAT) by as much as 14 °C greater than the modern Cape MAATs (~17 °C). Palynofloras, based on nearest living relative associations, suggest an equitable climate along the south-west coast with tropical to subtropical conditions. Seasonality or glacial/interglacial cycles, more likely, seem to play a role at Noordhoek and Rondeberg sites with the presence of charcoal, palynodebris, reduced palynomorph numbers and charred logs at specific intervals being indicators of high temperatures and lowered rainfall. Palynological information was further used to determine if sites are biostratigraphically correlated and to provide broad age-limits for each site by the comparison of palynomorphs found over specified intervals. Known botanical affinities of palynomorphs show establishment of swamp, forest trees and shrubs as well as herbs, but the exact composition of the palaeoflora, however, cannot be determined precisely from the pollen abundance due to the differences in preservation, production and dispersal (Traverse, 1988).

The branched tetraether membrane lipids derived from peaty-clays and organic-rich clays at the Noordhoek, Langebaanweg and Rietvlei sites yielded positive results, and indicate the potential for the use of MBT-CBT proxy in southern Africa. Employing the novel CBT/MBT proxy has complemented, to an extent, previous and present palynological studies and palaeoclimate interpretations. Climate interpretation using palynoflora in conjunction with tetraether lipid membranes provides convincing evidence for the useful nature of the new proxy. It not only builds on palynological evidence but allows for the detailing of palaeotemperatures and palaeoenvironmental change. The further refinement of the proxy through calibration using local soils may increase the success of the tool in

Southern African palaeoenvironment reconstruction. The use of this proxy in relatively young sediments that lie close to the surface is cautioned. This is due to the fact that modern bacteria producing branched tetraethers in sediment/water column may be incorporated, via natural processes (such as bioturbation), contributing to the fossil concentrations. This is where the indices are of importance.

Currently studies of the Middle Miocene Climatic Optimum suggest multiple hypotheses and models as to the generation of this periodic warming (Flower and Kennett, 1993; Ennyu and Arthur, 2004; Kutzbach and Behling, 2004). These range from the geographical and tectonic, such as closure of key gateways leading to differences in ocean circulation allowing for efficient heat flow (Zachos *et al.*, 2001; Steppuhn *et al.*, 2006), to changes in the levels of atmospheric carbon dioxide (Cerling 1991; Pearson and Palmer, 2000; Kürschner *et al.*, 2008; Retallack, 2009; Tripathi *et al.*, 2010). The generation and continuous refinement of numerous Miocene climate models provides constraints on certain variables, such as carbon dioxide concentration. This will provide a better understanding and explanation as to the environmental change recorded (Micheels *et al.*, 2009). A greater understanding of these factors will influence the understanding of continental climate change relative to global scenarios.

7.1 Future research

The use of biogeochemical proxies where organic-rich sediments are available would contribute to a more informed insight into regional climate change in Southern Africa. Moreover, there would be potential for global climate change comparisons in the Southern and Northern Hemisphere. The molecular proxy may complement many previously attempted palaeoclimatic and palaeoecological studies of Neogene age, more specially the wealth of Pleistocene, Holocene and Quaternary palynological studies (Scott, 1982, 1993, 1994, 1996; Scott and Vogel, 2000; Scott and Woodborne, 2007). This type of research has potential to provide palaeoenvironmental information where other proxies may be absent. Several sites along the south-west coast and south coast have enormous potential for the application of this new proxy, and would further test the proxy and supplement current and previous research, e.g. the Knysna lignites (Thiergart *et al.*, 1963; Thwaites and Jacobs, 1989; Carr *et al.*, 2010b), the Wonderkrater pollen core with reliable dates from the Pleistocene-Holocene (Scott *et al.*, 1995). Importantly, detailed environmental knowledge would augment

archaeological studies. For example, the Elands Bay and Pinnacle Point (Mossel Bay) sites may benefit from a greater understanding of the palaeoenvironment in order to improve current knowledge of the 'palaeoscape', and contribute to theories on the habitation of early humans in these areas. Further afield, application of molecular fossils to organic-rich Miocene to Pleistocene fossiliferous lacustrine and playa sediments from Etosha Pan, Namibia (Pickford *et al.*, accepted manuscript) would extend current understanding of the aridification that took place along the Southern African west coast from the Late Oligocene. The age of the deposits seems of lesser concern when the reliability of the tetraether membrane lipids is considered; so long as the GDGTs are sufficiently preserved and of substantial quantity to give reliable and reproducible results (Powers *et al.*, 2004).

8 References

- Adams, C.G., Lee, D.E. and Rosen, B.R. 1990. Conflicting isotopic and biotic evidence for tropical sea-surface temperatures during the Tertiary. *Palaeogeography, Palaeoclimatology, Palaeoecology*, **77**: 289-313.
- Adelana, S., Xu, Y., and Vrbka, P. 2010. A conceptual model for the development and management of the Cape Flats aquifer, South Africa. *Water SA*, **36**: 461-474.
- Albers, S-J., Van De Vossenberg, J .L. C. M., Driessen, J. M., and Konings, W.N. 2000. Adaptations of the Archaeal cell membrane to heat stress. *Frontiers in Bioscience*, **5**: 813-820.
- Anon 1. 2010. African pollen database (APD). Available, (online): <http://medias3.mediasfrance.org/apd/accueil.htm> [Accessed 25/04/2009].
- Ansorge, I.J., and Lutjeharms, J.R.E. 2007. The Cetacean Environment off Southern Africa. *In*: Best, P.B. 2007 (Ed.), *Whales and Dolphins of the Southern African Subregion*. Cambridge University Press. Cape Town. Pp. 5-13.
- Axelrod, D.I. and Raven, P.H. 1978. Late Cretaceous and Tertiary vegetation history of Africa. *In*: Werger, M.J.A. (Ed.). 1978. *Biogeography and Ecology of Southern Africa*. Junk. The Hague. Pp. 77 – 130.
- Ballantyne, A. P., Greenwood, D.R., Sinninghe Damste, J.S., Csank, A Z., Eberle, J.J., and Rybczynski, N. 2010. Significantly warmer Arctic surface temperatures during the Pliocene indicated by multiple independent proxies. *Geology*, **38**: 603-606.
- Bechtel, A., Gratzner, R., Sachsenhofer, R., Gusterhuber, J. Lucke, A., and Puttmann, W. 2008. Biomarker and carbon isotope variation in coal and fossil wood of Central Europe through the Cenozoic. *Palaeogeography, Palaeoclimatology, Palaeoecology*, **262**: Jun. 166-175.
- Bice, K., Scotese, C., Seidov, D., and Barron, E. 2000. Quantifying the role of geographic change in Cenozoic ocean heat transport using uncoupled atmosphere and ocean models. *Palaeogeography, Palaeoclimatology, Palaeoecology*, **161**: 295-310.
- Billups, K., Kelly, C., and Pierce, E. 2008. The Late Miocene to Early Pliocene Climate Transition in the Southern Ocean. *Palaeogeography, Palaeoclimatology, Palaeoecology*, **267**: 31–40.
- Bindler, R. 2006. Mired in the past — looking to the future: Geochemistry of peat and the analysis of past environmental changes. *Global and Planetary Change*, **53**: 209-221.
- Birks, H.J.B., and Gordon, A.D. 1985. *Numerical Methods in Quaternary Pollen Analysis*. Academic Press, London. Pp.317.

- Camberlin, P., Janicot, S., Pocard, I. 2001. Seasonality and Atmospheric Dynamics of the Teleconnection between African Rainfall and tropical Sea-Surface Temperature: Atlantic vs. ENSO. *International Journal of Climatology*, **21**: 973-1005.
- Carr, A.S., Thomas, D.S.G., Bateman, M.D., Meadows, M.E., and Chase, B. 2006a. Late Quaternary palaeoenvironments of the winter-rainfall zone of southern Africa: Palynological and sedimentological evidence from the Agulhas Plain. *Palaeogeography, Palaeoclimatology, Palaeoecology*, **239**: 147-165.
- Carr, A. S., Thomas, D.S.G., and Bateman, M.D. 2006b. Climatic and sea level controls on Late Quaternary aeolian activity on the Agulhas Plain, South Africa. *Quaternary Research*, **65**: 252 – 263.
- Carr, A. S., Boom, A., and Chase, B. M. 2010a. The potential of plant biomarker evidence derived from rock hyrax middens as an indicator of palaeoenvironmental change. *Palaeogeography, Palaeoclimatology, Palaeoecology*, **385**: 321-330.
- Carr, A. S., Dunajko, A., Bateman, M. D., Holmes, P.J., and Berrio, J-C. 2010b. New evidence for the age and palaeoecology of the Knysna Formation. *South African Journal of Geology*, **113**: 241-256.
- Carr, A.S., Boom, A., Chase, B.M., Roberts, D.L., and Roberts, Z.E. 2010c. Molecular fingerprinting of wetland organic matter using pyrolysis-GC/MS: an example from the southern Cape coastline of South Africa. *Journal of Paleolimnology*, **44**: 947-961.
- Carr, A.S., Bateman, M.D., Roberts, D.L., Murray-Wallace, C.V., Jacobs, Z., and Holmes, P.J. 2010d. The last interglacial sea-level high stand on the southern Cape coastline of South Africa. *Quaternary Research*, **73**: 351-363.
- Cerling, T.E. 1991. Carbon dioxide in the atmosphere: evidence from Cenozoic and Mesozoic paleosols. *American Journal of Science*, **291**: 377-400.
- Cerling, T.E., Harris, J.M., MacFadden, B.J., Leakey, M, Quade, J., Eiseenmann, V., and Ehleringer, J.R. 1997. Global vegetation change through the Miocene/Pliocene boundary. *Nature*, **389**: 153-158.
- Chase, B. M. 2010. South African palaeoenvironments during marine oxygen isotope stage 4: a context for the Howiesons Poort and Still Bay industries. *Journal of Archaeological Science*, **37**: 1359-1366.

- Chase, B.M., and Meadows, M.E. 2007. Late Quaternary dynamics of southern Africa's winter rainfall zone. *Earth Science Reviews*, **84**: 103-138.
- Chesworth, W., Camps Arbestainm M., Macias, F., and Martinez-Cortizas, A. 2008. Humic substances. In: Chesworth, W. (Ed). 2008. *Encyclopedia of soil science*. Springer. The Netherlands. Pp. 323-326.
- Christensen, B.A., and Giraudeau, J. 2002. Foreword: Neogene and Quaternary evolution of the Benguela upwelling system. *Marine Geology*, **180**: 1-2.
- Clarke, J., and Crame, J. O. 1992. The Southern Ocean Benthic Fauna and Climate Change: A Historical Perspective [and Discussion]. *Philosophical Transactions of the Royal Society B: Biological Sciences*, **338**: 299-309.
- Coetzee, J.A. 1978a. Late Cainozoic palaeoenvironments of southern Africa. In: Van Zinderen Bakker, E.M., (Ed.), *Antarctic glacial history and world palaeoenvironments*. A.A. Balkema. Rotterdam. Pp. 115-127.
- Coetzee, J.A. 1978b. Climatic and biological changes in South-western Africa during the Late Cainozoic. In: Van Zinderen Bakker, E.M., and Coetzee, J.A. (Eds.). *Palaeoecology of Africa and the surrounding Islands*. Vol. 10. A.A. Balkema. Rotterdam. Pp. 13-29.
- Coetzee, J.A. 1980. Tertiary environmental changes along the south-western African coast. *Palaeontologia Africana*, **23**: 197-203.
- Coetzee, J.A. 1981. A palynological record of very primitive Angiosperms in Tertiary deposits of south-western Cape Province, South Africa. *South African Journal of Science*, **77**: 341-342.
- Coetzee, J.A. 1983. Intimations on the Tertiary vegetation of southern Africa. *Bothalia*, **14**: 345- 354.
- Coetzee, J.A. 1986. Palynological evidence for major vegetation and climatic change in the Miocene and Pliocene of the south-western Cape. *South African Journal of Science*, **82**: 71-72.
- Coetzee, J.A., and Muller, J. 1984. The phytogeographic significance of some extinct Gondwana pollen types from the Tertiary of the south-western Cape (South Africa). *Annals of the Missouri Botanical Garden*, **71**: 1088-1099.
- Coetzee, J.A., and Praglowski, J. 1984. Pollen evidence for the occurrence of *Casuarina* and *Myrica* in the Tertiary of South Africa. *Grana*, **23**: 23-41.

- Coetzee, J.A., and Rogers, J. 1982. Palynological and lithological evidence for the Miocene palaeoenvironment in the Saldanha Region (South Africa). *Palaeogeography, Palaeoclimatology, Palaeoecology*, **39**: 71-85.
- Coetzee, J.A., Scholtz, A., and Deacon, H.J. 1983. Palynological studies and the vegetation history of the Fynbos. In: Deacon, H.j., Hendey, Q.B., and Lambrecht, J.J.N. (Eds). 1983. *Fynbos Palaeoecology: A Preliminary Synthesis*. South African National Scientific Programmes Report, **75**. Pretoria. Pp. 156-173.
- Cole, D.I., and Roberts, D.L. 1996. Lignite from the western coastal plain of South Africa. *Journal of African Earth Sciences*, **23**: 95-117.
- Coûteaux, M.-M., Bottner P., and Berg, B. 1995. Litter decomposition climate and litter quality, *Trends in Evolution and Ecology*, **10**: 63–66.
- Cowling, R.M., Procheş, S., and Partridge, T.C. 2009. Explaining the uniqueness of the Cape flora: incorporating geomorphic evolution as a factor for explaining its diversification. *Molecular phylogenetics and evolution*, **51**: 64-74.
- Craig, H. 1957. Isotopic standards for carbon and oxygen and correction factors for mass-spectrometric analysis of carbon dioxide: *Geochimica et Cosmochimica Acta*, **12**:133–149.
- Day, S.P. 1996. Dogs, Deer and Diet at Star Carr: a Reconsideration of C-isotope Evidence from Early Mesolithic Dog Remains from the Vale of Pickering, Yorkshire, England. *Journal of Archaeological Science*, **23**: 783–787.
- Deacon, H.J., Deacon, J., Scholtz, A., Thackeray, J.F., Brink, J.S., Vogel, J.C. 1984. Correlation of palaeoenvironmental data from the Late Pleistocene and Holocene deposits at Boomplaas cave, southern Cape. In: Vogel, J.C. (Ed.). *Late Cainozoic Palaeoenvironments of the Southern Hemisphere*. A.A. Balkema. Rotterdam. Pp. 339–352.
- DeConto, R.M. and Pollard, D. 2003. Rapid Cenozoic glaciation of Antarctica induced by declining atmospheric CO₂. *Nature*, **421**: 245-249.
- Denton, G.H. 1985. Did the Antarctic ice sheet influence Late Cainozoic climate and evolution in the southern hemisphere? *South African Journal of Science*, **81**: 224-229.
- Derry, L.A., and France-Lanord, C. 1996. Neogene growth of the sedimentary organic carbon reservoir. *Paleoceanography*, **11**: 267 – 275.
- de Villiers, S.E. 1997. The Palynology of Tertiary sediments from a palaeochannel in Namaqualand. PhD thesis (unpubl.). University of Witwatersrand, Johannesburg.

- de Villiers, S.E., and Cadman, A. 1997. The palynology of Tertiary sediments from a palaeochannel in Namaqualand, South Africa. *Palaeontologia Africana*, **34**: 69-99.
- de Villiers, S.E., and Cadman, A. 2001. An analysis of the palynomorphs obtained from Tertiary sediments at Koingnaas, Namaqualand, South Africa. *Journal of African Earth Sciences*, **33**: 17 - 47.
- Diester-Haass, L., Meyers, P.A., Vidal, L., Wefer, G., 2001. Data report: Sand fraction, carbonate, and organic carbon contents of Late Miocene sediments from Site 1085, middle Cape Basin. In: *Proc. ODP, Sci. Res.* **175**, Available, (online): <http://www.odp.tamu.edu/publications/175-SR/chap-01>. [Accessed 12/09/2010].
- Diester-Haass, L., Meyers, P.A., and Vidal, L. 2002. The late Miocene onset of high productivity in the Benguela Current upwelling system as part of a global pattern. *Marine Geology*, **180**: 87-103.
- Dingle, R. V. 1973. Post-Palaeozoic stratigraphy of the eastern Agulhas Bank, South African continental margin. *Marine Geology*, **15**: 1-23.
- Dommenget, D. 2009. The Ocean's Role in Continental Climate Variability and Change. *Journal of Climate*, **22**: 4939 – 4952.
- Donders, T.H., Weijers, J.W.H., Munsterman, D.K., Kloosterboer-van Hoeve, M.L., Buckles, L.K., Pancost, R.D., Schouten, S., Sinninghe Damsté, J. S., and Brinkhuis, H. 2009. Strong climate coupling of terrestrial and marine environments in the Miocene of northwest Europe. *Earth and Planetary Science Letters*, **281**: 215- 225.
- Dowsett, H. J., and Willard D. 1996. Southeast Atlantic marine and terrestrial response to middle Pliocene climate change. *Marine Micropaleontology*, **27**: 181–193.
- Doyle, J. A. 1998. Molecules, morphology, fossils, and the relationship of angiosperms and Gnetales. *Molecular phylogenetics and evolution*, **9**: 448-462.
- Dupont, L. M.; Rommerskirchen, F.; Condon, T.; Mollenhauer, G.; Schefuss, E. 2009. Environmental changes in South-west Africa during the Miocene C4 plant expansion. *American Geophysical Union*, Fall Meeting 2009, abstract #PP13B-1396.
- Du Toit, A.L. 1933. Crustal movement as a factor in the geographical evolution of South Africa. *South African Journal of Geography*, **16**: 3-21.
- Eagles, G., Livermore, R. and Morris, P. 2006. Small basins in the Scotia Sea; The Eocene Drake Passage gateway. *Earth and Planetary Science Letters*, **242**: 343-353.

- Ennyu, A. and Arthur, M.A. 2004. Early to middle Miocene paleoceanography in the southern high latitudes off Tasmania. *In: Exon, N.F., Kennett, J.P., and Malone, M.J. (Eds.). The Cenozoic Southern Ocean: Tectonics, Sedimentation and Climate Change Between Australia and Antarctica. Geophysical Monograph Series, 151: 215-233.*
- Erdtman, G. 1969. *Handbook of palynology; An introduction to the study of pollen grains and spores.* Munksgaard. Copenhagen. Pp 486.
- Fægri, K and Iverson, J. 1964. *Textbook of Pollen Analysis.* Munksgaard. Denmark. Pp. 229.
- Farquhar, G.D., O'Leary, M.H., and Berry, J.A. 1982. On the relationship between carbon isotope discrimination and the intercellular carbon dioxide concentration in leaves. *Australian Journal of Plant Physiology, 9: 121–137.*
- Flower, B.P., and Kennet, J.P. 1993. Relations between Monterey Formation deposition and middle Miocene global cooling: Naples Beach section, California. *Geology, 23:877- 880.*
- Flower, B.P., and Kennett, J.P. 1994. The middle Miocene climatic transition: East Antarctic ice sheet development, deep ocean circulation and global carbon cycling. *Palaeogeography, Palaeoclimatology, Palaeoecology, 108: 537–555.*
- Franz-Odendaal TA. 2001. Environmental stress five million years ago on the West Coast of South Africa? *Science in Africa.* Available, (online): <http://www.scienceinAfrica.co.za/2001/june/fossils.htm> [Accessed 08/09/2010].
- Franz-Odendaal, T.A., Lee-Thorp, J. A., and Chinsamy, A. 2002. New evidence for the lack of C₄ grassland expansions during the early Pliocene at Langebaanweg, South Africa. *Paleobiology, 28: 378-388.*
- Franz-Odendaal, T.A., Lee-Thorp, J. A., and Chinsamy, A. 2003. Insights from stable light isotopes on enamel defects and weaning in Pliocene herbivores. *Journal of Biosciences, 28: 101-109.*
- Gallagher, S.J., Smith, A.J., Jonasson, K., Wallace, M.W., Holdgate, G.R. Daniels, J., and Taylor, D. 2001. The Miocene palaeoenvironmental and palaeoceanographic evolution of the Gippsland Basin , Southeast Australia: a record of Southern Ocean change. *Palaeogeography, Palaeoclimatology, Palaeoecology, 172: 53-80.*
- Gersonde, B., and Censarek, R. 2006. Middle- Late Miocene Southern Ocean climate development and its implications on Antarctica Ice sheet development-Diatom evidence from Atlantic sector ODP sites. *Geophysical Research Abstracts 8.*

- Germeraad, J.H., Hopping, C.A., and Muller, J. 1968. Palynology of Tertiary sediments of tropical areas. *Review Palaeobotany and Palynology*, **6**: 189–348.
- Gheerbrant, E., and Rage, J.C. 2006. Paleobiogeography of Africa: How distinct from Gondwana and Laurasia? *Palaeogeography, Palaeoclimatology, Palaeoecology*, **241**: 224–246.
- Goldblatt, P., and Manning, J.C. 2002. Plant diversity of the Cape Region of Southern Africa. *Annals of the Missouri Botanical Garden*, **89**: 281-302.
- Gray, J. 1965. Part III. Extraction techniques. In: Kummel, B., and Raup, D. (Eds.). 1965. *Handbook of Paleontological Techniques*. W.H. Freeman and Co. San Francisco. Pp. 530–587.
- Gröcke, D.R., 2002. The carbon isotope composition of ancient CO₂ based on higher plant organic matter. *Philosophical Transactions of the Royal Society, London. A* **360**: 633–658.
- Hanekom, N., Randall, R. M., Nel, P., and Kruger, N. 2009. West Coast National Park - state of knowledge report. *South African National Parks*. Pp. 1-65.
- Haq, B.V., Hardenbol, J., and Vail, P.R. 1987. Chronology of fluctuating sea levels since the Triassic. *Science*, **35**: 1156-1166.
- Hay, W.H. 2010. Can humans force a return to a ‘Cretaceous’ climate? *Sedimentary Geology*, doi:10.1016/j.sedgeo.2010.04.015.
- Helme, N.A., and Trinder-Smith, T.H. 2006. The endemic flora of the Cape Peninsula, South Africa. *South African Journal of Botany*, **72**: 205 – 210.
- Hendey, Q.B. 1974. Faunal dating of the Late Cenozoic of Southern Africa, with special reference to the Carnivora. *Quaternary Research*, **4**: 149-161.
- Hendey, Q.B. 1981. Geological succession at Langebaanweg, Cape Province, and global events of the late Tertiary. *South African Journal of Science*, **77**: 33-38.
- Hendey, Q.B. 1982. *Langebaanweg; A record of past life*. The Rustica Press, Ltd. Cape Town. Pp. 71.
- Hendey, Q.B. 1983. Cenozoic geology and palaeogeography of the Fynbos region. In: Deacon, H.J., Hendey, Q.B. and Lambrechts, J.J.N. (Eds), *Fynbos palaeoecology: a preliminary synthesis*. South African National Scientific 1591 Programmes Report No. 75, 35-60.
- Holbourn, A., Kuhnt, W., Schulz, M and Erlenkeuser, H. 2005. Impacts of orbital forcing and atmospheric carbon dioxide on Miocene ice-sheet expansion. *Nature*, **438**: 483-487.

- Holbourn, A., Kuhnt, W., Schulz, M., Flores, J-A., and Andersen, N. 2007. Orbitally-paced climate evolution during the middle Miocene “Monterey” carbon-isotope excursion. *Earth and Planetary Science Letters*, **261**: 534–550.
- Holdgate, G., McGowran, B., Fromhold, T., Wagstaff, B., Gallagher, S., Wallace, M., Sluiter, I., and Whitelaw, M. 2009. Eocene–Miocene carbon-isotope and floral record from brown coal seams in the Gippsland Basin of southeast Australia. *Global and Planetary Change*, **65**: 89-103.
- Hopmans, E.C., Weijers, J.W.H., Schefuss, E., Herfort, L., Sinninghe Damsté, J.S., Schouten, S., 2004. A novel proxy for terrestrial organic matter in sediments based on branched and isoprenoid tetraether lipids. *Earth and Planetary Science Letters*, **224**: 107–116.
- Huguet, C., Hopmans, E.C., Febo-Ayala, W., Thompson, D.H., Sinninghe Damste, J. S., and Schouten, S. 2006. An improved method to determine the absolute abundance of glycerol dibiphytanyl glycerol tetraether lipids. *Organic Geochemistry*, **37**: 1036- 1041.
- Ivanov, D., Utescher, T., Mosbrugger, V., Syabryaj, S. , Djordjević-Milutinović, D., and Molchanoff, S. 2010. Miocene vegetation and climate dynamics in Eastern and Central Paratethys (Southeastern Europe). *Palaeogeography, Palaeoclimatology, Palaeoecology*, doi.org/10.1016/j.palaeo.2010.07.006.
- Jacquemet, A., Barbeau, J., Lemiègre, L., and Benvegnu, T. 2009. Archaeal tetraether bipolar lipids: structure, function and applications. *Biochimie*, : **91**: 711-717.
- Jenkins, D.A. 1989. Trace element geochemistry in archaeological sites. *Environmental Geochemistry and Health*, **11**: 257-62.
- Jenkyns, H.C., Gröcke, D.R., and Hesselbo, S. P. 2001. Nitrogen isotope evidence for water mass denitrification during the Early Toarcian (Jurassic) oceanic anoxic event. *Paleoceanography*, **16**: 593 - 603.
- Jiménez-Moreno, G., Rodríguez-Tovar, F.-J., Pardo-Igúzquiza, E., Fauquette, S., Suc, J.-P., Müller, P., 2005. High-resolution palynological analysis in late early-middle Miocene core from the Pannonian Basin, Hungary: climatic changes, astronomical forcing and eustatic fluctuations in the Central Paratethys. *Palaeogeography, Palaeoclimatology, Palaeoecology*, **216**:73–97.
- Jiménez-Moreno, G., and Suc, J.-P. 2007. Middle Miocene latitudinal climatic gradient in western Europe: evidence from pollen records. *Palaeogeography, Palaeoclimatology, Palaeoecology*, **253**: 224–241.

- Jiménez-Moreno, G., Fauquette, S., and Suc, J.-P. 2010. Miocene to Pliocene vegetation reconstruction and climate estimates in the Iberian Peninsula from pollen data. *Review of Palaeobotany and Palynology*, **162**: 403-415.
- Karl, T.E., and Trenberth, K.E. 2003. Modern Global Climate Change. *Science*, **302**: 1719-1723.
- Kemp, E.M., and Harris, W.K. 1975. The vegetation of Tertiary islands on the Ninetyeast Ridge. *Nature*, **258**: 303- 307.
- Kennett, J.P. 1977. Cenozoic evolution of Antarctic glaciation, the circum-Antarctic Ocean, and their impact on global paleoceanography. *Journal of Geophysical Research*, **82**: 3843-3860.
- Kennett, J.P. 1986. Miocene to early Pliocene oxygen and carbon isotope stratigraphy in the southwest Pacific, Deep Sea Drilling Project, Leg 90. In: Kennett, J. P., van der Borch, C. C. *et al.* (Ed.). *Initial Reports of the Deep Sea Drilling Project*, **90**: 1383-1411.
- Killops, S., and Killops, V. 2005. *Introduction to Organic Geochemistry*. 2nd Edition. Blackwell Publishing. Oxford. Pp. 393.
- Kim, J.-H., Schouten, S., Buscail, R., Ludwig, W., Bonnin, J., Sinninghe Damsté, J.S., Bourrin, F., 2006. Origin and distribution of terrestrial organic matter in the NW Mediterranean (Gulf of Lions): exploring the newly developed BIT index. *Geochemistry, Geophysics, Geosystems* **7**. doi:10.1029/2006GC001306.
- Kim, J.-H., Hugué, C., Zonneveld, K.A.F., Versteegh, G.J.M., Roeder, W., Sinninghe Damsté, J.S., and Schouten, S. 2009. An experimental field study to test the stability of lipids used for the TEX₈₆ and U^K₃₇ palaeothermometers. *Geochimica et Cosmochimica Acta*, **73**: 2888–2898.
- Kirchheimer, F. 1934. On pollen from the upper Cretaceous dysodil of Banke, Namaqualand (South Africa). *Transactions of the Royal society of South Africa*, **21**: 41-50.
- Koen, J.H. and Crowe, T.M. 1987. Animal-habitat relationships in the Knysna Forest, South Africa: discrimination between forest types by birds and invertebrates. *Oecologia*, **72**:414-422.
- Kominz, M.A., Miller, K.G., and Browning, J.V. 1998. Long-term and short-term global Cenozoic sea-level estimates. *Geology*, **26**: 311 – 314.
- Kruger, A.C. 2004. *Climate of South Africa: Climate Regions*. South African Weather Service, Pretoria, South Africa. WS 45. Pp 19.

- Kürschner, W.M., Kvaček, Z., and Dilcher, D.L. 2008. The impact of Miocene atmospheric carbon dioxide fluctuations on climate and the evolution of terrestrial ecosystems. *Proceedings of the National Academy of Sciences of the United States of America*, **105**: 449-53.
- Kutzbach, J.E., and Behling, P. 2004. Comparison of simulated changes of climate in Asia for two scenarios: Early Miocene to present, and present to future enhanced greenhouse. *Global and Planetary Change*, **41**: 157–165.
- Lakhanpal, R.N. 1970. Tertiary floras of India and their bearing on the historical geology of the region. *Taxon*, **19**: 675-694.
- Linder, H.P. 1987. The evolutionary history of the Poales/Restionales-a hypothesis. *Kew Bulletin*, **42**: 297-318.
- Liu, Y., Ma, L., Leavitt, S.W., Cai, Q., and Liu, W. 2004. Seasonal precipitation reconstruction from tree-ring stable carbon isotopes at Mt. Helan, China, since AD 1804, *Global Planet Change*, **41**: 229–239.
- Logan, P., Curd1, S., Downie, B., Weston, J. and Shaw, D. 2009. Exploration on the Frontier: Towards an Understanding of the Albert Basin. Search and Discovery Article #10192. Available, Online: <http://www.searchanddiscovery.com/documents/2009/50180shaw/index.htm> [Accessed 12/05/2010].
- Lovett, J.C., Ruffo, C.K., Gereau, R.E and Taplin, J.R.D. 2007. *Field Guide to the Moist Forest Trees of Tanzania*. Frontier. Pp. 303.
- Lunt, D.J., Flecker, R., Valdes, P.J., Salzmann, U., Gladstone, R., and Haywood, A. 2008. A methodology for targeting palaeo proxy data acquisition: A case study for the terrestrial late Miocene. *Earth and Planetary Science Letters*, **271**: 53-62.
- Lutjeharms, J.R.E., Monteiro, P.M.S., Tyson P.D. and Obura D. 2001. The oceans around southern Africa and regional effects of global change. *South African Journal of Science*, **97**:119-130.
- McLachlan, I.R., and Pieterse, E. 1978. Preliminary palynological results: Site 361, Leg 40, Deep Sea Drilling Project. *Initial Reports Deep Sea Drilling Project*, **40**: 857-881.
- Macphail, M., and Cantrill, D. 2006. Age and implications of the Forest Bed, Falkland Islands, south-west Atlantic Ocean: Evidence from fossil pollen and spores. *Palaeogeography, Palaeoclimatology, Palaeoecology*, **240**: 602-629.

- Majewski, W and Bohaty, S. 2010. Surface-water cooling and salinity decrease during the Middle Miocene climate transition at the Southern Ocean ODP Site 747 (Kerguelen Plateau). *Marine micropaleontology*, **74**:1-14.
- Markgraf, V, McGlone, M., and Hope, G. 1995. Neogene palaeoenvironmental and climatic change in southern temperate ecosystems – a southern perspective. *Tree*, **10**: 143 – 147.
- Marlow, J.R., Lange, C. B., Wefer, G., and Rosell-Melé, A. 2000. Upwelling Intensification as part of the Pliocene-Pleistocene Climate Transition. *Science*, **290**: 2288 – 2291.
- Martin, H.A. and McMinn, A. 1993. Palynology of Sites 815 and 823: the Neogene vegetation history of coastal Northeastern Australia. *Proceedings of the Ocean Drilling Program, Scientific Results*, **133**: 115-125.
- Maslin, M. A., and Christensen, B. 2007. Tectonics, orbital forcing, global climate change, and human evolution in Africa: introduction to the African paleoclimate special volume. *Journal of human evolution*, **53**: 443-64.
- Matthews, T., Denys, C. and Parkington, J. E. 2006. An analysis of the mole rats (Mammalia : Rodentia) from Langebaanweg (Mio-Pliocene, South Africa). *Geobios*, **39**(6):853-864.
- Matthews, T., Denys C., and Parkington, J.E. 2007. Community evolution of Neogene micromammals from LBW 'E' Quarry and other west coast fossil sites, south-western Cape, South Africa. *Palaeogeography, Palaeoclimatology, Palaeoecology*, **245**: 332-352.
- Meadows, M.E. 1988. Late Quaternary peat accumulation in southern Africa. *Catena*, **15**: 459-472.
- Mercer, J.H. 1978. Glacial development and temperate trends in Antarctica and in South America. In: van Zinderen Bakker, E.M., (Ed.). 1978. *Antarctic Glacial History and World Palaeoenvironments*. A.A. Balkema. Rotterdam. Pp. 73-94.
- Meyers, P.A., 1997. Organic geochemical proxies of paleoceanographic, paleolimnologic and paleoclimatic processes. *Organic Geochemistry*, **27**: 213–250.
- Meyers, P.A., 2003. Applications of *Organic Geochemistry* to paleolimnological reconstructions: a summary of examples from the Laurentian Great Lakes. *Organic Geochemistry*, **34**: 261–289.
- Meyers, P.A. and Lallier-Vergés, E. 1999. Lacustrine sedimentary organic matter records of Late Quaternary palaeoclimates. *Journal of Paleolimnology*, **21**: 345-372.
- Miall, A.D. 1985. Architectural-element analysis: A new method of facies analysis applied to fluvial deposits. *Earth-Science Reviews*, **22**(4), pp.261-308.

- Mielnik, L., Piotrowicz, R., and Klimaszuk, P. 2009. Chemical properties of bottom sediments in throughflow lakes located in Drawieński National Park. *Oceanological and Hydrobiological Studies*, vol. XXXVIII: 69-76.
- Micheels, A., Eronen, J., and Mosbrugger, V. 2009. The Late Miocene climate response to a modern Sahara desert. *Global and Planetary Change*, **67**: 193-204.
- Miller, K.G., and Fairbanks, R.G. 1985. Cainozoic $\delta^{18}\text{O}$ record of climate and sea level. *South African Journal of Science*, **81**: 248-249.
- Miller, K.G., Fairbanks, R.G., and Mountain, G.S. 1987. Tertiary oxygen isotope synthesis, sea level history, and continental margin erosion. *Paleoceanography*, **2**(1):1-19.
- Miller, K.G., Kominz, M.A., Browning, J.V., Wright, J.D., Mountain, G.S., Katz, M.E., Sugarman, P.J., Cramer, B.S., Christie-blick, N., and Pekar, S.F. 2005. The Phanerozoic record of global sea-level change. *Science*, **310**: 1293 - 1298.
- Moore, A., Blenkinsop, T., and Cotterill, F. 2009. Southern African topography and erosion history: plumes or plate tectonics? *Terra Nova*, **21**: 310-315.
- Morgan, R. 1978. Albian to Senonian palynology of Site 364, Angolan Basin. *Initial Reports Deep Sea Drilling Project*, **40**: 915-951.
- Muller, 1981. Fossil pollen records of extant angiosperms. *Botanical Review*, **47**: 1-142.
- Negri, A., Ferretti, A., Wagner, T., and Meyers, P.A. 2009. Organic-carbon-rich sediments through the Phanerozoic: Processes, progress, and perspectives. *Palaeogeography, Palaeoclimatology, Palaeoecology*, **273**: 213-217.
- Nichols, G., and Fisher, J., 2007. Processes, facies and architecture of fluvial distributary system deposits. *Sedimentary Geology*, **195**(1-2): 75-90.
- Norrish, K., and Hutton, J.T., 1969. An accurate X-ray spectrographic method for the analysis of a wide range of geological samples. *Geochimica et Cosmochimica Acta*, **33**: 431-453.
- O'Leary, M. 1981. Carbon isotope fractionation in plants. *Phytochemistry*, **20**: 553 - 567.
- Orwa, C., Mutua, A., Kindt, R., Jamnadass, R., and Simons, A. 2009. Agroforestry Database: a tree reference and selection guide version 4.0. Available, (online): <http://www.worldagroforestry.org/af/treedb/> [Accessed 10/08/2010].

- Pagani, M., Zachos, J.C., Freeman, K.H., Tipple, B., and Bohaty, S. 2005. Marked decline in atmospheric carbon dioxide concentrations during the Palaeogene. *Science*, **309**: 600–603.
- Park, R and Epstein, S. 1960. Carbon isotope fractionation during Photosynthesis. *Geochimica et Cosmochimica Acta*, **21**:110 -126.
- Partridge, T.C. 1985. The palaeoclimatic significance of Cainozoic terrestrial stratigraphic and tectonic evidence from Southern Africa: a review. *South African Journal of Science*, **81**: 245-247.
- Partridge, T.C., and Maud, R.R., 1987. Geomorphic evolution of South Africa since the Mesozoic. *South African Journal of Geology*, **90**:179-208.
- Paton, D. A. 2006. Influence of crustal heterogeneity in normal fault dimensions and evolution: southern South Africa extensional system. *Journal of Structural Geology*, **28**: 868-886.
- Pearson, P.N., and Palmer, M.R. 2000. Atmospheric carbon dioxide concentrations over the past 60 million years. *Nature*, **406**: 695–699.
- Pegion, P.J., and Kumar, A. 2010. Multimodel Estimates of Atmospheric Response to Modes of SST Variability and Implications for Droughts. *Journal of Climate*, **23** (16): 4327-4341.
- Peterse, F., Schouten, S., van der Meer, J., van der Meer, M.T.J., Sinninghe Damsté, J.S. 2009a. Distribution of branched tetraether lipids in geothermally heated soils: Implications for the MBT/CBT temperature proxy. *Organic Geochemistry*, **40**: 201–205.
- Peterse, F., Kim, J-H., Schouten, S., Klitgaard Kristensen, D., Koc, N., Sinninghe Damsté, J.S. 2009b. Constraints on the application of the MBT/CBT palaeothermometer at high latitude environments (Svalbard, Norway). *Organic Geochemistry*, **40**: 692-699.
- Peterse, F., Nicol, G. W., Schouten, S and Sinninghe Damsté, J.S. 2010. Influence of soil pH on the abundance and distribution of core and intact polar lipid-derived branched GDGTs in soil. *Organic Geochemistry*, 1171-1175.
- Pether, J., Roberts, D.L., and Ward, J.D. 2000. Deposits of the West Coast. In: Partridge, T.C., and Maud, R.R. (Eds). 2000. *The Cenozoic of Southern Africa*. Oxford University Press. Oxford. Pp. 33-54.
- Pickford, M., Senut, B., Hipondoka, M., Person, A., Segalen, L., Plet, C., Jousse, H., Mein, P., Guerin, C., Morales, J., and Mourer-Chauvire, C. Accepted. Mio-Pleistocene geology and palaeobiology of Etosha Pan, Namibia. *Communications of the geology survey of Namibia*.

- Potter, P.E. and Szatmari, P. 2009. Global Miocene tectonics and the modern world. *Earth-Science Reviews*, **96**: 279-295.
- Powers, L. A., Werne, J.P., Johnson, T.C., Hopmans, E.C., Sinninghe Damsté, J.S., and Schouten, S. 2004. Crenarchaeotal membrane lipids in lake sediments: A new paleotemperature proxy for continental paleoclimate reconstruction? *Geology*, **32**:613-616.
- Punt, W., Hoen, P.P., Blackmore, S., Nilsson, S. and Le Thomas, A., 2007. Glossary of pollen and spore terminology. *Review of Palaeobotany and Palynology*, **143** (1-2): 1-81.
- Raine, J.I., Mildenhall, D.C., and Kennedy, E.M. 2008. New Zealand fossil spores and pollen: an illustrated catalogue. 3rd edition. GNS Science miscellaneous series no. 4. Available, (online):http://www.gns.cri.nz/what/earthhist/fossils/spore_pollen/catalog/index.html Accessed [20.08.2010].
- Retallack, G.J. 2009. Refining a pedogenic carbonate CO₂ paleobarometer to quantify a middle Miocene greenhouse spike. *Palaeogeography, Palaeoclimatology, Palaeoecology*, **281**:57-85.
- Robert C. and Chamley, H., 1987. Cenozoic evolution of continental humidity and paleoenvironment, deduced from the kaolinite content of oceanic sediments. *Palaeogeography Palaeoclimatology, Palaeoecology*, **60**:171-187.
- Roberts, D.L., 2006a. Lithostratigraphy of the Sandveld Group. *South African Committee for Stratigraphy Lithostratigraphic Series* **9**: 25-26.
- Roberts, D.L., 2006b. Lithostratigraphy of the Elandsfontyn Formation. *South African Committee for Stratigraphy Lithostratigraphic Series* **9**: 25-26.
- Roberts, D.L., 2006c. Lithostratigraphy of the Prospect Hill Formation (Sandveld Group). *South African Committee for Stratigraphy Lithostratigraphic Series* **9**: 17-20.
- Roberts, D.L., 2006d. Lithostratigraphy of the Varswater Formation (Sandveld Group). *South African Committee for Stratigraphy Lithostratigraphic Series* **9**: 27-31.
- Roberts, D.L., 2006e. Lithostratigraphy of the Langebaan Formation (Sandveld Group). *South African Committee for Stratigraphy Lithostratigraphic Series* **9**: 9-12.
- Roberts, D.L., and Brink, J., 2002. Dating and correlation of Neogene coastal deposits in the Western Cape, South Africa: implications for Neotectonism. *South African Journal of Geology*, **105**: 337–352.

- Roberts, D.L., Botha, G.A., Maud, R.R., and Pether, J. 2006. Coastal Cenozoic deposits. *In*: Johnson, M.R., Anhaeusser, C.R., and Thomas, R.J. (Eds.). 2006. *The Geology of South Africa*. Geological Society of South Africa, Johannesburg/Council for Geoscience, Pretoria, 605-628.
- Roberts, D.L., Murray-Wallace, C. V., Bateman, M. D., Carr, A. S., Holmes, P. J. 2008. Fossil elephant trackways, sedimentation and diagenesis in OSL/AAR-dated Late Quaternary coastal aeolianites: Still Bay, South Africa. *Palaeogeography, Palaeoclimatology, Palaeoecology*, **257**: 261-279.
- Roberts, D.L., Bateman, M. D., Murray-Wallace, C. V., Carr, A. S., Holmes, P. J. 2009. West coast dune plumes: Climate driven contrasts in dunefield morphogenesis along the western and southern South African coasts. *Palaeogeography, Palaeoclimatology, Palaeoecology*, **271**: 24-38.
- Roberts, D.L., Matthews, T., Herries, A. I. R., Boulter, C., Scott, L., Musekiwa, C., Mthembia, P., Browning, C., Smith, R. M. H., Haarhoff, P., and Bateman, M. D. In review. Regional and global context of the Late Cenozoic Langebaanweg (LBW) Palaeontological site: West Coast of South Africa. *Earth Science Reviews*.
- Rogers, J. 1982. Lithostratigraphy of Cenozoic sediments between Cape Town and Eland's Bay. *Palaeoecology of Africa*, **15**: 121-137.
- Romero, O., Armand, L., Crosta, X., and Pichon, J. 2005. The biogeography of major diatom taxa in Southern Ocean surface sediments: 3. Tropical/Subtropical species. *Palaeogeography, Palaeoclimatology, Palaeoecology*, **223**: 49-65.
- Royer, D.L. 2006. CO₂-forced climate thresholds during the Phanerozoic. *Geochemica et Cosmochimica Acta*, **70**: 5665-5675.
- Sachs, J.P., Pahnke, K., Smittenberg, R., and Zhang, Z. 2007. Biomarker Indicators of Past Climate. *In*: Elias, S. (Ed.). *Encyclopaedia of Quaternary Science*. Available, (online): <http://faculty.washington.edu/jsachs/lab/www/Sachs-Biomarkers-EcyclQuatSci06proofs.pdf> [Accessed 19.10.2010].
- Sancetta, C., Heusser, L. and Hall, M.A. 1992. Late Pliocene climate in the Southeast Atlantic: preliminary results from a multi-disciplinary study of DSDP Site 532. *Marine Micropaleontology*, **20**: 59 - 75.
- Schalke, H.J.W.G. 1973. The Upper Quaternary of the Cape Flats Area (Cape Province, South Africa). *Scripta Geol.*, **15**: 1-57.

- Schidlowski, M. 1995. Isotope fractionations in the terrestrial carbon cycle: A brief overview. *Advanced space Research*, **15**: 441-449.
- Schindler, D. W. 1999. The Mysterious Missing Sink. *Nature*, **398**: 105-106.
- Schleser, G. H., Helle, G., Lücke, A., and Vos, H. 1999. Isotope signals as climate proxies: the role of transfer functions in the study of terrestrial archives. *Quaternary Science Reviews*, **18**:927-943.
- Schmittner, A., Oschlies, A., Matthews, H. D., and Galbraith, E.D. 2008. Future changes in climate, ocean circulation, emissions, ecosystems, and biogeochemical cycling simulated for a business-as-usual CO₂ emission scenario until year 4000 AD. *Global Biogeochemical Cycles*, **22**, GB1013, doi:10.1029/2007GB002953.
- Scholtz, A. 1985. The palynology of the upper lacustrine sediments of Arnot pipe, Banke, Namaqualand. *Annals of the South Africa Museum*, **95**: 1-1-09.
- Schouten, S., Hopmans, E.C., Pancost, R.D., and Sinninghe Damste', J.S., 2000. Widespread occurrence of structurally diverse tetraether membrane lipids: Evidence for the ubiquitous presence of low-temperature relatives of hyperthermophiles: *National Academy of Sciences Proceedings*, **97**:14,421–14,426.
- Schouten, S., Hopmans, E.C., Schefuß, E., and Sinninghe Damste', J.S. 2002 Distributional variations in marine crenarchaeotal membrane lipids: A new tool for reconstructing ancient sea water temperatures? *Earth and Planetary Science Letters*, **204**: 265–274.
- Schouten, S., Hopmans, E., Forster, A., van Breugel, Y., Kuypers, M.M.M., and Sinninghe Damste', J.S., 2003a. Extremely high sea-surface temperatures at low latitudes during the middle Cretaceous as revealed by archaeal membrane lipids: *Geology*, **31**: 1069–1072.
- Schouten, S., Hopmans, E.C., Schefuß, E., and Sinninghe Damste', J.S., 2003b, Distributional variations in marine crenarchaeotal membrane lipids: A new tool for reconstructing ancient sea water temperatures? Corrigendum: *Earth and Planetary Science Letters*, **211**: 205–206.
- Schouten, S., Huguet, C., Hopmans, E.C., Kienhuis, M.V.M., and Sinninghe Damsté, J.S. 2007. Analytical methodology for TEX₈₆ paleothermometry by high-performance liquid chromatography/atmospheric pressure chemical ionization-mass spectrometry. *Analytical chemistry*, **79**: 2940-2944.
- Schouten, S., Eldrett, J., Greenwood, D.R., Harding, I., Baas, M., and Sinninghe Damsté, J.S. 2008. Onset of long-term cooling of Greenland near the Eocene–Oligocene boundary as revealed by branched tetraether lipids. *Geology*, **36**: 147–150.

- Scott, L., 1982. A Late Quaternary pollen record from the Transvaal bushveld, South Africa. *Quaternary Research*, **17**: 339–370.
- Scott, L., 1993. Palynological evidence for Late Quaternary warming episodes in southern Africa. *Palaeogeography Palaeoclimatology, Palaeoecology*, **101**: 229–235.
- Scott, L., 1994. Palynology of Late Pleistocene hyrax middens, south-western Cape Province, South Africa: a preliminary report. *Historical Biology*, **9**: 71–81.
- Scott, L., 1996. Palynology of hyrax middens: 2000 years of palaeoenvironmental history in Namibia. *Quaternary International*, **33**: 73–79.
- Scott, A. C and. Jones, T. P. 1994. The nature and influence of fire in Carboniferous ecosystems. *Palaeogeography, Palaeoclimatology, Palaeoecology*, **106**: 91- 112.
- Scott, L., Anderson, H.M., and Anderson, J.M., 1997. Vegetation History. In: Cowling, R.M, Richardson, D.M., and Pierce, S.M. (Eds.). 1997. *The Vegetation of Southern Africa*. Cambridge University Press. Cambridge. Pp. 62–84.
- Scott, L., and Vogel, J.C., 2000. Evidence for environmental conditions during the last 20,000 years in southern Africa from $\delta^{13}C$ in fossil hyrax dung. *Global and Planetary Change*, **26**: 207–215.
- Scott, L. Cadman, A., and Mcmillan, I. 2006. Early history of Cainozoic Asteraceae along the Southern African west coast, *Review of Palaeobotany and Palynology*, **142**: 47-52.
- Scott, L., and Woodborne, S., 2007. Vegetation history inferred from pollen in Late Quaternary faecal deposits (*hyraceum*) in the Cape winter-rain region and its bearing on past climates in South Africa. *Quaternary Science Reviews*, **26**: 941–953.
- Shackleton, N. J. 1995. New data on the evolution of Pliocene climate variability. In: Vrba, E. S., Denton, G. H., Partridge, T. C., and Burkle, L. H. (Eds). 1995. *Paleoclimate and Evolution, with emphasis on human origins*. Yale University Press. New Haven. Pp. 242-248.
- Shackleton, N.J., and Kennet, J.P. 1975a. Palaeotemperature history of the Cenozoic and the initiation of Antarctic glaciations: oxygen and carbon isotope analyses of DSDP Sites 277, 279 and 281: *Initial Reports of the Deep Sea Drilling Project*, **29**:743-755.
- Shackleton, N.J., and Kennet, J.P. 1975b. Late Cenozoic oxygen and carbon isotopic changes at DSDP Site 284: implications for glacial history of the Northern Hemisphere and Antarctica. *Initial Reports of the Deep Sea Drill. Project*, **29**: 801-807.

- Shah, S., Mollenhauer, G., Ohkouchi, N., Eglinton, T. I., and Pearson, A. 2008. Origins of archaeal tetraether lipids in sediments: Insights from radiocarbon analysis. *Geochimica et Cosmochimica Acta*, **72**: 4577-4594.
- Sharp, Z. 2007. *Principles of stable isotope geochemistry*. Pearson Prentice Hall. Pp. 344.
- Shaw, D., Logan, P.C., and Weston, J. 2008. A palynological study of Neogene and Holocene Sediments from Lake Albert, Uganda, with implications for vegetation and climatic changes in East Africa. Search and Discovery Article, #50180. Available, (online): <http://www.searchanddiscovery.net/documents/2009/50180shaw/images/shaw.pdf> [Accessed 16/04/2010].
- Shevenell, A.E., Kennett, J.P., Lea, D.W., 2004. Middle Miocene Southern Ocean cooling and Antarctic cryosphere expansion. *Science*, **304**: 1766–1770.
- Shi, N., Dupont, L.M., Beug, H-J., and Schneider, R. 2000. Correlation between vegetation in South-western Africa and oceanic upwelling in the past 21,000 years. *Quaternary Research*, **54**: 72-80.
- Shunk, A. J., Driese, S.G., Farlow, J.O., Zavada, M.S., and Zobaa, M.K. 2009. Late Neogene paleoclimate and paleoenvironment reconstructions from the Pipe Creek Sinkhole, Indiana, USA. *Palaeogeography, Palaeoclimatology, Palaeoecology*, **274**: 173–184.
- Siesser, W.G. 1978. Aridification of the Namib Desert: Evidence from oceanic cores. *In*: Van Zinderen Bakker, E.M. (Ed). 1978. *Antarctic glacial history and world palaeoenvironment*. Balkema, Rotterdam. Pp. 105–113
- Siesser, W.G., and Dingle, R.V. 1981. Tertiary sea-level movements around southern Africa. *Journal of Geology*, **89**: 83-96.
- Sinninghe Damsté, J.S., Hopmans, E.C., Pancost, R.D., Schouten, S., and Geenevasen, J.A.J. 2000. Newly discovered non-isoprenoid dialkyl diglycerol tetraether lipids in sediments. *Journal of the Chemical Society, Chemical Communications (2000)*, 1683–1684.
- Sinninghe Damsté, J. S., Ossebaar, J., Schouten, S., and Verschuren, D. 2008. Altitudinal shifts in the branched tetraether lipid distribution in soil from Mt. Kilimanjaro (Tanzania): Implications for the MBT/CBT continental palaeothermometer. *Organic Geochemistry*, **39**: 1072-1076.
- Spicer, R.A. 1993. Palaeoecology, past climates and C₃/C₄ photosynthesis. *Chemosphere*, **27**: 947-978.

- Steppuhn, A., Micheels, A., Bruch, A. A., Uhl, D., Utescher, T., and Mosbrugger, V. 2007. The sensitivity of ECHAM4/ML to a double CO₂ scenario for the Late Miocene and the comparison to terrestrial proxy data. *Global and Planetary Change*, **57**: 189-212.
- Stevens, P. F. 2001. Angiosperm Phylogeny Website. Version 9, June 2008 [continuously updated since 2008]. Available, (online): <http://www.mobot.org/MOBOT/research/APweb> [Accessed 2009/2010].
- Stokes, S., Thomas, D.S.G., and Washington, R. 1997. Multiple episodes of aridity in southern Africa since the last interglacial period. *Nature*, **388**: 154 - 158.
- Tankard, A.J., Rogers, J., 1978. Late Cenozoic palaeoenvironments on the west coast of southern Africa. *Journal of Biogeography*, **5**: 319-337.
- Thomazo, C., Pinti, D.L., Busigny, V., Ader, M., Hashizume, K., and Philippot, P. 2009. Biological activity and the Earth's surface evolution: Insights from carbon, sulfur, nitrogen and iron stable isotopes in the rock record. *Comptes Rendus Palevol*, **8**: 665-678.
- Thomson, K. 1999. Role of continental break-up mantle plume development and fault reactivation in the evolution of the Gamtoos Basin, South Africa. *Marine and Petroleum Geology*, **16**: 409-429.
- Thwaites, R.N., and Jacobs, E.O. 1989. The Cenozoic history of the coastal landscape of the Southern Cape Province, South Africa: A review. *Quaternary Science Reviews*, **8**: 283-293.
- Tierney, J.E., and Russell, J.M. 2009. Distribution of branched GDGTs in a tropical lake system: Implications for lacustrine application of the MBT/CBT paleoproxy. *Organic Geochemistry*, **40**: 1032-1036.
- Tong, J.A., You, Y., Müller, R.D., and Seton, M. 2009. Climate model sensitivity to atmospheric CO₂ concentrations for the middle Miocene. *Global and Planetary Change*, **67**: 129-140.
- Traverse, A. 1957. The Nomenclatural Problem of Plant Microfossil Species Belonging to Extant Genera. *Micropaleontology*, **3**: 255- 258.
- Traverse, A. 1988. *Palaeopalynology*. Unwin Hyman. Boston. Pp. 600.
- Tripathi, A.K., Roberts, C.D., and Eagle, R. 2009. Coupling of CO₂ and ice sheet stability over major climate transitions of the last 20 million years. *Science*, **326**: 1394-1397.
- Tyson, P.D., and Preston-Whyte, R.A. 2000. Chapter 16: Climatic change and variability. In: Tyson, P.D., and Preston-Whyte, R.A. 2000. *The Weather and Climate of Southern Africa* (Second edition). Oxford University Press. Cape Town. Pp. 305- 338.

- Uenzelmann-Neben, G., Schluter, P., and Weigell, E. 2007. Cenozoic oceanic circulation within the South African gateway: indications from seismic stratigraphy. *Geological Society of South Africa*, **110**: 275-294.
- Van der Merwe, N.J., and Medina, E. 1989. Photosynthesis and $^{13}\text{C}/^{12}\text{C}$ ratios in Amazonian rain forests. *Geochimica et Cosmochimica Acta*, **53**:1091-1094.
- Van der Merwe, N.J., and Medina, E. 1991. The Canopy Effect, Carbon Isotope Ratios and Foodwebs in Amazonia. *Journal of Archaeological Science*, **18**: 249-259.
- Van Zinderen Bakker, E.M., and Mercer, J.H. 1986. Major Late Cainozoic climatic events and palaeoenvironmental changes in Africa viewed in a worldwide context. *Palaeogeography, Palaeoclimatology, Palaeoecology*, **56**: 217-235.
- Verducci, M., Foresi, L.M., Scott, G.H., Tiepolo, M., Sprovieri, M., and Lirer, F. 2007. East Antarctic Ice Sheet fluctuations during the Middle Miocene climatic transition inferred from faunal and biogeochemical data on planktonic foraminifera (Kerguelen Plateau). U.S. Geological Survey and the National Academics; USGS OF-2007-1047: Short Research Paper, vol. 037. doi:10.3133/of2007-1047.srp037.
- Vincent, E., and Berger, W.H. 1985. Carbon dioxide and polar cooling in the Miocene: the Monterey hypothesis. In: Sundquist, E.T., and Broecker, W.S. (Eds.). 1985. *The Carbon Cycle and Atmospheric CO₂: Natural Variations Archean to Present*. Geophysical. Monograph, 32: 455-468.
- Vogel, C. 2003. Climate and climatic change: causes and consequences. Fox, R., and Rowntree, K. (Eds.). 2003. *The geography of South Africa in a changing world*. Oxford University Press Southern Africa. Cape Town. Pp. 284 – 303.
- Webb, P.N. and Harwood, D.M. 1991 Late Cenozoic glacial history of the Ross Embayment, Antarctica. *Quaternary Science Reviews*, **10**: 215-223.
- Weijers, J.W.H. 2007. Part I: Introduction. In: Weijers, J.W.H. 2007. Soil-derived branched tetraether membrane lipids in marine sediments: reconstruction of past continental climate and soil organic matter fluxes to the ocean. PhD thesis. *Geologica Ultraiectina*, University of Utrecht, 275. Pp. 9-51.
- Weijers, J.W.H., Schouten, S., Hopmans, E.C., Geenevasen, J.A.J., David, O.R.P., Coleman, J.M., Pancost, R.D., Sinninghe Damsté, J.S., 2006a. Membrane lipids of mesophilic anaerobic bacteria thriving in peats have typical archaeal traits. *Environmental Microbiology*, **8**: 648–657.

- Weijers, J.W.H., Schouten, S., Spaargaren, O.C., Sinninghe Damsté, J.S., 2006b. Occurrence and distribution of tetraether membrane lipids in soils: Implications for the use of the TEX₈₆ proxy and the BIT index. *Organic Geochemistry*, **37**: 1680–1693.
- Weijers, J.W.H., Schefuss, E., Schouten, S., Sinninghe Damsté, J.S., 2007a. Coupled thermal and hydrological evolution of tropical Africa over the last deglaciation. *Science*, **315**: 1701–1704.
- Weijers, J.W.H., Schouten, S., Sluijs, A., Brinkhuis, H., Sinninghe Damsté, J.S., 2007b. Warm arctic continents during the Palaeocene–Eocene thermal maximum. *Earth and Planetary Science Letters*, **261**: 230–238.
- Weijers, J.W.H., Schouten, S., van den Donker, J.C., Hopmans, E.C., Sinninghe Damsté, J.S., 2007c. Environmental controls on bacterial tetraether membrane lipid distribution in soils. *Geochimica et Cosmochimica Acta*, **71**: 703–713.
- Westerhold, T., Bickert, T., Röhl, U. 2005. Middle to late Miocene oxygen isotope stratigraphy of ODP site 1085 (SE Atlantic): new constraints on Miocene climate variability and sea-level fluctuations. *Palaeogeography, Palaeoclimatology, Palaeoecology*, **217**: 205–222.
- Wigley, R. A., and Compton, J.S. 2006. Late Cenozoic evolution of the outer continental shelf at the head of the Cape Canyon, South Africa. *Marine Geology*, **226**: 1–23.
- Wolfe, J.A. 1985. Distribution of major vegetational types during the Tertiary. *Geophysical Monograph*, **32**: 357–375.
- You, Y., Huber, M., Müller, D., Poulsen, C.J., and Ribbe, J. 2009. Simulation of the Middle Miocene Climate Optimum. *Geophysical Research Letters*, **36**, L04702, doi:10.1029/2008GL036571.
- Zachos, J., Pagani, M., Sloan, L., Thomas, E., and Billups, K. 2001. Trends, rhythms, and aberrations in global climate 65Ma to present. *Science*, **292**: 686–693.
- Zamaloa, M.C. 2004. Miocene algae and spores from Tierra del Fuego, Argentina. *Alcheringa*, **28**: 205–227.
- Zavada, M.S., and de Villiers, S.E. 2000. Pollen of the Asteraceae from the Paleocene-Eocene of South Africa. *Grana*, **39**: 39–45.
- Zink, K.-G. , Vandergoes, M.J., Mangelsdorf, K., Dieffenbacher-Krall, A.C., and Schwark, L. 2010. Application of bacterial glycerol dialkyl glycerol tetraethers (GDGTs) to develop modern and past temperature estimates from New Zealand lakes. *Organic Geochemistry*, **41**: 1060–1066.

9 Appendices

NOORDHOEK

Table A. 1. Noordhoek sample depths and sedimentological descriptions.

SAMPLE#	Depth (m)	Depth above/below sea level (m)	Description	Colour	Charcoal fragments	Sulphide horizons
N1	1.00	+1.50				
N2	2.50	+0.00				
N3	18.00	-15.50	fine grained sand with high (~80%) clay component	dark brown		
N4	19.40	-16.90	fine grained sand with high (~80%) clay component	dark brown		
N5	20.50	-18.00	silty organic-rich clay	dark brown		
N6	21.40	-18.90	silty organic-rich clay	dark brown		
N7	22.50	-20.00	clay	dark brown		
N8	24.00	-21.50	clayey- peat	dark brown		
N9	25.80	-23.30	clayey- peat	dark brown		
N10	27.10	-24.60	peat	dark brown		
N11	29.10	-26.60	peat	dark brown		present; 26.50m
N12	31.10	-28.60	clayey-peat	brown		
N13	31.30	-28.80	clayey-peat	brown	present	
N14	32.40	-29.90	clayey-peat	grey	present	present; 32.50m
N15	33.30	-30.80	fine grained sand with high (~80%) clay component	grey	present	
N16	35.50	-33.00	peaty silt with high (~80%) clay component	dark brown		
N17	36.60	-34.10	peaty silt with high (~80%) clay component	dark brown		
N18	37.50	-35.00	peaty silt with high (~80%) clay component	dark brown		
N19	39.50	-37.00	clayey-peat	dark brown	present	
N20	43.50	-41.00	peat	dark brown		
N21	44.00	-41.50	peat	dark brown		
N22	44.80	-42.30	clayey-peat	dark brown		
N23	45.50	-43.00	peaty fine sand	dark brown		

Table A. 2. The bulk organic geochemistry of the Noordhoek samples.

SAMPLE#	Depth (m)	Depth above/ below sea level (m)	TOC	$\delta^{13}\text{C}$ (‰ vs PDB)	TN	$\delta^{15}\text{N}$ (‰vs. AIR)	$\text{C}_{\text{org}}/\text{N}_{\text{org}}$ (atomic)	TOC/TN
N1	1.00	1.50	15.4	-26.6	0.23	0.84	76.5	66
N2	2.50	0.00	0.7	-26.1	0.02	-0.09	46.1	40
N3	18.00	-15.50	0.1	-24.3	0.01	1.52	5.9	5
N4	19.40	-16.90	0.7	-25.1	0.03	4.76	28.6	24
N5	20.50	-18.00	46.9	-25.8	0.32	2.60	170.1	146
N6	21.40	-18.90	58.8	-25.4	0.57	2.57	120.1	103
N7	22.50	-20.00	19.7	-26.1	0.28	2.53	82.7	71
N8	24.00	-21.50	49.3	-26.3	0.33	2.93	176.2	151
N9	25.80	-23.30	60.0	-25.6	0.77	1.36	91.4	78
N10	27.10	-24.60	63.4	-26.7	0.44	1.11	166.5	143
N11	29.10	-26.60	63.2	-26.8	0.68	2.60	108.7	93
N12	31.10	-28.60	60.8	-27.1	0.55	2.55	129.9	111
N13	31.30	-28.80	51.9	-26.0	0.57	3.70	106.9	92
N14	32.40	-29.90	1.1	-26.9	0.03	4.16	38.0	33
N15	33.30	-30.80	0.6	-26.3	0.01	3.11	67.0	57
N16	35.50	-33.00						-
N17	36.60	-34.10	38.3	-26.1	0.45	1.43	99.2	85
N18	37.50	-35.00	17.1	-26.7	0.24	0.77	82.5	71
N19	39.50	-37.00	16.5	-25.8	0.24	0.94	79.7	68
N20	43.50	-41.00	15.0	-25.8	0.08	0.42	225.2	193

SAMPLE#	Depth (m)	Depth above/ below sea level (m)	TOC	$\delta^{13}\text{C}$ (‰ vs PDB)	TN	$\delta^{15}\text{N}$ (‰ vs. AIR)	C/N (atomic)	TOC/TN
N22	44.80	-42.30	48.9	-25.0	0.19	0.03	306.4	263
N23	45.50	-43.00	1.4	-25.4	0.04	0.99	43.8	38
Mean			31.23	-25.95	0.28	2.02	117.52	100.8
Std. Dev.			25.07	0.72	0.23	1.36	84.36	72.3

Table A. 3. Comparison of the charcoal presence, pollen counts and total organic carbon content (TOC) of all Noordhoek samples.

Depth (m)	Charcoal presence	Total pollen per slide	TOC (%)
1.00	Sparse charcoal	600	15.4
2.50	Charcoal fragments	12	0.7
18.00	-	9	0.1
19.40	No pollen; sparse charcoal	24	0.7
20.50	-	564	46.9
21.40	-	86	58.8
22.50	-	480	19.7
24.00	-	206	49.3
25.80	-	53	60.0
27.10	-	163	63.4
29.10	-	273	63.2
31.10	-	233	60.8
31.30	-	91	51.9
32.40	Charcoal fragments	30	1.1
33.30	Charcoal fragments	61	0.6
35.50	-	424	
36.60	-	82	38.3
37.50	-	381	17.1
39.50	-	393	16.5
43.50	Charcoal fragments	12	15.0
44.00	Charcoal fragments	27	57.4
44.80	Charcoal fragments	1	48.9
45.50	Charcoal fragments	12	1.4

Table A. 4. The Noordhoek Branched vs. Isoprenoid index of Tetraethers (BIT), Methylation index of Branched Tetraethers (MBT), and Cyclisation ratio of Branched Tetraethers (CBT) with the calculated Mean annual temperature (MAAT) and pH values, obtained from the CBT/MBT proxy.

Sample #	Depth from surface (m)	BIT	MBT	CBT	MAAT (°C)	pH
N1	1.00	0.99	0.63	1.42	12.21	5.03
N2	2.50	1.00	0.65	1.65	10.88	4.45
N3	18.00	0.99	0.78	1.13	22.13	5.80
N4	19.40	1.00	0.86	0.98	27.75	6.18
N5	20.50	0.97	0.88	0.74	30.86	6.82
N6	21.40	1.00	0.79	1.10	22.92	5.86
N7	22.50	1.00	0.79	1.35	20.59	5.20
N8	24.00	1.00	0.85	1.14	25.93	5.77
N9	25.80	1.00	0.85	1.19	25.33	5.64
N10	27.10	1.00	0.89	1.12	28.08	5.82
N11	29.10	1.00	0.88	1.14	27.50	5.77
N12	31.10					
N13	31.30	1.00	0.80	1.16	22.95	5.70
N14	32.40	1.00	0.81	1.55	19.96	4.69
N15	33.30	1.00	0.77	1.51	18.30	4.80
N16	35.50					
N17	36.60	1.00	0.76	1.32	19.69	5.29
N18	37.50	1.00	0.79	1.45	19.61	4.94
N19	39.50	1.00	0.68	1.30	15.66	5.33
N20	43.50	1.00	0.69	1.86	11.17	3.87
N21	44.70					
N22	44.80	1.00	0.75	1.94	13.09	3.67
N23	45.50	1.00	0.88	1.48	24.14	4.88

LANGEBAAWEG (LBW)

Table A.5 Lithological description of the Langebaanweg (LBW) samples received from the Council for Geoscience.

Sample #	Depth below sea level (m)	Lithology	Colour
L1	17.00	clay	black
L2	18.40	clay	black
L3	19.04	clay	black
L4	19.50	silty-clay	dark brown
L5	25.40	silty-clay	dark brown
L6	25.50	silty-clay	dark brown
L7	33.00	silty-clay	dark brown

Table A. 6. Langebaanweg (LBW) samples bulk organic geochemical parameter data.

Metres below sea level	TOC (%)	TN	$\delta^{13}\text{C}$ (‰ vs PDB)	$\delta^{15}\text{N}$ (‰ vs AIR)	C/N (atomic)	TOC/TN
17.00	4.5	0.12	-24.64	3.71	42.1	37.5
18.40	2.7	0.09	-24.27	3.23	33.1	30.0
19.14	5.1	0.15	-24.37	2.37	39.7	34.0
19.50	10.7	0.22	-25.52	3.44	57.4	48.6
25.40	-	-	-	-	-	
25.50	4.9	0.13	-24.78	2.58	45.8	37.7
33.00	2.3	0.1	-25.48	2.94	27	23.0
average:	5.0	0.1	-24.8	3.0	40.9	37.3
stdev:	3.01	0.05	0.54	0.51	10.52	64.3

Correlation coefficient between TOC and $\delta^{15}\text{N}$ (‰ vs AIR) 0.227
 Correlation coefficient between TN and $\delta^{15}\text{N}$ (‰ vs AIR) 0.093
 Correlation coefficient between $\delta^{13}\text{C}$ (‰ vs PDB) and MAAT 0.543

Table A. 7. The Langebaanweg Branched vs. Isoprenoid index of Tetraethers (BIT), Methylation index of Branched Tetraethers (MBT), and Cyclisation ratio of Branched Tetraethers (CBT) with the calculated Mean annual temperature (MAAT) and pH values, obtained from the CBT/MBT proxy.

Metres below sea level	BIT	MBT	CBT	pH	MAAT (°C)
17.00	0.8	0.7	1.0	6.2	21.5
18.40	0.7	0.8	0.9	6.4	26.6
19.04	1.0	0.6	1.0	6.3	15.4
19.50	1.0	0.6	1.1	5.8	14.0
25.40	1.0	0.8	1.3	5.4	21.1
25.50	1.0	0.7	1.7	4.4	12.4
33.00	1.0	0.8	1.6	4.5	16.2

RONDEBERG CLAY PIT

Table A. 8. Rondeberg Clay Pit samples depths and descriptions.

Vertical Height Above Sea Level (M)	Sample #	Distance Between Samples (cm)	Grain Size	Colour	Organics	Wood	Additional Comments
0	RCP -8	0	clay	yellow-brown	-	-	potential basement rock of weathered Malmesbury Group
0.2	RCP -7	40	clay	yellow-brown	-	-	
0.4	RCP -6	20	clay	yellow-brown	-	-	
0.6	RCP -5	20	clay	yellow-brown	-	-	
0.77	RCP -4	20	clay	yellow-brown	-	-	
0.94	RCP -3	20	clay	yellow-brown	-	-	
1.11	RCP -2	20	clay	yellow-brown	-	LOGS in situ	
1.28	RCP -1	20	clay	yellow-brown	-	LOGS in situ	
1.45	RCP 0	20	clay	yellow-brown	-	LOGS in situ	
1.62	RCP 1	20	clay	darker brown	-	wood fragments	
1.79	RCP 2	20	clay	darker brown	-	wood fragments	
1.96	RCP 3	20	clay	darker brown	-	wood fragments	
2.13	RCP 4	20	clay	darker brown	-	wood fragments	
2.34	RCP 5	20	clay	darker brown	-	-	
2.55	RCP 6	20	clay	darker brown	-	-	
2.76	RCP 7	20	clay	darker brown	-	-	
2.97	RCP 8	20	clay	very dark brown	-	-	
3.18	RCP 9	20	clay	black	homogeneous organic layer of ~ 30 cm thick	-	

Vertical Height Above Sea Level (M)	Sample #	Distance Between Samples (cm)	Grain Size	Colour	Organics	Wood	Additional Comments
3.39	RCP 10	20	clay	dark brown		-	
3.6	RCP 11	20	clay	yellow-brown		-	
3.98	RCP 12	20	clay	yellow-brown	containing 2 cm black horizon	-	
4.36	RCP 13	20	clay	pale orange	-	-	
4.74	RCP 14	20	clay	pale orange	-	-	
5.12	RCP 15	20	clay	olive green- brown cream	-	-	
5.42	RCP 16	20	clay	olive green- brown cream	-	-	
5.72	RCP 17	20	clay	olive green- brown cream	-	-	

Table A. 9. RCP samples' organic potential with charcoal estimations based on thin section petrography.

SAMPLE #	Vertical height above sea level (m)	Organic material	Wood	Palynodebris	Charcoal estimation (%)
RCP -8	0	Fragmentary organics (cellular material and grains)	-	Fragmentary organics, amorphous plant material, microscopic charcoal	10
RCP -7	0.2	-	-	-	
RCP -6	0.4	-	-	-	
RCP -5	0.6	charcoal -not rounded, angular, small	-	Brown amorphous material, abundant microscopic charcoal fragments	55
RCP -4	0.77	-	-	-	
RCP -3	0.94	-	-	-	
RCP -2	1.11	Fragmentary organics and grains, charcoal subrounded to angular, <1.0um	LOG	-	35
RCP -1	1.28		LOG	-	
RCP 0	1.45		LOG	-	
RCP 1	1.62	charcoal -angular to sub-rounded. Pollen grains frequent (palm and podocarp); a lot of fragmentary organics	wood fragments	microscopic charcoal	45
RCP 2	1.79	palynological productive	wood fragments	-	5
RCP 3	1.96	palynological productive	wood fragments	-	5
RCP 4	2.13		wood fragments	-	
RCP 5	2.34	Very few Palmae, angular charcoal fragments, lots of fragmentary organics	-	microscopic charcoal	65
RCP 6	2.55		-		
RCP 7	2.76	Fragmentary organics and grains, charcoal subrounded to angular, <1.0um	-	microscopic charcoal	75
RCP 8	2.97		-		
RCP 9	3.18	Abundant charcoal; rare palynomorphs	-	microscopic charcoal	75

SAMPLE #	Vertical height above sea level (m)	Organic material	Wood	Palynodebris	Charcoal estimation (%)
RCP 10	3.39	Highly frequent rounded charcoal, fragmentary organics	-	microscopic charcoal	75
RCP 11	3.6		-		
RCP 12	3.98	barren - little palynomorphs, subrounded charcoal fragments < 1.0um	-	microscopic charcoal	75
RCP 13	4.36	-	-	-	-
RCP 14	4.74	-	-	-	-
RCP 15	5.12	-	-	-	-
RCP 16	5.42	-	-	-	-
RCP 17	5.72	-	-	-	-
RCP 18	6.02	-	-	-	-
RCP 19	6.32	-	-	-	-
RCP 20	6.97	-	-	-	-
RCP 21	7.62	-	-	-	-
RCP 22	8.27	-	-	-	-
RCP 23	8.92	-	-	-	-
RCP 24	9.72	-	-	-	-
RCP 25	10.52	-	-	-	-
RCP 26	11.04	-	-	-	-

Table A. 11. Rondeberg Clay Pit (RCP) X.R.F trace element geochemistry data.

Vertical Height above pit base(m)	Sample # (RCP)	Mo	Nb	Zr	Y	Sr	U	Rb	Th	Pb
0	RCP-8	9.8	78.5	879.3	71.4	106.7	7.7	15.1	28.1	73.8
0.2	-7	11.9	104.6	838.2	97.4	115	10.8	20	41.1	96.5
0.4	-6	9	87.1	552.6	81.5	101.6	7.6	29.6	37.6	86.3
0.6	-5	7.6	70	408.3	63.4	87	9	33	34.9	73
0.77	-4	8.2	63.8	391.8	60.2	89.9	8.4	35.5	32.5	72.8
0.94	-3	6.8	56.7	335.8	56.9	91	7.6	39.2	28.5	70.2
1.11	-2	4.9	47	257.8	44.2	71.4	6.9	45.7	23.9	55
1.28	-1	8.7	68.1	432.1	66.1	95	7.4	32.7	34.4	76.4
1.45	0	6	58.1	326.4	56.3	72.6	6.3	37.5	22.6	32.1
1.62	1	5.8	54.9	357.8	130.4	95.7	13.3	29.2	40.6	79.8
1.79	2	7.9	67	896.4	63.2	64.1	7.8	21.2	21.2	54.8
1.96	3	6.4	47.7	290.8	61.9	83.1	10.4	27.6	38.2	110.9
2.13	4	7.7	64.7	355	63.4	89.7	7.7	44.2	29.5	73.1
2.34	5	6.9	53	389.2	100.3	95.5	10.6	31.5	39.2	78.5
2.55	6	8.4	60.9	352	76.5	83.8	8.9	33.4	28.1	71.1
2.76	7	10	66.1	346.7	65.3	85.9	7.5	39	30.5	81.1
2.97	8	7.5	60.8	343	62.3	63.4	7.7	30	23.2	72.5
3.18	9	0.2	65.1	567.7	491.8	207	40.2	14.6	125.9	96.9
3.39	10	5.9	55.1	332.3	119.1	84.4	13.5	38.4	36.2	66.8
3.6	11	7.6	56.7	357.9	57.4	85.1	8.9	40.6	39.1	73.6
3.98	12	8.7	67.3	400.6	57.2	83	8.8	33	23.3	64.4
4.36	13									
4.74	14	4.1	41.7	240.3	36	68.4	8.2	28	13.2	67.8
5.12	15	5	45.1	271.8	37.8	66.4	7.5	30	19.9	53.7
5.42	16	4.9	44.3	502.8	40.4	62.1	6.2	25.5	13.7	33.6
5.72	17	5.2	59	386.3	49.1	74.5	8.2	30.8	16.4	43
6.02	18	5.1	44	567.8	40.6	135.7	7	20.5	16.4	34.1
6.32	19	4.6	26.8	715.9	27.7	25.8	3.6	9.6	4.1	10.3
6.97	20	4.8	29.9	754.3	31	21.6	4.4	7.3	6	11.4
7.62	21	5.2	77.8	522.7	58.1	69	6.2	15.8	18.9	29.6
8.27	22	8.3	58.1	340.8	51.5	981.7	6.6	26.7	24.1	91.4
8.92	23	5.4	47	341.1	45.8	1171.7	3.6	29.7	28	76.7
9.72	24	5.2	29.1	602.8	24.3	275	1.7	20.5	21.2	60.2
10.52	25	5.2	15.2	732.3	18.2	36.2	1.8	18.4	12.7	26.5
11.04	26	3.9	11.2	595.7	17.4	23.8	2.1	15.4	12.5	16.5

Table A.11. Continued..

Vertical Height above pit base (m)	Sample # (RCP)	Ce	Nd	La	Co	Cr	V	Zn	Cu	Ni
0	RCP-8	157.3	63	85.5	3.1	71.1	162.2	8.9	3.2	9.6
0.2	-7				5.2	92.9	227.2	15.5	5.8	17.3
0.4	-6	163.7	68.1	93.4	4.6	109.6	229.7	19.6	12.1	19.1
0.6	-5	132.8	55.1	74.2	7.9	104.9	217.2	19.9	13.1	22.1
0.77	-4	131.7	55.8	76.2	5.3	109.3	223.8	19.7	13.2	22.3
0.94	-3	123.8	53	68.6	5.6	123.2	243.5	20.6	13.6	19.8
1.11	-2	99.7	43.5	59.4	21.1	105.2	200.6	30	9.4	23.6
1.28	-1	151.9	61.7	84.3	15.1	112.4	236.2	24.6	11.3	24.8
1.45	0	126.1	54.7	72.3	65	111.6	210.9	299.4	17.6	52.8
1.62	1	241.1	132.7	99.3	5.1	191.6	293.7	16.2	46.9	20.9
1.79	2	91	38.2	51.6	4.2	77.8	134.7	14.8	13	15.1
1.96	3	124.4	61.2	64.4	6.4	184.4	409.3	399.2	80.5	20
2.13	4	143.3	63.9	81.5	11	113	272.7	23.6	35.4	20.5
2.34	5	192.4	99.3	86.6	9.9	167.9	280.9	17	34.3	19.1
2.55	6	159.9	76	83.4	11.5	125.1	311.6	15.3	16.8	21.2
2.76	7	149.7	69.4	86.4	5.2	135.8	389.9	17.7	28.2	17.5
2.97	8	110.3	52.1	60.5	11.2	112.9	328.4	15	22.1	21.6
3.18	9	941	530.7	325.1	-1.1	514.9	290	13.5	73.8	24.2
3.39	10	211.2	118.2	94.3	11.3	163	356.6	27.8	37.2	24
3.6	11	112.8	47.1	64.5	3.9	127.8	299.3	17.7	36.6	19.4
3.98	12	117.5	43.5	71.7	4.3	130.1	320	7.5	36.4	22.9
4.36	13									
4.74	14	65.1	22.1	36.3	4.2	53	96.4	11.9	13.3	16.1
5.12	15	102.8	35.6	61.1	4.7	87.1	169.5	14.4	17.3	18.6
5.42	16	106.5	32.9	48.6	9.4	75.7	113.7	12.6	6.1	11.3
5.72	17				3.9	76.1	144.3	16.7	6.9	13.8
6.02	18				5.3	90.4	204.4	10.1	9	11.5
6.32	19	35.9	14.5	21.2	0.9	31.2	36.8	4.9	2.3	2.2
6.97	20	33.6	14.3	18.7	0.2	27.3	36.9	3.8	2.8	2.7
7.62	21	71.8	29.9	39.9	1.7	65.2	112.9	10.2	4.3	8
8.27	22	150.9	69.2	96.1	7.6	133.2	286.6	14.2	58.9	23.3
8.92	23	160.6	66.3	93.2	6.3	147.6	240.3	10.7	35.1	20.2
9.72	24	107.5	22.4	78	8.9	134.6	212.3	10	17.6	18.5
10.52	25	47.7	19.4	27.4	6.6	74.5	179.8	4.8	3.7	13.2
11.04	26	55.6	21.6	30.2	7.1	74.7	173.6	4.2	2.1	10.8

Table A. 12. Rondeberg Clay Pit (RCP) X.R.F major element geochemistry data.

Elevation above pit base (m)	Sample	SiO ₂	TiO ₂	Al ₂ O ₃	Fe ₂ O ₃	FeO	MnO	MgO	CaO
0	RCP-8								
0.2	RCP-7	56.565	4.457	19.013	0.893	0.000	0.003	0.456	0.072
0.4	RCP-6	47.350	3.496	21.989	1.070	0.000	0.005	0.571	0.130
0.6	RCP-5	45.058	2.980	24.399	1.360	0.000	0.005	0.631	0.125
0.77	RCP-4								
0.94	RCP-3	44.463	2.399	24.891	1.292	0.000	0.011	0.669	0.164
1.11	RCP-2	41.155	1.825	25.194	1.359	0.000	0.003	0.663	0.141
1.28	RCP-1	39.988	2.469	23.487	1.097	0.000	0.007	0.574	0.120
1.45	RCP0	42.549	2.542	24.363	1.348	0.000	0.009	1.117	0.149
1.62	RCP1	40.688	2.222	22.921	1.070	0.000	0.006	0.620	0.235
1.79	RCP2	54.285	2.415	13.178	0.717	0.000	0.001	0.348	0.062
1.96	RCP3	27.279	1.836	15.210	0.882	0.000	0.000	0.550	0.183
2.13	RCP4	37.018	2.285	20.978	1.117	0.000	0.003	0.613	0.301
2.34	RCP5	36.652	1.931	18.275	1.095	0.000	0.005	0.496	0.115
2.55	RCP6	42.048	2.551	23.764	1.057	0.000	0.000	0.666	0.145
2.76	RCP7	40.325	2.748	23.028	1.132	0.000	0.009	0.813	0.204
2.97	RCP8	49.064	2.696	25.729	1.194	0.000	0.013	0.596	0.148
3.18	RCP9	30.715	3.075	16.860	0.783	0.000	0.006	1.121	1.188
3.39	RCP10	44.735	2.492	26.052	1.420	0.000	0.005	0.761	0.251
3.6	RCP11	51.281	2.609	26.139	1.482	0.000	0.000	0.919	0.125
3.98	RCP12	51.506	2.987	24.728	0.798	0.000	0.008	0.722	0.113
4.36	RCP13	50.184	2.286	27.242	2.054	0.000	0.006	0.592	0.141
4.74	RCP14	52.099	1.966	28.222	2.103	0.000	0.000	0.654	0.112
5.12	RCP15	51.749	1.937	27.633	2.071	0.000	0.005	0.541	0.062
5.42	RCP16	68.722	1.893	15.245	1.159	0.000	0.004	0.369	0.042
5.72	RCP17	59.707	2.409	18.684	1.615	0.000	0.006	0.453	0.057
6.02	RCP18	69.420	1.894	13.576	0.919	0.000	0.006	0.307	0.043
6.32	RCP19	89.123	1.214	3.588	0.316	0.000	0.004	0.173	0.036
6.97	RCP20	92.381	1.327	2.718	0.284	0.000	0.014	0.090	0.019
7.62	RCP21	72.031	3.152	11.292	0.866	0.000	0.006	0.259	0.036
8.27	RCP22	38.691	2.424	28.827	3.297	0.000	0.004	0.554	0.082
8.92	RCP23	42.643	2.250	31.472	1.839	0.000	0.002	0.980	0.183
9.72	RCP24	51.762	1.294	26.147	1.450	0.000	0.000	0.366	0.081
10.52	RCP25	79.829	0.690	10.835	1.610	0.000	0.004	0.368	0.076
11.04	RCP26	82.571	0.511	9.239	2.559	0.000	0.003	0.213	0.057

Table A. 12. Continued..

Elevation above pit base (m)	Sample	Na ₂ O	K ₂ O	P ₂ O ₅	Cr ₂ O ₃	NiO	LOI	H ₂ O-
0	RCP-8							
0.2	RCP-7	0.273	0.406	0.102	0.000	0.000	12.881	4.275
0.4	RCP-6	0.346	0.515	0.085	0.000	0.000	20.596	4.152
0.6	RCP-5	0.352	0.556	0.076	0.000	0.000	16.206	8.406
0.77	RCP-4							
0.94	RCP-3	0.387	0.686	0.068	0.000	0.000	14.747	9.761
1.11	RCP-2	0.319	0.707	0.059	0.000	0.000	19.421	8.913
1.28	RCP-1	0.399	0.523	0.072	0.000	0.000	20.768	9.591
1.45	RCP0	4.107	0.624	0.070	0.000	0.000	16.434	8.645
1.62	RCP1	0.440	0.505	0.055	0.000	0.000	20.847	10.148
1.79	RCP2	0.480	0.306	0.041	0.000	0.000	19.801	8.405
1.96	RCP3	0.759	0.467	0.048	0.000	0.000	33.587	19.428
2.13	RCP4	0.535	0.703	0.061	0.000	0.000	27.546	9.080
2.34	RCP5	0.620	0.482	0.049	0.000	0.000	27.255	13.202
2.55	RCP6	0.531	0.593	0.059	0.000	0.000	22.842	5.139
2.76	RCP7	0.356	0.785	0.053	0.000	0.000	18.851	10.988
2.97	RCP8	0.345	0.564	0.053	0.000	0.000	15.431	3.444
3.18	RCP9	1.887	0.295	0.075	0.000	0.000	37.312	6.467
3.39	RCP10	0.657	0.689	0.058	0.000	0.000	17.314	4.911
3.6	RCP11	20.442	0.777	0.066	0.000	0.000	10.482	5.261
3.98	RCP12	2.938	0.417	0.061	0.000	0.000	10.781	5.445
4.36	RCP13	3.878	0.515	0.079	0.000	0.000	10.491	3.960
4.74	RCP14	46.429	0.492	0.063	0.000	0.000	10.876	3.550
5.12	RCP15	0.433	0.459	0.050	0.000	0.000	10.130	3.199
5.42	RCP16	0.411	0.425	0.038	0.000	0.000	6.169	4.853
5.72	RCP17	0.475	0.518	0.044	0.000	0.000	8.911	6.992
6.02	RCP18	0.539	0.315	0.045	0.000	0.000	5.354	7.108
6.32	RCP19	3.965	0.162	0.016	0.000	0.000	2.539	1.889
6.97	RCP20	0.204	0.121	0.013	0.000	0.000	1.214	0.520
7.62	RCP21	0.281	0.224	0.033	0.000	0.000	4.674	5.812
8.27	RCP22	1.076	0.409	0.190	0.000	0.000	13.500	10.949
8.92	RCP23	7.106	0.487	0.236	0.000	0.000	14.801	4.516
9.72	RCP24	1.508	0.323	0.097	0.000	0.000	15.282	2.316
10.52	RCP25	16.482	0.189	0.015	0.000	0.000	6.046	1.596
11.04	RCP26	0.405	0.156	0.012	0.000	0.000	4.198	1.020

NOORDHOEK POLLEN ASSEMBLAGE

**Avondrustvlei drill-core,
Avondrustvlei Farm, Noordhoek
South Africa**

Descriptive/Systematic Palynology

Noordhoek Pollen Catalogue 2010

Introduction

The following pollen catalogue serves to illustrate many of the morphological types represented within the Noordhoek Avondrustvlei core. Photomicrographs were taken using transmitted light microscopy and all scale bars represent 10µm.

References

- Terminology used in this catalogue is in accordance with Erdtman (1969), and Faegri and Iversen (1964).
- Unless stated information has been obtained from:

African pollen database. 2010. Available, (online): <http://medias3.mediasfrance.org/pollen/> [Accessed 2009/2010].

Coetzee, J.A. 1978a. Late Cainozoic palaeoenvironments of southern Africa. In: Van Zinderen Bakker, E.M., (Ed.). *Antarctic glacial history and world palaeoenvironments*. A.A. Balkema. Rotterdam. Pp.115-127.

Coetzee, J.A. 1978b. Climatic and biological changes in South-western Africa during the Late Cainozoic. In: Van Zinderen Bakker, E.M., and Coetzee, J.A. (Eds.). *Palaeoecology of Africa and the surrounding Islands*. Vol. 10. A.A. Balkema. Rotterdam. Pp. 13-29.

Coetzee, J.A., and Muller, J. 1984. The phytogeographic significance of some extinct Gondwana pollen types from the Tertiary of the southwestern Cape (South Africa). *Annals of the Missouri Botanical Garden*, **71**: 1088-1099.

Coetzee, J.A., and Praglowski, J. 1984. Pollen evidence for the occurrence of Casuarina and Myrica in the Tertiary of South Africa. *Grana*, **23**: 23-41.

Coetzee, J.A., and Rogers, J. 1982. Palynological and lithological evidence for the Miocene palaeoenvironment in the Saldanha Region (South Africa). *Palaeogeography, Palaeoclimatology, Palaeoecology*, **39**: 71-85.

de Villiers, S.E.; Cadman, A., 1997: The palynology of Tertiary sediments from a palaeochannel in Namaqualand, South Africa. *Palaeontologia africana*, **34**: 69-99.

de Villiers, S.E., and Cadman, A. 2001. An analysis of the palynomorphs obtained from Tertiary sediments at Koingnaas, Namaqualand, South Africa. *Journal of African Earth Sciences*, **33**: 17 - 47.

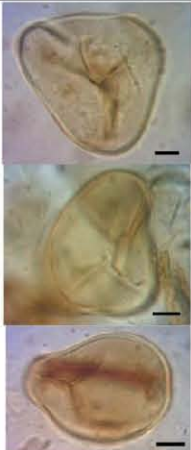
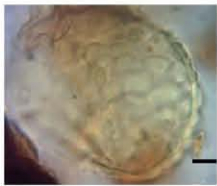


Muller, 1981. Fossil pollen records of extant angiosperms. *Botanical Review*, **47**: 1-142.

Raine, J.I., Mildenhall, D.C., and Kennedy, E.M. 2008. New Zealand fossil spores and pollen: an illustrated catalogue. 3rd edition. GNS Science miscellaneous series no. 4. Available, (online):http://www.gns.cri.nz/what/earthhist/fossils/spore_pollen/catalog/index.htm

Stevens, P. F. 2001. Angiosperm Phylogeny Website. Version 9, June 2008 [continuously updated since]. Available, (online): <http://www.mobot.org/MOBOT/research/APweb> [Accessed 2009/2010].





Zavada, M.S., and de Villiers, S.E. 2000. Pollen of the Asteraceae from the Paleocene-Eocene of South Africa. *Grana* **39**: 39-45.

SPORES

<p>Pteridaceae, <i>Pellaea</i>-type</p> <p>Description:</p> <p>Shape of the amb: Circular Number of lasurae: Trilete, rays are straight and slightly gaping Exospore: 1-2.5µm thickness Ornamentation: Psilate Dimensions: Equatorial diameter (average for 10 specimens): 39+/- 5µm</p>	<p>Polypodiaceae, <i>Polypodiisporites</i> sp.</p> <p>Description:</p> <p>Shape of the amb: Plano-convex but oval in proximal view Number of lasurae: Monolete. Exospore: 3-4 µm thickness Ornamentation: Verrucae Dimensions: Equatorial diameter (average for 10 specimens): 25+/- 3µm</p>	<p>Pteridaceae, <i>Verrucate</i> sp. A</p> <p>Description:</p> <p>Shape of the amb: Spherical Number of lasurae: Trilete, rays are straight. Exospore: 1-2.5µm thickness Ornamentation: psilate Dimensions: Equatorial diameter (average for 10 specimens): 39+/- 5µm <i>Pellaea</i></p>	<p>Pteridaceae, Filicopsida: Gleicheniaceae</p> <p>Description:</p> <p>Shape of the amb: Triangular, convex sides Number of lasurae: Trilete, rays are straight. Tricrassate Exospore: 1-2 µm thickness Ornamentation: psilate Dimensions: Equatorial diameter (average for 10 specimens): 39+/- 5µm</p>
<p>Remarks:</p> <p>Botanical affinities to <i>Pellaea</i> Geological occurrence: Tertiary</p>	<p>Remarks:</p> <p>Botanical affinities: Resembles <i>Polypodiisporites</i> sp Potonie'1931; also described by deVilliers (1997) from Koinznaas, and <i>Polypodiisporites</i> sp. described by Kemp and Harris (1977) which has an age range from Upper Eocene to Miocene. Geological occurrence: Cenozoic</p>	<p>Remarks:</p>	<p>Remarks:</p>
			

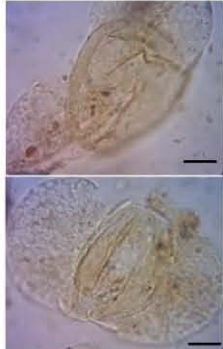
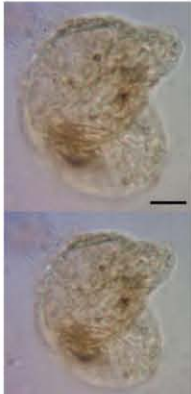
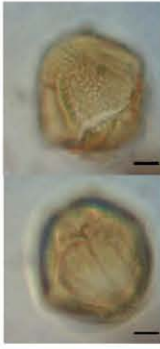
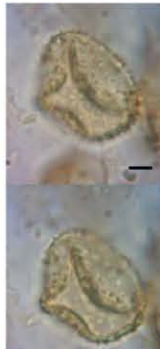
SPORES





Pteridaceae





Monosulcate psilate A	Monosulcate psilate B	Trilete, cingulate triangular spore	Trilete, acingulate, psilate spore
<p>Description:</p> <p>Shape of the amb: biconvex to plano-convex in lateral view</p> <p>Number of lasurae: Monolete</p> <p>Exospore: 1-2 μm thickness</p> <p>Ornamentation: psilate</p> <p>Dimensions: Length (average for 10 specimens): 42\pm 3μm; height: 15\pm 2μm</p>	<p>Description:</p> <p>Shape of the amb: biconvex to plano-convex in lateral view</p> <p>Number of lasurae: Monolete</p> <p>Exospore: 1-2 μm thickness</p> <p>Ornamentation: psilate</p> <p>Dimensions: Length(average for 10 specimens): 70\pm 2μm; height: 32μm</p>	<p>Description:</p> <p>Shape of the amb: triangular with straight sides</p> <p>Number of lasurae: Trilete, rays reach to border.</p> <p>Exospore: 3-4 μm thickness</p> <p>Ornamentation: psilate</p> <p>Dimensions: Equatorial diameter (average for 10 specimens): 40\pm 1μm</p>	<p>Description:</p> <p>Shape of the amb: Sub-circular</p> <p>Number of lasurae: Trilete, rays are short and straight, commissure slightly gaping.</p> <p>Exospore: 1-2 μm thickness</p> <p>Ornamentation: Psilate</p> <p>Dimensions: Equatorial diameter (average for 10 specimens): 47\pm 3μm</p>
<p>Remarks:</p>	<p>Remarks:</p>	<p>Remarks:</p>	<p>Remarks:</p>
			





POLLEN

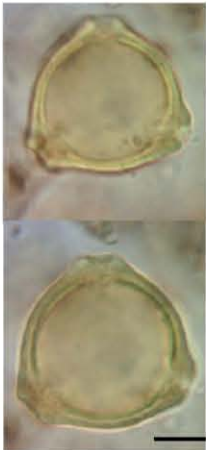



SACCATES

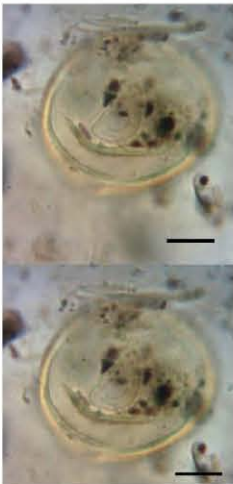



Gymnospermopsida : Coniferophyta, Podocarpidites sp. A	Gymnospermopsida : Coniferophyta, Podocarpidites sp.B	Angiospermae	Compositae, Tubuliflorae group
<p>Description:</p> <p>Corpus: Circular Dimensions fo corpus: Av. length: 43+/-2µm diameter (10 specimens) Sacci: Two semi-circular Ornamentation: finely sculptured Dimensions: Equatorial diameter (average for 10 specimens): 39+/- 5µm</p>	<p>Description:</p> <p>Corpus: Circular Dimensions fo corpus: Av. length: 34+/-2µm diameter (10 specimens) Sacci: Two semi-circular Ornamentation: fine sculpturing</p>	<p>Description:</p> <p>Shape of the amb: Prolate Number of colpi: 4 or more which are meridionally lined Exine:~1µm Dimensions: Equatorial diameter (average for 10 specimens): 30+/- 3µm</p>	<p>Description:</p> <p>Shape of the amb: Spherical Colpi: Number of pores: Three - not well seen Exine:1-2 µm Ornamentation: Echinata, spines are low (<1 µm) and regularly distributed Dimensions: Equatorial diameter (average for 10 specimens): 30+/-5µm</p>
<p>Remarks:</p> <p>Botanical affinity: Podocarpaceae (<i>Podocarpus</i>). Geological occurrence: Cretaceous to Neogene</p>	<p>Remarks:</p> <p>Botanical affinity: Podocarpaceae (<i>Podocarpus</i>). Geological age rangc: Cretaceous to Neogene.</p>	<p>Remarks:</p> <p>Baculae look longer at the poles</p> <p>Botanical affinities: Angiospermae Geological occurrence:</p>	<p>Remarks:</p> <p>Botanical affinities: Compositae; appears to resemble <i>Mutisia</i>. Geological occurrence: Cretaceous- present</p>
			





<p>Angiospermae: Carpacoce-type</p> <p>Description:</p> <p>Shape of the amb: Prolate to subprolate Colpi: Three Number of pores: Three Exine: 2µm Ornatmentation: Regulate Dimensions: Equatorial diameter (average for 10 specimens):25+/- 5µm</p>	<p>Angiospermae: Celastrales, Celastraceae</p> <p>Description:</p> <p>Shape of the amb: Circular to subprolate Colpi: Tricolpate Exine: Thick >3µm Ornamentation: reticulate Dimensions: Equatorial diameter (average for 10 specimens): 25µm +/- 5µm</p>	<p>Angiospermae: Celtis-type</p> <p>Description:</p> <p>Shape of the amb:spherical Number of colpi: Triporate: Exine: <2µm Ornamentation: fine regulate scuplturing to psilate Dimensions: Equatorial diameter (average for 10 specimens): 25+/- 5µm</p>	<p>Chloranthaceae: Ascarina-type (Clavatipollenites- Ascarina complex)</p> <p>Description:</p> <p>Shape of the amb: Prolate Number of colpi: Monocolpate Number of pores: - Exine:thick, 2-4µm Ornamentation: Retsiculate Dimensions: Equatorial diameter (average for 10 specimens): 30+/- 5µm</p>
<p>Remarks:</p> <p>Modern genus and endemic to the Cape (Robbretch, 1985). Only found in the upper metre at Noordhoek.</p> <p>Botanical affinities: Rubiaceae (Robbretch, 1985) Geological occurrence: Cenozoic - Modern</p>	<p>Remarks:</p> <p>Botanical affinities: Celastraceae (Perveen and Qaiser, 2008) Geological occurrence: Cretaceous - present (http://www.mobot.org/mobot/research/apweb/orders/celastralesweb.html)</p>	<p>Remarks:</p> <p>Botanical affinities: Ulmaceae (Muller, 1981) Geological occurrence: Cretaceous (Tortonian) - present (Muller, 1981).</p>	<p>Remarks:</p> <p>Occurrence interval within Noordhoek core:</p> <p>Botanical affinities: Chloranthaceae Geological occurrence: Cretaceous (Aptian) - present (Muller, 1981).</p>
			


<p>Angiospermae: Compositae A, <i>Tricolpites</i> sp.</p> <p>Description:</p> <p>Shape of the amb: Circular Number of colpi: Tricolpate Exine: <1µm Ornamentation: fine regulate sculpturing Dimensions: Equatorial diameter (average for 10 specimens): 25+/- 3µm</p>	<p>Angiospermae: <i>Cupuliferoideapollen ites</i> sp.</p> <p>Description:</p> <p>Shape of the amb: Circular to spherical Number of colpi: Tricolpate Exine: 1µm Ornamentation: Psilate Dimensions: Equatorial diameter (average for 10 specimens): 12+/- 2µm</p>	<p>Angiospermae: Compositae B, <i>Tricolpites</i> sp.</p> <p>Description:</p> <p>Shape of the amb: Circular to trilobate Number of colpi: Tricolpate Exine: <1µm Ornamentation: fine regulate sculpturing Dimensions: Equatorial diameter (average for 10 specimens): 45+/- 3µm</p>	<p>Angiospermae: Sarcolaenaceae, <i>Xyloolaena</i>-type (Coetzee and Muller, 1984)</p> <p>Description:</p> <p>Shape of the amb: Tetrad; Circular to spherical Thickening around apertures is roughly 2µm Ornamentation: Psilate Dimensions: Equatorial diameter of entire tetrad: 35+/- 2µm</p>
<p>Remarks:</p> <p>Botanical affinities: Compositae Geological occurrence:</p>	<p>Remarks:</p> <p>Resembles that described by DeVilliers (1997)</p> <p>Botanical affinities: Unknown Geological occurrence: Cretaceous (?)</p>	<p>Remarks:</p> <p>Botanical affinities: Compositae Geological occurrence: Unknown</p>	<p>Remarks:</p> <p>Endemic to Madagascar (Carlquist (1964). Resembles that described by Coetzee and Muller (1984) which resemble <i>Xyloolaena</i> of Carlquist (1964) for Noordhoek S20 core.</p> <p>Botanical affinities: Sarcolaenaceae Geological occurrence: At least from the early Miocene</p>
			





<p>Angiospermae: <i>Euphorbia</i>-type</p> <p>Description:</p> <p>Shape of the amb: Trilobate Number of colpi: Tricolpate Exine: <1µm Ornamentation: Psilate Dimensions: Equatorial diameter (average for 10 specimens): 7+/- 3µm</p>	<p>Angiospermae: Arecaceae/Palmae, 'Large Palm'</p> <p>Description:</p> <p>Shape of the amb: Oval Number of colpi: Monocolpate Exine: 1-2µm Ornamentation: Psilate Dimensions: Pole-pole length (average for 10 specimens): 50+/- 5µm</p>	<p>Arecaceae/Palmae, 'Small Palm' <i>Arecipites waitakiensis</i> (McIntyre 1968) Mildenhall & Pocknall 1989</p> <p>Description:</p> <p>Shape of the amb: Oval ('boat shaped') Number of colpi: Monocolpate Exine: 1µm Ornamentation: Psilate Dimensions: Equatorial diameter (av.): 25+/- 5µm</p>	<p>Angiospermae: Liliaceae, Liliacidites (?)</p> <p>Description:</p> <p>Shape of the amb: Oval Number of colpi: Monocolpate Exine: 1µm Ornamentation: Finely reticulate Dimensions: Equatorial diameter (average for 10 specimens): 30+/- 5µm</p>
<p>Remarks:</p> <p>Botanical affinities: <i>Euphorbia</i>-type? Geological occurrence: Unknown</p>	<p>Remarks:</p> <p>Botanical affinities: Resembles modern <i>Jubaeopsis</i>. Geological occurrence: Paleogene to Neogene</p>	<p>Remarks:</p> <p>Botanical affinities: Arecaceae Geological occurrence: Paleogene to Neogene</p>	<p>Remarks:</p> <p>Botanical affinities: Liliaceae Geological occurrence: Paleogene to present</p>
			

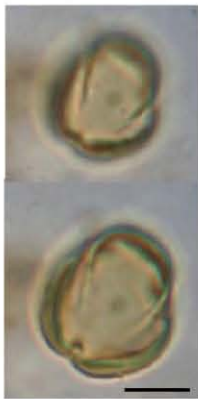
<p>Angiospermae: Myricaceae/Casuarina- ceae, Myrica/Casuarina- type</p> <p>Description:</p> <p>Shape of the amb: Triangular with convex sides Pores: Triporate; pores at equator Exine: 1-3µm Ornamentation: psilate Dimensions: Equatorial</p>	<p>Angiospermae: Myrtaceidites parvus Cookson and Pike 1954</p> <p>Description:</p> <p>Shape of the amb: Triangular Syn-tricolporate Exine: <1µm Ornamentation: Psilate Dimensions: Equatorial diameter (average for 10 specimens): 12+/- 2µm</p>	<p>Angiospermae: Oleaceae, Olea-type</p> <p>Description:</p> <p>Shape of the amb: Trilobate - polar view Pores: Colporate Exine: 3µm - thick sexine with long baculae Ornamentation: Reticulate Dimensions: Equatorial diameter (average for 10 specimens): 30+/- 2µm</p>	<p>Angiospermae: Proteaceae, Proteacidites sp.</p> <p>Description:</p> <p>Shape of the amb: Triangular Triporate Exine: 1-2µm Ornamentation: Finely reticulate Dimensions: Diameter (average for 10 specimens): 35+/- 5µm</p>
<p>Remarks: Hard to differentiate between <i>Myrica</i> and <i>Casuarina</i> pollen. All pollen in this thesis has been referred to as '<i>Myrica</i>'.</p> <p>Botanical affinities: Myricaceae/ Casuarinaceae Geological occurrence: Paleogene to Neogene(<i>Casuarina</i>) Palaeogene to present (<i>Myrica</i> - now termed <i>Morella</i>)</p>	<p>Remarks: Similar to grains described by Coetzee (1983) which resemble <i>Myrtaceidites parvus</i> Cookson and Pike 1954.</p> <p>Botanical affinities: Myrtaceae Geological occurrence: Paleogene to Modern</p>	<p>Remarks:</p> <p>Botanical affinities: Oleaceae Geological occurrence: Paleogene to present http://www.jstor.org/stable/4113738</p>	<p>Remarks: The reticulate mesh appeared wider around pores.</p> <p>Botanical affinities: Proteaceae Geological occurrence: Neogene</p>
			





<p>Angiospermae: Restionaceae</p> <p>Description:</p> <p>Shape of the amb: Circular/spherical Pores: Monoporate, pore width: 2µm Exine: 1-2µm Ornamentation: Psilate Dimensions: Equatorial diameter (average for 10 specimens): 30+/-5µm</p>	<p>Angiospermae: Sapotaceae</p> <p>Description:</p> <p>Shape of the amb: Prolate Colpi: Three meridionally aligned colpi Pores: Four (4th not visible in photomicrograph) (Stephanocolporate) Exine: 2µm Ornamentation: Psilate Dimensions: Diameter (average for 10 specimens): 40+/- 2µm</p>	<p>Angiospermae: Tubulifloridites sp Partridge (1978)</p> <p>Description:</p> <p>Shape of the amb: Trilobate Colpi: Three Pores: Three Tricolporate Exine: 1µm Ornamentation: Reticulate Dimensions: Equatorial diameter (average for 10 specimens): 20+/-5µm</p>	<p>Angiospermae: Stephanocolporites pollen</p> <p>Description:</p> <p>Shape of the amb: Prolate Colpi: Four meridionally aligned colpi Pores: Four Exine: 1-2.5µm Ornamentation: Psilate Dimensions: Diameter (average for 10 specimens): 35+/- 2µm</p>
<p>Remarks:</p> <p>Botanical affinities: Restionaceae Geological occurrence: Cenozoic</p>	<p>Remarks:</p> <p>Botanical affinities: Sapotaceae Geological occurrence: Paleogene to Neogene.</p>	<p>Remarks:</p> <p>Deep colpi; tricolporate reticulate <i>Tricolporites</i> spp. found by Coetzee and Rogers (1982).</p> <p>Botanical affinities: Asteraceae Geological occurrence: Paleogene to Modern.</p>	<p>Remarks:</p> <p>Botanical affinities: Unknown - Angiospermae? Geological occurrence: Unknown</p>
			

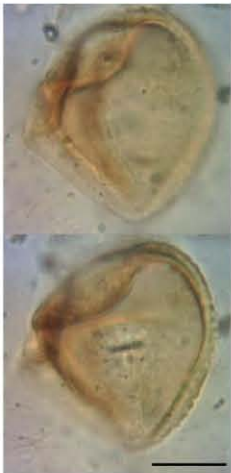

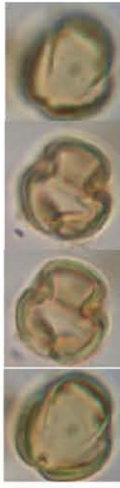

<p>Angiospermae: Rosaceae, <i>Cliffortia</i> spp. (?)</p> <p>Description:</p> <p>Shape of the amb: Triangular, straight sides Colpi: Three Pores: Three Tricolporate Exine: 2µm; sexine thicker than the nexine Ornamentation: Finely reticulate Dimensions: Equatorial diameter: 30+/-5µm</p>	<p>Angiospermae: “<i>Croton</i>”-type <i>sculpturing</i> <i>Tricolporites</i> sp.</p> <p>Description:</p> <p>Shape of the amb: Circular Colpi: Three Pores: Three Exine: 2.-35µm Ornamentation: Reticulate Dimensions: Diameter (average for 10 specimens): 25+/- 2µm</p>	<p>Angiospermae: <i>Tricolporites</i> <i>reticulate</i> sp. C</p> <p>Description:</p> <p>Shape of the amb: Prolate (equatorial view) Colpi: Three- meridionally aligned Tricolporate Pores: Three at equator Exine: 2-3µm- columellae appear longer at the pole Ornamentation: Strongly reticulate, wide mesh. Dimensions: Equatorial diameter (av. 10 specimens): 30+/-5µm</p>	<p>Angiospermae: <i>Tricolporites</i> <i>reticulate</i> sp. D</p> <p>Description:</p> <p>Shape of the amb: Prolate (equatorial view) Colpi: Three- meridionally aligned Pores: Three at equator Tricolporate Exine: 1µm, Ornamentation: Very finely reticulate Dimensions: Equatorial diameter (average for 10</p>
<p>Remarks:</p> <p>Botanical affinities: Rosaceae, or could be Rubiaceae Geological occurrence: Neogene to present</p>	<p>Remarks:</p> <p>Botanical affinities: Unknown - Angiospermae Geological occurrence: Unknown</p>	<p>Remarks:</p> <p>Appears to resemble <i>Calodendrum</i> sp. identified by Coetzee (1983). Botanical affinities: Rutaceae Geological occurrence: Paleogene to Modern.</p>	<p>Remarks:</p> <p>Botanical affinities: Unknown Geological occurrence: . Unknown</p>
			

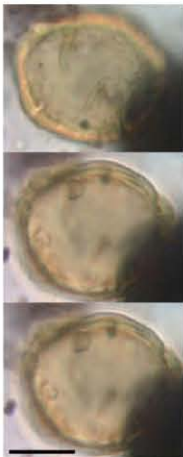


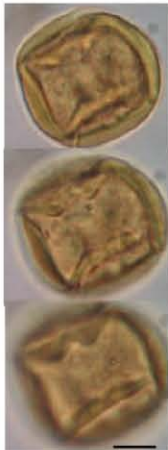
Angiospermae: <i>Tricolporites</i> <i>reticulate</i> sp. A	Angiospermae: <i>Tricolporites</i> <i>reticulate</i> sp. B	Angiospermae: <i>Tricolporites</i> <i>reticulate</i> sp. E	Angiospermae: <i>Tricolporites coarse</i> <i>reticulate</i> sp.
<p>Description:</p> <p>Shape of the amb: Triangular (equatorial view) Colpi: Three-meridionally aligned Pores: Three at equator Tricolporate Exine: 1-2 μm Ornamentation: Reticulate Dimensions: Equatorial diameter (average for 10</p>	<p>Description:</p> <p>Shape of the amb: Oblate Colpi: Three-meridionally aligned Pores: Three at equator Tricolporate Exine: 1-3μm, Ornamentation: Very finely reticulate Dimensions: Equatorial diameter (average for 10 specimens): 30+/-5μm</p>	<p>Description:</p> <p>Shape of the amb: Triangular (equatorial view) Colpi: Three-meridionally aligned Pores: Three at equator Tricolporate Exine: 1-2 μm; but thick exine at poles Ornamentation: Reticulate Dimensions: 28μm</p>	<p>Description:</p> <p>Shape of the amb: Triangular Colpi: Three-meridionally aligned Pores: Three at equator - Maybe syncolporate (?) Exine: 1-3μm, Ornamentation: Coarsely reticulate Dimensions: (average for 10 specimens): 32+/-2μm</p>
<p>Remarks:</p> <p>Botanical affinities: Unknown Geological occurrence: Unknown.</p>	<p>Remarks:</p> <p>Botanical affinities: Unknown Geological occurrence: . Unknown</p>	<p>Remarks:</p> <p>Botanical affinities: Unknown Geological occurrence: Unknown.</p>	<p>Remarks:</p> <p>Borehole depth at Noordhoek: only found at 22.5m depth below surface.</p> <p>Botanical affinities: Unknown (Angiospermae?) Geological occurrence: . Unknown</p>
			

<p><i>Tricolporites spp.</i> (<i>Striatricolpites spp.</i>)</p> <p>Description:</p> <p>Shape of the amb: (equatorial view) Colpi: Three- meridionally aligned Pores: Three at equator Tricolporate Exine: 1-2 μm; Ornamentation: Striate reticulate Dimensions: Equatorial diameter: 30+/-5μm</p>	<p>Angiospermae: <i>Tricolporites psilate</i> sp. A</p> <p>Description:</p> <p>Shape of the amb: Circular Colpi: Three- meridionally aligned Pores: Three at equator Tricolporate Exine: 1-3μm, Ornamentation: Psilate Dimensions: Equatorial diameter (average for 10 specimens):12+/-5μm</p>	<p><i>Tricolporites psilate</i> sp. B</p> <p>Description:</p> <p>Shape of the amb:Triangular trilobate (equatorial view) Colpi: Three- meridionally aligned Pores: Three at equator Tricolporate Exine: 1-2 μm; Ornamentation: Psilate Dimensions: Equatorial diameter (average for 10 specimens): 32+/-5μm</p>	<p><i>Tricolporites psilate</i> sp. C</p> <p>Description:</p> <p>Shape of the amb: Circular Colpi: Three- meridionally aligned Pores: Three at equator Tricolporate Exine: 1-3μm, Ornamentation: Psilate Dimensions: Equatorial diameter (average for 10 specimens):30+/-5μm</p>
<p>Remarks:</p> <p>Botanical affinities: Unknown Geological occurrence: Unknown</p>	<p>Remarks:</p> <p>Botanical affinities: Unknown Geological occurrence: Unknown</p>	<p>Remarks:</p> <p>Botanical affinities: Unknown Geological occurrence: Unknown</p>	<p>Remarks:</p> <p>Botanical affinities: Unknown. (Angiospermae?) Geological occurrence: Unknown</p>
			

<p>Angiospermae: <i>Tricolporites psilate</i> sp. D</p> <p>Description:</p> <p>Shape of the amb: Prolate Colpi: Three-meridionally aligned Pores: Three at equator Tricolporate Exine: 1.5 - 2 μm; Ornamentation: psilate Dimensions: Equatorial diameter (average for 10 specimens): 30μm</p>	<p>Angiospermae: <i>Tricolporites psilate</i> sp. E</p> <p>Description:</p> <p>Shape of the amb: Oblate Colpi: Three-meridionally aligned Pores: Three at equator Tricolporate Exine: 1-3μm, Ornamentation: Psilate Dimensions: Equatorial diameter (average for 10 specimens): 20\pm 2μm</p>	<p><i>Tricolporites spp.</i> Coarse reticulate</p> <p>Description:</p> <p>Shape of the amb: Prolate (equatorial view) Colpi: Three-meridionally aligned Pores: Three at equator Tricolporate Exine: 5μm; Ornamentation: Wide mesh (2-3μm) reticulate Dimensions: Length: 50\pm 3 μm</p>	<p>Angiospermae: <i>Tricolpites reticulate</i> sp. A</p> <p>Description:</p> <p>Shape of the amb: Trilobate Colpi: Three-meridionally aligned Exine: 1-3μm Ornamentation: Microreticulate Dimensions: Equatorial diameter (average for 10 specimens): 20\pm 5μm</p>
<p>Remarks:</p> <p>Botanical affinities: Unknown Geological occurrence: Unknown.</p>	<p>Remarks:</p> <p>Botanical affinities: Unknown Geological occurrence: Unknown.</p>	<p>Remarks:</p> <p>Botanical affinities: Unknown Geological occurrence: Unknown</p>	<p>Remarks:</p> <p>Botanical affinities: Unknown Geological occurrence: Unknown</p>
 <p>Two micrographs showing the morphology of <i>Tricolporites psilate</i> sp. D. The top image shows a single specimen with a prolate shape and three colpi. The bottom image shows another specimen with a similar morphology. A scale bar is present in the bottom right of the second image.</p>	 <p>Two micrographs showing the morphology of <i>Tricolporites psilate</i> sp. E. The top image shows a single specimen with an oblate shape and three colpi. The bottom image shows another specimen with a similar morphology. A scale bar is present in the bottom right of the second image.</p>	 <p>Three micrographs showing the morphology of <i>Tricolporites</i> spp. Coarse reticulate. The top image shows a single specimen with a prolate shape and three colpi. The middle and bottom images show other specimens with similar morphology. A scale bar is present in the bottom right of the bottom image.</p>	 <p>Two micrographs showing the morphology of <i>Tricolpites reticulate</i> sp. A. The top image shows a single specimen with a trilobate shape and three colpi. The bottom image shows another specimen with a similar morphology. A scale bar is present in the bottom right of the second image.</p>

<p>Angiospermae: <i>Tricolpites reticulata</i> sp. B</p> <p>Description:</p> <p>Shape of the amb: Prolate Colpi: Three-meridionally aligned Exine: 2-3µm; Ornamentation: Reticulate Dimensions: Length: 35+/-3 µm</p>	<p>Angiospermae: <i>Tricolpites reticulata</i> sp. C</p> <p>Description:</p> <p>Shape of the amb: Prolate Colpi: Three-meridionally aligned Exine: 1µm, Ornamentation: Microreticulate Dimensions: Equatorial diameter (average for 10 specimens):10+/- 5µm</p>	<p>Angiospermae: <i>Tricolpites reticulata</i> sp. D</p> <p>Description:</p> <p>Shape of the amb: Prolate Colpi: Three-meridionally aligned Exine: 1µm, Ornamentation: Psilate Dimensions: Equatorial diameter (average for 10 specimens):12+/- 5µm</p>	<p>Angiospermae: <i>Tricolpites reticulata</i> sp. E</p> <p>Description:</p> <p>Shape of the amb: Prolate Colpi: Three-meridionally aligned Exine: 3-5µm; Ornamentation: Pronounced reticulum; long baculae Dimensions: Length: 25+/-3 µm</p>
<p>Remarks:</p> <p>Botanical affinities: Unknown Geological occurrence: Unknown</p>	<p>Remarks:</p> <p>Botanical affinities: Unknown Geological occurrence: Unknown</p>	<p>Remarks:</p> <p>Botanical affinities: Unknown Geological occurrence: Unknown</p>	<p>Remarks:</p> <p>Botanical affinities: Unknown Geological occurrence: Unknown</p>
			

<p>Angiospermae: <i>Tricolpites reticulata</i> sp. F</p> <p>Description:</p> <p>Shape of the amb: Circular Colpi: Three Exine: 2.5-3 μm, Ornamentation: Reticulate Dimensions: Equatorial diameter (average for 10 specimens): 35\pm5 μm</p>	<p>Angiospermae: <i>Tricolpites psilate</i> sp. A</p> <p>Description:</p> <p>Shape of the amb: Trilobate Colpi: Three- meridionally aligned Exine: 1-2 μm; Ornamentation: Psilate Dimensions: Length: 15\pm3 μm</p>	<p>Angiospermae: <i>Tricolpites psilate</i> sp. B</p> <p>Description:</p> <p>Shape of the amb: Trilobate Colpi: Three Exine: 2.5 μm, Ornamentation: Psilate Dimensions: Equatorial diameter (average for 10 specimens): 15\pm5 μm</p>	<p>Angiospermae: <i>Tricolpites psilate</i> sp. C</p> <p>Description:</p> <p>Shape of the amb: Circular Colpi: Three- meridionally aligned Exine: 1-2 μm; Ornamentation: Psilate Dimensions: Length: 15\pm5 μm</p>
<p>Remarks:</p> <p>Botanical affinities: Unknown Geological occurrence: Unknown</p>	<p>Remarks:</p> <p>Botanical affinities: Unknown Geological occurrence: Unknown</p>	<p>Remarks:</p> <p>Botanical affinities: Unknown Geological occurrence: Unknown</p>	<p>Remarks:</p> <p>Botanical affinities: Unknown Geological occurrence: Unknown</p>
			

<p>Stephanoporate sp. A</p> <p>Description:</p> <p>Shape of the amb: Circular Pores: Six or more Exine: 2.5 μm, Ornamentation: Psilate Dimensions: Equatorial diameter (average for 10 specimens): 25\pm 5 μm</p>	<p>Stephanoporate sp. B</p> <p>Description:</p> <p>Shape of the amb: Circular Pores: Six, aligned equatorially and oval in shape. Exine: 2-4 μm; Ornamentation: Echinate, spines wider at base. Dimensions: Equatorial diameter (average for 10 specimens): 15\pm 5 μm</p>	<p>Stephanoporate sp. C</p> <p>Description:</p> <p>Shape of the amb: Circular Pores: Six, placed equatorially and circular in shape possessing annulae. Exine: 2 μm; Ornamentation: Microreticulate Dimensions: Equatorial diameter (average for 10 specimens): 30\pm 5 μm</p>	<p>Stephanoporate sp. D</p> <p>Description:</p> <p>Shape of the amb: Square in polar view Pores: Four, aligned equatorially Exine: 3-4 μm, Ornamentation: Psilate to finely granular Dimensions: Equatorial diameter (average for 10 specimens): 25\pm 5 μm</p>
<p>Remarks:</p> <p>Botanical affinities: Unknown - Angiospermae(?) Geological occurrence: Unknown</p>	<p>Remarks:</p> <p>Botanical affinities: Angiospermae(?) Geological occurrence: Unknown</p>	<p>Remarks:</p> <p>Botanical affinities: Angiospermae(?) Geological occurrence: Unknown</p>	<p>Remarks:</p> <p>Botanical affinities: Unknown - Angiospermae(?) Geological occurrence: Unknown</p>
			

Periporate

Description:

Shape of the amb:

Circular

Pores: Four, equatorially aligned, circular and possessing annulae.

Exine: 1-2 μm

Ornamentation:

Microreticulate

Dimensions: Equatorial diameter (average for 10 specimens): $25\pm 3\ \mu\text{m}$

Remarks:

Botanical affinities:

Unknown

Geological occurrence:

Unknown

